CONTACT MECHANICS OF FGM COATINGS

Fazil Erdogan
and
Mehmet Ali Guler

Lehigh University
Bethlehem, PA 18015

October 2000

AIR FORCE OFFICE OF SCIENTIFIC RESEARCH
GRANT F49620-98-1-0028

DTIC CONVERSATION RECORD FOR DISTRIBUTION STATEMENT REQUEST

DTIC Personnel Making Call	Date	Time
JACK RIKE	17 April 02	1420
Authorizing Official	**Phone**	
F. Erdogan		
Agency		
LEHIGH UNIV. MECH. Engineering & Mechanics		
Title		
Internet Document URL *(if applicable)*		

Distribution Statement *(Please check one box)*

☑ DISTRIBUTION STATEMENT A: Approved for public release. Distribution is unlimited.

☐ DISTRIBUTION STATEMENT B: Distribution authorized to U.S. Government Agencies only.

☐ DISTRIBUTION STATEMENT C: Distribution authorized to U.S. Government Agencies and their contractors.

☐ DISTRIBUTION STATEMENT D: Distribution authorized to U.S. Department of Defense (DoD) and U.S DoD contractors only.

☐ DISTRIBUTION STATEMENT E: Distribution authorized to U.S. Department of Defense (DoD) components only.

☐ DISTRIBUTION STATEMENT F: Further dissemination only as directed by the controlling DoD office indicated below or by higher authority.

☐ DISTRIBUTION STATEMENT X: Distribution authorized to U.S. Government agencies and private individuals or enterprises eligible to obtain export-controlled technical data in accordance with DoD Directive 5230.25, Withholding of Unclassified Technical Data from Public Disclosure, 6 Nov 84.

Reason for the above identified distribution statement *(in accordance with DoD Directive 5230.24)*

Controlling Office	Date of Distribution Statement Determination

AQ Number *(For DTIC-OCA Use Only)*

Abstract

The concept of grading the thermo-mechanical properties of materials provides an important tool to design new materials for certain specific functions. To take full advantage of this new tool research is needed not only for developing efficient processing methods and material characterization techniques but also for carrying out basic mechanics studies relating to the safety and durability of the FGM components. These studies may help to protect certain components against abrasion and wear at the surface where the maximum stress often occurs.

Graded materials, also known as *functionally graded materials* (FGMs), are generally two-phase composites with continuously varying volume fractions. Used as coatings and interfacial zones they can reduce thermally and mechanically induced stresses resulting from material property mismatch, increase the bonding strength and provide protection against adverse environments.

In this study the contact problem for the FGM coatings is considered. The objective of the study is to obtain a series of analytical benchmark solutions for examining the influence of such factors as material inhomogeneity constants, the coefficient of friction, curvatures and various length parameters on the critical stresses that may have a bearing on the fatigue and fracture of the components with FGM coatings.

In the first part of this study an FGM layer bonded to a homogeneous substrate loaded by a rigid stamp is considered. It is assumed that the coating is inhomogeneous, isotropic and linearly elastic, and the problem is one of plane strain. The shear

modulus of the FGM coating is represented by an exponential function. The Poisson's ratio is assumed to be constant. With the applications to load transfer components and abradable seals in mind, it is also assumed that the contacting surfaces are in relative motion with constant coefficient of friction. The related contact problem is solved for various different stamp profiles including flat, triangular, semicircular and cylindrical.

In the second part of this study the contact problem for two elastic load transfer components with FGM coating have been solved. The load transfer components are typically gears, cams, bearings and machine tools, where two elastic solids of given curvatures move relative to each other. The curvatures may be positive or negative. In these components ceramic coatings may be used to increase the wear resistance, whereas the material property grading would improve the toughness, reduce the stress levels and again increase the bonding strength

After solving the half space problem the Green's functions necessary for the solution of the problem in load transfer components are obtained. A parametric study has been done to find the effects of the parameters such as coefficient of friction, material property grading and surface shear modulus of elasticity of upper/lower or inner/outer cylinders. The contact stresses at the surface of the FGM coating are given and discussed.

Chapter 1

Introduction

Many of the present and potential applications of functionally graded materials (FGMs) involve contact problems. These are the basic load transfer problems between two solids, generally in the presence of friction. In the near future FGMs are expected to be used in three groups of practical applications that will require studying the problem from a view point of contact mechanics. The first is tribological applications of FGM coatings in such load transfer components as bearings, gears and cams. In this case the contacting solids are both elastic and one or both may have an FGM coating. The second application of the concept would be in cylinder linings, brake discs and other automotive components for the purpose of improving the wear resistance. In the related contact problem one of the opposing components (e.g., piston rings and brake pads) may have sharp corners. The third area of potential application of FGM coatings involving contact mechanics is in the field of abradable seal design in stationary gas turbines. The concept of abradable seals was developed some years ago to reduce or to eliminate the gas leakage between the tips of the blades and the shroud. With such a design the gain due to increased efficiency seems to outweigh the power loss due to friction. In this case the layered medium consists of the substrate(a superalloy) the FGM(substrate/dense YSZ), and porous ceramic(porous YSZ). The

contact is between porous ceramic and the blade. In these applications, the corresponding mechanics problem may be approximated by a quasi-static contact problem for a rigid punch of given profile moving over a graded medium in the presence of friction.

1.1 Functionally Graded Materials(FGMs)

In recent years the requirements of materials in severe environments have become more demanding. Ultimate purpose of the materials research in advancing technologies such as power generation, transportation, aerospace and micro-electronics is the development of new materials that can withstand these environments. Material scientists considered two ways to overcome the shortcomings of the conventional materials. One is to develop a completely different homogeneous material and the other is to develop new compositions by using the existing materials. The second approach leads to the design of composites and intermetallics having homogeneous bulk properties.

In recent past a wide variety of composites have been developed with fiber or filament reinforced, particulate or layered structure. A common feature of these composites is having different material characteristics on separate surfaces or in separate parts. An example of such a composite is a coated or joined material designed to improve material's surface characteristics to prevent failure caused by corrosion, wear and fatigue. Coated materials have a wide range of applications such as the blades in gas turbine engines which are subjected to high stresses and highly corrosive atmosphere, combustion chambers, machine tools, gears, bearings, cams and abradable seals.

The disadvantage of these piecewise homogeneous materials is that they consist of bonded dissimilar components which lead to discontinuities in the material's mechanical, physical, and chemical properties along the interfaces. The consequences of

this are higher residual, thermal and mechanical stresses, weaker bonding strength, low toughness and tendency toward cracking and spallation.

An alternative concept which may also be used to overcome some of the shortcomings of layered dissimilar materials would be the introduction of interfacial regions or coatings with graded thermomechanical properties.[1]-[6]. The approach is to synthesize inhomogeneous composites, in which the material's mechanical, physical, and chemical properties change continuously by varying the volume fractions of the constituents between zero to hundred percent. These materials are called Functionally Graded Materials (FGM). Apart from increasing the bond strength[7] and reducing the thermal stresses, grading also seems to improve the fracture toughness and fatigue and corrosion crack growth resistance parameters of thermal barrier coatings. For example, in joining tungsten to zirconia by introducing layers that contain $80/20, 60/40, 40/60$ and $20/80$ percent W/ZrO_2, it was shown that the peak value of the residual stress becomes approximately one-sixth of that obtained from direct W-ZrO_2 bonding[1].

The objective of the early research on the FGMs was to develop a new class of metal/ceramic composites with graded volume fractions to achieve the required high temperature resistance, toughness, strength and heat conductivity. An up to date summary and description of the recent research on the subject may be found in the proceedings of the international symposia on FGMs [4],[8],[9], [5].

Even though initially the FGM research was largely motivated by the practical application of the concept in thermal shielding problems in gas turbine and engine components, combustion chambers and high speed air and space transport, materials with graded physical properties have almost unlimited potential in many technological applications. However, in the near future the applications of FGMs will most likely be limited to thermal barrier coatings, corrosion-resistant coatings and wear-resistance

coatings.

1.2 Wear-Resistant Coatings/Abradable Seals

Surface treatments and coatings are being used more and more frequently to solve various critical tribological problems. They offer several significant benefits when applied to metals. Increased corrosion resistance, reduced sliding wear, and increased rolling contact fatigue life are some of the major benefits. Examples of the above include electrodeposited thin steel films(such as 52100, M50 and M50 NiL) for increased corrosion resistance [10], and hard ceramic coatings(such as TiN and TiC [11]), solid lubricant coatings(such as Cu[12]) and diamond-like carbon(DLC) [13] for increased wear and fatigue [14] resistance.

In most homogeneous coatings, the main failure mechanism is the delamination and subsequent spallation at the coating-substrate interface. The spallation would expose the bare metal surfaces to adverse environment and mechanical contact and would accelerate the corrosion and wear process. These failures can be controlled by controlling the material properties near and at the surface. In such applications it is necessary to provide the bulk material with a protective coating of a more resistant material such as monolithic structural ceramics and fiber reinforced ceramics including carbon-carbon composites.

Ceramic materials are used in many industrial applications. Cutting tools,for example, are a common application where the material is subjected to high thermal and abrasive environment and high stresses. Ceramics are also being used to provide the necessary hardness or wear resistance to surfaces of structural components transmitting forces through contact, such as gears, bearings and cams.

Ceramics based on oxides such as Al_2O_3 are well known and used in continuous turning of cast iron and steel. By adding TiC, it is possible to improve thermal

stability. Ceramics based on silicon nitride(Si_3N_4) are used for milling and cutting operations of cast iron with higher rate of cut. Problems can occur because of the diffusion of silicon into iron at high temperatures. This effect can be reduced by a coating of the Si_3N_4- ceramics with Al_2O_3.

Generally, ceramic materials have high hardness, relatively low density and depending on the kind of ceramic, low thermal conductivity. The thermal expansion in the case of Si_3N_4 and Al_2O_3 is very low and cause the development of thermal stresses in films obtained by physical vapor deposition(PVD).

One of the main disadvantages of these ceramics is their brittle nature. Intuitively it is clear that the fatigue life of these components may be improved quite considerably if one uses a graded rather than a homogeneous ceramic coating on the metallic substrate. In load transfer components FGM coatings would provide the necessary surface hardness without sacrificing the overall toughness.

In the past wear and corrosion-resistant coatings have been used quite extensively in industrial machinery. The coating material has been metals such as stainless steels, Mo-based alloys and WC-Co as well as ceramics such as Al_2O_3, TiO_2 and Cr_2O_3. For example, WC-Co and Cr_3C_2/NiCr have been extensively used in aircraft industry to coat various turbine/compressor components and mid-span stiffeners for improved wear resistance. Other applications of wear-resistant coatings have been in printing rolls, steel mills, petrochemical industry, and automobile industry. Most of these coatings have been deposited by using a thermal spray process. Since thermal spray technique is readily suitable for grading the composition of the coating, service life improvements can be obtained in all applications of wear resistant coatings by using the FGM concept.

1.3 Contact problems in Graded Materials

The contact problems involving graded materials may be considered in two major categories, namely the abradable seals and load transfer components. Abradable seals are used in some stationary gas turbines to reduce or eliminate the leakage between turbine blades and the shroud. The seal is a very low density ceramic deposited over the shroud metal structure through a graded interfacial region[15]. Because of the large difference between the stiffness of the blade and low density ceramic, the blade may be modelled as a rigid stamp pressed against and moving relative to an elastic medium. In this particular application the reason for grading the medium is to reduce the magnitude of the stresses and to improve the bonding strength. A related potential application of this particular concept is the wear control in aluminum alloy cylinders used in internal combustion engines. Here the piston rings are pressed against the cylinder and wear control is accomplished by coating the cylinder.

Load transfer components are typically gears, cams, bearings and machine tools, where two elastic solids of given curvatures move relative to each other. The curvatures may be positive or negative. In these components ceramic coatings may be used to increase the wear resistance, whereas the material property grading would improve the toughness, reduce the stress levels and again increase the bonding strength.

1.4 Literature review on Contact Mechanics

Contact problems have been a topic of interest within the theory of elasticity for over 100 years. The problem of determining the stress distribution in a semi infinite elastic solid under the compressive action of a rigid body was first considered by Boussinesq. Hence problems of this kind are referred to as *Boussinesq problems.* The general description of the problem may be found in the classical paper by Hertz [16] who

gave birth to an area of research which has grown into the present day field of contact mechanics.

The foundation of contact mechanics analysis rests on the Hertz assumption. If the contact area is small compared to the geometry of the contacting bodies and if it is far removed from other surfaces, then the contacting bodies can be approximated as semi-infinite planes or spaces. This generally reduces the complexity of the original problem and simplifies the solution process, allowing closed form solutions in many cases. This Hertz assumption has provided a great stimulus for analyzing contact problems for half planes and half spaces.

Harding and Sneddon [17] obtained the general solution of the Boussinesq problem for an axisymmetric punch. Using the Boussinesq solution for point loading on half space, the contact problem may be formulated as a Fredholm integral equation of the first kind. Remarkable progress was made by Shtaerman(see book by Galin[18]), who showed that polynomial solutions multiplied by a square root term could be achieved for the related integral equation if the contact region on a half space is elliptic. Later, Shtaerman's result was developed to handle the contact problem for an inhomogeneous isotropic medium by Rostovtsev[19] ,[20] and a homogeneous anisotropic medium by Willis[21], [22].

Either the Integral transformation approach or the finite element method can be used for computing stresses. In terms of actual implementation for practical design the finite element model can be effectively used for arbitrary complex geometry, but the integral formulation is limited to simplified contact configurations. On the other hand the finite element models require some effort in the pre and post processing of the data and overall setup of the problem, while the use of the numerical integral model is very straightforward. Depending on the complexity of the application both

models may have a notable practical significance. For material selection and preliminary design the Integral transform approach may be very efficient. For final design development in critical and complex applications the finite element approach may provide acceptable design solutions with a minimum number of model assumptions and limitations. Analytical solutions to contact problems have technologically significant applications in the aircraft, automotive and marine industries. For instance, the knowledge of contact pressure distribution allows the calculation of internal stresses in order to determine those regions where potential damage may occur as a consequence of the application of concentrated loads.

Even though such solutions can be obtained numerically by using finite-difference or finite element approaches, the analytical approach presented here allows one to generate these solutions efficiently thereby facilitating parametric studies wherein the geometric parameters are varied to ascertain their effect on the resulting contact pressure. The present solution when employed in conjunction with the current punch testing methods for the determination of the in situ elastic moduli of constituent materials in a layered composite.

Solutions to many plane as well as axisymmetric problems can be found in the work of Galin. A general solution of such problems using integral transforms was given by Sneddon [23].

The general method of solving frictionless plane contact problems was given by Muskhelishvili[24]. Much of the literature in this area deals with an elastic slab, either loaded symmetrically from both surfaces or loaded from one surface and rigidly fixed on the other surface. A survey of these two types of elasticity problems, tackled by the method of integral transforms, may be found in the book by Uflyand [25].

In subsequent studies a layer between the punch and the subspace was introduced. A systematic treatment of this kind of problems can be found in [27]-[29]. Recently,

Kasmalkar solved the axisymmetric contact problem for a layer bonded to substrate for different indenter geometries [30].

Ratwani and Erdoğan [31] have considered the plane contact problem for an elastic layer lying frictionlessly on an elastic half space. Civelek and Erdoğan[32] have solved the problem in axisymmetric case.

Frictional phenomena have to be considered when the tangential part of the motion is important in the response of two or more bodies coming into contact during static or dynamic load transfer. Most of the formulation relies on the law of Coulomb. However, in some cases local micro-mechanical phenomena within the contact interface has to be taken into account. An extensive overview may be found in [33]. For the physical background of the frictional phenomena reader is referred to [34].

For frictional contact problems of linear elasticity, most of the solutions given are approximate solutions , obtained by using either finite element method or a more specific variational formulation. The finite element method has been used by many investigators to study contact problems. Chan and Tuba [35], Tsuta and Yamaji [36] and Ohte [37] studied contact problems for plane and axisymmetric problems. In these studies, an ideal type of Coulomb friction has been included. Lindeman [38] has used the finite element method to study shrink fit problems.

Although considerable research is being carried out in components involving FGMs, there is not much work done in the area of contact mechanics. However, in recent years fracture mechanics of FGMs have been extensively studied by Erdogan and coworkers.

Contact problems of a rigid punch on a non-homogeneous medium were solved approximately for small values of the non-homogeneity parameter, by Bakirtas [39]. Bakırtaş considered the frictionless elastostatic problem of a rigid punch on an elastic half place [40]. Guler[41] solved the same problem for the stiffening medium including

friction.

1.5 Statement of the Problem

1.5.1 Introduction

The main cause of failure in mechanical structures is fracture and fatigue. Crack initiation and propagation take place essentially in areas of high stresses or in areas where friction and wear are present. In contact zones in a variety of load transmission components quasi-static loads can lead to friction and to high stresses which results in erosion and fatigue. It is thus necessary to predict the magnitude of contact stresses, in order to design these elements

The contact problems can be categorized into two broad sections,namely frictionless and with friction.In the first, the friction between the contacting solids are neglected which simplifies the problem significantly. For contact problems that arise in well-lubricated components, this assumption is well justified. In the second group, forces of friction are not small. Therefore, the effect of friction can not be neglected. Here two cases can arise. In the fist case, one elastic solid moves relative to the other and the movement is so slow that the dynamic effect can be neglected. This is the case in the proposed study. In the second case no displacement of the punch as a whole with respect to the elastic body takes place. However, when $\sigma_{xy} < \eta\sigma_{yy}$ a rigid linkage (stick), and when $\sigma_{xy} > \eta\sigma_{yy}$ a relative displacement (slip) would take place between the contacting solids.

In this study, dynamic effects are neglected and it is assumed that forces of friction obey Coulomb's law which states that

$$\sigma_{xy} = \eta\sigma_{yy}$$

where η is the coefficient of friction.

1.5.2 Description of the problem

In this study two classes of problems will be considered namely; contact problems for rigid stamps (e.g. abradable seals) and contact problems in load transfer components.

The contact problems to be studied for abradable seals are described in Fig.1.1. Here the blade will be represented by a rigid stamp and the abradable seal by a (ceramic-rich) graded metal/low density ceramic layer. In the analytical solution to be carried out the metal substrate will be modeled as an elastic half plane. It will be assumed that the stamp and the coated medium are in relative motion and the coefficient of friction η along the contact region is constant (i.e., $Q = \eta P$). Four basic stamp geometries shown in Fig.1.1 will be considered. Also the stamp problems shown in Fig.1.1c and Fig.1.1d will be studied separately for both positive and negative directions of the tangential force Q. The main calculated results in these problems are the contact stresses which may then be used with appropriate kernels to evaluate the desired stresses and displacements.

In the load-transfer components shown in Fig.1.2, it will be assumed that the contacting solids locally have shallow curvatures(that is, the contact zone size $(b+a)$ is "small" compared to R_1 and R_2. Thus, in formulating the problem one may make the standard Hertzian assumption to the effect that the Green's functions for the concentrated surface tractions in a cylindrical medium may be approximated by that of a half plane. The contacting solids consist of dissimilar homogeneous materials coated by graded elastic layers of known thickness. Locally the solids will be represented by circular cylinders with positive/negative (Fig.1.2a) or positive/positive (Fig.1.2b) curvatures. The problem will be considered with or without friction. The main calculated quantities will again be the contact stresses and the load versus the contact zone size curves.

In these problems it will be assumed that a coating layer of thickness h_2 or h_3

is perfectly bonded to the homogeneous substrate. The coating is nonhomogeneous where the nonhomogeneity is assumed to be in the thickness direction only and may be approximated by $\mu_3(y) = \mu_{30}e^{\gamma_3 y}$, μ_{30} being the shear modulus of the FGM coating on the surface at $y = 0$. The Poisson's ratio is assumed to be constant for both materials.

The result of this study may be applicable to a great variety of structural components such as connecting-rods, bolted connections, shrink fits, rolling mills, turbine blade roots, ball and roller bearings, foundations, pavements in roads and runways, and other structures consisting of layered media.

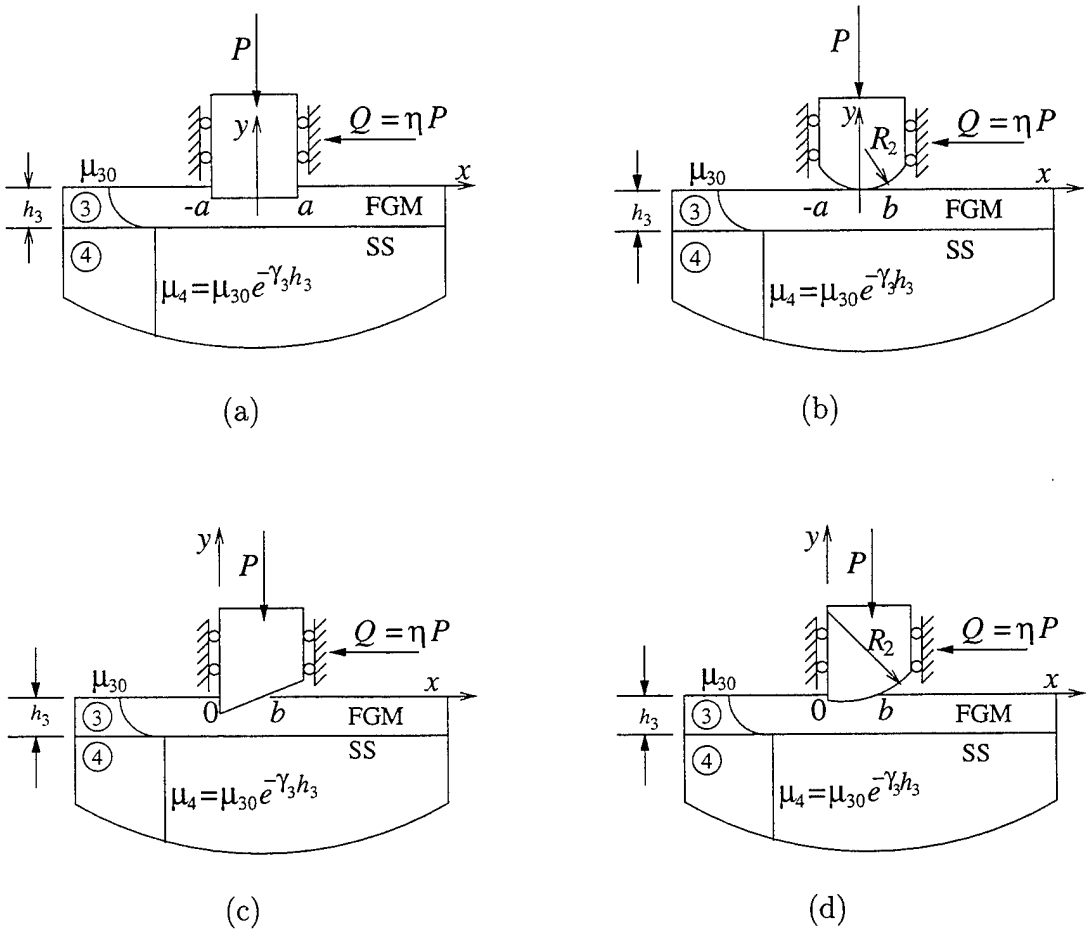

Figure 1.1: Contact problems for abradable seals

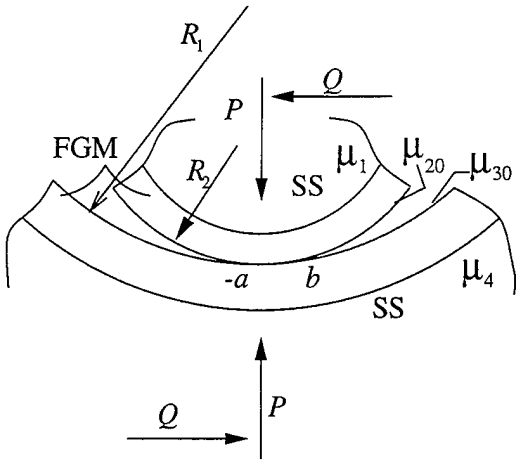

(a)

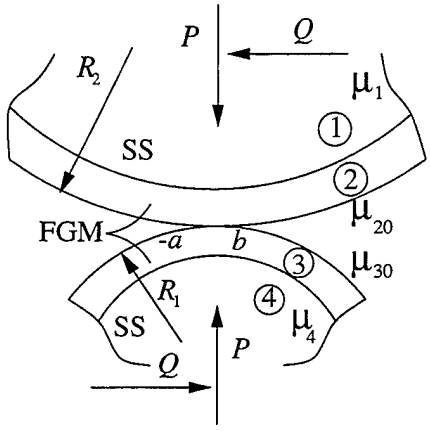

(b)

Figure 1.2: Contact problems for load transfer components

Chapter 2

Formulation of the Upper Half Plane

2.1 Solution of Differential Equations

In this chapter the Greens functions for the upper half plane will be developed. The standard elasticity analysis of the upper half plane composed of a homogeneous substrate and an FGM coating will be carried out under the mixed boundary conditions along the surface. By using an exponential variation for the shear modulus of the FGM coating and applying Fourier transforms, the Navier's equations will be reduced to a sistem of ordinary differential equations. These differential equations will be solved by applying continuity of the stress and displacement conditions along the interface and the mixed boundary conditions along the surface. Finally the Greens functions for the displacement gradients in x directions will be found by taking the inverse transforms.

Consider the plane elasticity punch problem shown in Figure 2.1. The medium(1) is a homogeneous substrate and medium (2) is the FGM coating with a thickness

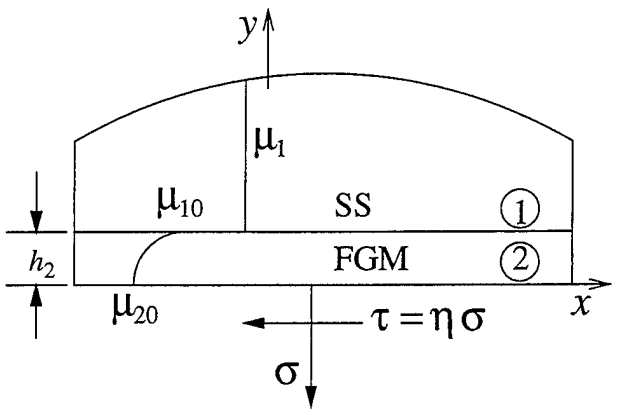

Figure 2.1: Geometry of the problem for the upper half plane

of h_2. The elastic constants of the homogeneous substrate is represented by μ_1 and κ_1. The non-homogeneity of the FGM coating is assumed to be such that its shear modulus, μ_2 is approximated by

$$\mu_2(y) = \mu_{20} e^{\gamma_2 y}, \qquad 0 < y < h_2. \tag{2.1}$$

Thus

$$\mu_{10} = \mu_{20} e^{\gamma_2 h_2}, \tag{2.2}$$

where the non-homogeneity parameter is

$$\gamma_2 h_2 = \ln \Gamma_2, \tag{2.3}$$

$$\Gamma_2 = \frac{\mu_{10}}{\mu_{20}}. \tag{2.4}$$

We define another parameter, χ_2

$$\chi_2 = \frac{\mu_{10}}{\mu_1}$$

For the plane contact problem under consideration, we start by writing the equations of elastisity

$$\sigma_{ij,j} = 0, \tag{2.5}$$

$$\varepsilon_{ij} = \frac{1}{2}\left(u_{i,j} + u_{j,i}\right), \tag{2.6}$$

$$\sigma_{ij} = 2\mu\varepsilon_{ij} + \lambda\varepsilon_{kk}\delta_{ij}. \tag{2.7}$$

Hooke's law for the medium (1) and (2) can be written as

$$\sigma_{1xx}(x,y) = \frac{\mu_1}{\kappa_1 - 1}\left[(\kappa_1+1)\frac{\partial u_1}{\partial x} + (3-\kappa_1)\frac{\partial v_1}{\partial y}\right], \tag{2.8}$$

$$\sigma_{1yy}(x,y) = \frac{\mu_1}{\kappa_1 - 1}\left[(3-\kappa_1)\frac{\partial u_1}{\partial x} + (\kappa_1+1)\frac{\partial v_1}{\partial y}\right], \qquad h_2 < y < \infty \tag{2.9}$$

$$\sigma_{1xy}(x,y) = \mu_1\left[\frac{\partial u_1}{\partial y} + \frac{\partial v_1}{\partial x}\right], \tag{2.10}$$

$$\sigma_{2xx}(x,y) = \frac{\mu_{20}e^{\gamma_2 y}}{\kappa_2 - 1}\left[(\kappa_2+1)\frac{\partial u_2}{\partial x} + (3-\kappa_2)\frac{\partial v_2}{\partial y}\right], \tag{2.11}$$

$$\sigma_{2yy}(x,y) = \frac{\mu_{20}e^{\gamma_2 y}}{\kappa_2 - 1}\left[(3-\kappa_2)\frac{\partial u_2}{\partial x} + (\kappa_2+1)\frac{\partial v_2}{\partial y}\right], \qquad 0 < y < h_2 \tag{2.12}$$

$$\sigma_{2xy}(x,y) = \mu_{20}e^{\gamma_2 y}\left[\frac{\partial u_2}{\partial y} + \frac{\partial v_2}{\partial x}\right], \tag{2.13}$$

where $\kappa_2 = 3 - 4\nu_2$ for plane strain and $\kappa_2 = (3-\nu_2)/(1+\nu_2)$ for the generalized plane stress conditions. In the absence of body forces, the equations of equilibrium can be written as

$$\frac{\partial \sigma_{1xx}}{\partial x} + \frac{\partial \sigma_{1xy}}{\partial y} = 0, \tag{2.14}$$

$$\frac{\partial \sigma_{1xy}}{\partial x} + \frac{\partial \sigma_{1yy}}{\partial y} = 0, \tag{2.15}$$

$$\frac{\partial \sigma_{2xx}}{\partial x} + \frac{\partial \sigma_{2xy}}{\partial y} = 0, \tag{2.16}$$

$$\frac{\partial \sigma_{2xy}}{\partial x} + \frac{\partial \sigma_{2yy}}{\partial y} = 0. \tag{2.17}$$

Substituting stresses found from equations (2.8)-(2.13) into the equations of equilibrium (2.14)-(2.17), we obtain the Navier's equations as follows

$$(\kappa_1+1)\frac{\partial^2 u_1}{\partial x^2} + (\kappa_1-1)\frac{\partial^2 u_1}{\partial y^2} + 2\frac{\partial^2 v_1}{\partial x \partial y} = 0, \tag{2.18}$$

$$(\kappa_1+1)\frac{\partial^2 v_1}{\partial y^2} + (\kappa_1-1)\frac{\partial^2 v_1}{\partial x^2} + 2\frac{\partial^2 u_1}{\partial x \partial y} = 0, \tag{2.19}$$

$$
\begin{aligned}
(\kappa_2+1)\frac{\partial^2 v_2}{\partial y^2}+(\kappa_2-1)\frac{\partial^2 v_2}{\partial x^2}+2\frac{\partial^2 u_2}{\partial x\partial y}& \\
+\gamma_2(3-\kappa_2)\frac{\partial u_2}{\partial x}+\gamma_2(\kappa_2+1)\frac{\partial v_2}{\partial y} &= 0, \qquad (2.20)\\
(\kappa_2+1)\frac{\partial^2 u_2}{\partial x^2}+(\kappa_2-1)\frac{\partial^2 u_2}{\partial y^2}+2\frac{\partial^2 v_2}{\partial x\partial y}& \\
+\gamma_2(\kappa_2-1)\frac{\partial u_2}{\partial y}+\gamma_2(\kappa_2-1)\frac{\partial v_2}{\partial x} &= 0. \qquad (2.21)
\end{aligned}
$$

To solve the Navier's equations we define the Fourier transforms of the four displacement components, $u_1(x,y)$, $u_2(x,y)$, $v_1(x,y)$ and $v_2(x,y)$, as

$$
\begin{aligned}
F_1(\alpha,y) &= \int_{-\infty}^{\infty} u_1(x,y)e^{-i\alpha x}dx, \qquad (2.22)\\
F_2(\alpha,y) &= \int_{-\infty}^{\infty} u_2(x,y)e^{-i\alpha x}dx, \qquad (2.23)\\
G_1(\alpha,y) &= \int_{-\infty}^{\infty} v_1(x,y)e^{-i\alpha x}dx, \qquad (2.24)\\
G_2(\alpha,y) &= \int_{-\infty}^{\infty} v_2(x,y)e^{-i\alpha x}dx. \qquad (2.25)
\end{aligned}
$$

The functions $u_1(x,y)$, $u_2(x,y)$ and $v_1(x,y)$, $v_2(x,y)$ are given by the following inverse transforms;

$$
\begin{aligned}
u_1(x,y) &= \frac{1}{2\pi}\int_{-\infty}^{\infty} F_1(\alpha,y)e^{i\alpha x}d\alpha, \qquad (2.26)\\
u_2(x,y) &= \frac{1}{2\pi}\int_{-\infty}^{\infty} F_2(\alpha,y)e^{i\alpha x}d\alpha, \qquad (2.27)\\
v_1(x,y) &= \frac{1}{2\pi}\int_{-\infty}^{\infty} G_1(\alpha,y)e^{i\alpha x}d\alpha, \qquad (2.28)\\
v_2(x,y) &= \frac{1}{2\pi}\int_{-\infty}^{\infty} G_2(\alpha,y)e^{i\alpha x}d\alpha. \qquad (2.29)
\end{aligned}
$$

Substituting (2.26)-(2.29) into (2.18)-(2.21) yields the following system of differential equations with constant coefficients.

$$
\begin{aligned}
(\kappa_1-1)\frac{d^2F_1}{dy^2}-(\kappa_1+1)\alpha^2F_1+2i\alpha\frac{dG_1}{dy} &= 0, \qquad (2.30)\\
(\kappa_1+1)\frac{d^2G_1}{dy^2}-(\kappa_1-1)\alpha^2G_1+2i\alpha\frac{dF_1}{dy} &= 0, \qquad (2.31)
\end{aligned}
$$

$$(\kappa_2-1)\frac{d^2F_2}{dy^2}+\gamma_2(\kappa_2-1)\frac{dF_2}{dy}-(\kappa_2+1)\alpha^2F_2$$
$$+2i\alpha\frac{dG_2}{dy}+i\alpha\gamma_2(\kappa_2-1)G_2 = 0, \tag{2.32}$$
$$(\kappa_2+1)\frac{d^2G_2}{dy^2}+\gamma_2(\kappa_2+1)\frac{dG_2}{dy}-(\kappa_2-1)\alpha^2G_2$$
$$+2i\alpha\frac{dF_2}{dy}+i\alpha\gamma_2(3-\kappa_2)F_2 = 0. \tag{2.33}$$

The solution of equations (2.30) and (2.31) can be expressed as

$$F_1(\alpha,y) = [A_{11}(\alpha)+A_{12}(\alpha)y]\,e^{|\alpha|y}+[A_{13}(\alpha)+A_{14}(\alpha)y]\,e^{-|\alpha|y}, \tag{2.34}$$
$$G_1(\alpha,y) = [A_{21}(\alpha)+A_{22}(\alpha)y]\,e^{|\alpha|y}+[A_{23}(\alpha)+A_{24}(\alpha)y]\,e^{-|\alpha|y}. \tag{2.35}$$

For (2.32) and (2.33), if we assume a solution of the form

$$F_2(\alpha,y) = A_3(\alpha)e^{ny}, \tag{2.36}$$
$$G_2(\alpha,y) = A_4(\alpha)e^{ny}, \tag{2.37}$$

we obtain

$$F_2(\alpha,y) = \sum_{j=1}^{4}A_{3j}(\alpha)e^{n_jy}, \tag{2.38}$$
$$G_2(\alpha,y) = \sum_{j=1}^{4}A_{4j}(\alpha)e^{n_jy}, \tag{2.39}$$

where n_j, $(j=1,\ldots,4)$ satisfies the following characteristic equation

$$(n_j^2-\alpha^2+\gamma_2n_j)^2+\delta_2^2|\alpha|^2|\gamma_2|^2=0, \tag{2.40}$$

with

$$n_j^2+\gamma_2n_j = |\alpha|^2+i\,|\alpha|\,\delta_2\,|\gamma_2|\,, \qquad j=1,2 \tag{2.41}$$
$$n_j^2-\gamma_2n_j = |\alpha|^2-i\,|\alpha|\,\delta_2\,|\gamma_2|\,, \qquad j=3,4 \tag{2.42}$$
$$\delta_2^2 = \frac{3-\kappa_2}{\kappa_2+1}. \tag{2.43}$$

The roots of the characteristic equation are given by

$$n_1 = \frac{1}{2}\left(-\gamma_2 + \sqrt{\gamma_2^2 + 4(\alpha^2 + i|\alpha||\gamma_2|\delta_2)}\right), \tag{2.44}$$

$$n_2 = \frac{1}{2}\left(-\gamma_2 - \sqrt{\gamma_2^2 + 4(\alpha^2 + i|\alpha||\gamma_2|\delta_2)}\right), \tag{2.45}$$

$$n_3 = \frac{1}{2}\left(-\gamma_2 + \sqrt{\gamma_2^2 + 4(\alpha^2 - i|\alpha||\gamma_2|\delta_2)}\right), \tag{2.46}$$

$$n_4 = \frac{1}{2}\left(-\gamma_2 - \sqrt{\gamma_2^2 + 4(\alpha^2 - i|\alpha||\gamma_2|\delta_2)}\right). \tag{2.47}$$

The functions $A_{1j}(\alpha)$, $A_{2j}(\alpha)$, $A_{3j}(\alpha)$ and $A_{4j}(\alpha)$, $(j = 1 \ldots 4)$ are unknown functions and are not independent. The relationship between them can be found by substituting (2.34), (2.35) into (2.30), (2.31) and (2.38), (2.39) into (2.32), (2.33)

$$A_{11}(\alpha) = i\left[\frac{|\alpha|}{\alpha}A_{21}(\alpha) + \frac{\kappa_1}{\alpha}A_{22}(\alpha)\right], \tag{2.48}$$

$$A_{12}(\alpha) = i\frac{|\alpha|}{\alpha}A_{22}(\alpha), \tag{2.49}$$

$$A_{13}(\alpha) = i\left[-\frac{|\alpha|}{\alpha}A_{23}(\alpha) + \frac{\kappa_1}{\alpha}A_{24}(\alpha)\right], \tag{2.50}$$

$$A_{14}(\alpha) = -i\frac{|\alpha|}{\alpha}A_{24}(\alpha), \tag{2.51}$$

$$A_{3j}(\alpha) = a_j(\alpha)A_{4j}(\alpha), \qquad j = 1, 2 \tag{2.52}$$

$$A_{3j}(\alpha) = -\overline{a}_{j-2}(\alpha)A_{4j}(\alpha), \qquad j = 3, 4 \tag{2.53}$$

where

$$a_j(\alpha) = -\frac{(\kappa_2 + 1)\left[n_j^2 + \gamma_2 n_j\right] - (\kappa_2 - 1)\,\alpha^2}{i\alpha\left[2n_j + \gamma_2\,(3 - \kappa_2)\right]}. \tag{2.54}$$

Using equations (2.41) and (2.42), (2.54) it may be seen that

$$a_j(\alpha) = \frac{1}{\alpha}\frac{2i\alpha^2 - |\alpha|(\kappa_2 + 1)\delta_2\gamma_2}{2n_j + \gamma_2(3 - \kappa_2)}, \qquad j = 1, 2 \tag{2.55}$$

$$a_j(\alpha) = \frac{1}{\alpha}\frac{2i\alpha^2 + |\alpha|(\kappa_2 + 1)\delta_2\gamma_2}{2n_j + \gamma_2(3 - \kappa_2)}, \qquad j = 3, 4 \tag{2.56}$$

$$a_j(\alpha) = -\overline{a}_{j-2}(\alpha), \qquad j = 3, 4. \tag{2.57}$$

2.2 Boundary and Continuity Conditions

2.2.1 Continuity conditions along the interface

The first four conditions are the displacement and stress continuity conditions along the interface at $y = h_2$ which can be written as,

$$u_1(x, h_2) = u_2(x, h_2), \tag{2.58}$$

$$v_1(x, h_2) = v_2(x, h_2), \tag{2.59}$$

$$\sigma_{1yy}(x, h_2) = \sigma_{2yy}(x, h_2), \tag{2.60}$$

$$\sigma_{1xy}(x, h_2) = \sigma_{2xy}(x, h_2). \tag{2.61}$$

Since both σ_{1yy} and σ_{1xy} vanish as $|x^2 + y^2| \to \infty$, in the solution given by (2.34) and (2.35), A_{11} and A_{12} must be set to zero. Thus (2.34) and (2.35) reduce to

$$F_1(\alpha, y) = [A_{13}(\alpha) + A_{14}(\alpha)y]\, e^{-|\alpha|y}, \tag{2.62}$$

$$G_1(\alpha, y) = [A_{23}(\alpha) + A_{24}(\alpha)y]\, e^{-|\alpha|y}. \tag{2.63}$$

Using (2.58) and (2.59) we obtain

$$\begin{bmatrix} -i\frac{|\alpha|}{\alpha} & \frac{i}{\alpha}(\kappa_1 - |\alpha|h_2) \\ 1 & h_2 \end{bmatrix} \begin{Bmatrix} A^*_{23} \\ A^*_{24} \end{Bmatrix} = \begin{bmatrix} a_1 & a_2 & -\overline{a_1} & -\overline{a_2} \\ 1 & 1 & 1 & 1 \end{bmatrix} \begin{Bmatrix} A^*_{41} \\ A^*_{42} \\ A^*_{43} \\ A^*_{44} \end{Bmatrix}, \tag{2.64}$$

where

$$A_{23}^* = A_{23}e^{|\alpha|h_2}, \tag{2.65}$$

$$A_{24}^* = A_{24}e^{|\alpha|h_2}, \tag{2.66}$$

$$A_{41}^* = A_{41}e^{n_1h_2}, \tag{2.67}$$

$$A_{42}^* = A_{42}e^{n_2h_2}, \tag{2.68}$$

$$A_{43}^* = A_{43}e^{\overline{n_1}h_2}, \tag{2.69}$$

$$A_{44}^* = A_{44}e^{\overline{n_2}h_2}. \tag{2.70}$$

Solving for A_{23}^* and A_{24}^* from (2.64), we have

$$\begin{Bmatrix} A_{23}^* \\ A_{24}^* \end{Bmatrix} = \begin{bmatrix} 1-h_2b_1 & 1-h_2b_2 & 1-h_2\overline{b_1} & 1-h_2\overline{b_2} \\ b_1 & b_2 & \overline{b_1} & \overline{b_2} \end{bmatrix} \begin{Bmatrix} A_{41}^* \\ A_{42}^* \\ A_{43}^* \\ A_{44}^* \end{Bmatrix}, \tag{2.71}$$

where

$$b_1 = \frac{|\alpha|}{\kappa_2} - i\frac{\alpha}{\kappa_2}a_1, \tag{2.72}$$

$$b_2 = \frac{|\alpha|}{\kappa_2} - i\frac{\alpha}{\kappa_2}a_2. \tag{2.73}$$

By using the third and fourth boundary conditions (i.e. (2.60) and (2.61)) we obtain

$$\begin{bmatrix} s_1 & \overline{s_1} \\ t_1 & -\overline{t_1} \end{bmatrix} \begin{Bmatrix} A_{41}^* \\ A_{43}^* \end{Bmatrix} = \begin{bmatrix} -s_2 & -\overline{s_2} \\ -t_2 & \overline{t_2} \end{bmatrix} \begin{Bmatrix} A_{42}^* \\ A_{44}^* \end{Bmatrix}, \tag{2.74}$$

where

$$s_1 = i\lambda_2\alpha a_1 + \Lambda_2(\kappa_2+1)n_1\kappa_1 + \left(\kappa_1^2-1\right)|\alpha| \tag{2.75}$$

$$s_2 = i\lambda_2\alpha a_2 + \Lambda_2(\kappa_2+1)n_2\kappa_1 + \left(\kappa_1^2-1\right)|\alpha| \tag{2.76}$$

$$t_1 = a_1\left[\chi_2\kappa_1 n_1 + |\alpha|(\kappa_1+1)\right] + i\alpha\left[\kappa_1\chi_2 - (\kappa_1-1)\right], \tag{2.77}$$

$$t_2 = a_2\left[\chi_2\kappa_1 n_2 + |\alpha|(\kappa_1+1)\right] + i\alpha\left[\kappa_1\chi_2 - (\kappa_1-1)\right], \tag{2.78}$$

$$\lambda_2 = \kappa_1^2 + \kappa_1\left(\Lambda_2(3-\kappa_2)-2\right)+1 \tag{2.79}$$

$$\Lambda_2 = \chi_2\frac{\kappa_1-1}{\kappa_2-1} \tag{2.80}$$

$$\chi_2 = \frac{\mu_{10}}{\mu_1} \tag{2.81}$$

Solving for A_{41}^* and A_{43}^* , we obtain

$$\left\{\begin{array}{c} A_{41}^* \\ A_{43}^* \end{array}\right\} = \left[\begin{array}{cc} r_1 & \overline{r_3} \\ r_3 & \overline{r_1} \end{array}\right]\left\{\begin{array}{c} A_{42}^* \\ A_{44}^* \end{array}\right\}, \tag{2.82}$$

where

$$r_1 = \frac{1}{\Delta_2}\left(s_2\overline{t_1} + \overline{s_1}t_2\right), \tag{2.83}$$

$$r_3 = \frac{1}{\Delta_2}\left(s_2 t_1 - s_1 t_2\right), \tag{2.84}$$

$$\Delta_2 = \left|\begin{array}{cc} s_1 & \overline{s_1} \\ t_1 & -\overline{t_1} \end{array}\right| = -(s_1\overline{t_1} + \overline{s_1}t_1). \tag{2.85}$$

2.2.2 Boundary conditions

The other two boundary conditions come from the tractions along the surface. Substituting u_2 and v_2 into (2.12), we have

$$\frac{\kappa_2-1}{\mu_{20}e^{\gamma_2 y}}\sigma_{2yy}(x,y) = \frac{1}{2\pi}\int_{-\infty}^{\infty}\left[(3-\kappa_2)(i\alpha)F_2 + (\kappa_2+1)\frac{\partial G_2}{\partial y}\right]e^{i\alpha x}d\alpha. \tag{2.86}$$

Taking the inverse transform of (2.86), we obtain

$$(3-\kappa_2)(i\alpha)F_2+(\kappa_2+1)\frac{\partial G_2}{\partial y}=\frac{\kappa_2-1}{\mu_{20}e^{\gamma_2 y}}\int_{-\infty}^{\infty}\sigma_{2yy}(t,y)e^{-i\alpha t}dt \tag{2.87}$$

Defining the contact stresses on the surface as

$$\sigma_{2yy}(x,0) = \sigma(x), \tag{2.88}$$

$$\sigma_{2xy}(x,0) = \tau(x), \tag{2.89}$$

Fourier transforms of the tractions on the surface becomes

$$P(\alpha)=\int_{-\infty}^{\infty}\sigma(t)e^{-i\alpha t}dt, \tag{2.90}$$

$$Q(\alpha)=\int_{-\infty}^{\infty}\tau(t)e^{-i\alpha t}dt. \tag{2.91}$$

Therefore taking the limit of equation (2.87) as $y\to 0$ we have

$$(3-\kappa_2)(i\alpha)F_2(\alpha,y)+(\kappa_2+1)\frac{\partial G_2}{\partial y}(\alpha,y)=\frac{\kappa_2-1}{\mu_{20}e^{\gamma_2 y}}P(\alpha). \tag{2.92}$$

Substituting u_2 and v_2 into (2.13) we find

$$\sigma_{2xy}(x,y)=\mu_{20}e^{\gamma_2 y}\frac{1}{2\pi}\int_{-\infty}^{\infty}\left[\frac{\partial F_2}{\partial y}(\alpha,y)+(i\alpha)G_2(\alpha,y)\right]e^{i\alpha x}d\alpha. \tag{2.93}$$

Taking the inverse transform of (2.93) we have

$$\frac{\partial F_2}{\partial y}(\alpha,y)+(i\alpha)G_2(\alpha,y)=\frac{1}{\mu_{20}e^{\gamma_2 y}}Q(\alpha). \tag{2.94}$$

By substituting $F_2(\alpha,y)$ and $G_2(\alpha,y)$ into equations (2.92) and (2.94) we obtain

$$\begin{bmatrix} z_{11} & z_{12} & \overline{z_{11}} & \overline{z_{12}} \\ z_{21} & z_{22} & -\overline{z_{21}} & -\overline{z_{22}} \end{bmatrix}\begin{Bmatrix} A_{41} \\ A_{42} \\ A_{43} \\ A_{44} \end{Bmatrix}=\frac{1}{\mu_{20}}\begin{Bmatrix} (\kappa_2-1)P(\alpha) \\ Q(\alpha) \end{Bmatrix}. \tag{2.95}$$

Also, substituting $A_{41}$and A_{43} into (2.95) we have

$$\begin{bmatrix} r_2 & \overline{r_2} \\ r_4 & -\overline{r_4} \end{bmatrix} \begin{Bmatrix} A_{42} \\ A_{44} \end{Bmatrix} = \frac{1}{\mu_{20}} \begin{Bmatrix} (\kappa_2 - 1)\, P(\alpha) \\ Q(\alpha) \end{Bmatrix}, \tag{2.96}$$

where

$$r_2 = z_{12} + z_{11} r_1 e^{-h_2(n_1 - n_2)} + \overline{z_{11}} r_3 e^{-h_2(\overline{n_1} - n_2)}, \tag{2.97}$$

$$r_4 = z_{22} + z_{21} r_1 e^{-h_2(n_1 - n_2)} - \overline{z_{21}} r_3 e^{-h_2(\overline{n_1} - n_2)}, \tag{2.98}$$

$$z_{11} = (3 - \kappa_2)(i\alpha) a_1 + (\kappa_2 + 1) n_1, \tag{2.99}$$

$$z_{12} = (3 - \kappa_2)(i\alpha) a_2 + (\kappa_2 + 1) n_2, \tag{2.100}$$

$$z_{21} = a_1 n_1 + i\alpha, \tag{2.101}$$

$$z_{22} = a_2 n_2 + i\alpha. \tag{2.102}$$

Therefore, solving for A_{42} and A_{44} we have

$$A_{42} = -\frac{1}{\mu_{20} \Delta_3} \left[(\kappa_2 - 1) P(\alpha) \overline{r_4} + \overline{r_2} Q(\alpha) \right], \tag{2.103}$$

$$A_{44} = \frac{1}{\mu_{20} \Delta_3} \left[r_2 Q(\alpha) - (\kappa_2 - 1) P(\alpha) r_4 \right], \tag{2.104}$$

where

$$\Delta_3 = \begin{vmatrix} r_2 & \overline{r_2} \\ r_4 & -\overline{r_4} \end{vmatrix} = -(r_2 \overline{r_4} + \overline{r_2} r_4). \tag{2.105}$$

2.3 The surface displacement gradients

So far, we have found all the constants A_{ij}, $(i = 1, ..., 4, \quad j = 1, ..., 4)$ to determine $u_2(x, y)$ and $v_2(x, y)$ in the Fourier domain in (2.34),(2.35), (2.38) and (2.39). Since displacement vector is specified on the part of the boundary $y = 0$ and the traction vector is specified on the remainder, our problem is a mixed boundary value problem.

Input to the problem is the y component of the displacement gradient at the surface, $\frac{\partial}{\partial x}v_2(x,0)$ and the unknowns are the contact stresses $\sigma_{2xy}(x,0)$ and $\sigma_{2yy}(x,0)$.

Thus the displacement gradients can be found by writing the derivatives of (2.29) and (2.27) with respect to x giving

$$\lim_{y\to 0}\frac{\partial}{\partial x}v_2(x,y) = \lim_{y\to 0}\frac{1}{2\pi}\int_{-\infty}^{\infty} i\alpha G_2(\alpha,y)e^{i\alpha x}d\alpha, \tag{2.106}$$

$$\lim_{y\to 0}\frac{\partial}{\partial x}u_2(x,y) = \lim_{y\to 0}\frac{1}{2\pi}\int_{-\infty}^{\infty} i\alpha F_2(\alpha,y)e^{i\alpha x}d\alpha. \tag{2.107}$$

Substituting (2.36) and (2.37) into (2.106)and (2.107) we obtain

$$\begin{aligned}\lim_{y\to 0}2\pi\mu_{20}\frac{\partial}{\partial x}v_2(x,y) &= \int_{-\infty}^{\infty}K_{11}(x,y,t)\sigma_{2yy}(t,0)dt \\ &\quad + \int_{-\infty}^{\infty}K_{12}(x,y,t)\sigma_{2xy}(t,0)dt,\end{aligned} \tag{2.108}$$

$$\begin{aligned}\lim_{y\to 0}2\pi\mu_{20}\frac{\partial}{\partial x}u_2(x,y) &= \int_{-\infty}^{\infty}K_{21}(x,y,t)\sigma_{2xy}(t,0)dt \\ &\quad + \int_{-\infty}^{\infty}K_{22}(x,y,t)\sigma_{2yy}(t,0)dt,\end{aligned} \tag{2.109}$$

where

$$K_{11}(x,y,t) = \lim_{y\to 0}\int_{-\infty}^{\infty}h_{11}(\alpha,y)e^{-i\alpha(t-x)}d\alpha, \tag{2.110}$$

$$K_{21}(x,y,t) = \lim_{y\to 0}\int_{-\infty}^{\infty}h_{21}(\alpha,y)e^{-i\alpha(t-x)}d\alpha, \tag{2.111}$$

$$K_{12}(x,y,t) = \lim_{y\to 0}\int_{-\infty}^{\infty}h_{12}(\alpha,y)e^{-i\alpha(t-x)}d\alpha, \tag{2.112}$$

$$K_{22}(x,y,t) = \lim_{y\to 0}\int_{-\infty}^{\infty}h_{22}(\alpha,y)e^{-i\alpha(t-x)}d\alpha, \tag{2.113}$$

$$h_{11}(\alpha,y) = -\frac{i\alpha(\kappa_2-1)}{\Delta_3}\left(y_1\overline{r_4}+\overline{y_1}r_4\right), \tag{2.114}$$

$$h_{12}(\alpha,y) = \frac{i\alpha}{\Delta_3}\left(-y_1\overline{r_2}+\overline{y_1}r_2\right), \tag{2.115}$$

$$h_{21}(\alpha,y) = -\frac{i\alpha}{\Delta_3}\left(y_2\overline{r_2}+\overline{y_2}r_2\right), \tag{2.116}$$

$$h_{22}(\alpha,y) = -\frac{i\alpha(\kappa_2-1)}{\Delta_3}\left(y_2\overline{r_4}-\overline{y_2}r_4\right), \tag{2.117}$$

$$y_1(\alpha,y) = e^{n_2y}+r_1e^{-h_2(n_1-n_2)+n_1y}+r_3e^{-h_2(\overline{n_1}-n_2)+\overline{n_1}y}, \tag{2.118}$$

$$y_2(\alpha,y) = a_2e^{n_2y}+a_1r_1e^{-h_2(n_1-n_2)+n_1y}-\overline{a_1}r_3e^{-h_2(\overline{n_1}-n_2)+\overline{n_1}y}. \tag{2.119}$$

The singularities in the kernels come from the asymptotic behavior of the integrands. The asymptotic analysis has to be performed in order to extract the singularities as $\alpha\to\infty$. The details of asymptotic expansion of the kernels $K_{11}(x,y,t)$, $K_{12}(x,y,t)$, $K_{21}(x,y,t)$ and $K_{22}(x,y,t)$ are given in Appendix E. For $\alpha\to\infty$ the asymptotic behavior of $h_{11}(\alpha,y)$, $h_{12}(\alpha,y)$, $h_{21}(\alpha,y)$ and $h_{22}(\alpha,y)$ are as follows:

$$h_{11}(\alpha,y) = i\frac{\alpha}{|\alpha|}e^{-|\alpha|y}\left(-\frac{\kappa_2+1}{4}+\frac{(5+\kappa_2)}{8}\frac{\gamma_2}{|\alpha|}+\mathcal{O}\left(\frac{1}{\alpha^2}\right)\right), \tag{2.120}$$

$$h_{12}(\alpha,y) = e^{-|\alpha|y}\left(-\frac{\kappa_2-1}{4}+\frac{(\kappa_2+1)}{8}\frac{\gamma_2}{|\alpha|}+\mathcal{O}\left(\frac{1}{\alpha^2}\right)\right), \tag{2.121}$$

$$h_{21}(\alpha,y) = i\frac{\alpha}{|\alpha|}e^{-|\alpha|y}\left(-\frac{\kappa_2+1}{4}+\frac{(\kappa_2+1)}{8}\frac{\gamma_2}{|\alpha|}+\mathcal{O}\left(\frac{1}{\alpha^2}\right)\right), \tag{2.122}$$

$$h_{22}(\alpha,y) = e^{-|\alpha|y}\left(\frac{\kappa_2-1}{4}-\frac{(\kappa_2+1)}{8}\frac{\gamma_2}{|\alpha|}+\mathcal{O}\left(\frac{1}{\alpha^2}\right)\right). \tag{2.123}$$

We may now write K_{11}, K_{21}, K_{12}, K_{22} as

$$K_{11}(x,y,t) = \int_{-\infty}^{+\infty}\left(h_{11}(\alpha,y)+i\frac{\kappa_2+1}{4}\frac{\alpha}{|\alpha|}e^{-|\alpha|y}\right)e^{-i\alpha(t-x)}d\alpha+K_{11\infty}, \tag{2.124}$$

$$K_{12}(x,y,t) = \int_{-\infty}^{+\infty}\left(h_{12}(\alpha,y)+\frac{\kappa_2-1}{4}e^{-|\alpha|y}\right)e^{-i\alpha(t-x)}d\alpha+K_{12\infty}, \tag{2.125}$$

$$K_{21}(x,y,t) = \int_{-\infty}^{+\infty}\left(h_{21}(\alpha,y)+i\frac{\kappa_2+1}{4}\frac{\alpha}{|\alpha|}e^{-|\alpha|y}\right)e^{-i\alpha(t-x)}d\alpha+K_{21\infty}, \tag{2.126}$$

$$K_{22}(x,y,t) = \int_{-\infty}^{+\infty}\left(h_{22}(\alpha,y)-\frac{\kappa_2-1}{4}e^{-|\alpha|y}\right)e^{-i\alpha(t-x)}d\alpha+K_{22\infty}, \tag{2.127}$$

where

$$K_{11\infty}(x,y,t) = -\frac{\kappa_2+1}{4}\int_{-\infty}^{\infty} i\frac{\alpha}{|\alpha|}e^{-|\alpha|y}e^{-i\alpha(t-x)}d\alpha, \tag{2.128}$$

$$K_{12\infty}(x,y,t) = -\frac{\kappa_2-1}{4}\int_{-\infty}^{\infty} e^{-|\alpha|y}e^{-i\alpha(t-x)}d\alpha, \tag{2.129}$$

$$K_{21\infty}(x,y,t) = -\frac{\kappa_2+1}{4}\int_{-\infty}^{\infty} i\frac{\alpha}{|\alpha|}e^{-|\alpha|y}e^{-i\alpha(t-x)}d\alpha, \tag{2.130}$$

$$K_{22\infty}(x,y,t) = +\frac{\kappa_2-1}{4}\int_{-\infty}^{\infty} e^{-|\alpha|y}e^{-i\alpha(t-x)}d\alpha. \tag{2.131}$$

The first integrals in (2.124)- (2.127) are bounded and, when substituted into (2.108) and (2.109) limit can be put under the integral sign. Using the following relations

$$\int_{-\infty}^{+\infty} i\frac{|\alpha|}{\alpha}e^{-|\alpha|y}e^{-i\alpha(t-x)}d\alpha = \frac{2(t-x)}{(t-x)^2+y^2}, \qquad y>0 \tag{2.132}$$

$$\int_{-\infty}^{+\infty} e^{-|\alpha|y}e^{-i\alpha(t-x)}d\alpha = \frac{2y}{(t-x)^2+y^2}, \qquad y>0 \tag{2.133}$$

it may easily be shown that

$$K_{11\infty}(x,y,t) = -\frac{\kappa_2+1}{2}\frac{t-x}{(t-x)^2+y^2}, \tag{2.134}$$

$$K_{12\infty}(x,y,t) = -\frac{\kappa_2-1}{2}\frac{y}{(t-x)^2+y^2}, \tag{2.135}$$

$$K_{21\infty}(x,y,t) = -\frac{\kappa_2+1}{2}\frac{t-x}{(t-x)^2+y^2}, \tag{2.136}$$

$$K_{22\infty}(x,y,t) = +\frac{\kappa_2-1}{2}\frac{y}{(t-x)^2+y^2}. \tag{2.137}$$

By taking the limit as $y \to 0$ in equations (2.134)-(2.137) and noting that

$$\lim_{y\to 0}\frac{y}{(t-x)^2+y^2} = \pi\delta(t-x), \tag{2.138}$$

we obtain

$$\lim_{y\to 0}K_{11\infty}(x,y,t) = -\frac{\kappa_2+1}{2}\frac{1}{t-x}, \tag{2.139}$$

$$\lim_{y\to 0}K_{12\infty}(x,y,t) = -\frac{\kappa_2-1}{2}\pi\delta(t-x), \tag{2.140}$$

$$\lim_{y\to 0}K_{21\infty}(x,y,t) = -\frac{\kappa_2+1}{2}\frac{1}{t-x}, \tag{2.141}$$

$$\lim_{y\to 0}K_{22\infty}(x,y,t) = +\frac{\kappa_2-1}{2}\pi\delta(t-x). \tag{2.142}$$

Therefore equations (2.108) and (2.109) becomes

$$\begin{aligned} 2\pi\mu_{20}\frac{\partial}{\partial x}v_2(x,y) &= \int_{-\infty}^{\infty}\left[K_{11}(x,y,t)-K_{11\infty}(x,y,t)\right]\sigma_{2yy}(t,y)dt \\ &+\int_{-\infty}^{\infty}\left[K_{12}(x,y,t)-K_{12\infty}(x,y,t)\right]\sigma_{2xy}(t,y)dt \\ &+\int_{-\infty}^{\infty}K_{11\infty}(x,y,t)\sigma_{2yy}(t,y)dt \\ &+\int_{-\infty}^{\infty}K_{12\infty}(x,y,t)\sigma_{2xy}(t,y)dt, \end{aligned} \tag{2.143}$$

$$\begin{aligned} 2\pi\mu_{20}\frac{\partial}{\partial x}u_2(x,y) &= \int_{-\infty}^{\infty}\left[K_{21}(x,y,t)-K_{21\infty}(x,y,t)\right]\sigma_{2xy}(t,y)dt \\ &+\int_{-\infty}^{\infty}\left[K_{22}(x,y,t)-K_{22\infty}(x,y,t)\right]\sigma_{2yy}(t,y)dt \\ &+\int_{-\infty}^{\infty}K_{21\infty}(x,y,t)\sigma_{2xy}(t,y)dt \\ &+\int_{-\infty}^{\infty}K_{22\infty}(x,y,t)\sigma_{2yy}(t,y)dt. \end{aligned} \tag{2.144}$$

Multiplying (2.143) and (2.144) by $\dfrac{2}{\pi\,(\kappa_2+1)}$ and taking the limit as $y \to 0$.

$$\begin{aligned} \frac{4\mu_{20}}{\kappa_2+1}\frac{\partial}{\partial x}v_2(x,0) &= \frac{2}{\pi(\kappa_2+1)}\int_{-\infty}^{\infty}\sigma_{2yy}(t,0)I_{11}(t,x)dt \\ &+\frac{2}{\pi(\kappa_2+1)}\int_{-\infty}^{\infty}\sigma_{xy}(t,0)I_{12}(t,x)dt \\ &-\frac{1}{\pi}\int_{-\infty}^{\infty}\frac{\sigma_{2yy}(t,0)}{t-x}dt-\frac{\kappa_2-1}{\kappa_2+1}\sigma_{2xy}(x,0), \end{aligned} \tag{2.145}$$

$$\begin{aligned} \frac{4\mu_{20}}{\kappa_2+1}\frac{\partial}{\partial x}u_2(x,0) &= \frac{2}{\pi(\kappa_2+1)}\int_{-\infty}^{\infty}\sigma_{2xy}(t,0)I_{21}(t,x)dt \\ &+\frac{2}{\pi(\kappa_2+1)}\int_{-\infty}^{\infty}\sigma_{yy}(t,0)I_{22}(t,x)dt \\ &-\frac{1}{\pi}\int_{-\infty}^{\infty}\frac{\sigma_{2xy}(t,0)dt}{t-x}+\frac{\kappa_2-1}{\kappa_2+1}\sigma_{2yy}(x,0), \end{aligned} \tag{2.146}$$

where

$$I_{11}(t,x) = \int_{-\infty}^{\infty} \left(h_{11}(\alpha,0) + i\frac{\kappa_2+1}{4}\frac{\alpha}{|\alpha|} \right) e^{-i\alpha(t-x)} d\alpha, \quad (2.147)$$

$$I_{12}(t,x) = \int_{-\infty}^{\infty} \left(h_{12}(\alpha,0) + \frac{\kappa_2-1}{4} \right) e^{-i\alpha(t-x)} d\alpha, \quad (2.148)$$

$$I_{21}(t,x) = \int_{-\infty}^{+\infty} \left(h_{21}(\alpha,0) + i\frac{\kappa_2+1}{4}\frac{\alpha}{|\alpha|} \right) e^{-i\alpha(t-x)} d\alpha, \quad (2.149)$$

$$I_{22}(t,x) = \int_{-\infty}^{+\infty} \left(h_{22}(\alpha,0) - \frac{\kappa_2-1}{4} \right) e^{-i\alpha(t-x)} d\alpha. \quad (2.150)$$

Further refinements can be made by analyzing the kernels $I_{11}(t,x)$,$I_{21}(t,x)$,$I_{12}(t,x)$ and $I_{22}(t,x)$ in equation (2.145) and (2.146). Observing that

$$I_{11} = 2\int_0^{\infty} \Re\left[i\Phi_{11}(\alpha) e^{-i\alpha(t-x)} \right] d\alpha = 2\int_0^{\infty} \Phi_{11}(\alpha) \sin\alpha(t-x) d\alpha, \quad (2.151)$$

$$I_{12} = 2\int_0^{\infty} \Re\left[\Phi_{12}(\alpha) e^{-i\alpha(t-x)} \right] d\alpha = 2\int_0^{\infty} \Phi_{12}(\alpha) \cos\alpha(t-x) d\alpha, \quad (2.152)$$

$$I_{21} = 2\int_0^{\infty} \Re\left[i\Phi_{21}(\alpha) e^{-i\alpha(t-x)} \right] d\alpha = 2\int_0^{\infty} \Phi_{21}(\alpha) \sin\alpha(t-x) d\alpha, \quad (2.153)$$

$$I_{22} = 2\int_0^{\infty} \Re\left[\Phi_{22}(\alpha) e^{-i\alpha(t-x)} \right] d\alpha = 2\int_0^{\infty} \Phi_{22}(\alpha) \cos\alpha(t-x) d\alpha, \quad (2.154)$$

where

$$\Phi_{11}(\alpha) = -\frac{\alpha(\kappa_2-1)}{\Delta_3}\left(y_1\overline{r_4} + \overline{y_1}r_4 \right) + \frac{\kappa_2+1}{4}, \quad (2.155)$$

$$\Phi_{12}(\alpha) = \frac{i\alpha}{\Delta_3}\left(-y_1\overline{r_2} + \overline{y_1}r_2 \right) + \frac{\kappa_2-1}{4}, \quad (2.156)$$

$$\Phi_{21}(\alpha) = -\frac{\alpha}{\Delta_3}\left(y_2\overline{r_2} + \overline{y_2}r_2 \right) + \frac{\kappa_2+1}{4}, \quad (2.157)$$

$$\Phi_{22}(\alpha) = -\frac{i\alpha(\kappa_2-1)}{\Delta_3}\left(y_2\overline{r_4} - \overline{y_2}r_4 \right) - \frac{\kappa_2-1}{4}, \quad (2.158)$$

we can write (2.145) and (2.146) as;

$$-\omega_2\sigma_{2xy}(x,0) - \frac{1}{\pi}\int_{-\infty}^{\infty}\left[\frac{1}{t-x} + k_{11}(t,x)\right]\sigma_{2yy}(t,0)dt$$
$$-\frac{1}{\pi}\int_{-\infty}^{\infty}\sigma_{2xy}(t,0)k_{12}(t,x)dt = f_2(x), \quad (2.159)$$

$$\omega_2\sigma_{2yy}(x,0) - \frac{1}{\pi}\int_{-\infty}^{\infty}\left[\frac{1}{t-x} + k_{21}(t,x)\right]\sigma_{2xy}(t,0)dt$$
$$-\frac{1}{\pi}\int_{-\infty}^{\infty}\sigma_{2yy}(t,0)k_{22}(t,x)dt = g_2(x), \quad (2.160)$$

where

$$\omega_2 = \frac{\kappa_2 - 1}{\kappa_2 + 1}, \quad (2.161)$$

$$f_2(x) = \lambda_2\frac{\partial}{\partial x}v_2(x,0), \quad (2.162)$$

$$g_2(x) = \lambda_2\frac{\partial}{\partial x}u_2(x,0), \quad (2.163)$$

$$\lambda_2 = \frac{4\mu_{20}}{\kappa_2 + 1}, \quad (2.164)$$

$$k_{11}(t,x) = -\frac{4}{\kappa_2 + 1}\int_0^{\infty}\Phi_{11}(\alpha)\sin\alpha(t-x)d\alpha, \quad (2.165)$$

$$k_{12}(t,x) = -\frac{4}{\kappa_2 + 1}\int_0^{\infty}\Phi_{12}(\alpha)\cos\alpha(t-x)d\alpha, \quad (2.166)$$

$$k_{21}(t,x) = -\frac{4}{\kappa_2 + 1}\int_0^{\infty}\Phi_{21}(\alpha)\sin\alpha(t-x)d\alpha, \quad (2.167)$$

$$k_{22}(t,x) = -\frac{4}{\kappa_2 + 1}\int_0^{\infty}\Phi_{22}(\alpha)\cos\alpha(t-x)d\alpha. \quad (2.168)$$

Chapter 3

Formulation of the lower half plane

3.1 Solution of Differential Equations

Consider the plane elasticity problem shown in Figure 3.1. The medium (4) is a homogeneous substrate and medium (3) is the FGM coating with a thickness h_3. The elastic constants of the homogeneous substrate is represented by μ_4 and κ_4. The non-homogeneity of the FGM coating is assumed to be such that its shear modulus, μ_3 is approximated by

$$\mu_3(y) = \mu_{30} e^{\gamma_3 y}, \qquad -h_3 < y < 0. \tag{3.1}$$

Thus

$$\mu_{40} = \mu_{30} e^{-\gamma_3 h_3}, \tag{3.2}$$

where the non-homogeneity parameter is

$$\gamma_3 h_3 = -\ln \Gamma_3, \tag{3.3}$$

$$\Gamma_3 = \frac{\mu_{40}}{\mu_{30}}. \tag{3.4}$$

We define another parameter, χ_3

$$\chi_3 = \frac{\mu_{40}}{\mu_4}$$

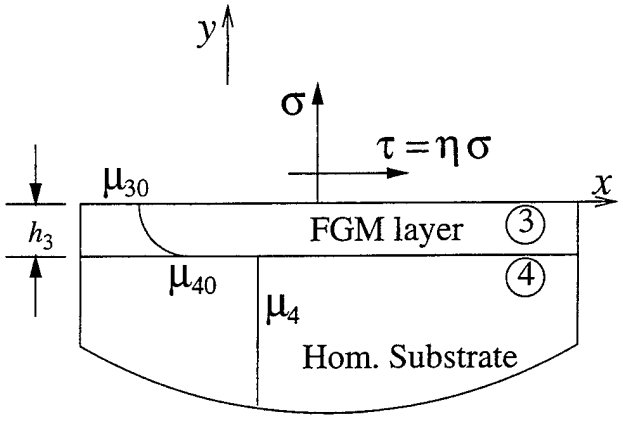

Figure 3.1: Geometry of the problem for the lower half plane

For the plane contact problem under consideration the Hooke's law can be written as

$$\sigma_{3xx}(x,y) = \frac{\mu_{30}e^{\gamma_3 y}}{\kappa_3 - 1}\left[(\kappa_3+1)\frac{\partial u_3}{\partial x} + (3-\kappa_3)\frac{\partial v_3}{\partial y}\right], \tag{3.5}$$

$$\sigma_{3yy}(x,y) = \frac{\mu_{30}e^{\gamma_3 y}}{\kappa_3 - 1}\left[(3-\kappa_3)\frac{\partial u_3}{\partial x} + (\kappa_3+1)\frac{\partial v_3}{\partial y}\right], -h_3 < y < 0 \tag{3.6}$$

$$\sigma_{3xy}(x,y) = \mu_{30}e^{\gamma_3 y}\left[\frac{\partial u_3}{\partial y} + \frac{\partial v_3}{\partial x}\right], \tag{3.7}$$

$$\sigma_{4xx}(x,y) = \frac{\mu_4}{\kappa_4 - 1}\left[(\kappa_4+1)\frac{\partial u_4}{\partial x} + (3-\kappa_4)\frac{\partial v_4}{\partial y}\right], \tag{3.8}$$

$$\sigma_{4yy}(x,y) = \frac{\mu_4}{\kappa_4 - 1}\left[(3-\kappa_4)\frac{\partial u_4}{\partial x} + (\kappa_4+1)\frac{\partial v_4}{\partial y}\right], -\infty < y < -h_3 \tag{3.9}$$

$$\sigma_{4xy}(x,y) = \mu_4\left[\frac{\partial u_4}{\partial y} + \frac{\partial v_4}{\partial x}\right], \tag{3.10}$$

where $\kappa_3 = 3 - 4\nu_3$ for plane strain and $\kappa_3 = (3-\nu_3)/(1+\nu_3)$ for the generalized plane stress conditions. The governing equations are the equilibrium equations and

in the absence of body forces, they can be written as

$$\frac{\partial \sigma_{4xx}}{\partial x} + \frac{\partial \sigma_{4xy}}{\partial y} = 0, \tag{3.11}$$

$$\frac{\partial \sigma_{4xy}}{\partial x} + \frac{\partial \sigma_{4yy}}{\partial y} = 0, \tag{3.12}$$

$$\frac{\partial \sigma_{3xx}}{\partial x} + \frac{\partial \sigma_{3xy}}{\partial y} = 0, \tag{3.13}$$

$$\frac{\partial \sigma_{3xy}}{\partial x} + \frac{\partial \sigma_{3yy}}{\partial y} = 0. \tag{3.14}$$

Substituting stresses found from equations (3.8)-(3.7) into equations of equilibrium (3.11)-(3.14), we obtain the Navier's equations as follows

$$\begin{aligned}(\kappa_3+1)\frac{\partial^2 v_3}{\partial y^2} + (\kappa_3-1)\frac{\partial^2 v_3}{\partial x^2} + 2\frac{\partial^2 u_3}{\partial x \partial y} \\ +\gamma_3(3-\kappa_3)\frac{\partial u_3}{\partial x} + \gamma_3(\kappa_3+1)\frac{\partial v_3}{\partial y} &= 0,\end{aligned} \tag{3.15}$$

$$\begin{aligned}(\kappa_3+1)\frac{\partial^2 u_3}{\partial x^2} + (\kappa_3-1)\frac{\partial^2 u_3}{\partial y^2} + 2\frac{\partial^2 v_3}{\partial x \partial y} \\ +\gamma_3(\kappa_3-1)\frac{\partial u_3}{\partial y} + \gamma_3(\kappa_3-1)\frac{\partial v_3}{\partial x} &= 0,\end{aligned} \tag{3.16}$$

$$(\kappa_4+1)\frac{\partial^2 u_4}{\partial x^2} + (\kappa_4-1)\frac{\partial^2 u_4}{\partial y^2} + 2\frac{\partial^2 v_4}{\partial x \partial y} = 0, \tag{3.17}$$

$$(\kappa_4+1)\frac{\partial^2 v_4}{\partial y^2} + (\kappa_4-1)\frac{\partial^2 v_4}{\partial x^2} + 2\frac{\partial^2 u_4}{\partial x \partial y} = 0. \tag{3.18}$$

To solve the Navier's equations we define the Fourier transforms of the four displacement components, $u_3(x,y)$, $v_3(x,y)$, $u_4(x,y)$, and $v_4(x,y)$ as

$$F_3(\alpha, y) = \int_{-\infty}^{\infty} u_3(x,y)e^{-i\alpha x}dx, \tag{3.19}$$

$$F_4(\alpha, y) = \int_{-\infty}^{\infty} u_4(x,y)e^{-i\alpha x}dx, \tag{3.20}$$

$$G_3(\alpha, y) = \int_{-\infty}^{\infty} v_3(x,y)e^{-i\alpha x}dx, \tag{3.21}$$

$$G_4(\alpha, y) = \int_{-\infty}^{\infty} v_4(x,y)e^{-i\alpha x}dx. \tag{3.22}$$

The functions $u_3(x,y)$, $u_4(x,y)$ and $v_3(x,y)$, $v_4(x,y)$ are given by the following inverse transforms;

$$u_3(x,y) = \frac{1}{2\pi}\int_{-\infty}^{\infty} F_3(\alpha,y)e^{i\alpha x}d\alpha, \tag{3.23}$$

$$u_4(x,y) = \frac{1}{2\pi}\int_{-\infty}^{\infty} F_4(\alpha,y)e^{i\alpha x}d\alpha, \tag{3.24}$$

$$v_3(x,y) = \frac{1}{2\pi}\int_{-\infty}^{\infty} G_3(\alpha,y)e^{i\alpha x}d\alpha, \tag{3.25}$$

$$v_4(x,y) = \frac{1}{2\pi}\int_{-\infty}^{\infty} G_4(\alpha,y)e^{i\alpha x}d\alpha. \tag{3.26}$$

Substituting (3.23)-(3.26) into (3.17)-(3.16) yields the following system of differential equations with constant coefficients:

$$\begin{aligned}(\kappa_3-1)\frac{d^2F_3}{dy^2}+\gamma_3(\kappa_3-1)\frac{dF_3}{dy}-(\kappa_3+1)\alpha^2F_3 & \\ +2i\alpha\frac{dG_3}{dy}+i\alpha\gamma_3(\kappa_3-1)G_3 &= 0,\end{aligned} \tag{3.27}$$

$$\begin{aligned}(\kappa_3+1)\frac{d^2G_3}{dy^2}+\gamma_3(\kappa_3+1)\frac{dG_3}{dy}-(\kappa_3-1)\alpha^2G_3 & \\ +2i\alpha\frac{dF_3}{dy}+i\alpha\gamma_3(3-\kappa_3)F_3 &= 0,\end{aligned} \tag{3.28}$$

$$(\kappa_4-1)\frac{d^2F_4}{dy^2}-(\kappa_4+1)\alpha^2F_4+2i\alpha\frac{dG_4}{dy} = 0, \tag{3.29}$$

$$(\kappa_4+1)\frac{d^2G_4}{dy^2}-(\kappa_4-1)\alpha^2G_4+2i\alpha\frac{dF_4}{dy} = 0. \tag{3.30}$$

We can express the solution of (3.29) and (3.30) as

$$F_4(\alpha,y) = [A_{75}(\alpha)+A_{76}(\alpha)y]\,e^{|\alpha|y}+[A_{77}(\alpha)+A_{78}(\alpha)y]\,e^{-|\alpha|y}, \tag{3.31}$$

$$G_4(\alpha,y) = [A_{85}(\alpha)+A_{86}(\alpha)y]\,e^{|\alpha|y}+[A_{87}(\alpha)+A_{88}(\alpha)y]\,e^{-|\alpha|y}. \tag{3.32}$$

Assuming a solution of the form

$$F_3(\alpha,y) = A_5(\alpha)e^{ny}, \tag{3.33}$$

$$G_3(\alpha,y) = A_6(\alpha)e^{ny}, \tag{3.34}$$

we obtain the solution of (3.27) and (3.28) as

$$F_3(\alpha, y) = \sum_{j=5}^{8} A_{5j}(\alpha) e^{n_j y}, \tag{3.35}$$

$$G_3(\alpha, y) = \sum_{j=5}^{8} A_{6j}(\alpha) e^{n_j y}, \tag{3.36}$$

where $n_j, (j = 5, \ldots, 8)$ satisfies the following characteristic equation

$$(n_j^2 - \alpha^2 + \gamma_3 n_j)^2 + \delta_3^2 |\alpha|^2 |\gamma_3|^2 = 0, \tag{3.37}$$

with

$$n_j^2 + \gamma_3 n_j = |\alpha|^2 + i\,|\alpha|\,\delta_3\,|\gamma_3|\,, \qquad j = 5, 6 \tag{3.38}$$

$$n_j^2 - \gamma_3 n_j = |\alpha|^2 - i\,|\alpha|\,\delta_3\,|\gamma_3|\,, \qquad j = 7, 8 \tag{3.39}$$

$$\delta_3^2 = \frac{3 - \kappa_3}{\kappa_3 + 1}. \tag{3.40}$$

The roots of the characteristic equation are found to be

$$n_5 = \frac{1}{2}\left(-\gamma_3 + \sqrt{\gamma_3^2 + 4(\alpha^2 + i|\alpha||\gamma_3|\delta_3)}\right), \tag{3.41}$$

$$n_6 = \frac{1}{2}\left(-\gamma_3 - \sqrt{\gamma_3^2 + 4(\alpha^2 + i|\alpha||\gamma_3|\delta_3)}\right), \tag{3.42}$$

$$n_7 = \frac{1}{2}\left(-\gamma_3 + \sqrt{\gamma_3^2 + 4(\alpha^2 - i|\alpha||\gamma_3|\delta_3)}\right), \tag{3.43}$$

$$n_8 = \frac{1}{2}\left(-\gamma_3 - \sqrt{\gamma_3^2 + 4(\alpha^2 - i|\alpha||\gamma_3|\delta_3)}\right). \tag{3.44}$$

The functions $A_{5j}(\alpha)$, $A_{6j}(\alpha)$, $A_{7j}(\alpha)$ and $A_{8j}(\alpha)$ $(j = 5 \ldots 8)$ are unknown functions and are not independent. The relationship between them can be written as

$$A_{75}(\alpha) = i\left[\frac{|\alpha|}{\alpha} A_{85}(\alpha) + \frac{\kappa_4}{\alpha} A_{86}(\alpha)\right], \tag{3.45}$$

$$A_{76}(\alpha) = i\frac{|\alpha|}{\alpha} A_{86}(\alpha), \tag{3.46}$$

$$A_{77}(\alpha) = i\left[-\frac{|\alpha|}{\alpha} A_{87}(\alpha) + \frac{\kappa_4}{\alpha} A_{88}(\alpha)\right], \tag{3.47}$$

$$A_{78}(\alpha) = -i\frac{|\alpha|}{\alpha} A_{88}(\alpha), \tag{3.48}$$

$$A_{5j}(\alpha) = a_j(\alpha)A_{6j}(\alpha), \qquad j = 5,6 \tag{3.49}$$

$$A_{5j}(\alpha) = -\overline{a}_{j-2}(\alpha)A_{6j}(\alpha), \qquad j = 7,8 \tag{3.50}$$

where

$$a_j(\alpha) = -\frac{(\kappa_3+1)\left[n_j^2+\gamma_3 n_j\right]-(\kappa_3-1)\,\alpha^2}{i\alpha\left[2n_j+\gamma_3\,(3-\kappa_3)\right]}, \qquad j = 5,...,8. \tag{3.51}$$

Using equations (3.38) and (3.39), (3.51) becomes

$$a_j(\alpha) = \frac{1}{\alpha}\frac{2i\alpha^2-|\alpha|(\kappa_3+1)\delta_3\gamma_3}{2n_j+\gamma_3(3-\kappa_3)}, \qquad j = 5,6 \tag{3.52}$$

$$a_j(\alpha) = \frac{1}{\alpha}\frac{2i\alpha^2+|\alpha|(\kappa_3+1)\delta_3\gamma_3}{2n_j+\gamma_3(3-\kappa_3)}, \qquad j = 7,8 \tag{3.53}$$

$$a_j(\alpha) = -\overline{a}_{j-2}(\alpha), \qquad j = 7,8 \tag{3.54}$$

3.2 Boundary and Continuity Conditions

3.2.1 Continuity conditions along the interface

The unknowns A_{ij}, $(i = 5,...,8, \quad j = 5,...,8)$ are obtained from the following displacement and stress continuity conditions along the interface:

$$u_3(x,-h_3) = u_4(x,-h_3), \tag{3.55}$$

$$v_3(x,-h_3) = v_4(x,-h_3), \tag{3.56}$$

$$\sigma_{3yy}(x,-h_3) = \sigma_{4yy}(x,-h_3), \tag{3.57}$$

$$\sigma_{3xy}(x,-h) = \sigma_{4xy}(x,-h_3). \tag{3.58}$$

Since both σ_{4yy} and σ_{4xy} vanish as $|x^2+y^2| \to -\infty$, in the solution given by (3.31) and (3.32), A_{77} , A_{78}, A_{87} and A_{88} must be set to zero. Thus (3.31) and (3.32) reduce to

$$F_4(\alpha,y) = \left[A_{75}(\alpha)+A_{76}(\alpha)y\right]e^{|\alpha|y}, \tag{3.59}$$

$$G_4(\alpha,y) = \left[A_{85}(\alpha)+A_{86}(\alpha)y\right]e^{|\alpha|y}. \tag{3.60}$$

Using (3.55) and (3.56) we obtain

$$\begin{bmatrix} i\frac{|\alpha|}{\alpha} & \frac{i}{\alpha}(\kappa_4 - |\alpha|h_3) \\ 1 & -h_3 \end{bmatrix} \begin{Bmatrix} A^*_{85} \\ A^*_{86} \end{Bmatrix} = \begin{bmatrix} a_5 & a_6 & -\overline{a_5} & -\overline{a_6} \\ 1 & 1 & 1 & 1 \end{bmatrix} \begin{Bmatrix} A^*_{65} \\ A^*_{66} \\ A^*_{67} \\ A^*_{68} \end{Bmatrix}, \tag{3.61}$$

where

$$A^*_{85} = A_{85}e^{-|\alpha|h_3}, \tag{3.62}$$

$$A^*_{86} = A_{86}e^{-|\alpha|h_3}, \tag{3.63}$$

$$A^*_{65} = A_{65}e^{-n_5h_3}, \tag{3.64}$$

$$A^*_{66} = A_{66}e^{-n_6h_3}, \tag{3.65}$$

$$A^*_{67} = A_{67}e^{-\overline{n_5}h_3}, \tag{3.66}$$

$$A^*_{68} = A_{68}e^{-\overline{n_6}h_3}. \tag{3.67}$$

Solving for A^*_{85} and A^*_{86}, we obtain

$$\begin{Bmatrix} A^*_{85} \\ A^*_{86} \end{Bmatrix} = \begin{bmatrix} 1+h_3b_5 & 1+h_3b_6 & 1+h_3\overline{b_5} & 1+h_3\overline{b_6} \\ b_5 & b_6 & \overline{b_5} & \overline{b_6} \end{bmatrix} \begin{Bmatrix} A^*_{65} \\ A^*_{66} \\ A^*_{67} \\ A^*_{68} \end{Bmatrix}, \tag{3.68}$$

where

$$b_5 = -\frac{|\alpha|}{\kappa_4} - i\frac{\alpha}{\kappa_4}a_5, \tag{3.69}$$

$$b_6 = -\frac{|\alpha|}{\kappa_4} - i\frac{\alpha}{\kappa_4}a_6, \tag{3.70}$$

Using the third and fourth continuity conditions (i.e. (3.57) and (3.58)) we obtain

$$\begin{bmatrix} s_6 & \overline{s_6} \\ t_6 & -\overline{t_6} \end{bmatrix} \begin{Bmatrix} A^*_{66} \\ A^*_{68} \end{Bmatrix} = \begin{bmatrix} -s_5 & -\overline{s_5} \\ -t_5 & \overline{t_5} \end{bmatrix} \begin{Bmatrix} A^*_{65} \\ A^*_{67} \end{Bmatrix}, \tag{3.71}$$

where

$$s_5 = i\lambda_3\alpha a_5 + \Lambda_3(\kappa_3+1)n_5\kappa_4 - (\kappa_4^2-1)|\alpha| \quad (3.72)$$

$$s_6 = i\lambda_3\alpha a_6 + \Lambda_3(\kappa_3+1)n_6\kappa_4 - (\kappa_4^2-1)|\alpha| \quad (3.73)$$

$$t_5 = a_5[\chi_3\kappa_4 n_5 - |\alpha|(\kappa_4+1)] + i\alpha[\kappa_4\chi_3 - (\kappa_4-1)], \quad (3.74)$$

$$t_6 = a_6[\chi_3\kappa_4 n_6 - |\alpha|(\kappa_4+1)] + i\alpha[\kappa_4\chi_3 - (\kappa_4-1)], \quad (3.75)$$

$$\lambda_3 = \kappa_4^2 + \kappa_4(\Lambda_3(3-\kappa_3)-2)+1 \quad (3.76)$$

$$\Lambda_3 = \chi_3\frac{\kappa_4-1}{\kappa_3-1} \quad (3.77)$$

$$\chi_3 = \frac{\mu_{40}}{\mu_4} \quad (3.78)$$

Solving for A_{66}^* and A_{68}^* we obtain

$$\begin{Bmatrix} A_{66}^* \\ A_{68}^* \end{Bmatrix} = \begin{bmatrix} r_5 & \overline{r_7} \\ r_7 & \overline{r_5} \end{bmatrix} \begin{Bmatrix} A_{65}^* \\ A_{67}^* \end{Bmatrix}, \quad (3.79)$$

where

$$r_5 = \frac{1}{\Delta_4}\left(s_5\overline{t_6} + \overline{s_6}t_5\right), \quad (3.80)$$

$$r_7 = \frac{1}{\Delta_4}\left(s_5 t_6 - s_6 t_5\right), \quad (3.81)$$

$$\Delta_4 = -\left(s_6\overline{t_6} + \overline{s_6}t_6\right). \quad (3.82)$$

3.2.2 Boundary conditions

The two boundary conditions for the unknowns A_{65} and A_{67} come from the tractions along the surface. Substituting u_3 and v_3 into (3.6) and (3.7) we have

$$\sigma_{3yy}(x,y) = \frac{\mu_{30}e^{\gamma_3 y}}{\kappa_3-1}\frac{1}{2\pi}\int_{-\infty}^{\infty}\left[(3-\kappa_3)(i\alpha)F_3 + (\kappa_3+1)\frac{\partial G_3}{\partial y}\right]e^{i\alpha x}d\alpha, \quad (3.83)$$

$$\sigma_{3xy}(x,y) = \mu_{30}e^{\gamma_3 y}\frac{1}{2\pi}\int_{-\infty}^{\infty}\left[\frac{\partial F_3}{\partial y} + (i\alpha)G_3\right]e^{i\alpha x}d\alpha. \quad (3.84)$$

Taking the inverse Fourier transform we have

$$(3-\kappa_3)(i\alpha)F_3+(\kappa_3+1)\frac{\partial G_3}{\partial y} = \frac{\kappa_3-1}{\mu_{30}e^{\gamma_3 y}}\int_{-\infty}^{\infty}\sigma_{3yy}(t,y)e^{-i\alpha t}dt, \quad (3.85)$$

$$\frac{\partial F_3}{\partial y}+(i\alpha)G_3 = \frac{1}{\mu_{30}e^{\gamma_3 y}}\int_{-\infty}^{\infty}\sigma_{3xy}(t,y)e^{-i\alpha t}dt. \quad (3.86)$$

Defining the contact stresses on the surface as

$$\sigma_{3yy}(x,0) = \sigma(x), \quad (3.87)$$

$$\sigma_{3xy}(x,0) = \tau(x), \quad (3.88)$$

Fourier transforms of the tractions on the surface becomes

$$P(\alpha)=\int_{-\infty}^{\infty}\sigma(t)e^{-i\alpha t}dt, \quad (3.89)$$

$$Q(\alpha)=\int_{-\infty}^{\infty}\tau(t)e^{-i\alpha t}dt. \quad (3.90)$$

Therefore taking the limit of equations (3.85) and (3.86) as $y \to 0$ we have

$$(3-\kappa_3)(i\alpha)F_3+(\kappa_3+1)\frac{\partial G_3}{\partial y} = \frac{\kappa_3-1}{\mu_{30}e^{\gamma_3 y}}P(\alpha), \quad (3.91)$$

$$\frac{\partial F_3}{\partial y}+(i\alpha)G_3 = \frac{1}{\mu_{30}e^{\gamma_3 y}}Q(\alpha). \quad (3.92)$$

Substituting $F_3(\alpha,y)$ and $G_3(\alpha,y)$ into equations (3.91) and (3.92) we find

$$\begin{bmatrix} z_{55} & z_{56} & \overline{z_{55}} & \overline{z_{56}} \\ z_{65} & z_{66} & -\overline{z_{65}} & -\overline{z_{66}} \end{bmatrix} \begin{Bmatrix} A_{65} \\ A_{66} \\ A_{67} \\ A_{68} \end{Bmatrix} = \frac{1}{\mu_{30}} \begin{Bmatrix} (\kappa_3-1)P(\alpha) \\ Q(\alpha) \end{Bmatrix}, \quad (3.93)$$

where

$$z_{55} = (3-\kappa_3)(i\alpha)a_5+(\kappa_3+1)n_5, \quad (3.94)$$

$$z_{56} = (3-\kappa_3)(i\alpha)a_6+(\kappa_3+1)n_6, \quad (3.95)$$

$$z_{65} = a_5 n_5 + i\alpha, \quad (3.96)$$

$$z_{66} = a_6 n_6 + i\alpha. \quad (3.97)$$

Substituting A_{66} and A_{68} into (3.93) we obtain

$$\begin{bmatrix} r_6 & \overline{r_6} \\ r_8 & -\overline{r_8} \end{bmatrix} \begin{Bmatrix} A_{65} \\ A_{67} \end{Bmatrix} = \frac{1}{\mu_{30}} \begin{Bmatrix} (\kappa_3 - 1)\, P(\alpha) \\ Q(\alpha) \end{Bmatrix}, \tag{3.98}$$

where

$$r_6 = z_{55} + z_{56} r_5 e^{-h_3(n_5 - n_6)} + \overline{z_{56}} r_7 e^{-h_3(n_5 - \overline{n_6})}, \tag{3.99}$$

$$r_8 = z_{65} + z_{66} r_5 e^{-h_3(n_5 - n_6)} - \overline{z_{66}} r_7 e^{-h_3(n_5 - \overline{n_6})}. \tag{3.100}$$

Thus, the unknowns A_{65} and A_{67} become

$$A_{65} = -\frac{1}{\mu_{30}\Delta_5} \left[(\kappa_3 - 1) P(\alpha) \overline{r_8} + \overline{r_6} Q(\alpha) \right], \tag{3.101}$$

$$A_{67} = \frac{1}{\mu_{30}\Delta_5} \left[r_6 Q(\alpha) - (\kappa_3 - 1) P(\alpha) r_8 \right], \tag{3.102}$$

where

$$\Delta_5 = \begin{vmatrix} r_6 & \overline{r_6} \\ r_8 & -\overline{r_8} \end{vmatrix} = -(r_6 \overline{r_8} + \overline{r_6} r_8). \tag{3.103}$$

3.3 The surface displacement gradients

So far, we have found all the constants A_{ij}, $(i = 5, ..., 8, \quad j = 5, ..., 8)$ to determine $u_3(x, y)$ and $v_3(x, y)$ in the Fourier domain. Since displacement vector is specified on the part of the boundary $y = 0$ and the traction vector is specified on the remainder, our problem is a mixed boundary value problem. Input to the problem is the y component of the displacement gradient at the surface $\frac{\partial}{\partial x} v_3(x, 0)$ and the unknowns are the contact stresses $\sigma_{3xy}(x, 0) = \tau(x)$ and $\sigma_{3yy}(x, 0) = \sigma(x)$. Thus writing the displacement gradients at the surface by taking the derivatives of (3.24) and (3.26) with respect to x gives

$$\lim_{y \to 0} \frac{\partial}{\partial x} v_3(x, y) = \lim_{y \to 0} \frac{1}{2\pi} \int_{-\infty}^{\infty} i\alpha G_3(\alpha, y) e^{i\alpha x} d\alpha, \tag{3.104}$$

$$\lim_{y \to 0} \frac{\partial}{\partial x} u_3(x, y) = \lim_{y \to 0} \frac{1}{2\pi} \int_{-\infty}^{\infty} i\alpha F_3(\alpha, y) e^{i\alpha x} d\alpha. \tag{3.105}$$

Substituting (3.35) and (3.36) into (3.104)and (3.105) we obtain

$$\lim_{y\to 0} 2\pi\mu_{30}\frac{\partial}{\partial x}v_3(x,y) = \int_{-\infty}^{\infty} K_{31}(x,y,t)\sigma(t)dt + \int_{-\infty}^{\infty} K_{32}(x,y,t)\tau(t)dt, \tag{3.106}$$

$$\lim_{y\to 0} 2\pi\mu_{30}\frac{\partial}{\partial x}u_3(x,y) = \int_{-\infty}^{\infty} K_{41}(x,y,t)\tau(t)dt + \int_{-\infty}^{\infty} K_{42}(x,y,t)\sigma(t)dt. \tag{3.107}$$

where

$$K_{31}(x,y,t) = \lim_{y\to 0}\int_{-\infty}^{\infty} h_{31}(\alpha,y)e^{-i\alpha(t-x)}d\alpha, \tag{3.108}$$

$$K_{32}(x,y,t) = \lim_{y\to 0}\int_{-\infty}^{\infty} h_{32}(\alpha,y)e^{-i\alpha(t-x)}d\alpha, \tag{3.109}$$

$$K_{41}(x,y,t) = \lim_{y\to 0}\int_{-\infty}^{\infty} h_{41}(\alpha,y)e^{-i\alpha(t-x)}d\alpha, \tag{3.110}$$

$$K_{42}(x,y,t) = \lim_{y\to 0}\int_{-\infty}^{\infty} h_{42}(\alpha,y)e^{-i\alpha(t-x)}d\alpha, \tag{3.111}$$

$$h_{31}(\alpha,y) = -\frac{i\alpha(\kappa_3-1)}{\Delta_5}\left(y_3\overline{r_8}+\overline{y_3}r_8\right), \tag{3.112}$$

$$h_{32}(\alpha,y) = \frac{i\alpha}{\Delta_5}\left(-y_3\overline{r_6}+\overline{y_3}r_6\right), \tag{3.113}$$

$$h_{41}(\alpha,y) = -\frac{i\alpha}{\Delta_5}\left(y_4\overline{r_6}+\overline{y_4}r_6\right), \tag{3.114}$$

$$h_{42}(\alpha,y) = -\frac{i\alpha(\kappa_3-1)}{\Delta_5}\left(y_4\overline{r_8}-\overline{y_4}r_8\right), \tag{3.115}$$

$$y_3(\alpha,y) = e^{n_5 y} + r_5 e^{-h_3(n_5-n_6)+n_6 y} + r_7 e^{-h(n_5-\overline{n_6})+\overline{n_6}y}, \tag{3.116}$$

$$y_4(\alpha,y) = a_5 e^{n_5 y} + a_6 r_5 e^{-h_3(n_5-n_6)+n_6 y} - \overline{a_6} r_7 e^{-h_3(n_5-\overline{n_6})+\overline{n_6}y}. \tag{3.117}$$

The singularities in the kernels come from the asymptotic behavior of the integrands. The asymptotic analysis has to be performed in order to extract the singularities as

$\alpha \to \infty$. The details of asymptotic expansion of the kernels $K_{31}(x,y,t)$, $K_{32}(x,y,t)$, $K_{41}(x,y,t)$ and $K_{42}(x,y,t)$ are given in Appendix E. For $\alpha \to \infty$ the asymptotic behavior of $h_{31}(\alpha,y)$, $h_{32}(\alpha,y)$, $h_{41}(\alpha,y)$ and $h_{42}(\alpha,y)$ are as follows:

$$h_{31}(\alpha,y) = i\frac{\alpha}{|\alpha|}e^{|\alpha|y}\left(\frac{\kappa_3+1}{4}+\frac{(5+\kappa_3)}{8}\frac{\gamma_3}{|\alpha|}+O\left(\frac{1}{\alpha^2}\right)\right), \tag{3.118}$$

$$h_{32}(\alpha,y) = e^{|\alpha|y}\left(-\frac{\kappa_3-1}{4}-\frac{(\kappa_3+1)}{8}\frac{\gamma_3}{|\alpha|}+O\left(\frac{1}{\alpha^2}\right)\right), \tag{3.119}$$

$$h_{41}(\alpha,y) = i\frac{\alpha}{|\alpha|}e^{|\alpha|y}\left(\frac{\kappa_3+1}{4}+\frac{(\kappa_3+1)}{8}\frac{\gamma_3}{|\alpha|}+O\left(\frac{1}{\alpha^2}\right)\right), \tag{3.120}$$

$$h_{42}(\alpha,y) = e^{|\alpha|y}\left(\frac{\kappa_3-1}{4}+\frac{(\kappa_3+1)}{8}\frac{\gamma_3}{|\alpha|}+O\left(\frac{1}{\alpha^2}\right)\right). \tag{3.121}$$

We may now write (3.106) and (3.107) as

$$\begin{aligned}\lim_{y\to 0} 2\pi\mu_{30}\frac{\partial}{\partial x}v_3(x,y) = &\lim_{y\to 0}\int_{-\infty}^{\infty}\left[K_{31}(x,y,t)-K_{31\infty}(x,y,t)\right]\sigma(t)dt\\ &+\lim_{y\to 0}\int_{-\infty}^{\infty}\left[K_{32}(x,y,t)-K_{32\infty}(x,y,t)\right]\tau(t)dt\\ &+\lim_{y\to 0}\int_{-\infty}^{\infty}K_{31\infty}(x,y,t)\sigma(t)dt\\ &+\lim_{y\to 0}\int_{-\infty}^{\infty}K_{32\infty}(x,y,t)\tau(t)dt,\end{aligned} \tag{3.122}$$

$$\begin{aligned}\lim_{y\to 0} 2\pi\mu_{30}\frac{\partial}{\partial x}u_3(x,y) = &\lim_{y\to 0}\int_{-\infty}^{\infty}\left[K_{41}(x,y,t)-K_{41\infty}(x,y,t)\right]\tau(t)dt\\ &+\lim_{y\to 0}\int_{-\infty}^{\infty}\left[K_{42}(x,y,t)-K_{42\infty}(x,y,t)\right]\sigma(t)dt\\ &+\lim_{y\to 0}\int_{-\infty}^{\infty}K_{41\infty}(x,y,t)\tau(t)dt\\ &+\lim_{y\to 0}\int_{-\infty}^{\infty}K_{42\infty}(x,y,t)\sigma(t,y)dt,\end{aligned} \tag{3.123}$$

where

$$K_{31\infty}(x,y,t) = \frac{\kappa_3+1}{4}\int_{-\infty}^{\infty} i\frac{\alpha}{|\alpha|}e^{|\alpha|y}e^{-i\alpha(t-x)}d\alpha, \tag{3.124}$$

$$K_{32\infty}(x,y,t) = -\frac{\kappa_3-1}{4}\int_{-\infty}^{\infty} e^{|\alpha|y}e^{-i\alpha(t-x)}d\alpha, \tag{3.125}$$

$$K_{41\infty}(x,y,t) = \frac{\kappa_3+1}{4}\int_{-\infty}^{\infty} i\frac{\alpha}{|\alpha|}e^{|\alpha|y}e^{-i\alpha(t-x)}d\alpha, \tag{3.126}$$

$$K_{42\infty}(x,y,t) = \frac{\kappa_3-1}{4}\int_{-\infty}^{\infty} e^{|\alpha|y}e^{-i\alpha(t-x)}d\alpha. \tag{3.127}$$

The first integrals in (3.122)- (3.123) are bounded and, therefore limit can be put under the integral sign. Using the following relations for $y<0$

$$\int_{-\infty}^{+\infty} i\frac{|\alpha|}{\alpha}e^{|\alpha|y}e^{-i\alpha(t-x)}d\alpha = \frac{2(t-x)}{(t-x)^2+y^2}, \qquad y<0,$$

$$\int_{-\infty}^{+\infty} e^{|\alpha|y}e^{-i\alpha(t-x)}d\alpha = -\frac{2y}{(t-x)^2+y^2}, \qquad y<0,$$

it may easily be shown that

$$K_{31\infty}(x,y,t) = \frac{\kappa_3+1}{2}\frac{t-x}{(t-x)^2+y^2}, \tag{3.128}$$

$$K_{32\infty}(x,y,t) = \frac{\kappa_3-1}{2}\frac{y}{(t-x)^2+y^2}, \tag{3.129}$$

$$K_{41\infty}(x,y,t) = \frac{\kappa_3+1}{2}\frac{t-x}{(t-x)^2+y^2}, \tag{3.130}$$

$$K_{42\infty}(x,y,t) = -\frac{\kappa_3-1}{2}\frac{y}{(t-x)^2+y^2}. \tag{3.131}$$

Taking the limit as $y\to 0^-$ in equations (3.122)-(3.123) and noting that

$$\lim_{y\to 0^-}\frac{t-x}{(t-x)^2+y^2} = \frac{1}{t-x}, \tag{3.132}$$

$$\lim_{y\to 0^-}\frac{y}{(t-x)^2+y^2} = -\pi\delta(t-x), \tag{3.133}$$

we find

$$\lim_{y\to 0} K_{31\infty}(x,y,t) = +\frac{\kappa_3+1}{2}\frac{1}{t-x}, \tag{3.134}$$

$$\lim_{y\to 0} K_{32\infty}(x,y,t) = -\frac{\kappa_3-1}{2}\pi\delta(t-x), \tag{3.135}$$

$$\lim_{y\to 0} K_{41\infty}(x,y,t) = +\frac{\kappa_3+1}{2}\frac{1}{t-x}, \tag{3.136}$$

$$\lim_{y\to 0} K_{42\infty}(x,y,t) = +\frac{\kappa_3-1}{2}\pi\delta(t-x). \tag{3.137}$$

Substituting (3.134)-(3.126) into (3.122) and (3.123) it may be shown that

$$\begin{aligned}\lambda_3\frac{\partial}{\partial x}v_3(x,0) &= \frac{2}{\pi(\kappa_3+1)}\int_{-\infty}^{\infty}\sigma(t)I_{31}(t,x)dt \\ &\quad +\frac{2}{\pi(\kappa_3+1)}\int_{-\infty}^{\infty}\tau(t)I_{32}(t,x)dt \\ &\quad +\frac{1}{\pi}\int_{-\infty}^{\infty}\frac{\sigma(t)dt}{t-x}-\omega_3\tau(x),\end{aligned} \tag{3.138}$$

$$\begin{aligned}\lambda_3\frac{\partial}{\partial x}u_3(x,0) &= \frac{2}{\pi(\kappa_3+1)}\int_{-\infty}^{\infty}\tau(t)I_{41}(t,x)dt \\ &\quad +\frac{2}{\pi(\kappa_3+1)}\int_{-\infty}^{\infty}\sigma(t)I_{42}(t,x)dt \\ &\quad +\frac{1}{\pi}\int_{-\infty}^{\infty}\frac{\tau(t)dt}{t-x}+\omega_3\sigma(x),\end{aligned} \tag{3.139}$$

where

$$I_{31}(t,x) = \int_{-\infty}^{\infty} \left(h_{31}(\alpha,0) - i\frac{\kappa_3+1}{4}\frac{\alpha}{|\alpha|} \right) e^{-i\alpha(t-x)} d\alpha, \tag{3.140}$$

$$I_{32}(t,x) = \int_{-\infty}^{\infty} \left(h_{32}(\alpha,0) + \frac{\kappa_3-1}{4} \right) e^{-i\alpha(t-x)} d\alpha, \tag{3.141}$$

$$I_{41}(t,x) = \int_{-\infty}^{\infty} \left(h_{41}(\alpha,0) - i\frac{\kappa_3+1}{4}\frac{\alpha}{|\alpha|} \right) e^{-i\alpha(t-x)} d\alpha, \tag{3.142}$$

$$I_{42}(t,x) = \int_{-\infty}^{\infty} \left(h_{42}(\alpha,0) - \frac{\kappa_3-1}{4} \right) e^{-i\alpha(t-x)} d\alpha, \tag{3.143}$$

$$\omega_3 = \frac{\kappa_3-1}{\kappa_3+1}, \tag{3.144}$$

$$\lambda_3 = \frac{4\mu_{30}}{\kappa_3+1}. \tag{3.145}$$

Further refinements can be made by analyzing the kernels $I_{31}(t,x)$,$I_{32}(t,x)$,$I_{41}(t,x)$ and $I_{42}(t,x)$ in equation (3.138) and (3.139). Observing that

$$I_{31} = 2\int_0^{\infty} \Re\left[i\Phi_{31}(\alpha) e^{-i\alpha(t-x)} \right] d\alpha = 2\int_0^{\infty} \Phi_{31}(\alpha) \sin\alpha(t-x) d\alpha, \tag{3.146}$$

$$I_{32} = 2\int_0^{\infty} \Re\left[\Phi_{32}(\alpha) e^{-i\alpha(t-x)} \right] d\alpha = 2\int_0^{\infty} \Phi_{32}(\alpha) \cos\alpha(t-x) d\alpha, \tag{3.147}$$

$$I_{41} = 2\int_0^{\infty} \Re\left[i\Phi_{41}(\alpha) e^{-i\alpha(t-x)} \right] d\alpha = 2\int_0^{\infty} \Phi_{41}(\alpha) \sin\alpha(t-x) d\alpha, \tag{3.148}$$

$$I_{42} = 2\int_0^{\infty} \Re\left[\Phi_{42}(\alpha) e^{-i\alpha(t-x)} \right] d\alpha = 2\int_0^{\infty} \Phi_{42}(\alpha) \cos\alpha(t-x) d\alpha, \tag{3.149}$$

where

$$\Phi_{31}(\alpha) = -\frac{\alpha(\kappa_3-1)}{\Delta_6}\left(y_3\overline{r_8} + \overline{y_3}r_8 \right) - \frac{\kappa_3+1}{4}, \tag{3.150}$$

$$\Phi_{32}(\alpha) = \frac{i\alpha}{\Delta_6}\left(-y_3\overline{r_6} + \overline{y_3}r_6 \right) + \frac{\kappa_3-1}{4}, \tag{3.151}$$

$$\Phi_{41}(\alpha) = -\frac{\alpha}{\Delta_6}\left(y_4\overline{r_6} + \overline{y_4}r_6 \right) - \frac{\kappa_3+1}{4}, \tag{3.152}$$

$$\Phi_{42}(\alpha) = -\frac{i\alpha(\kappa_3-1)}{\Delta_6}\left(y_4\overline{r_8} - \overline{y_4}r_8 \right) - \frac{\kappa_3-1}{4}. \tag{3.153}$$

we can write (3.138) and (3.139) as;

$$-\omega_3\tau(x)+\frac{1}{\pi}\int_{-\infty}^{\infty}\left[\frac{1}{t-x}-k_{31}(t,x)\right]\sigma(t)dt$$
$$-\frac{1}{\pi}\int_{-\infty}^{\infty}\tau(t)k_{32}(t,x)dt = f_3(x), \tag{3.154}$$

$$\omega_3\sigma(x)+\frac{1}{\pi}\int_{-\infty}^{\infty}\left[\frac{1}{t-x}-k_{41}(t,x)\right]\tau(t)dt$$
$$-\frac{1}{\pi}\int_{-\infty}^{\infty}\sigma(t)k_{42}(t,x)dt = g_3(x), \tag{3.155}$$

where

$$f_3(x) = \lambda_3\frac{\partial}{\partial x}v_3(x,0), \tag{3.156}$$

$$g_3(x) = \lambda_3\frac{\partial}{\partial x}u_3(x,0), \tag{3.157}$$

$$\lambda_3 = \frac{4\mu_{30}}{\kappa_3+1} \tag{3.158}$$

$$k_{31}(t,x) = -\frac{4}{\kappa_3+1}\int_0^{\infty}\Phi_{31}(\alpha)\sin\alpha(t-x)d\alpha, \tag{3.159}$$

$$k_{32}(t,x) = -\frac{4}{\kappa_3+1)}\int_0^{\infty}\Phi_{32}(\alpha)\cos\alpha(t-x)d\alpha, \tag{3.160}$$

$$k_{41}(t,x) = -\frac{4}{\kappa_3+1}\int_0^{\infty}\Phi_{41}(\alpha)\sin\alpha(t-x)d\alpha, \tag{3.161}$$

$$k_{42}(t,x) = -\frac{4}{\kappa_3+1}\int_0^{\infty}\Phi_{42}(\alpha)\cos\alpha(t-x)d\alpha. \tag{3.162}$$

Chapter 4

The Integral Equation and Its Solution

If the direction of the forces P and Q are taken to be as in Fig. 4.1, boundary conditions become

$$\sigma_{3yy}(x,0) = \sigma(x) = \begin{cases} -p(x) & -a < x < b, \\ 0 & x < -a, \quad x > b. \end{cases} \tag{4.1}$$

Shear stress at the surface of the medium is related to the normal stress by coefficient of friction η as follows:

$$\sigma_{3xy}(x,0) = \tau(x) = \eta\,\sigma(x) = -\eta p(x), \tag{4.2}$$

Substituting (4.1) and (4.2) into eq (3.154) we have (3.155)

$$\omega_3 \eta p(x) + \frac{1}{\pi}\int_{-a}^{b}\left[-\frac{1}{t-x} + k_{31}(t,x) + \eta k_{32}(t,x)\right] p(t)dt = f_3(x), \tag{4.3}$$

$$-\omega_3 p(x) + \frac{1}{\pi}\int_{-a}^{b}\left[-\frac{\eta}{t-x} + \eta k_{41}(t,x) + k_{42}(t,x)\right] p(t)dt = g_3(x). \tag{4.4}$$

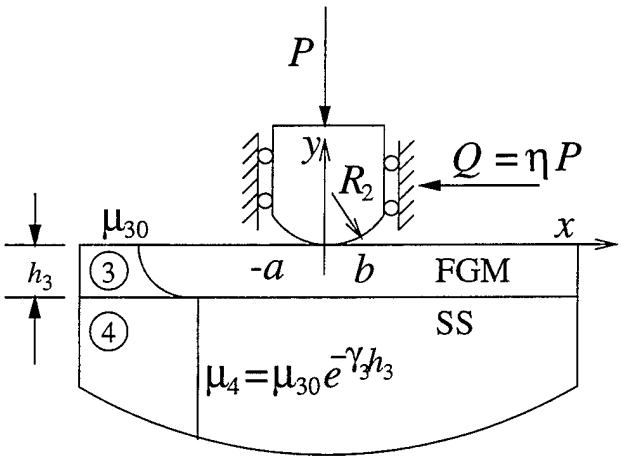

Figure 4.1: Problem geometry

where

$$f_3(x) = \lambda_3 \frac{\partial}{\partial x} v_3(x,0), \tag{4.5}$$

$$g_3(x) = \lambda_3 \frac{\partial}{\partial x} u_3(x,0), \tag{4.6}$$

$$\lambda_3 = \frac{4\mu_{30}}{\kappa_3 + 1}, \tag{4.7}$$

$$k_{31}(t,x) = -\frac{4}{\kappa_3+1}\int_0^\infty \Phi_{31}(\alpha)\sin\alpha(t-x)d\alpha, \tag{4.8}$$

$$k_{32}(t,x) = -\frac{4}{\kappa_3+1}\int_0^\infty \Phi_{32}(\alpha)\cos\alpha(t-x)d\alpha, \tag{4.9}$$

$$k_{41}(t,x) = -\frac{4}{\kappa_3+1}\int_0^\infty \Phi_{41}(\alpha)\sin\alpha(t-x)d\alpha, \tag{4.10}$$

$$k_{42}(t,x) = -\frac{4}{\kappa_3+1}\int_0^\infty \Phi_{42}(\alpha)\cos\alpha(t-x)d\alpha. \tag{4.11}$$

In the singular integral equation (4.3) the contact pressure $p(x)$ is unknown. a and b, on the other hand depends on the punch profile and is found by applying the equilibrium and, if needed, the consistency conditions. The equilibrium of the punch requires that the total pressure on the contact area should be equal to the total load applied to the punch. This can be expressed as

$$\int_{-a}^{b} p(t)dt = P. \tag{4.12}$$

where P is the known compressive force per unit depth in z direction, applied to the punch away from the contact region.

To solve the singular integral equation (4.3) we first normalize the interval $(-a, b)$ to $(-1, 1)$. This can be done by defining the new variables

$$l = \frac{b+a}{2}, \tag{4.13}$$

$$x = \frac{b+a}{2}r + \frac{b-a}{2}, \tag{4.14}$$

$$t = \frac{b+a}{2}s + \frac{b-a}{2}, \tag{4.15}$$

$$p(x) = \phi(r), \tag{4.16}$$

$$k_{31}(t, x) = \frac{1}{l}k_{31}^*(s, r), \tag{4.17}$$

$$k_{32}(t, x) = \frac{1}{l}k_{32}^*(s, r), \tag{4.18}$$

$$f_3(x) = f_3^*(r), \tag{4.19}$$

$$\alpha = \frac{1}{l}\zeta, \tag{4.20}$$

$$\Phi_{31}(\alpha) = \Phi_{31}^*(\zeta), \tag{4.21}$$

$$\Phi_{32}(\alpha) = \Phi_{32}^*(\zeta), \tag{4.22}$$

$$\gamma_3 = \frac{\gamma_3^*}{l} = \frac{1}{l}\gamma_3 h_3 \frac{l}{h_3}. \tag{4.23}$$

The singular integral equation (4.3) then becomes

$$A\phi(r)+\frac{1}{\pi}\int_{-1}^{1}\left[\frac{B}{s-r}+k_{31}^{*}(s,r)+\eta k_{32}^{*}(s,r)\right]\phi(s)ds=f_{3}^{*}(r), \tag{4.24}$$

where

$$A = \omega_3\eta, \tag{4.25}$$

$$B = -1, \tag{4.26}$$

$$k_{31}^{*}(s,r) = -\frac{4}{(\kappa_3+1)}\int_{0}^{\infty}\Phi_{31}^{*}(\zeta)\sin\zeta(s-r)d\zeta, \tag{4.27}$$

$$k_{32}^{*}(s,r) = -\frac{4}{(\kappa_3+1)}\int_{0}^{\infty}\Phi_{32}^{*}(\zeta)\cos\zeta(s-r)d\zeta, \tag{4.28}$$

$$\Phi_{31}^{*}(\zeta) = -\frac{\zeta(\kappa_3-1)}{\Delta_6(\zeta)}\left[y_3(\zeta)\overline{r_8}(\zeta)+\overline{y_3}(\zeta)r_8(\zeta)\right]-\frac{\kappa_3+1}{4}, \tag{4.29}$$

$$\Phi_{32}^{*}(\zeta) = \frac{i\zeta}{\Delta_6(\zeta)}\left[-y_3(\zeta)\overline{r_6}(\zeta)+\overline{y_3}(\zeta)r_6(\zeta)\right]+\frac{\kappa_3-1}{4}. \tag{4.30}$$

The method of evaluation of the Fredholm kernels $k_{31}^{*}(s,r)$ and $k_{32}^{*}(s,r)$ are shown in Appendix F. However when evaluating the Fredholm kernels we end up with the integration of sign function, $\frac{|s-r|}{s-r}$ and the logarithmic function $\log|s-r|$. In the integration of $k_{31}^{*}(s,r)$ and $k_{32}^{*}(s,r)$ from -1 to 1, we subtract and add this functions in order to regularize the integrand. Therefore we may write

$$\begin{aligned}k_{31}^{*}(s,r) = & -\frac{4}{(\kappa_3+1)}\left[\int_{0}^{\infty}\Phi_{31}^{*}(\zeta)\sin\zeta(s-r)d\zeta-\frac{(\kappa_3+5)\,\gamma_3^{*}}{8}\frac{\pi}{2}\frac{|s-r|}{s-r}\right]\\ & -\frac{4}{(\kappa_3+1)}\frac{(\kappa_3+5)\,\gamma_3^{*}}{8}\frac{\pi}{2}\frac{|s-r|}{s-r},\end{aligned}$$

$$\begin{aligned}k_{32}^{*}(s,r) = & -\frac{4}{(\kappa_3+1)}\left[\int_{0}^{\infty}\Phi_{32}^{*}(\zeta)\cos\zeta(s-r)d\zeta-\frac{(\kappa_3+1)\,\gamma_3^{*}}{8}\log|s-r|\right]\\ & -\frac{4}{(\kappa_3+1)}\frac{(\kappa_3+1)\,\gamma_3^{*}}{8}\log|s-r|.\end{aligned}$$

4.1 The fundamental function

The dominant part of the singular integral equation of the second kind (4.24) is of the form

$$A\phi(r) - \frac{1}{\pi}\int_{-1}^{1}\frac{\phi(s)}{s-r}ds = F(r), \qquad -1 < r < 1, \tag{4.31}$$

where the bounded function $F(r)$ contains part of the integral equation with the Fredholm kernels. Defining

$$\Phi(z) = \frac{1}{2\pi i}\int_{-1}^{1}\frac{\phi(s)}{s-z}ds, \tag{4.32}$$

and using the following general Plemelj formulas

$$\Phi^{+}(r) - \Phi^{-}(r) = \begin{cases} \phi(r) & -1 < r < 1, \\ 0 & r < -1, r > 1, \end{cases} \tag{4.33}$$

$$\Phi^{+}(r) + \Phi^{-}(r) = \begin{cases} \frac{1}{\pi i}\int_{-1}^{1}\frac{\phi(s)}{s-r}ds, & -1 < r < 1, \\ 2\Phi(r), & r < -1, r > 1. \end{cases} \tag{4.34}$$

we may reduce (4.31) to the following Riemann-Hilbert problem for the sectionally holomorphic function $\Phi(z)$:

$$\Phi^{+}(r) = G\Phi^{-}(r) + g(r), \tag{4.35}$$

where

$$G = \frac{A+i}{A-i}, \tag{4.36}$$

$$g(r) = \frac{F(r)}{A-i}. \tag{4.37}$$

Considering the corresponding homogeneous equation

$$X^{+}(r) - GX^{-}(r) = 0, \tag{4.38}$$

we obtain the fundamental solution $X(z)$ and the fundamental function $w(x)$ of (4.31) as [43]

$$X(z) = (z-1)^{\alpha}(z+1)^{\beta}, \tag{4.39}$$

$$w(r) = (1-r)^{\alpha}(r+1)^{\beta}, \tag{4.40}$$

where

$$\alpha = a_1 + ib_1 + N, \tag{4.41}$$

$$\beta = a_2 + ib_2 + M, \tag{4.42}$$

$$a_1 + ib_1 = \frac{\ln G}{2\pi i}, \tag{4.43}$$

$$a_2 + ib_2 = -\frac{\ln G}{2\pi i}. \tag{4.44}$$

If $A > 0$, we define the angle, θ, such that

$$\begin{aligned} A + i &= re^{i\theta}, \\ A - i &= re^{-i\theta}, \\ \theta &= \arctan\frac{1}{A} > 0. \end{aligned} \tag{4.45}$$

Therefore equation (4.43) and (4.44) becomes

$$a_1 + ib_1 = \frac{1}{2\pi i}\ln e^{2i\theta} = \frac{\theta}{\pi}, \tag{4.46}$$

$$a_2 + ib_2 = -\frac{1}{2\pi i}\ln e^{2i\theta} = -\frac{\theta}{\pi}, \tag{4.47}$$

yielding

$$\alpha = N + \frac{\theta}{\pi}, \tag{4.48}$$

$$\beta = M - \frac{\theta}{\pi}. \tag{4.49}$$

However, If $A = -A_0 < 0$,we define the angle, θ,

$$\theta = \arctan\left|\frac{1}{A}\right| > 0. \tag{4.50}$$

From equation (4.36) G becomes

$$G = \frac{A_0 - i}{A_0 + i}.$$

We define the angle, θ as

$$A_0 + i = re^{i\theta}, \tag{4.51}$$

$$A_0 - i = re^{-i\theta}, \tag{4.52}$$

$$\theta = \arctan\left(\frac{1}{A_0}\right) > 0. \tag{4.53}$$

Therefore equation (4.43) and (4.44) becomes

$$a_1 + ib_1 = \frac{1}{2\pi i} \ln e^{-2i\theta} = -\frac{\theta}{\pi}, \tag{4.54}$$

$$a_2 + ib_2 = -\frac{1}{2\pi i} \ln e^{-2i\theta} = \frac{\theta}{\pi}. \tag{4.55}$$

Consequently

$$\alpha = N - \frac{\theta}{\pi}, \tag{4.56}$$

$$\beta = M + \frac{\theta}{\pi}, \tag{4.57}$$

where N and M are arbitrary(positive,zero, or negative) integers and they are determined from the physics of the problem. The index of the integral equation is defined by

$$\kappa_0 = -(\alpha + \beta) = -(N + M). \tag{4.58}$$

we observe that in the punch problem with friction $A = \eta(\kappa_3 - 1)/(\kappa_3 + 1)$. Therefore, the powers of stress singularity α and β will depend only on the coefficient of friction η and the value of the Poisson's ratio on the surface of the FGM layer. In this study the Poisson's ratio is assumed to be constant, consequently α and β would be independent of the non-homogeneity parameter $\gamma_3 h_3$.

4.2 Numerical Procedure

We have derived the singular integral equation for the punch problem. The integral equation has a Cauchy kernel and two Fredholm kernels. The solution of the singular integral equation is generally obtained either through function theoretical technique as given by Muskhelishvili [43] or through numerical methods [44] and [45]. In this study the method of using orthogonal polynomials with the unknown functions represented by Jacobi polynomials, associated with the weight function $w(s)$ and described in [46] is used.

The singular integral equation does not have a closed form solution. Hence a numerical method has to be used. In this study Jacobi polynomials are used to reduce the singular integral equation to an infinite system of linear algebraic equations.

Once the fundamental function, $w(s)$ of the integral equation is determined, the solution of (4.24) may be expressed as

$$\phi(s) = G(s)w(s), \qquad -1 < s < 1, \tag{4.59}$$

where $G(s)$ is a bounded continuous function and can always be represented by an infinite series. Observing that $w(s)$ is the weight function of the Jacobi Polynomials, one may write

$$\phi(s) = \sum_{0}^{\infty} c_n w(s) P_n^{(\alpha,\beta)}(s), \tag{4.60}$$

where c_n, $(n = 0, 1, \dots)$ are undetermined constants.

By substituting (4.60) into (4.24) and making use of the property of the Jacobi polynomials(A.6), we find

$$\sum_{0}^{\infty} c_n \left[\frac{-2^{-\kappa_0} B}{sin\pi\alpha} P_{n-\kappa_0}^{(-\alpha,-\beta)}(r) + \mathcal{K}_{3n}(r) \right] = f_3^*(r), \qquad -1 < r < 1, \tag{4.61}$$

where

$$\mathcal{K}_{3n}(r) = \frac{1}{\pi} \int_{-1}^{1} \left[k_{31}^*(s,r) + \eta k_{32}^*(s,r) \right] P_n^{(\alpha,\beta)}(s) w(s) ds. \tag{4.62}$$

The functional equation (4.61) can be reduced to a system of algebraic equations in c_n through a suitable collocation technique. In the numerical solution of (4.61), higher accuracy is obtained when the density of the collocation points is increased near the ends by choosing the collocation points ($r_i, \quad i = 0, 1, ..., N$) as the roots of the Jacobi polynomials depending on the index of the problem.

4.3 The In-plane stress, σ_{xx} on the surface

Once we obtain the solution for the contact stresses $\sigma(x)$ and $\tau(x)$, we can find the in plane σ_{3xx} stresses on the surface of the FGM coating. The strains in y and z direction can be written as

$$\epsilon_{3yy} = \frac{1}{E_3}\left[\sigma_{3yy} - \nu_3(\sigma_{3xx} + \sigma_{3zz})\right], \tag{4.63}$$

$$\epsilon_{3zz} = \frac{1}{E_3}\left[\sigma_{3zz} - \nu_3(\sigma_{3xx} + \sigma_{3yy})\right], \tag{4.64}$$

In the plane strain case ($\epsilon_{3zz} = 0$) the stress in z direction becomes

$$\sigma_{3zz} = \nu_3(\sigma_{3xx} + \sigma_{3yy}). \tag{4.65}$$

Substituting this stress back into equation (4.63), we obtain

$$\epsilon_{3yy}(x, y) = \frac{1 - \nu_3^2}{E_3}\sigma_{3yy}(x, y) - \frac{\nu_3(1 + \nu_3)}{E_3}\sigma_{3xx}(x, y). \tag{4.66}$$

We also have

$$\kappa_3 = 3 - 4\nu_3, \tag{4.67}$$

$$E_{30} = 2\mu_{30}(1 + \nu_3) = \mu_{30}\frac{7 - \kappa_3}{2}, \tag{4.68}$$

$$1 - \nu_3^2 = -\frac{(\kappa_3 - 7)(\kappa_3 + 1)}{16}, \tag{4.69}$$

$$\nu_3(1 + \nu_3) = \frac{(3 - \kappa_3)(7 - \kappa_3)}{16}. \tag{4.70}$$

Thus

$$\frac{1-\nu_3^2}{E_{30}} = \frac{\kappa_3+1}{8\mu_{30}}, \tag{4.71}$$

$$\frac{\nu_3(1+\nu_3)}{E_{30}} = \frac{3-\kappa_3}{8\mu_{30}}. \tag{4.72}$$

Substituting (4.71) and (4.72) into equation (4.66) and taking the limit as $y \to 0$ we find

$$\epsilon_{3yy}(x,0) = \frac{\partial}{\partial y} v_3(x,0) = \frac{\kappa_3+1}{8\mu_{30}}\sigma_{3yy}(x,y) - \frac{3-\kappa_3}{8\mu_{30}}\sigma_{3xx}(x,y) \tag{4.73}$$

Substituting $\frac{\partial}{\partial x}u_3(x,0)$ and $\frac{\partial}{\partial y}v_3(x,0)$ from equations (4.4) and (4.73) into equation (3.5) and after some algebra it can be shown that

$$\begin{aligned}\sigma_{3xx}(x,0) &= \sigma(x) + \frac{2}{\pi}\int_{-a}^{b}\frac{\tau(t)}{t-x}dt \\ &\quad -\frac{2}{\pi}\int_{-a}^{b} k_{41}(t,x)\,\tau(t)dt - \frac{2}{\pi}\int_{-a}^{b} k_{42}(t,x)\,\sigma(t)dt \end{aligned} \tag{4.74}$$

where

$$k_{41}(t,x) = -\frac{4}{\kappa_3+1}\int_0^\infty \Phi_{41}(\alpha)\sin\alpha(t-x)d\alpha, \tag{4.75}$$

$$k_{42}(t,x) = -\frac{4}{\kappa_3+1}\int_0^\infty \Phi_{42}(\alpha)\cos\alpha(t-x)d\alpha, \tag{4.76}$$

or in a compact form

$$\sigma_{3xx}(x,0) = \sigma_{xx}^p(x,0) + \sigma_{xx}^q(x,0), \tag{4.77}$$

where

$$\sigma_{xx}^p(x,0) = \sigma(x) - \frac{2}{\pi}\int_{-a}^{b} k_{42}(t,x)\,\sigma(t)dt, \tag{4.78}$$

$$\sigma_{xx}^q(x,0) = \frac{2}{\pi}\int_{-a}^{b}\left[\frac{1}{t-x} - k_{41}(t,x)\right]\tau(t)dt. \tag{4.79}$$

Chapter 5

Results of Rigid Stamps

5.1 The Flat Stamp

Consider the contact problem for the FGM layer bonded to a homogeneous substrate shown in Fig. 5.1 where the stamp profile is given by

$$v_3(x,0) = -v_{30}. \tag{5.1}$$

From (5.1) it follows that

$$\frac{\partial}{\partial x} v_3(x,0) = 0. \tag{5.2}$$

We now define the tractions on the boundary

$$\begin{aligned} \sigma_{3yy}(t,0) &= -p(t), \qquad \sigma_{3xy}(t,0) = -\eta p(t), \qquad -a < t < a, \\ \sigma_{3yy}(t,0) &= \sigma_{3xy}(t,0) = 0, \qquad\qquad\qquad t < -a, t > a, \end{aligned} \tag{5.3}$$

and making use of the following change of variables

$$x = ar, \tag{5.4}$$

$$t = as, \tag{5.5}$$

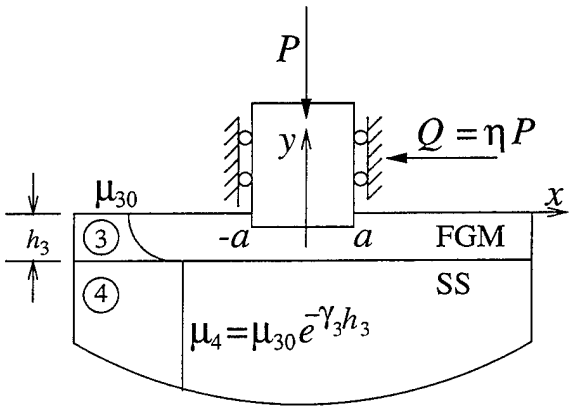

Figure 5.1: Geometry of the flat punch problem

and defining

$$p(t) = 2\sigma_0\phi(s), \tag{5.6}$$

$$\sigma_0 = \frac{P}{2a}, \tag{5.7}$$

and using the relations (4.17)-(4.23) integral equation (4.3) and the equilibrium equation (4.12) become

$$A\phi(r) + \frac{1}{\pi}\int_{-1}^{1}\left[-\frac{1}{s-r} + k_{31}^{*}(s,r) + \eta k_{32}^{*}(s,r)\right]\phi(s)ds = f_3^{*}(r), \tag{5.8}$$

$$\int_{-1}^{1}\phi(s)ds = 1, \tag{5.9}$$

where

$$A = \omega_3\eta, \tag{5.10}$$

$$f_3^{*}(r) = 0, \tag{5.11}$$

$$k_{31}(s,r) = \frac{1}{a}k_{31}^{*}(s,r), \tag{5.12}$$

$$k_{32}(s,r) = \frac{1}{a}k_{32}^{*}(s,r). \tag{5.13}$$

Since $p(x)$ has integrable singularities at $x = -a$, and $x = a$, from the physics of the problem we must require that both α and β be negative.

If $\eta > 0$ from equations (4.48) and (4.49) we have

$$\alpha = N + \frac{\theta}{\pi}, \quad \Longrightarrow \quad N = -1, \tag{5.14}$$

$$\beta = M - \frac{\theta}{\pi}, \quad \Longrightarrow \quad M = 0, \tag{5.15}$$

and if $\eta < 0$ equations (4.56) and (4.57) give

$$\alpha = N - \frac{\theta}{\pi}, \quad \Longrightarrow \quad N = 0, \tag{5.16}$$

$$\beta = M + \frac{\theta}{\pi}, \quad \Longrightarrow \quad M = -1. \tag{5.17}$$

The index of the integral equation is defined by

$$\kappa_0 = -(\alpha + \beta) = -(N + M) = 1. \tag{5.18}$$

α and β then become

$$\begin{aligned} \eta > 0: &\quad \alpha = -1 + \theta/\pi, \quad \beta = -\theta/\pi, \\ \eta = 0: &\quad \alpha = -0.5, \qquad\quad \beta = -0.5, \\ \eta < 0: &\quad \alpha = -\theta/\pi, \qquad\quad \beta = -1 + \theta/\pi, \end{aligned} \tag{5.19}$$

where

$$\theta = \arctan \left| \frac{\kappa_3 + 1}{\eta\,(\kappa_3 - 1)} \right|. \tag{5.20}$$

In Table 5.1 some values of the α and β are given for various values of η and $\nu = 0.3$.

Assuming a solution of the form

$$\phi(s) = w(s) \sum_{0}^{\infty} c_n P_n^{(\alpha,\beta)}(s), \tag{5.21}$$

$$w(s) = (1-s)^{\alpha} (1+s)^{\beta}, \tag{5.22}$$

considering the property of Jacobi Polynomials (A.6), letting

$$\mathcal{K}_{3n}(r) = \frac{1}{\pi} \int_{-1}^{1} \left[k_{31}^*(s,r) + \eta k_{32}^*(s,r) \right] w(s) P_n^{(\alpha,\beta)}(s) ds, \tag{5.23}$$

Table 5.1: Values of α and β for the index, $\kappa_0 = 1$

η	α	β
-0.3	-0.4728	-0.5272
-0.1	-0.4909	-0.5091
0	-0.5000	-0.5000
0.1	-0.5091	-0.4909
0.3	-0.5272	-0.4828

and truncating the series in (5.21) at N, equation (5.8) becomes

$$\sum_0^N c_n \left[\frac{1}{2\sin\pi\alpha} P_{n-1}^{(-\alpha,-\beta)}(r) + \mathcal{K}_{3n}(r) \right] = 0 \tag{5.24}$$

Equation (5.24) provides N equations for $N+1$ unknown constants $c_0, ..., c_N$. The additional equation for a unique solution is provided by the equilibrium condition (5.9), which becomes

$$\sum_0^N c_n \int_{-1}^{1} w(s) P_n^{(\alpha,\beta)}(s)\, ds = 1. \tag{5.25}$$

Using the orthogonality condition (A.7), we obtain the following $N+1$ equations

$$c_0\theta_0 = 1, \tag{5.26}$$

$$\sum_0^N c_n F_n(r_i) = 0, \qquad i = 1, ..., N, \tag{5.27}$$

where

$$F_n(r_i) = \frac{1}{2\sin\pi\alpha} P_{n-1}^{(-\alpha,-\beta)}(r_i) + \mathcal{K}_{3n}(r_i). \tag{5.28}$$

In (5.28) $r_i\,(i = 1, ..., N)$ are obtained by setting

$$P_{n-1}^{(\alpha+1,\beta+1)}(r_i) = 0, \qquad i = 1, ..., N. \tag{5.29}$$

From (5.6), it then follows that

$$\begin{aligned} p(r) &= 2\sigma_0\phi(r) \\ &= 2\sigma_0 w(r) \sum_0^N c_n P_n^{(\alpha,\beta)}(r). \end{aligned} \tag{5.30}$$

Or, in physical coordinates

$$\frac{p(x)}{\sigma_0} = 2\left(1-\frac{x}{a}\right)^{\alpha}\left(1+\frac{x}{a}\right)^{\beta}\sum_{0}^{N} c_n P_n^{(\alpha,\beta)}\left(\frac{x}{a}\right). \tag{5.31}$$

The contact stresses can then be obtained in nondimensional form as

$$\frac{\sigma_{2yy}(x,0)}{\sigma_0} = -\frac{p(x)}{\sigma_0} = -2\left(1-\frac{x}{a}\right)^{\alpha}\left(1+\frac{x}{a}\right)^{\beta}\sum_{0}^{N} c_n P_n^{(\alpha,\beta)}\left(\frac{x}{a}\right), \tag{5.32}$$

$$\frac{\sigma_{2yy}(x,0)}{\sigma_0} = -\eta\frac{p(x)}{\sigma_0}, \tag{5.33}$$

and by using equation (4.74).

$$\sigma_{3xx}(x,0) = \sigma(x) + \frac{2\eta}{\pi}\int_{-a}^{a}\frac{\sigma(t)}{t-x}dt - \frac{2}{\pi}\int_{-a}^{a}\left[k_{42}(t,x)+\eta k_{41}(t,x)\right]\sigma(t)\,dt. \tag{5.34}$$

It may also be shown that

$$\begin{aligned}\sigma_{3xx}(x,0) &= -p(x) - \frac{2\eta}{\pi}\int_{-a}^{a}\frac{p(t)}{t-x}dt + \frac{2}{\pi}\int_{-a}^{a}\left[k_{42}(t,x)+\eta k_{41}(t,x)\right]p(t)\,dt \\ &= 2\sigma_0\left[-\phi(r) - \frac{2\eta}{\pi}\int_{-1}^{1}\frac{\phi(s)}{s-r}dt + \frac{2}{\pi}\int_{-1}^{1}\left[k_{42}^{*}(s,r)+\eta k_{41}^{*}(s,r)\right]\phi(s)\,ds\right],\end{aligned}$$

Or defining

$$\sigma_{3xx}(x,0) = -2\sigma_0\psi(r), \tag{5.35}$$

$$\psi(r) = \phi(r) + \frac{2\eta}{\pi}\int_{-1}^{1}\frac{\phi(s)}{s-r}dt - \frac{2}{\pi}\int_{-1}^{1}\left[k_{42}^{*}(s,r)+\eta k_{41}^{*}(s,r)\right]\phi(s)\,ds \tag{5.36}$$

The nondimensional in-plane streses $\sigma_{3xx}(x,0)$ would then become

$$\frac{\sigma_{3xx}(x,0)}{\sigma_0} = -2\psi(r)$$

In Figure 5.2 - 5.3 the stress distribution on the surface of the FGM coating loaded by a rigid flat stamp is given for various values of the stiffness ratio $\Gamma_3 = \mu_4/\mu_{30}$ in the case of no friction and $a/h_3 = 0.1,\ 0.5$ respectively. The σ_{yy} stress distribution is symmetric and unbounded at the ends of the stamp. For the stiffenning coating

on the hard substrate($\Gamma_3 = 8$) the in-plane stress σ_{xx} at the surface of the coating is positive outside the contact zone. However for the softening coating on the soft substrate ($\Gamma_3 = 1/8$) σ_{xx} is negative everywhere along the surface of the coating. Also for the softening coating, the contact pressure σ_{yy} at the ends of the contact zone is higher than the stiffening coating.

Figures 5.4 -5.9 give the stress distribution on the surface of the FGM coating loaded by a flat stamp is given for various values of the stiffness ratio $\Gamma_3 = \mu_4/\mu_{30}$, a/h_3, and η. At the trailing edge of the contact the inplane stress σ_{xx} is positive infinite wheras at the leading edge the σ_{xx} is negative. Therefore the possible site of crack initiation is at the trailing edge.

5.1.1 Stress intensity factors

Mode I stress intensity factors at the ends of the stamp can be defined as

$$k_1(a) = \lim_{x\to a} \frac{p(x)}{2^\beta (a-x)^\alpha} = \frac{2\sigma_0}{a^\alpha} \sum_0^N c_n P_n^{(\alpha,\beta)}(1), \tag{5.37}$$

$$k_1(-a) = \lim_{x\to -a} \frac{p(x)}{2^\alpha (x+a)^\beta} = \frac{2\sigma_0}{a^\beta} \sum_0^N c_n P_n^{(\alpha,\beta)}(-1). \tag{5.38}$$

The non-dimensional stress intensity factors may then be expressed as

$$k_1^*(a) = \frac{a^\alpha}{2\sigma_0} k_1(a) = \sum_0^N c_n P_n^{(\alpha,\beta)}(1), \tag{5.39}$$

$$k_1^*(-a) = \frac{a^\beta}{2\sigma_0} k_1(-a) = \sum_0^N c_n P_n^{(\alpha,\beta)}(-1). \tag{5.40}$$

Table 5.2-5.3 gives the normalized stress intensity factors at the ends of the flat stamp by assuming $\nu = 0.3$, for $a/h_3 = 0.1$, 0.5 respectively.

Table 5.2: Stress intensity factors for flat stamp, $a/h_3 = 0.1$

	$\eta = 0.0$	$\eta = 0.1$		$\eta = 0.3$		$\eta = 0.5$	
	$\alpha = -0.5$ $\beta = -0.5$	$\alpha = -0.5091$ $\beta = -0.4909$		$\alpha = -0.5272$ $\beta = -0.4728$		$\alpha = -0.5452$ $\beta = -0.4548$	
Γ_3	$\frac{k_1(a)}{Pa^\beta}$	$\frac{k_1(-a)}{Pa^\alpha}$	$\frac{k_1(a)}{Pa^\beta}$	$\frac{k_1(-a)}{Pa^\alpha}$	$\frac{k_1(a)}{Pa^\beta}$	$\frac{k_1(-a)}{Pa^\alpha}$	$\frac{k_1(a)}{Pa^\beta}$
8	0.2802	0.2769	0.2833	0.2696	0.2885	0.2615	0.2926
2	0.3038	0.3025	0.3048	0.2991	0.3060	0.2949	0.3062
1	0.3183	0.3182	0.3182	0.3171	0.3171	0.3151	0.3151
1/2	0.3355	0.3366	0.3341	0.3382	0.3305	0.3386	0.3261
1/8	0.3813	0.3855	0.3768	0.3933	0.3673	0.3999	0.3572

Table 5.3: Stress intensity factors for flat stamp, $a/h_3 = 0.5$

	$\eta = 0.0$	$\eta = 0.1$		$\eta = 0.3$		$\eta = 0.5$	
	$\alpha = -0.5$ $\beta = -0.5$	$\alpha = -0.5091$ $\beta = -0.4909$		$\alpha = -0.5272$ $\beta = -0.4728$		$\alpha = -0.5452$ $\beta = -0.4548$	
Γ_3	$\frac{k_1(a)}{Pa^\beta}$	$\frac{k_1(-a)}{Pa^\alpha}$	$\frac{k_1(a)}{Pa^\beta}$	$\frac{k_1(-a)}{Pa^\alpha}$	$\frac{k_1(a)}{Pa^\beta}$	$\frac{k_1(-a)}{Pa^\alpha}$	$\frac{k_1(a)}{Pa^\beta}$
8	0.2086	0.1973	0.2199	0.1754	0.2422	0.1549	0.2635
2	0.2700	0.2657	0.2740	0.2565	0.2814	0.2467	0.2876
1	0.3183	0.3182	0.3182	0.3171	0.3171	0.3151	0.3151
1/2	0.3848	0.3895	0.3800	0.3979	0.3696	0.4053	0.3587
1/8	0.6011	0.6178	0.5844	0.6510	0.5511	0.6834	0.5185

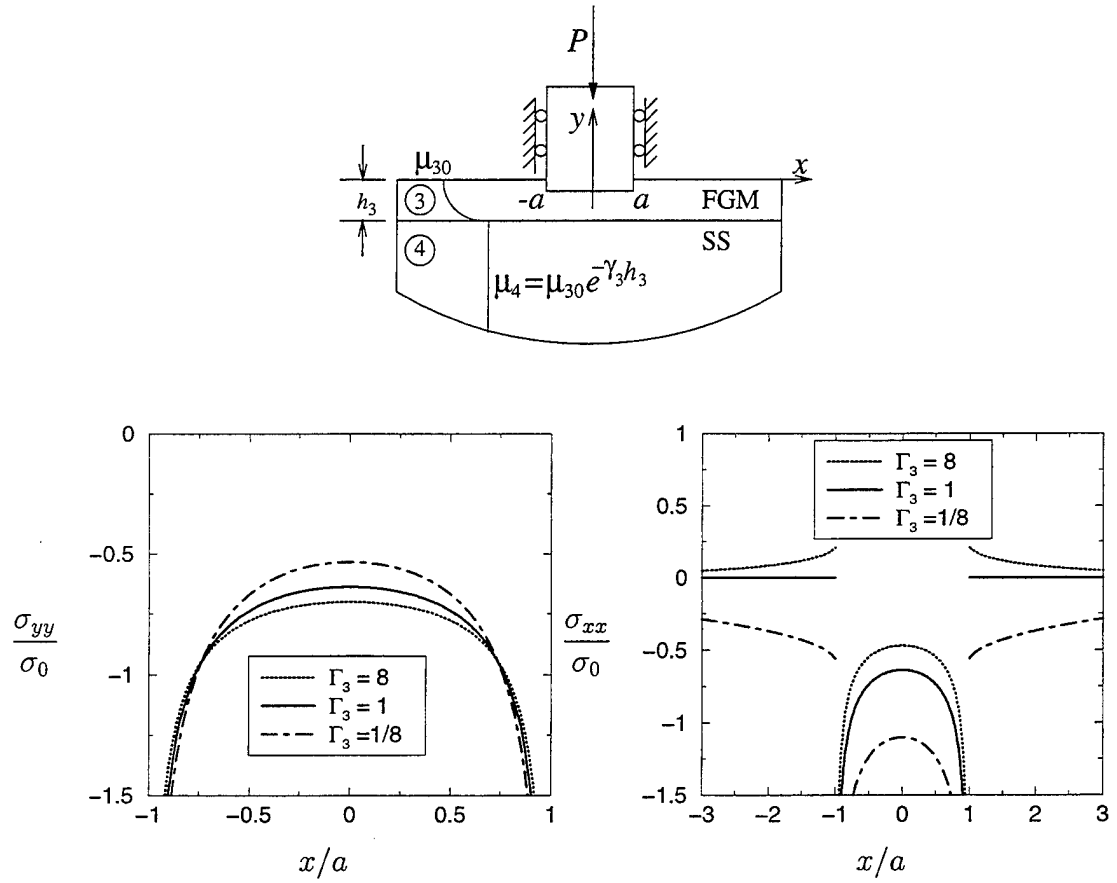

Figure 5.2: Stress distribution on the surface of the FGM coating loaded by a rigid flat stamp for various values of the stiffness ratios, $\Gamma_3 = \dfrac{\mu_4}{\mu_{30}}$, $\sigma_0 = \dfrac{P}{2a}$, $a/h_3 = 0.1$, $\eta = 0.0$.

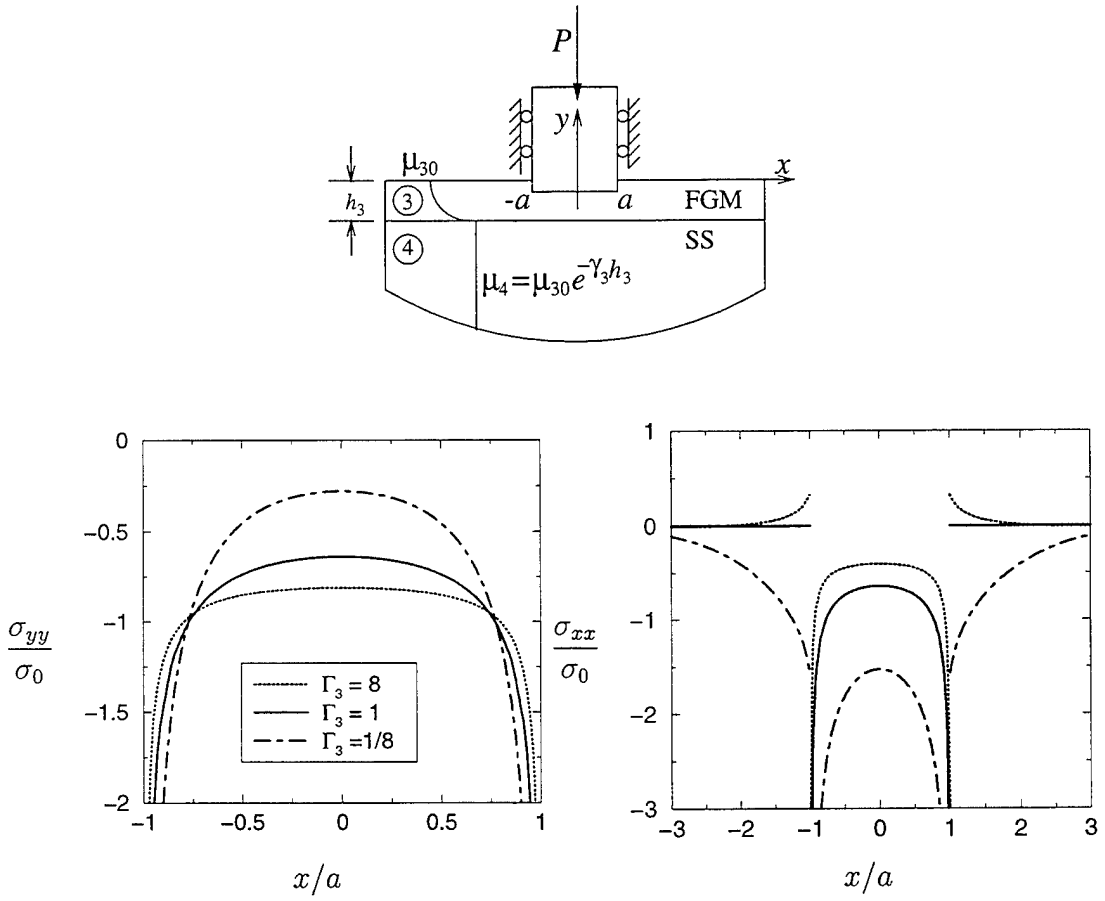

Figure 5.3: Stress distribution on the surface of the FGM coating loaded by a rigid flat stamp for various values of the stiffness ratios, $\Gamma_3 = \dfrac{\mu_4}{\mu_{30}}$, $\sigma_0 = \dfrac{P}{2a}$, $a/h_3 = 0.5$, $\eta = 0.0$.

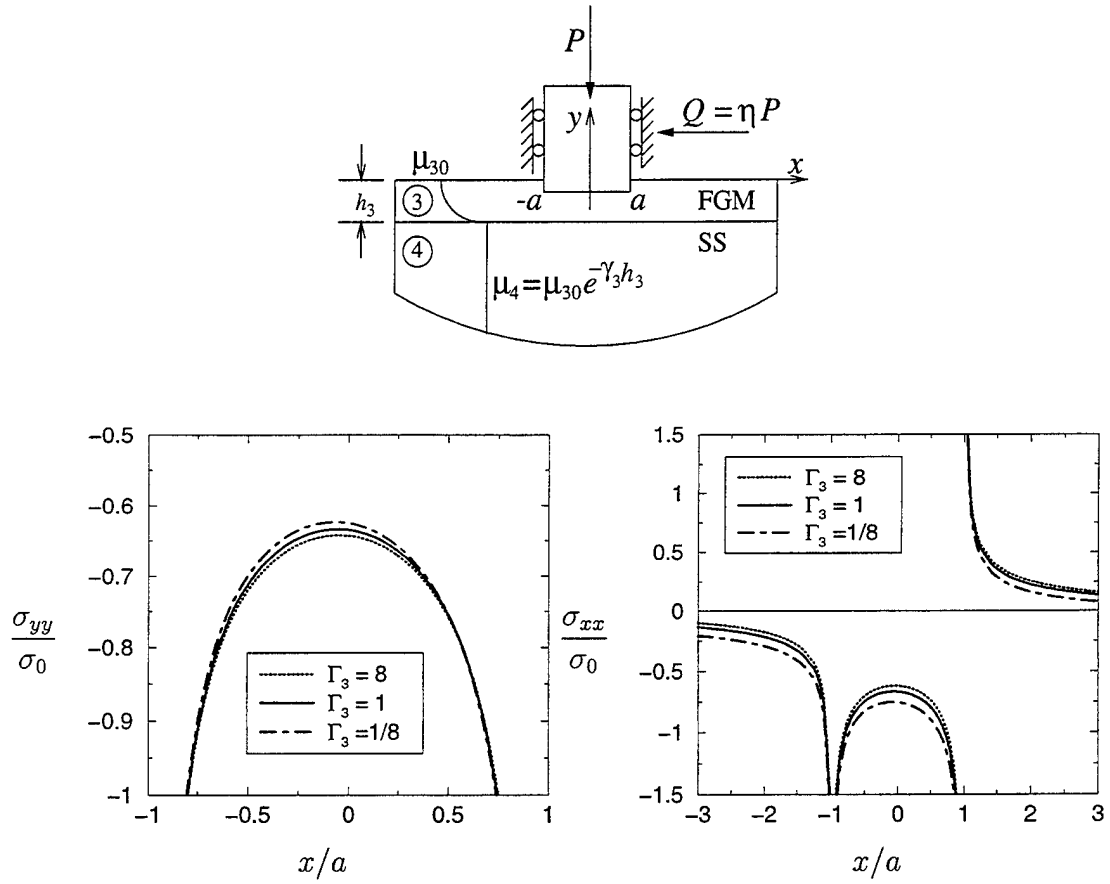

Figure 5.4: Stress distribution on the surface of the FGM coating loaded by a rigid flat stamp for various values of the stiffness ratios, $\Gamma_3 = \dfrac{\mu_4}{\mu_{30}}$, $\sigma_0 = \dfrac{P}{2a}$, $a/h_3 = 0.01$, $\eta = 0.3$.

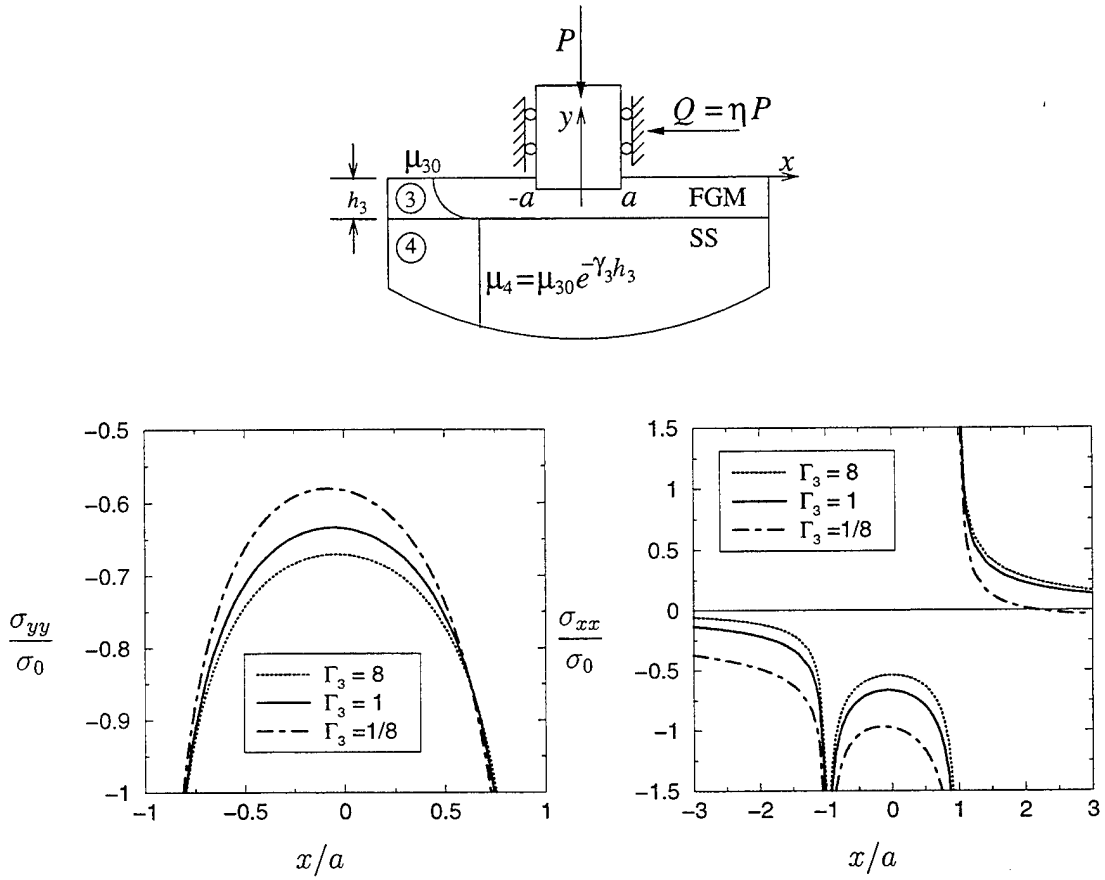

Figure 5.5: Stress distribution on the surface of the FGM coating loaded by a rigid flat stamp for various values of the stiffness ratios, $\Gamma_3 = \dfrac{\mu_4}{\mu_{30}}$, $\sigma_0 = \dfrac{P}{2a}$, $a/h_3 = 0.05$, $\eta = 0.3$.

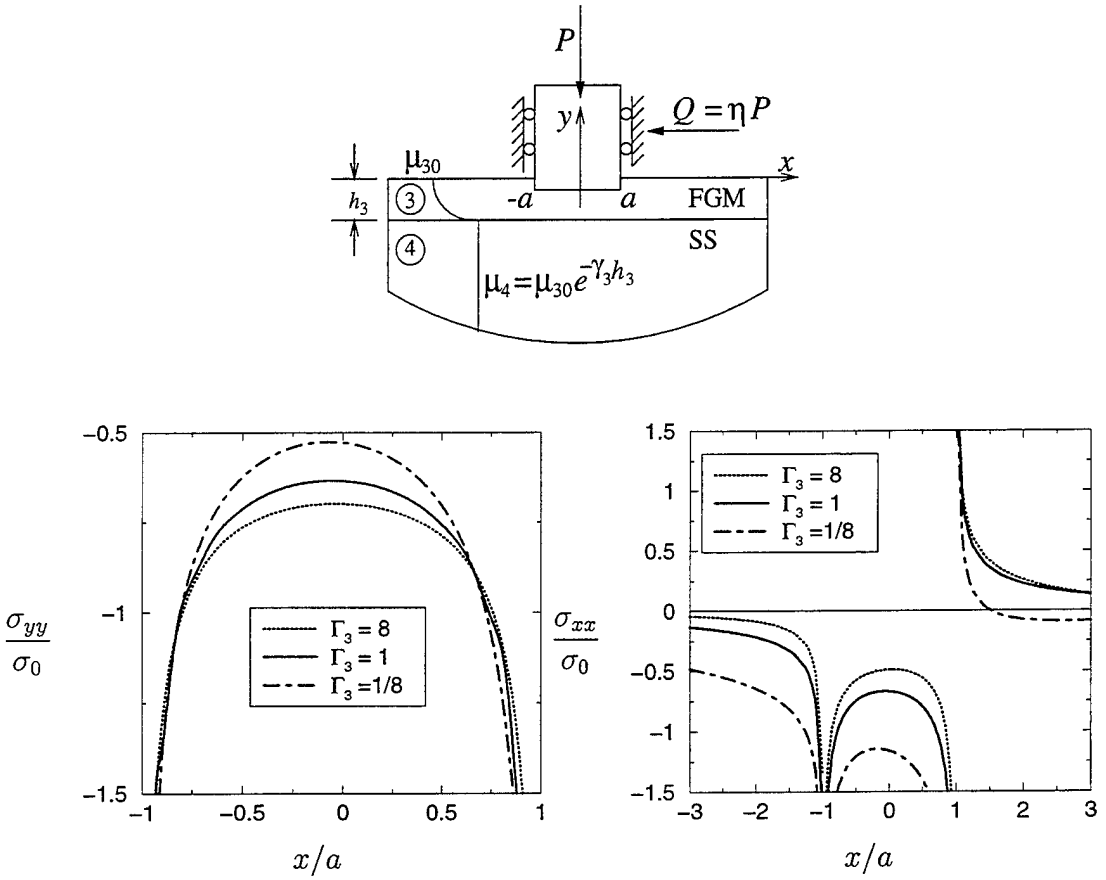

Figure 5.6: Stress distribution on the surface of the FGM coating loaded by a rigid flat stamp for various values of the stiffness ratios, $\Gamma_3 = \dfrac{\mu_4}{\mu_{30}}$, $\sigma_0 = \dfrac{P}{2a}$, $a/h_3 = 0.1$, $\eta = 0.3$.

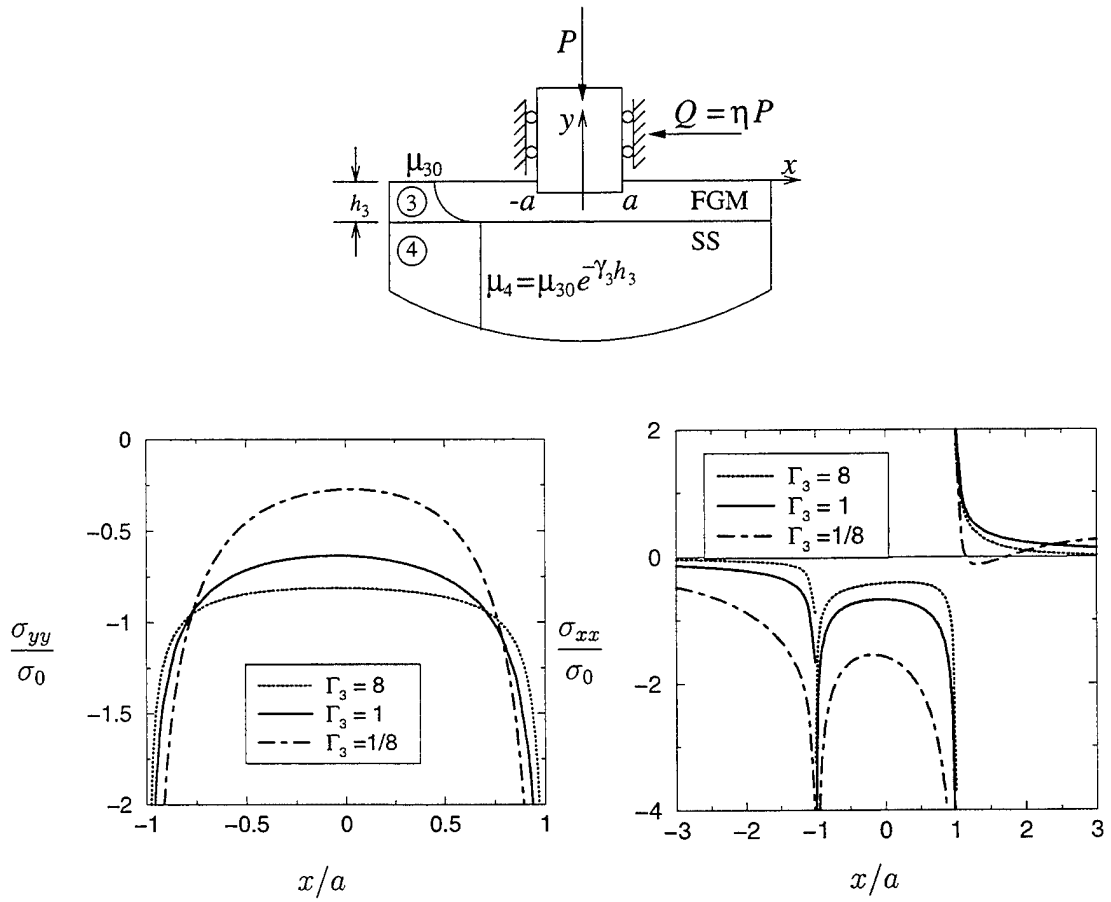

Figure 5.7: Stress distribution on the surface of the FGM coating loaded by a rigid flat stamp for various values of the stiffness ratios, $\Gamma_3 = \dfrac{\mu_4}{\mu_{30}}$, $\sigma_0 = \dfrac{P}{2a}$, $a/h_3 = 0.5$, $\eta = 0.3$.

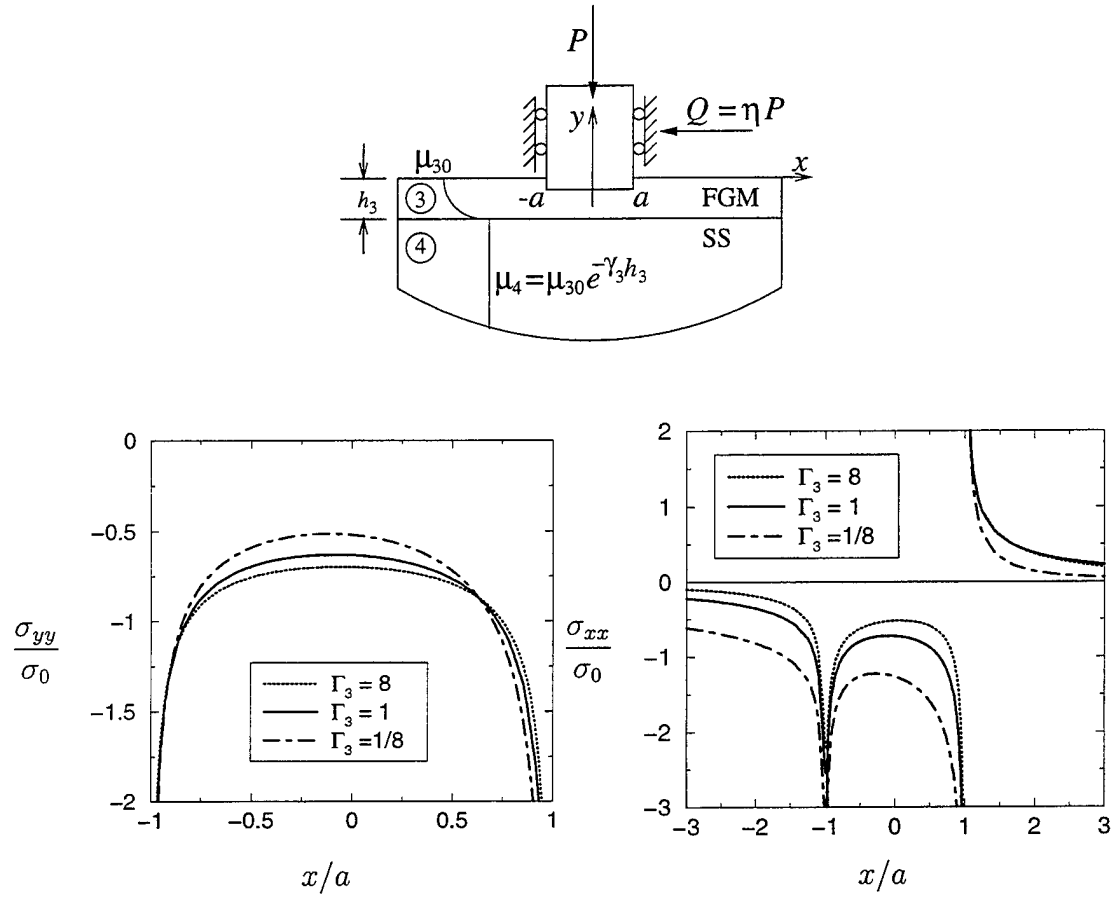

Figure 5.8: Stress distribution on the surface of the FGM coating loaded by a rigid flat stamp for various values of the stiffness ratios, $\Gamma_3 = \dfrac{\mu_4}{\mu_{30}}$, $\sigma_0 = \dfrac{P}{2a}$, $a/h_3 = 0.1$, $\eta = 0.5$.

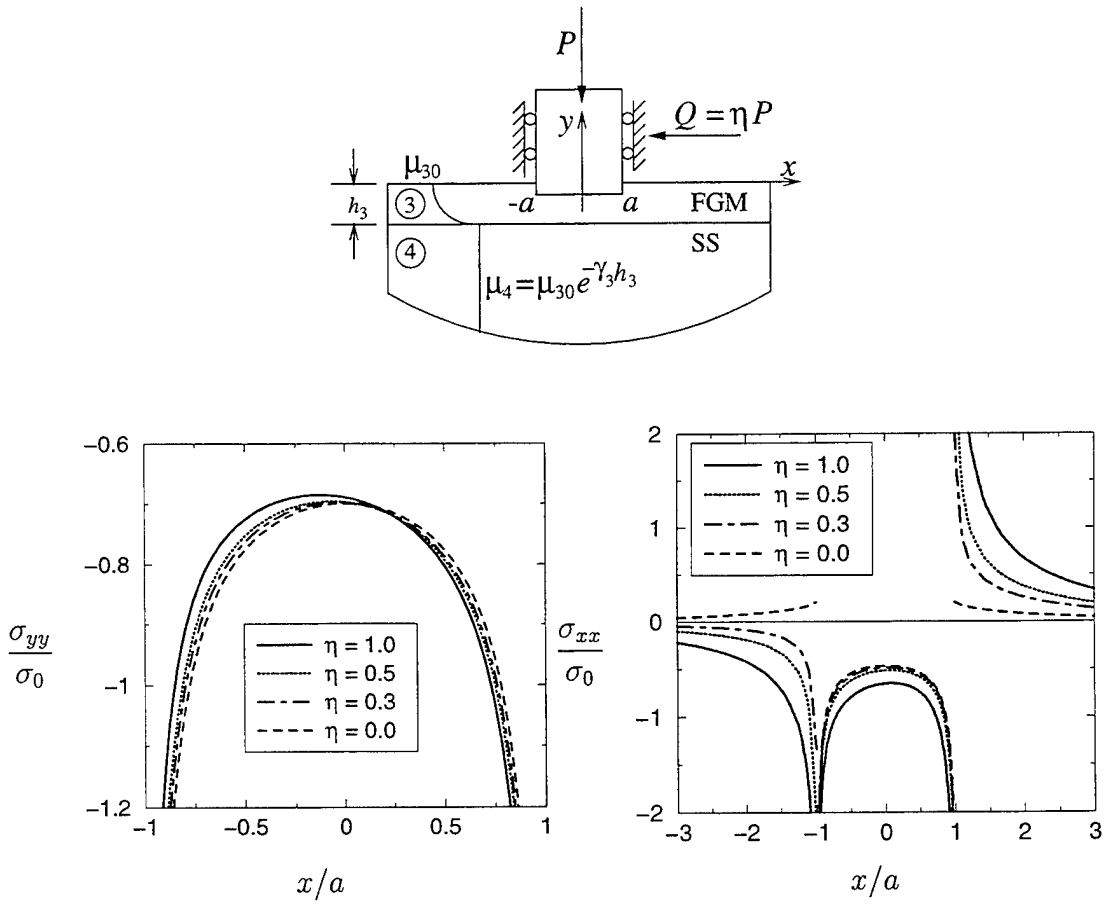

Figure 5.9: Stress distribution on the surface of the FGM coating loaded by a rigid flat stamp for various values of the coefficient of friction η, $\Gamma_3 = \dfrac{\mu_4}{\mu_{30}} = 8$, $\sigma_0 = \dfrac{P}{2a}$, $a/h_3 = 0.1$.

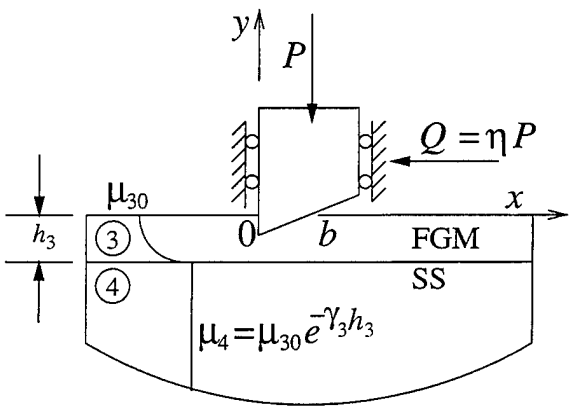

Figure 5.10: Geometry of the triangular stamp problem

5.2 The Triangular Stamp

Consider the stamp problem for the FGM layer bonded to a homogeneous substrate shown in Figure 5.10. The stamp profile is given as

$$v_3(x,0) = mx + C. \tag{5.41}$$

Therefore,

$$\frac{\partial}{\partial x} v_3(x,0) = m. \tag{5.42}$$

Letting

$$\begin{aligned} \sigma_{yy}(x,0) &= -p(x), \qquad \sigma_{xy}(x,0) = -\eta p(x), \qquad 0 < x < b, \\ \sigma_{yy}(x,0) &= \sigma_{xy}(x,0) = 0, \qquad\qquad\qquad\qquad x < 0, x > b, \end{aligned} \tag{5.43}$$

the integral equation (4.3) and the equilibrium equation (4.12) becomes

$$Ap(x) + \frac{1}{\pi}\int_0^b \left[-\frac{1}{t-x} + k_{31}(t,x) + \eta k_{32}(t,x)\right] p(t)dt = f_3(x), \tag{5.44}$$

$$\int_0^b p(t)dt = P, \tag{5.45}$$

where

$$A = \omega_3 \eta, \tag{5.46}$$

$$\omega_3 = \frac{\kappa_3 - 1}{\kappa_3 + 1}, \tag{5.47}$$

$$\lambda_3 = \frac{4\mu_{30}}{\kappa_3 + 1}, \tag{5.48}$$

$$f_3(x) = \lambda_3 \frac{\partial}{\partial x} v_3(x, 0) = \lambda_3 m. \tag{5.49}$$

Now, using the following change of variables in order to normalize the interval $(0, b)$

$$x = \frac{b}{2}(r + 1), \tag{5.50}$$

$$t = \frac{b}{2}(s + 1), \tag{5.51}$$

$$p(t) = \lambda_3 m \phi(s), \tag{5.52}$$

and using the relations (4.17)-(4.23) integral equation (5.44) and the equilibrium equation (5.45) become

$$A\phi(r) + \frac{1}{\pi} \int_{-1}^{1} \left[-\frac{1}{s - r} + k_{31}^*(s, r) + \eta k_{32}^*(s, r) \right] \phi(s) ds = 1, \tag{5.53}$$

$$\int_{-1}^{1} \phi(s) ds = \frac{2P}{\lambda_3 m b}, \tag{5.54}$$

where

$$k_{31}(s, r) = \frac{2}{b} k_{31}^*(s, r), \tag{5.55}$$

$$k_{32}(s, r) = \frac{2}{b} k_{32}^*(s, r). \tag{5.56}$$

Since the triangular stamp has a sharp corner at $x = 0$, and a smooth contact at $x = b$, from the physics of the problem we must require that α be positive and β be negative.

If $\eta > 0$ from equations (4.48) and (4.49) we have

$$\alpha = N + \frac{\theta}{\pi}, \quad \Longrightarrow \quad N = 0, \tag{5.57}$$

$$\beta = M - \frac{\theta}{\pi}, \quad \Longrightarrow \quad M = 0, \tag{5.58}$$

and for $\eta < 0$ from equations (4.56) and (4.57) it follows that

$$\alpha = N - \frac{\theta}{\pi}, \quad \Longrightarrow \quad N = 1, \tag{5.59}$$

$$\beta = M + \frac{\theta}{\pi}, \quad \Longrightarrow \quad M = -1. \tag{5.60}$$

The index of the integral equation is defined by and obtained as

$$\kappa_0 = -(\alpha + \beta) = -(N + M) = 0. \tag{5.61}$$

α and β then becomes

$$\begin{aligned} \eta > 0: &\quad \alpha = \theta/\pi, &\quad \beta = -\theta/\pi, \\ \eta = 0: &\quad \alpha = 0.5, &\quad \beta = -0.5, \\ \eta < 0: &\quad \alpha = 1 - \theta/\pi, &\quad \beta = -1 + \theta/\pi, \end{aligned} \tag{5.62}$$

where

$$\theta = \arctan \left| \frac{1}{A} \right|. \tag{5.63}$$

In Table 5.4 some values of α and β are given for various values of η.

Assuming a solution of the form

$$\phi(s) = w(s) \sum_{0}^{\infty} c_n P_n^{(\alpha,\beta)}(s), \tag{5.64}$$

$$w(s) = (1-s)^{\alpha} (1+s)^{\beta}, \tag{5.65}$$

considering the property of Jacobi Polynomials (A.6) and letting

$$\mathcal{K}_{3n}(r) = \frac{1}{\pi} \int_{-1}^{1} \left[k_{31}^*(s,r) + \eta k_{32}^*(s,r) \right] w(s) P_n^{(\alpha,\beta)}(s) ds, \tag{5.66}$$

Table 5.4: Values of α and β for the index, $\kappa_0 = 0$

η	α	β
-0.3	0.5272	-0.5272
-0.1	0.5091	-0.5091
0	0.5000	-0.5000
0.1	0.4909	-0.4909
0.3	0.4728	-0.4728

after truncating the series in (5.64) at N, the integral equation (5.53) becomes

$$\sum_{0}^{N} c_n \left[\frac{1}{\sin \pi\alpha} P_n^{(-\alpha,-\beta)}(r) + \mathcal{K}_{3n}(r) \right] = 1. \tag{5.67}$$

In this problem, after the application of a given load, one end of the contact length (i.e. b) is unknown. However for a given value of the contact length, equation (5.67) provides $N+1$ equations for $N+1$ unknown constants $(c_0, ..., c_N)$ as follows:

$$\sum_{0}^{N} c_n F_N(r_i) = 1, \qquad i = 1, ..., N+1, \tag{5.68}$$

where

$$F_N(r_i) = \frac{1}{\sin \pi\alpha} P_n^{(-\alpha,-\beta)}(r_i) + \mathcal{K}_{3n}, \tag{5.69}$$

and $r_i\,(i = 1, ..., N+1)$ are defined by

$$P_n^{(\alpha-1,\beta+1)}(r_i) = 0. \tag{5.70}$$

The relationship between P and b can be found from the equilibrium equation (5.54)

$$c_0\theta_0 = \frac{2P}{\lambda_3 m b}. \tag{5.71}$$

where θ_0 is given in (A.8)

$$\theta_0 = \frac{2\pi\alpha}{\sin \pi\alpha}. \tag{5.72}$$

The load versus contact relation can, therefore, be obtained from (5.71) as

$$\frac{P}{\mu_{30}m} = \frac{2c_0\theta_0}{\kappa_3+1}b.$$

The solution of the problem then becomes (5.52)

$$\begin{aligned} p(x) &= \lambda_3 m\phi(r) \\ &= \frac{4\mu_{30}m}{\kappa_3+1}\left(\frac{1-r}{1+r}\right)^{\alpha}\sum_{0}^{\infty}c_n P_n^{(\alpha,\beta)}(r). \end{aligned} \tag{5.73}$$

In nondimensional form, the contact stresses can be expressed as

$$\frac{\sigma_{3yy}(x,0)}{\mu_{30}m} = -\frac{4}{\kappa_3+1}\left(\frac{b-x}{x}\right)^{\alpha}\sum_{0}^{N}c_n P_n^{(\alpha,\beta)}(2x/b-1). \tag{5.74}$$

Defining

$$\sigma_{3xx}(x,0) = \lambda_3 m\psi(r) \tag{5.75}$$

the in-plane stresses, $\sigma_{3xx}(x,0)$ can be found by using equation (4.74), as follows:

$$\sigma_{3xx}(x,0) = \sigma(x) + \frac{2\eta}{\pi}\int_0^b \frac{\sigma(t)}{t-x}dt - \frac{2}{\pi}\int_0^b \left[k_{42}(t,x) + \eta k_{41}(t,x)\right]\sigma(t)\,dt, \tag{5.76}$$

Using equation (5.43), equation (5.76) becomes

$$\begin{aligned} \sigma_{3xx}(x,0) &= -p(x) - \frac{2\eta}{\pi}\int_0^b \frac{p(t)}{t-x}dt + \frac{2}{\pi}\int_0^b \left[k_{42}(t,x) + \eta k_{41}(t,x)\right]p(t)\,dt \\ &= \lambda_3 m\left[-\phi(r) - \frac{2\eta}{\pi}\int_{-1}^1 \frac{\phi(s)}{s-r}dt + \frac{2}{\pi}\int_{-1}^1 \left[k_{42}^*(s,r) + \eta k_{41}^*(s,r)\right]\phi(s)\,ds\right]. \end{aligned}$$

Thus, from (5.75) it may be seen that

$$\psi(r) = -\phi(r) - \frac{2\eta}{\pi}\int_{-1}^1 \frac{\phi(s)}{s-r}dt + \frac{2}{\pi}\int_{-1}^1 \left[k_{42}^*(s,r) + \eta k_{41}^*(s,r)\right]\phi(s)\,ds.$$

The nondimensional in-plane streses $\sigma_{3xx}(x,0)$ then becomes

$$\frac{\sigma_{3xx}(x,0)}{\mu_{30}m} = \frac{4}{\kappa_3+1}\psi(r).$$

Figure 5.11-5.12 give the stress distribution and the load versus contact length curves of an FGM coating loaded by a triangular stamp for various values of the stiffness ratio, $\Gamma_3 = \mu_4/\mu_{30}$ in the case of no friction and $b/h_3 = 0.2, 0.5$ respectively. The contact pressure σ_{yy} is bounded at $x = b$ and is zero. On the other hand, it is unbounded at the sharp edge $x = 0$. The σ_{yy} stresses for the stiff substrate and the stiffening coating(e.g.$\Gamma_3 = 8$) are greater than those of the soft substrate and the softening coating (e.g. $\Gamma_3 = 1/8$). The peculiar behavior of the in-plane stress σ_{xx} is such that it is tensile for $\Gamma_3 > 1$ and zero for $\Gamma_3 = 1$(homogeneous coating) and compressive for $\Gamma_3 < 1$ at $x < 0$. However at $x = b$ the σ_{xx} stresses have a peak as Γ_3 increases. Note that all the stress components are zero outside the contact zone for the homogenous coating. By looking at the load versus contact length curves we can deduce that for the same load P^* the contact length increases for the softening coating ($\Gamma_3 < 1$) and it decreases for the stiffening coating ($\Gamma_3 > 1$). Or in other words, for stiffening coatings $\Gamma_3 > 1$, it requires larger load to get the same contact length compared to the softening coatings ($\Gamma_3 > 1$). There is a linear relationship between the load and the contact length for the homogeneous coating. Also as the contact length b increases or the thickness of the coating h_3 decreases or in other words b/h_3 increases the magnitude of the contact stresses increase.

Figures 5.13-5.18 give the stress distribution and the load versus contact length curves of an FGM coating loaded by a triangular stamp for various values of the stiffness ratio, $\Gamma_3 = \mu_4/\mu_{30}$ by fixing the coefficient of friction, η and b/h_3. Again, the magnitude of σ_{yy} stresses increases as Γ_3 increases. The maximum tensile stress occurs at the trailing edge of the contact, $x = b$ for the stiffening coating $\Gamma_3 > 1$. Note that the homogeneous coating has also a peak at the trailing edge of the contact.

We now fix the stiffness ratio, Γ_3 and b/h to see the effect of the coefficient of friction on the contact stresses in Figures 5.19-5.20. For the stiffening coating on a

stiff substrate($\Gamma_3 = 8$) there is no significant change in the σ_{yy} stresses. However as η increases the σ_{xx} stresses increases at the trailing edge and are tensile. There is no significant change also in the load versus contact length curves due to the variation of the coefficient of friction. In the case of the softening coating on a soft substrate $\Gamma_3 = 1/8$ the behavior of the streses are the same except they are low in magnitude. The amount of load applied to the stamp P^* decreases as η increases for the same contact length b/h_3.

5.2.1 Stress intensity factor

The mode I stress intensity factor at the end of the stamp can be defined as

$$k_1(0) = \lim_{x \to 0} x^{\alpha} p(x) = \frac{4\mu_{30} m b^{\alpha}}{\kappa_3 + 1} \sum_{0}^{N} c_n P_n^{(\alpha,\beta)}(-1). \tag{5.77}$$

The non-dimensional stress intensity factor can be defined as

$$k_1^*(0) = \frac{k_1(0)}{\mu_{30} m b^{\alpha}} = \frac{4}{\kappa_3 + 1} \sum_{0}^{N} c_n P_n^{(\alpha,\beta)}(-1). \tag{5.78}$$

Tables 5.5-5.6 give the normalized stress intensity factor at the sharp end of the triangular punch according to the direction of application of the force Q by assuming $\nu = 0.3$. The stress intensity factor increases as Γ_3 increases. That is if the stiffness of the coating increases in the depth direction the stress intensity increases. The opposite is true for the coating whose stiffness decreases in the depth direction. Also for ($\Gamma_3 > 1$) the stress intensity factor increases as the coefficient of friction η increases, however for ($\Gamma_3 < 1$) the stress intensity factor decreases as the coefficient of friction η increases. Another point is the fact that for ($\Gamma_3 > 1$) stress intensity factor increase as b/h_3 increases however for ($\Gamma_3 < 1$) stress intensity factor decrease as b/h_3 increases.

Table 5.5: Stress intensity factors for triangular stamp, $b/h_3 = 0.2$

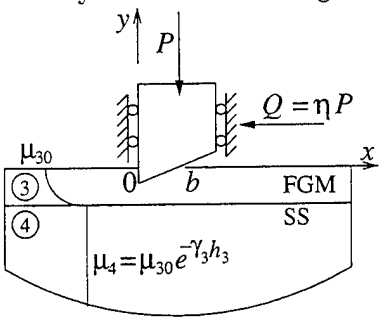

	$\eta = 0.0$	$\eta = 0.1$	$\eta = 0.3$	$\eta = 0.5$
	$\alpha = +0.5$ $\beta = -0.5$	$\alpha = +0.4909$ $\beta = -0.4909$	$\alpha = +0.4728$ $\beta = -0.4728$	$\alpha = +0.4548$ $\beta = -0.4548$
Γ_3	$\frac{k_1(0)}{\mu_{30} m b^\alpha}$	$\frac{k_1(0)}{\mu_{30} m b^\alpha}$	$\frac{k_1(0)}{\mu_{30} m b^\alpha}$	$\frac{k_1(0)}{\mu_{30} m b^\alpha}$
8	1.6247	1.6430	1.6751	1.7005
2	1.4976	1.5041	1.5128	1.5160
1	1.4286	1.4280	1.4234	1.4142
1/2	1.3550	1.3467	1.3279	1.3063
1/8	1.1912	1.1677	1.1224	1.0789

Table 5.6: Stress intensity factors for triangular stamp, $b/h_3 = 0.5$

	$\eta = 0.0$	$\eta = 0.1$	$\eta = 0.3$	$\eta = 0.5$
	$\alpha = +0.5$ $\beta = -0.5$	$\alpha = +0.4909$ $\beta = -0.4909$	$\alpha = +0.4728$ $\beta = -0.4728$	$\alpha = +0.4548$ $\beta = -0.4548$
Γ_3	$\frac{k_1(0)}{\mu_{30} m b^\alpha}$	$\frac{k_1(0)}{\mu_{30} m b^\alpha}$	$\frac{k_1(0)}{\mu_{30} m b^\alpha}$	$\frac{k_1(0)}{\mu_{30} m b^\alpha}$
8	2.1922	2.2358	2.3188	2.3951
2	1.6876	1.6976	1.7132	1.7228
1	1.4286	1.4280	1.4234	1.4142
1/2	1.1794	1.1736	1.1593	1.1418
1/8	0.7522	0.7470	0.7347	0.7203

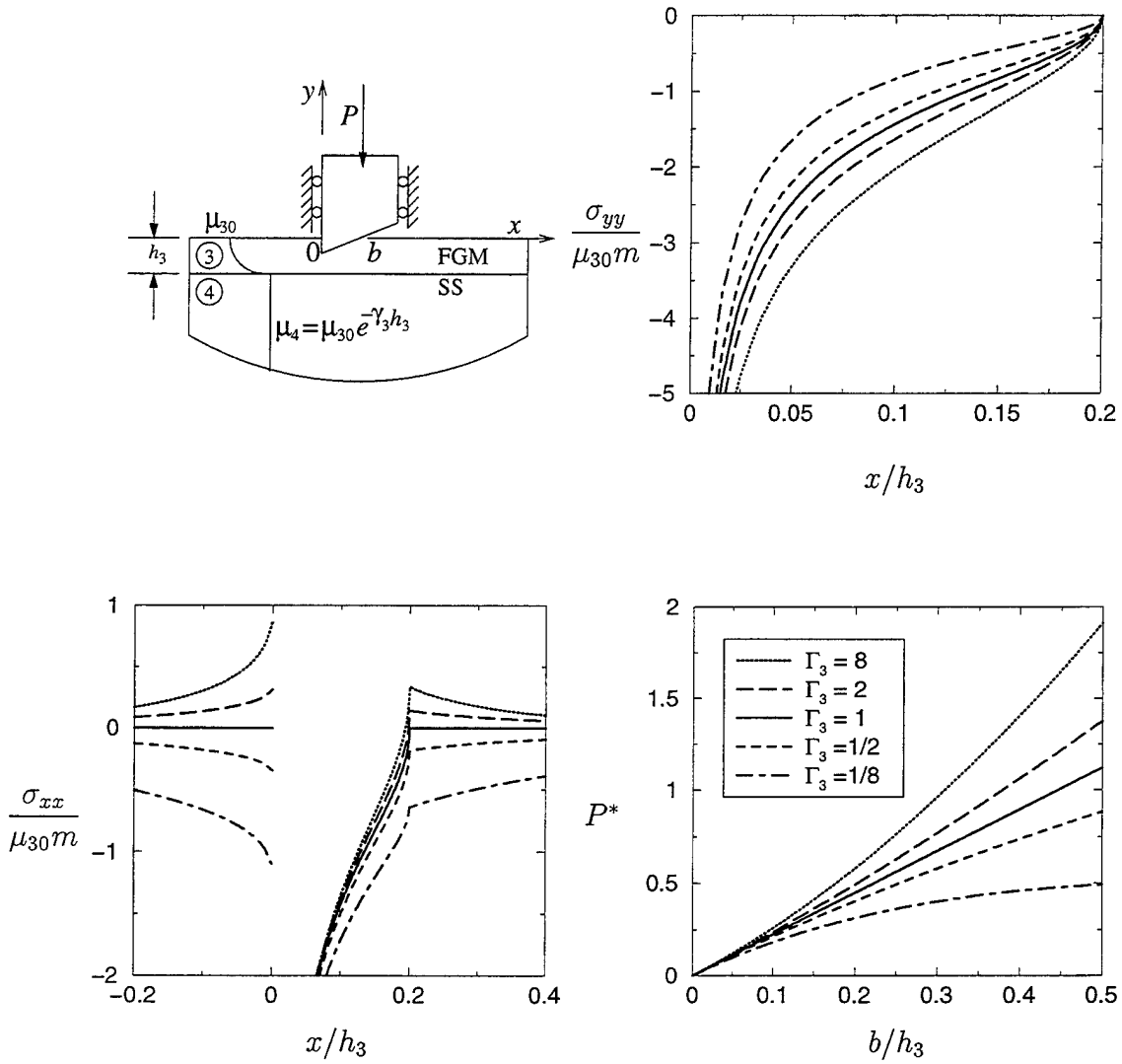

Figure 5.11: Stress distribution on the surface of an FGM coating loaded by a rigid triangular stamp for various values of the stiffness ratio, $\Gamma_3 = \mu_4/\mu_{30}$, $b/h_3 = 0.2$, $\eta = 0$, $P^* = P/(\mu_{30} m h_3)$.

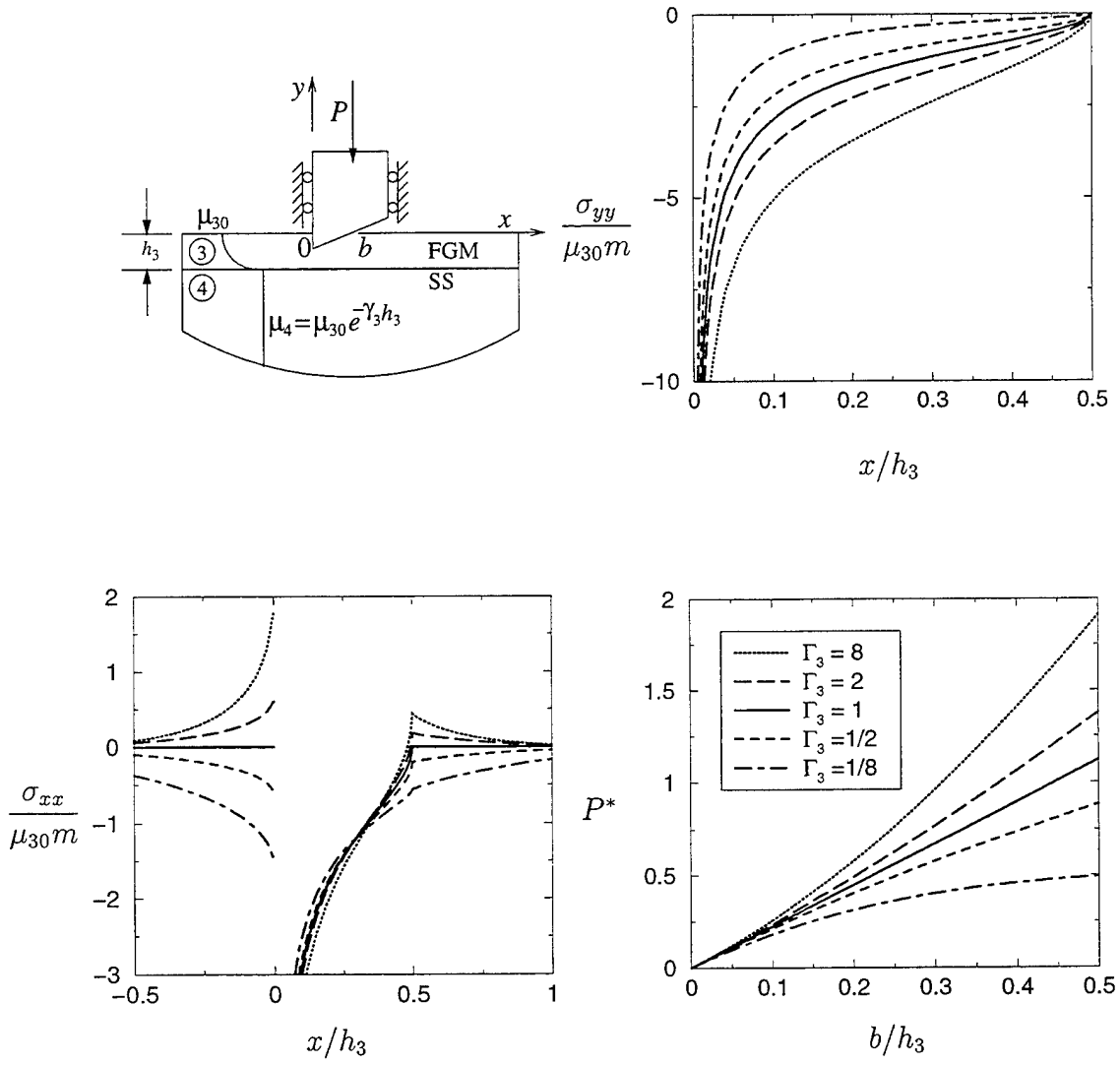

Figure 5.12: Stress distribution on the surface of an FGM coating loaded by a rigid triangular stamp for various values of the stiffness ratio, $\Gamma_3 = \mu_4/\mu_{30}$, $b/h_3 = 0.5$, $\eta = 0$, $P^* = P/(\mu_{30} m h_3)$.

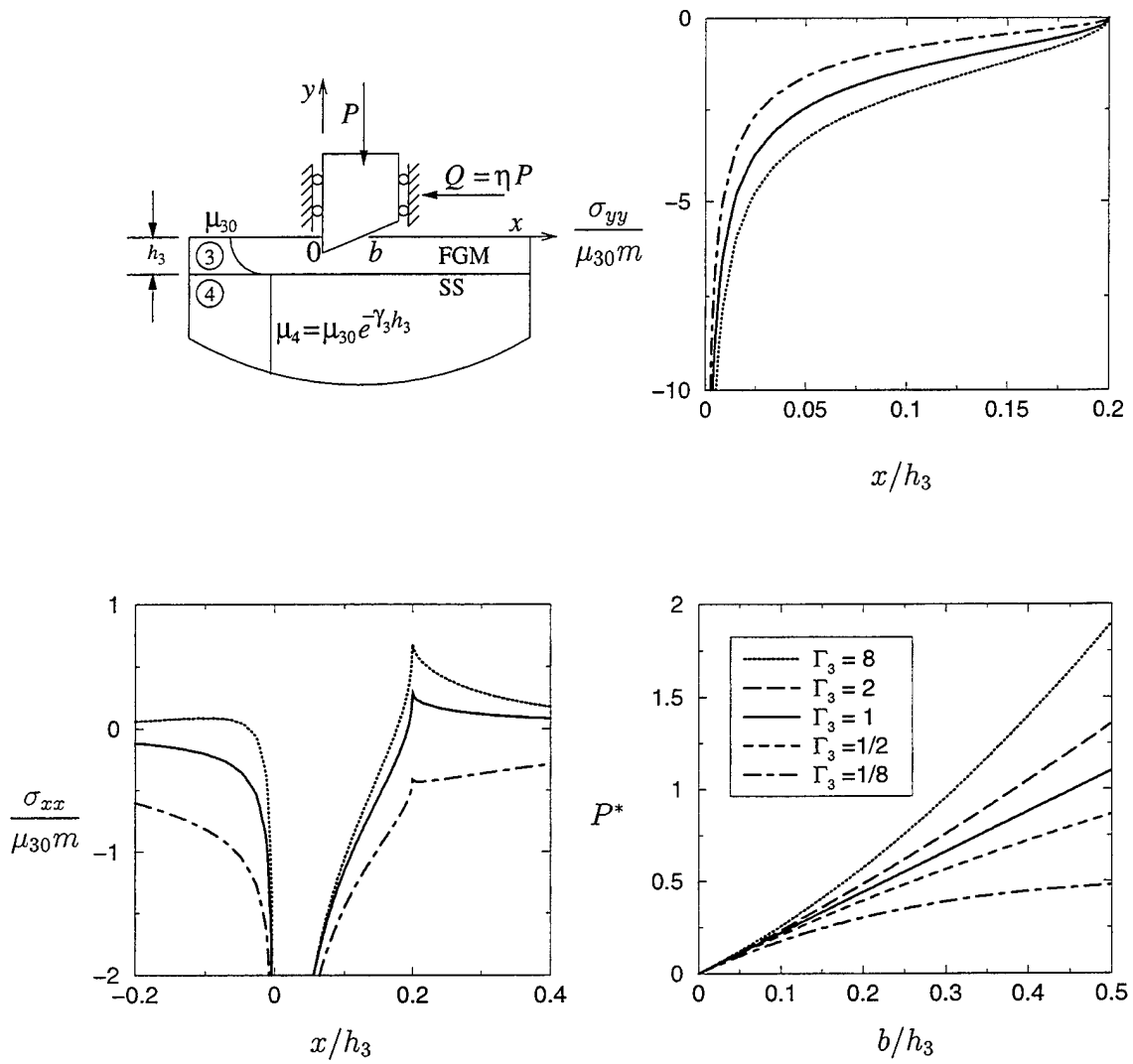

Figure 5.13: Stress distribution on the surface of an FGM coating loaded by a rigid triangular stamp for various values of the stiffness ratio, $\Gamma_3 = \mu_4/\mu_{30}$, $b/h_3 = 0.2$, $\eta = 0.1$, $P^* = P/(\mu_{30} m h_3)$.

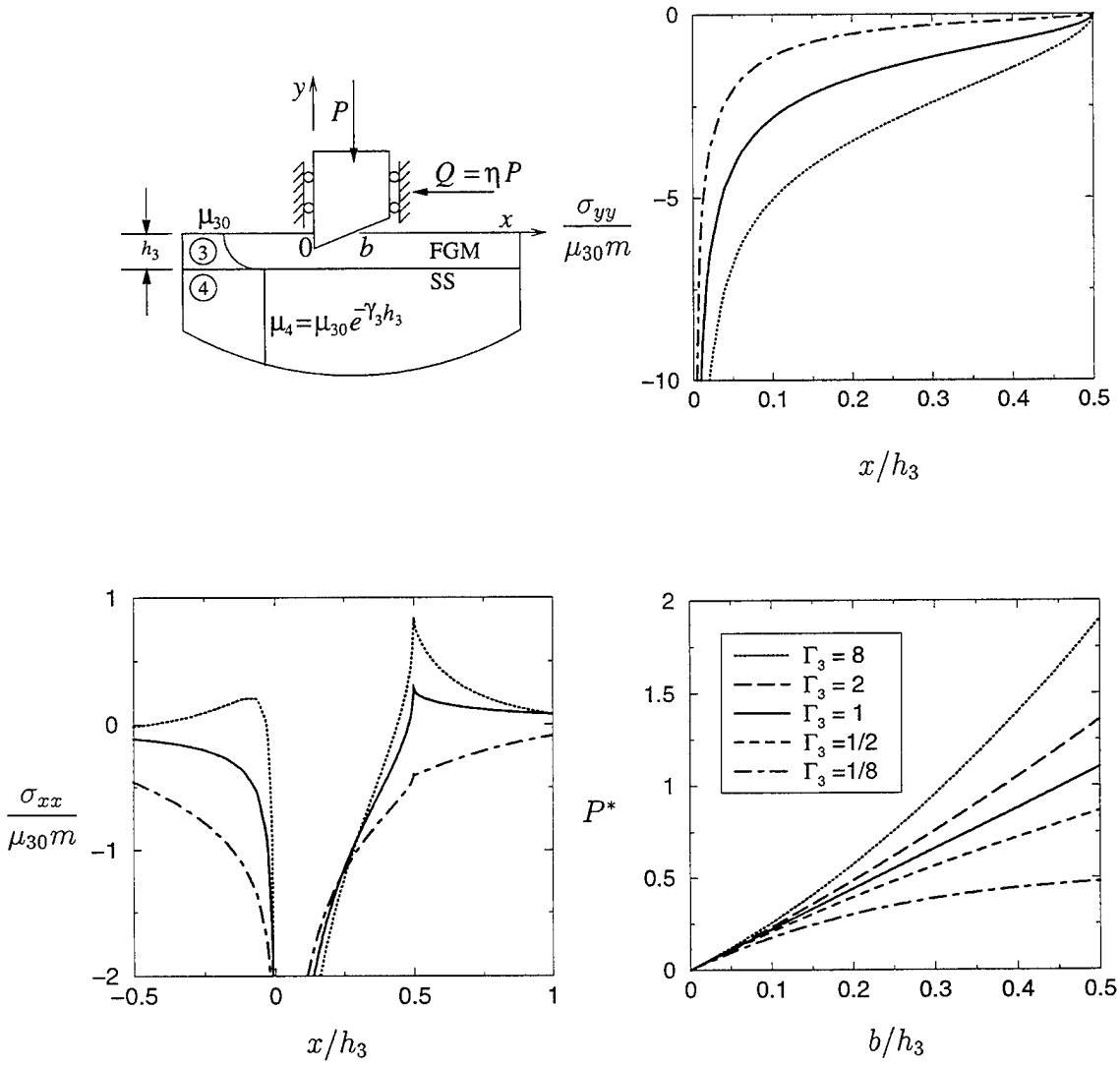

Figure 5.14: Stress distribution on the surface of an FGM coating loaded by a rigid triangular stamp for various values of the stiffness ratio, $\Gamma_3 = \mu_4/\mu_{30}$, $b/h_3 = 0.5$, $\eta = 0.1$, $P^* = P/(\mu_{30} m h_3)$.

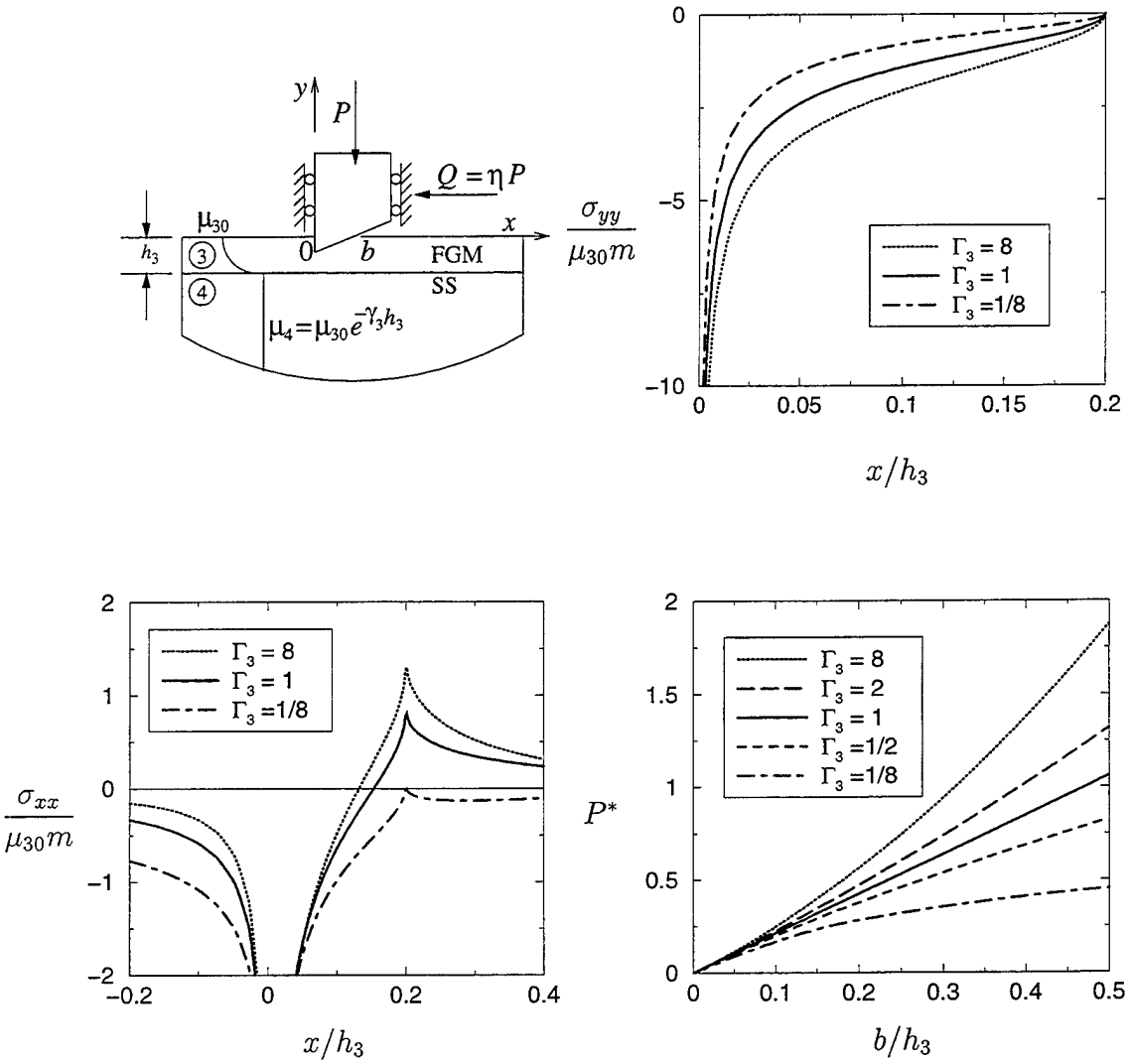

Figure 5.15: Stress distribution on the surface of an FGM coating loaded by a rigid triangular stamp for various values of the stiffness ratio, $\Gamma_3 = \mu_4/\mu_{30}$, $b/h_3 = 0.2$, $\eta = 0.3$, $P^* = P/(\mu_{30} m h_3)$.

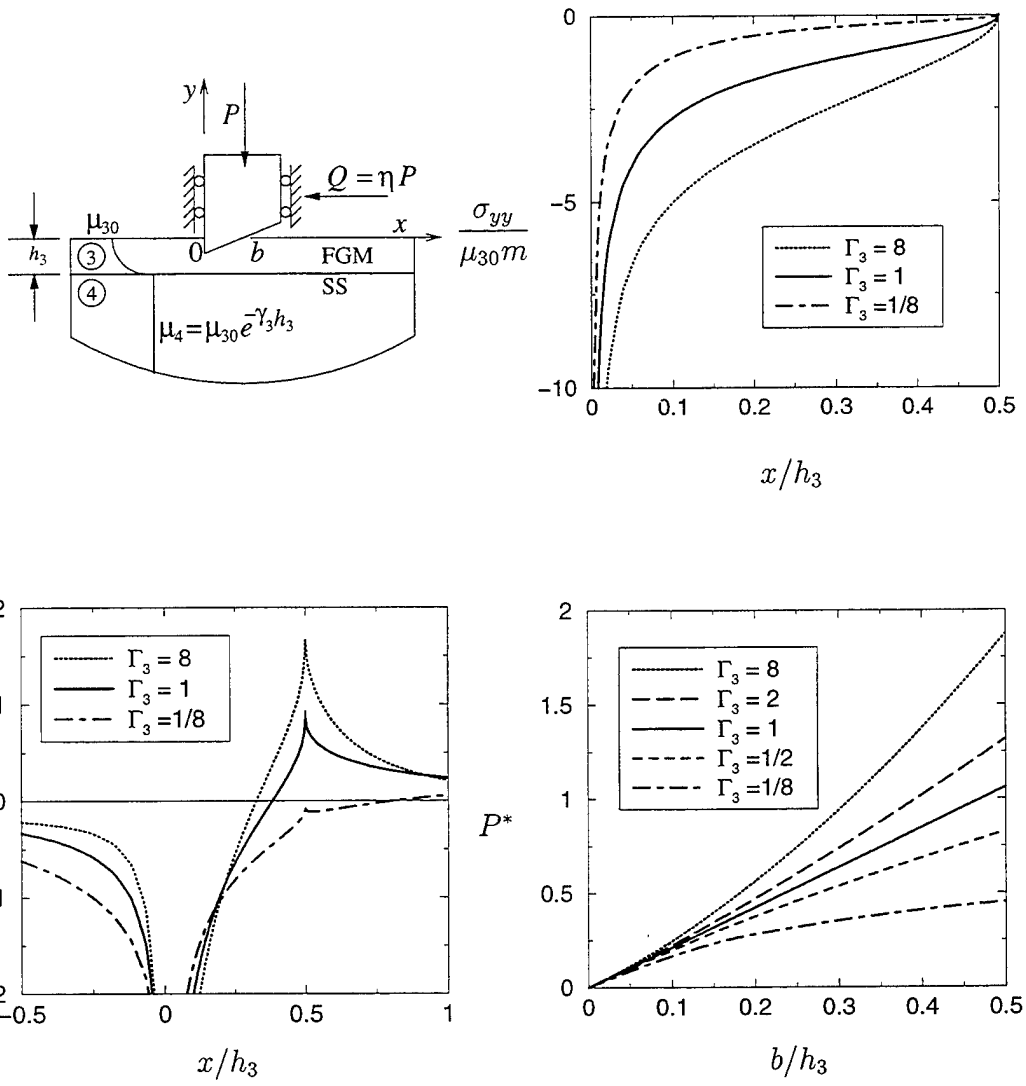

Figure 5.16: Stress distribution on the surface of an FGM coating loaded by a rigid triangular stamp for various values of the stiffness ratio, $\Gamma_3 = \mu_4/\mu_{30}$, $b/h_3 = 0.5$, $\eta = 0.3$, $P^* = P/(\mu_{30} m h_3)$.

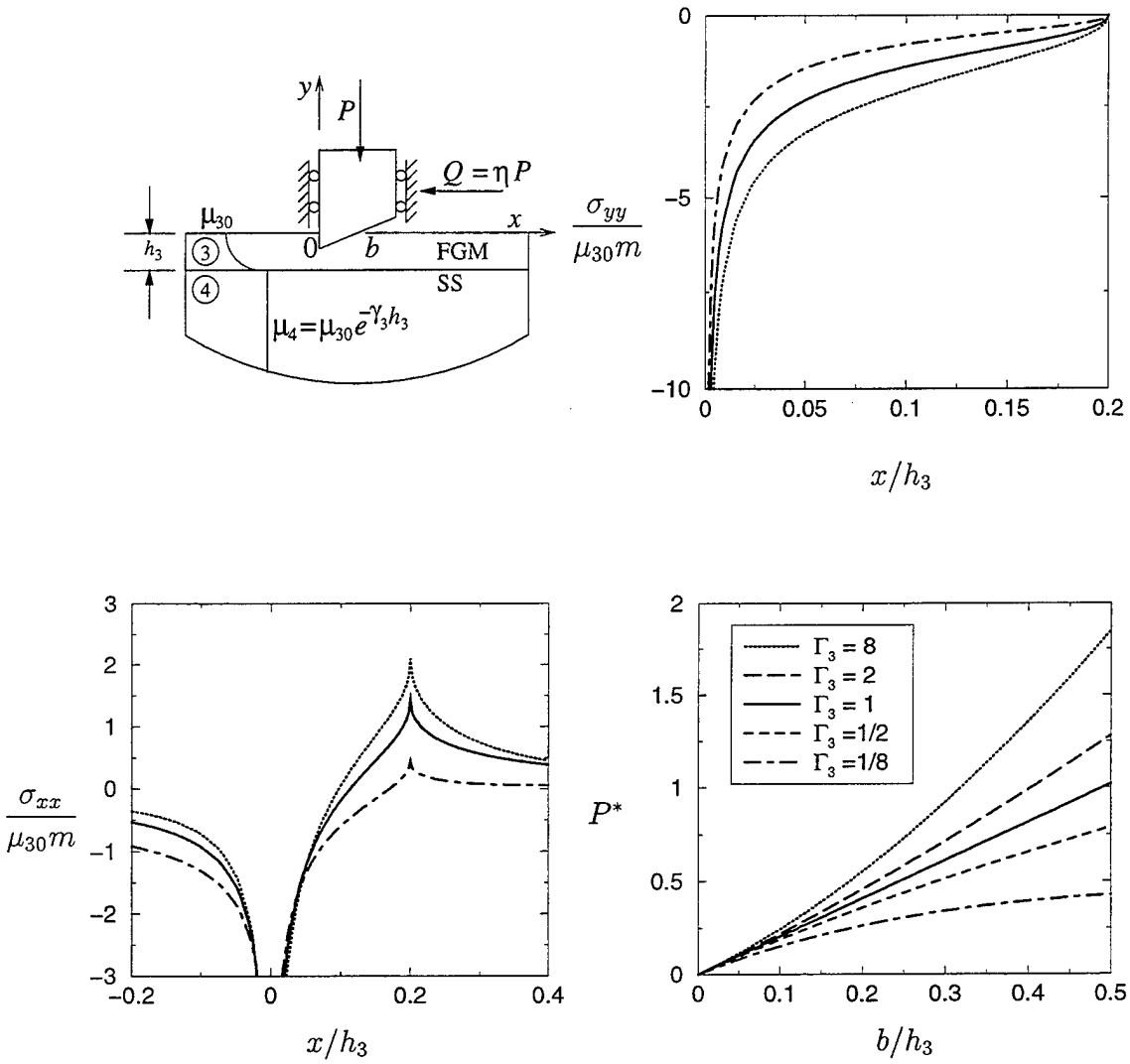

Figure 5.17: Stress distribution on the surface of an FGM coating loaded by a rigid triangular stamp for various values of the stiffness ratio, $\Gamma_3 = \mu_4/\mu_{30}$, $b/h_3 = 0.2$, $\eta = 0.5$, $P^* = P/(\mu_{30} m h_3)$.

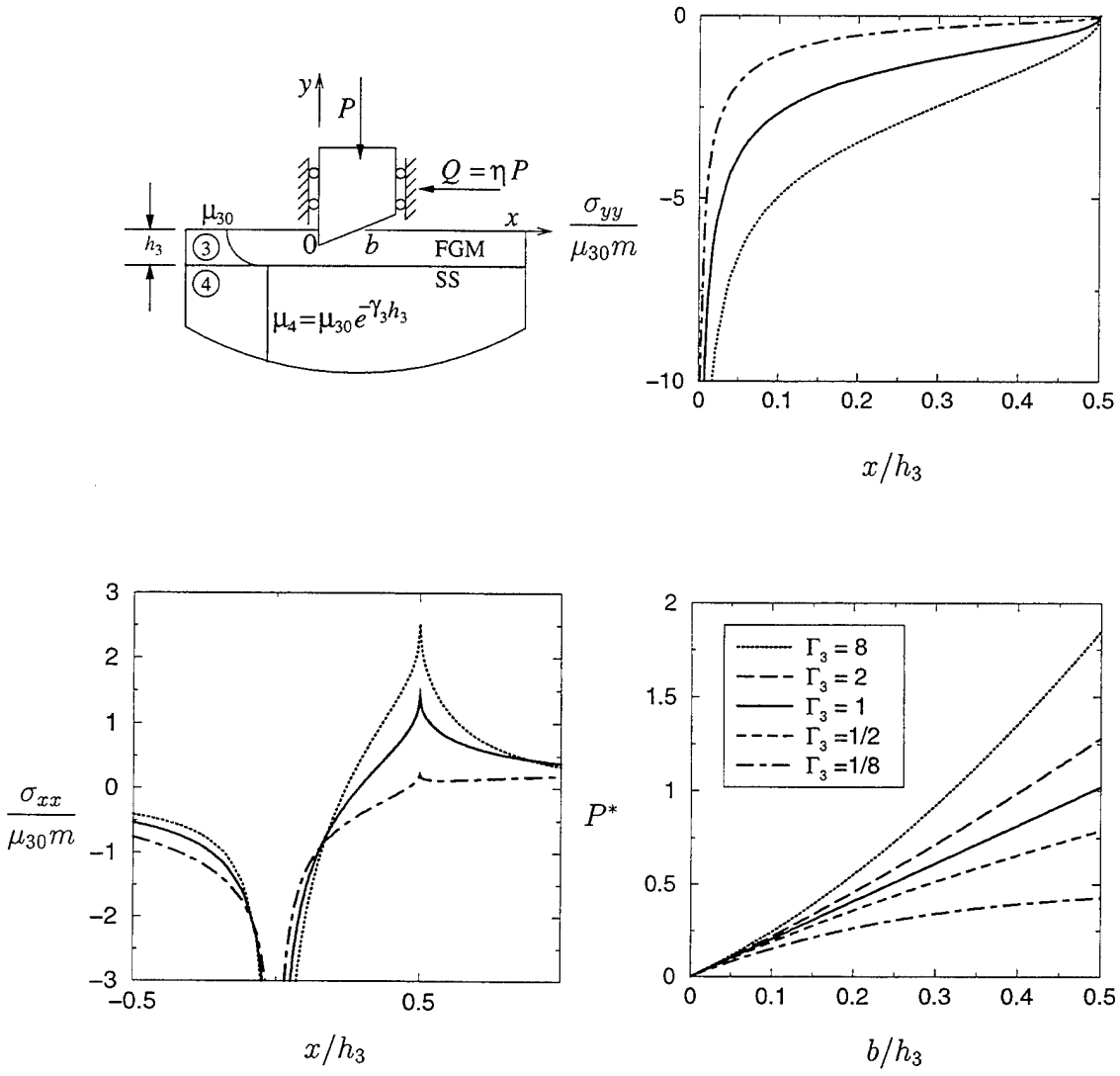

Figure 5.18: Stress distribution on the surface of an FGM coating loaded by a rigid triangular stamp for various values of the stiffness ratio, $\Gamma_3 = \mu_4/\mu_{30}$, $b/h_3 = 0.5$, $\eta = 0.5$, $P^* = P/(\mu_{30} m h_3)$.

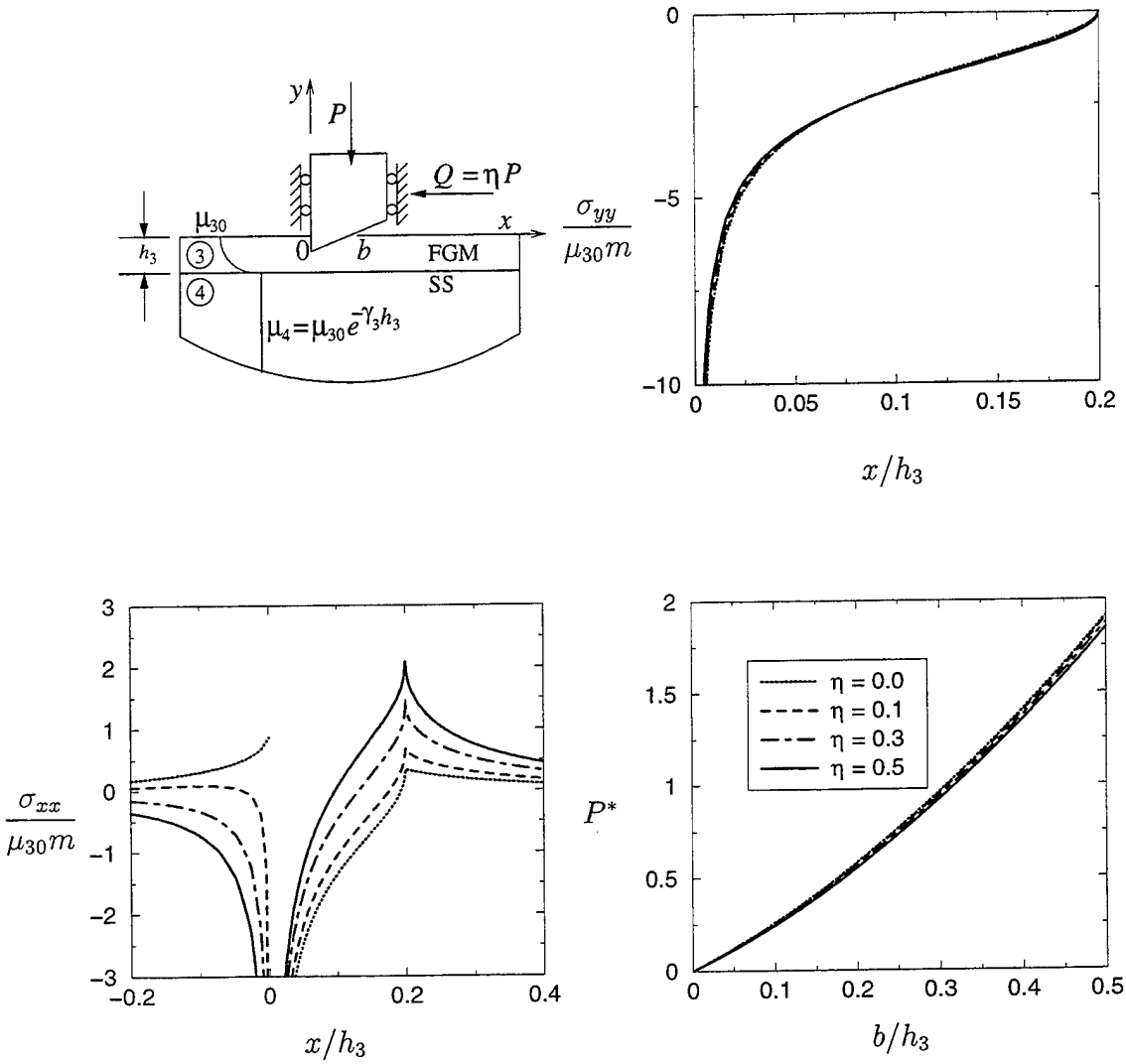

Figure 5.19: Stress distribution on the surface of an FGM coating loaded by a rigid triangular stamp for various values of the coefficient of friction, η, $\Gamma_3 = \mu_4/\mu_{30} = 8$, $b/h_3 = 0.2$, $P^* = P/(\mu_{30} m h_3)$.

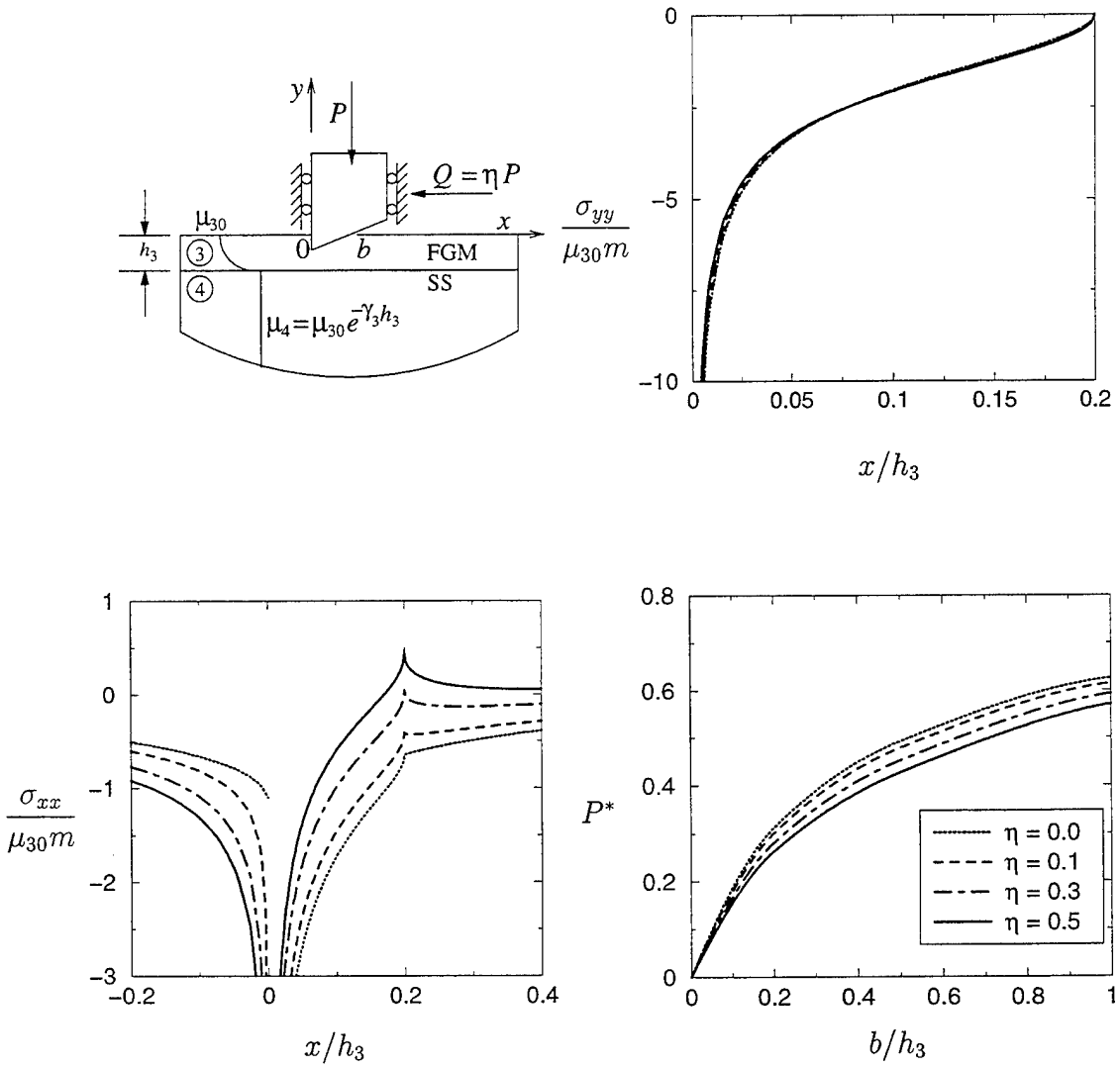

Figure 5.20: Stress distribution on the surface of an FGM coating loaded by a rigid triangular stamp for various values of the coefficient of friction, η, $\Gamma_3 = \mu_4/\mu_{30} = 1/8$, $b/h_3 = 0.2$, $P^* = P/(\mu_{30} m h_3)$.

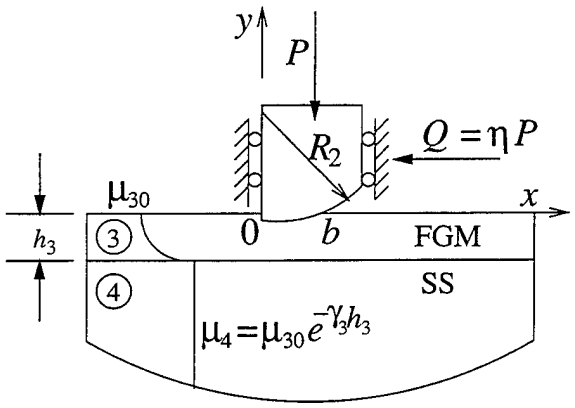

Figure 5.21: Geometry of the semi-circular stamp problem

5.3 The Semi-circular Stamp

The semi-circlar stamp shown in Figure 5.21 has a profile of the form

$$v_3(x,0) = -v_{30} + \frac{x^2}{2R_2}. \tag{5.79}$$

Thus,

$$\frac{\partial}{\partial x} v_3(x,0) = \frac{x}{R_2}. \tag{5.80}$$

The tractions on the boundary are defined as:

$$\begin{aligned} \sigma_{3yy}(x,0) &= -p(x), \qquad \sigma_{3xy}(x,0) = -\eta p(x), \qquad 0 < x < b, \\ \sigma_{3yy}(x,0) &= \sigma_{3xy}(x,0) = 0, \qquad\qquad\qquad\qquad x < 0, x > b. \end{aligned} \tag{5.81}$$

In order to solve the integral equation the limits of integration have to be normalized. Now setting

$$t = t^* R_2, \tag{5.82}$$

$$x = x^* R_2, \tag{5.83}$$

$$b = b^* R_2, \tag{5.84}$$

$$p(t) = p^*(t^*), \tag{5.85}$$

$$k_{31}(t,x) = \frac{1}{R_2} k_{31}^*(t^*,x^*), \tag{5.86}$$

$$k_{32}(t,x) = \frac{1}{R_2} k_{32}^*(t^*,x^*), \tag{5.87}$$

the integral equation (4.3) and the equilibrium equation (4.12) become

$$Ap^*(x^*) + \frac{1}{\pi}\int_0^{b^*} \left[-\frac{1}{t^*-x^*} + k_{31}^*(t^*,x^*) + \eta k_{32}^*(t^*,x^*) \right] p^*(t^*)dt^* = f_3^*(r), \tag{5.88}$$

$$\int_0^{b^*} p^*(t^*)dt^* = \frac{P}{R_2}. \tag{5.89}$$

Further normalizing the integration limit from $(0, b^*)$ to $(-1, 1)$ by the following change of variables

$$t^* = \frac{b^*}{2}(s+1), \qquad -1 < s < 1 \tag{5.90}$$

$$x^* = \frac{b^*}{2}(r+1), \qquad -1 < r < 1 \tag{5.91}$$

$$p^*(t^*) = \lambda_3 \frac{b^*}{2}\phi(s), \tag{5.92}$$

$$k_{31}^*(t^*,x^*) = \frac{2}{b^*}\widehat{k}_{31}(s,r), \tag{5.93}$$

$$k_{32}^*(t^*,x^*) = \frac{2}{b^*}\widehat{k}_{32}(s,r), \tag{5.94}$$

and using the relations (4.17)-(4.23) integral equation (5.88) and the equilibrium equation (5.89) become

$$A\phi(r) + \frac{1}{\pi}\int_{-1}^{1} \left[-\frac{1}{s-r} + \widehat{k}_{31}(s,r) + \eta\widehat{k}_{32}(s,r) \right] \phi(s)ds = f_3^*(r), \tag{5.95}$$

$$\int_{-1}^{1} \phi(s)ds = \frac{4}{b^{*2}} \frac{P}{\lambda_3 R_2}, \tag{5.96}$$

where

$$A = \frac{\kappa_3 - 1}{\kappa_3 + 1}\eta, \tag{5.97}$$

$$\lambda_3 = \frac{4\mu_{30}}{\kappa_3 + 1}, \tag{5.98}$$

$$f_3^*(r) = r + 1. \tag{5.99}$$

Since the index of the problem, $\kappa_0 = 0$, is the same as in the triangular stamp, the fundamental solution is also the same.

Assuming a solution of the form

$$\phi(s) = w(s) \sum_{0}^{\infty} c_n P_n^{(\alpha,\beta)}(s), \tag{5.100}$$

$$w(s) = (1-s)^{\alpha} (1+s)^{\beta}, \tag{5.101}$$

considering the property of Jacobi Polynomials (A.6), and letting

$$\mathcal{K}_{3n}(r) = \frac{1}{\pi} \int_{-1}^{1} \left[\widehat{k}_{31}(s,r) + \eta \widehat{k}_{32}(s,r) \right] w(s) P_n^{(\alpha,\beta)}(s) ds, \tag{5.102}$$

after truncating the series in (5.100) at N, (5.95) becomes

$$\sum_{0}^{N} c_n \left[\frac{1}{\sin \pi\alpha} P_n^{(-\alpha,-\beta)}(r) + \mathcal{K}_{3n}(r) \right] = r + 1. \tag{5.103}$$

By using a method of collocation, equation (5.103) provides $N+1$ equations for $N+1$ unknown constants $c_0, ..., c_N$ as follows:

$$\sum_{0}^{N} c_n F_N(r_i) = r_i + 1, \qquad i = 1, ..., N+1, \tag{5.104}$$

$$F_N(r_i) = \frac{1}{\sin \pi\alpha} P_n^{(-\alpha,-\beta)}(r_i) + \mathcal{K}_{3n}(r_i), \tag{5.105}$$

where r_i $(i = 1, ..., N+1)$ are defined by

$$P_n^{(\alpha-1,\beta+1)}(r_i) = 0. \tag{5.106}$$

The relationship between P and b can be found from the equilibrium equation (5.96) and using the orthogonality of Jacobi polynomials (A.7) as follows:

$$c_0\theta_0 = \frac{4}{b^{*2}}\frac{P}{\lambda_3 R_2}, \tag{5.107}$$

where from (A.8)

$$\theta_0 = \frac{2\pi\alpha}{\sin\pi\alpha}. \tag{5.108}$$

The load versus contact area relation can, therefore, be obtained from (5.107) as

$$P^* = \frac{P}{\mu_{30}R_2} = \frac{c_0\theta_0}{\kappa_3+1}b^{*2}. \tag{5.109}$$

The unknown b^* can then be found as follows:

$$b^* = \frac{b}{R_2} = \sqrt{\frac{\kappa_3+1}{c_0\theta_0}P^*}. \tag{5.110}$$

The solution then becomes

$$\begin{aligned} p^*(t^*) &= \frac{\lambda_3}{2}b^*\phi(s), \\ &= \frac{2\mu_{30}}{(\kappa_3+1)}b^*\left(\frac{b^*-t^*}{t^*}\right)^{\alpha}\sum_{n=0}^{1}c_nP_n^{(\alpha,\beta)}\left(\frac{2t^*}{b^*}-1\right). \end{aligned} \tag{5.111}$$

In Nondimensional form the contact stresses become

$$\frac{\sigma_{yy}(x^*,0)}{\mu_{30}} = -\frac{2}{\kappa_3+1}b^*\left(\frac{b^*-x^*}{x^*}\right)^{\alpha}\sum_{0}^{N}c_nP_n^{(\alpha,\beta)}(2x^*/b^*-1), \tag{5.112}$$

$$\sigma_{xy}(x^*,0) = \eta\sigma_{yy}(x^*,0). \tag{5.113}$$

Defining

$$\sigma_{3xx}(x,0) = \lambda_3\frac{b^*}{2}\psi(r), \tag{5.114}$$

the in-plane stress, $\sigma_{3xx}(x,0)$ can be found by using equation (4.74) as

$$\sigma_{3xx}(x,0) = \sigma(x) + \frac{2\eta}{\pi}\int_0^b\frac{\sigma(t)}{t-x}dt - \frac{2}{\pi}\int_0^b\left[k_{42}(t,x)+\eta k_{41}(t,x)\right]\sigma(t)\,dt. \tag{5.115}$$

Using equation (5.81), equation (5.115) becomes

$$\begin{aligned}\sigma_{3xx}(x,0) &= -p(x) - \frac{2\eta}{\pi}\int_0^b \frac{p(t)}{t-x}dt + \frac{2}{\pi}\int_0^b \left[k_{42}(t,x) + \eta k_{41}(t,x)\right] p(t)\,dt \\ &= \lambda_3 \frac{b^*}{2}\left[-\phi(r) - \frac{2\eta}{\pi}\int_{-1}^1 \frac{\phi(s)}{s-r}dt + \frac{2}{\pi}\int_{-1}^1 \left[k_{42}^*(s,r) + \eta k_{41}^*(s,r)\right]\phi(s)\,ds\right].\end{aligned}$$

Therefore, from (5.114) it is seen that

$$\psi(r) = -\phi(r) - \frac{2\eta}{\pi}\int_{-1}^1 \frac{\phi(s)}{s-r}dt + \frac{2}{\pi}\int_{-1}^1 \left[k_{42}^*(s,r) + \eta k_{41}^*(s,r)\right]\phi(s)\,ds. \qquad (5.116)$$

Thus, the nondimensional in-plane stress $\sigma_{3xx}(x,0)$ may be obtained from (5.114) and (5.116) as follows

$$\frac{\sigma_{3xx}(x,0)}{\mu_{30}} = \frac{2}{\kappa_3+1} b^* \psi(r).$$

Some results showing the effect of the stiffness ratio, $\Gamma_3 = \mu_4/\mu_{30}$ on the stress distribution and the load versus contact length are given in Figures 5.22-5.24 for an FGM coating loaded by a semi-circular stamp in the case of no friction and $b/h_3 = 0.01, 0.025, 0.05$ respectively. The stress σ_{yy} for the stiff substrate and the stiffening coating($\Gamma_3 = 8$) are greater than those of the soft substate and the softening coating ($\Gamma_3 = 1/8$). The in-plane stress σ_{xx} is tensile for $\Gamma_3 > 1$, zero for $\Gamma_3 = 1$(homogeneous coating) and compressive for $\Gamma_3 < 1$ for $x < 0$ as in the triangular stamp case. At $x = b$ the σ_{xx} take a peak as Γ_3 increases. Note that all the stress components are zero outside the contact zone for the homogenous coating. By looking at the load versus contact length curves we can deduce that for the same load P^* the contact length increases for the softening coating ($\Gamma_3 < 1$) and it decreases for the stiffening coating ($\Gamma_3 > 1$). There is a parabolic relationship between the load and the contact length for the homogeneous coating. Also as the contact length b increases or the thickness of the coating h_3 decreases or R_2 decreases, the magnitude of the contact stresses increase.

Figures 5.25-5.38 give the stress distribution and the load versus contact length curves for an FGM coating loaded by a semi-circular stamp for various values of the stiffness ratio, $\Gamma_3 = \mu_4/\mu_{30}$ by fixing the coefficient of friction, $\eta = 0.1, 0.3, 0.5$ and $b/R_2 = 0.01, 0.025, 0.05$ and $R_2/h_3 = 20$. Again, the magnitude of σ_{yy} increases as Γ_3 increases. The maximum tensile stress occurs at the trailing edge of the contact region, $x = b$ for the stiffening coating $\Gamma_3 > 1$. Note that the homogeneous coating has also a peak at the trailing edge of the contact.

We now fix the stiffness ratio, Γ_3 and b/h to see the effect of the coefficient of friction on the contact stresses. The results are given in Figures 5.37-5.38. For the stiffening coating on a stiff substrate($\Gamma_3 = 8$) there is no significant change in σ_{yy}. However, as η increases σ_{xx} increases at the trailing edge and are tensile. There is no significant change also in the load versus contact length curves due to the variation of the coefficient of friction. In the case of the softening coating on a soft substrate $\Gamma_3 = 1/8$ the behaviour of the streses are the same except they are low in magnitude. The amount of load applied to the stamp P^* decreses as η increases for the same contact length b/R_2.

5.3.1 Stress intensity factor

The mode I stress intensity factor at the end of the stamp, $x = 0$, can be defined and expressed as

$$k_1(0) = \lim_{x\to 0} x^{\alpha} p(x) = \frac{2\mu_{30}}{\kappa_3 + 1} \frac{b^{1+\alpha}}{R_2} \lim_{x\to 0} \sum_{0}^{N} c_n P_n^{(\alpha,\beta)}(-1). \tag{5.117}$$

The non-dimensional stress intensity factor then becomes

$$k_1^*(0) = \frac{k_1(0)}{(\mu_{30} b^{1+\alpha})/R_2} = \frac{2}{\kappa_3 + 1} \sum_{0}^{N} c_n P_n^{(\alpha,\beta)}(-1). \tag{5.118}$$

Tables 5.7-5.9 give the normalized stress intensity factors at the sharp end of the semi-circular punch according to the direction of application of the force Q by

Table 5.7: Stress intensity factors for semi-circular stamp, $b/R_2 = 0.01$, $R_2/h_3 = 20$

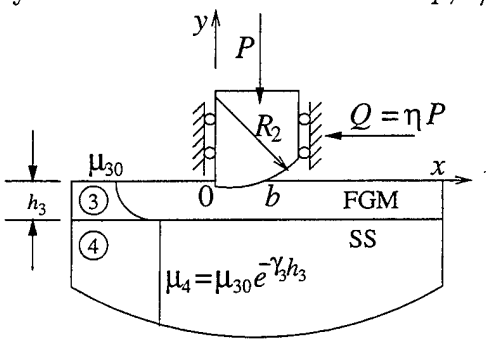

	$\eta = 0.0$	$\eta = 0.1$	$\eta = 0.3$	$\eta = 0.5$
	$\alpha = +0.5$ $\beta = -0.5$	$\alpha = +0.4909$ $\beta = -0.4909$	$\alpha = +0.4728$ $\beta = -0.4728$	$\alpha = +0.4548$ $\beta = -0.4548$
Γ_3	$\frac{k_1(0)}{(\mu_{30}b^{1+\alpha})/R_2}$	$\frac{k_1(0)}{(\mu_{30}b^{1+\alpha})/R_2}$	$\frac{k_1(0)}{(\mu_{30}b^{1+\alpha})/R_2}$	$\frac{k_1(0)}{(\mu_{30}b^{1+\alpha})/R_2}$
8	0.8123	0.8119	0.8082	0.8007
2	0.7488	0.7404	0.7214	0.6998
1	0.7143	0.7010	0.6729	0.6432
1/2	0.6775	0.6588	0.6209	0.5829
1/8	0.5956	0.5656	0.5087	0.4558

assuming $\nu = 0.3$. The stress intensity factor increases as Γ_3 increases. That is if the stiffness of the coating increases in the depth direction the stress intensity factor increases. The opposite is true for the coating whose stiffness decreases in the depth direction.

Table 5.8: Stress intensity factors for semi-circular stamp, $b/R_2 = 0.025$, $R_2/h_3 = 20$

	$\eta = 0.0$	$\eta = 0.1$	$\eta = 0.3$	$\eta = 0.5$
	$\alpha = +0.5$ $\beta = -0.5$	$\alpha = +0.4909$ $\beta = -0.4909$	$\alpha = +0.4728$ $\beta = -0.4728$	$\alpha = +0.4548$ $\beta = -0.4548$
Γ_3	$\frac{k_1(0)}{(\mu_{30}b^{1+\alpha})/R_2}$	$\frac{k_1(0)}{(\mu_{30}b^{1+\alpha})/R_2}$	$\frac{k_1(0)}{(\mu_{30}b^{1+\alpha})/R_2}$	$\frac{k_1(0)}{(\mu_{30}b^{1+\alpha})/R_2}$
8	0.9336	0.9411	0.9528	0.9603
2	0.7914	0.7847	0.7688	0.7500
1	0.7143	0.7010	0.6729	0.6432
1/2	0.6342	0.6157	0.5783	0.5408
1/8	0.4725	0.4501	0.4066	0.3653

Table 5.9: Stress intensity factors for semi-circular stamp, $b/R_2 = 0.05$, $R_2/h_3 = 20$

	$\eta = 0.0$	$\eta = 0.1$	$\eta = 0.3$	$\eta = 0.5$
	$\alpha = +0.5$ $\beta = -0.5$	$\alpha = +0.4909$ $\beta = -0.4909$	$\alpha = +0.4728$ $\beta = -0.4728$	$\alpha = +0.4548$ $\beta = -0.4548$
Γ_3	$\frac{k_1(0)}{(\mu_{30}b^{1+\alpha})/R_2}$	$\frac{k_1(0)}{(\mu_{30}b^{1+\alpha})/R_2}$	$\frac{k_1(0)}{(\mu_{30}b^{1+\alpha})/R_2}$	$\frac{k_1(0)}{(\mu_{30}b^{1+\alpha})/R_2}$
8	1.0961	1.1096	1.1336	1.1533
2	0.8438	0.8367	0.8201	0.8005
1	0.7143	0.7010	0.6729	0.6432
1/2	0.5897	0.5739	0.5415	0.5086
1/8	0.3761	0.3633	0.3374	0.3116

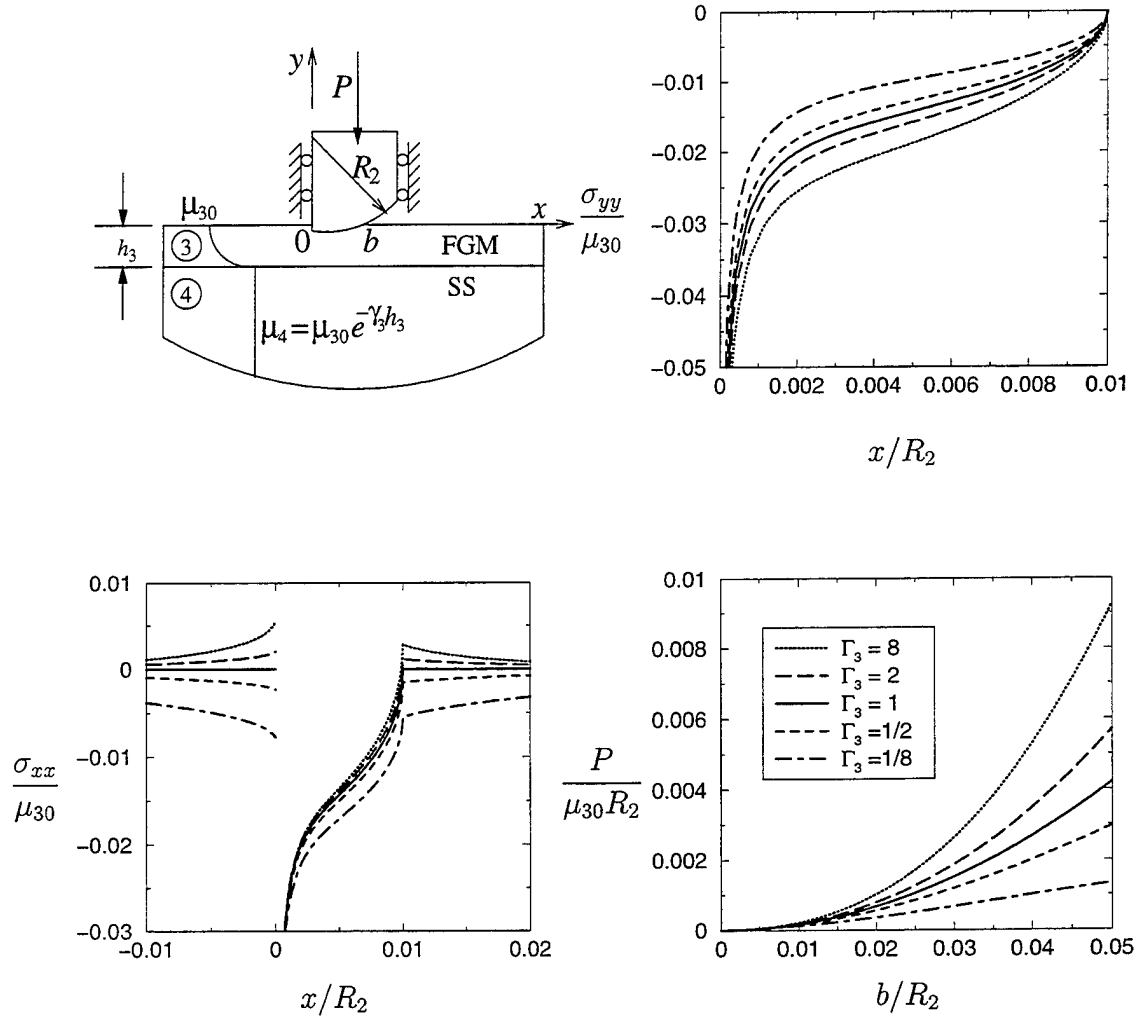

Figure 5.22: Stress distribution on the surface of an FGM coating loaded by a rigid semi-circular stamp for various values of the stiffness ratio, $\Gamma_3 = \mu_4/\mu_{30}$, $b/R_2 = 0.01$, $R_2/h_3 = 20$, $\eta = 0.0$.

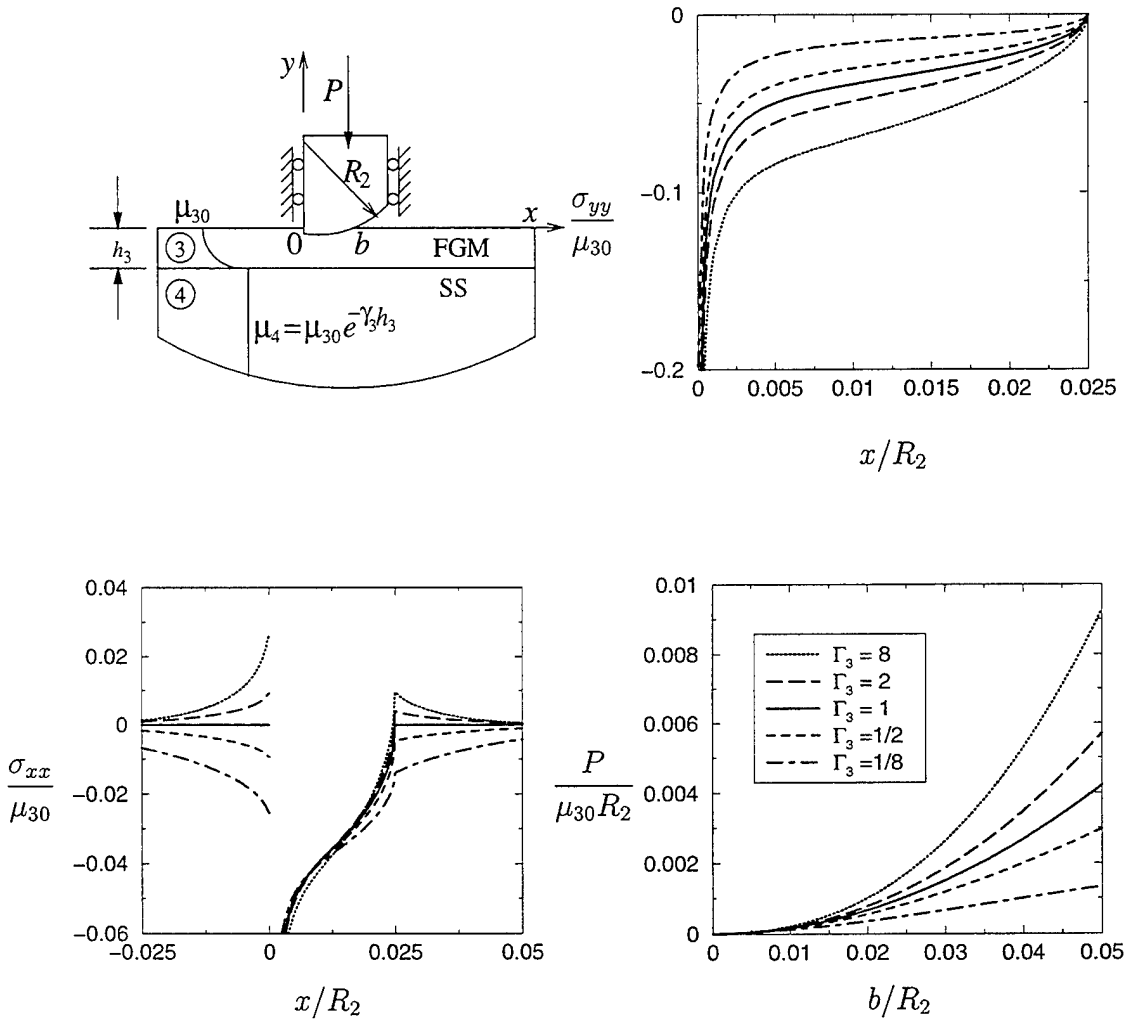

Figure 5.23: Stress distribution on the surface of an FGM coating loaded by a rigid semi-circular stamp for various values of the stiffness ratio, $\Gamma_3 = \mu_4/\mu_{30}$, $b/R_2 = 0.025$, $R_2/h_3 = 20$, $\eta = 0.0$.

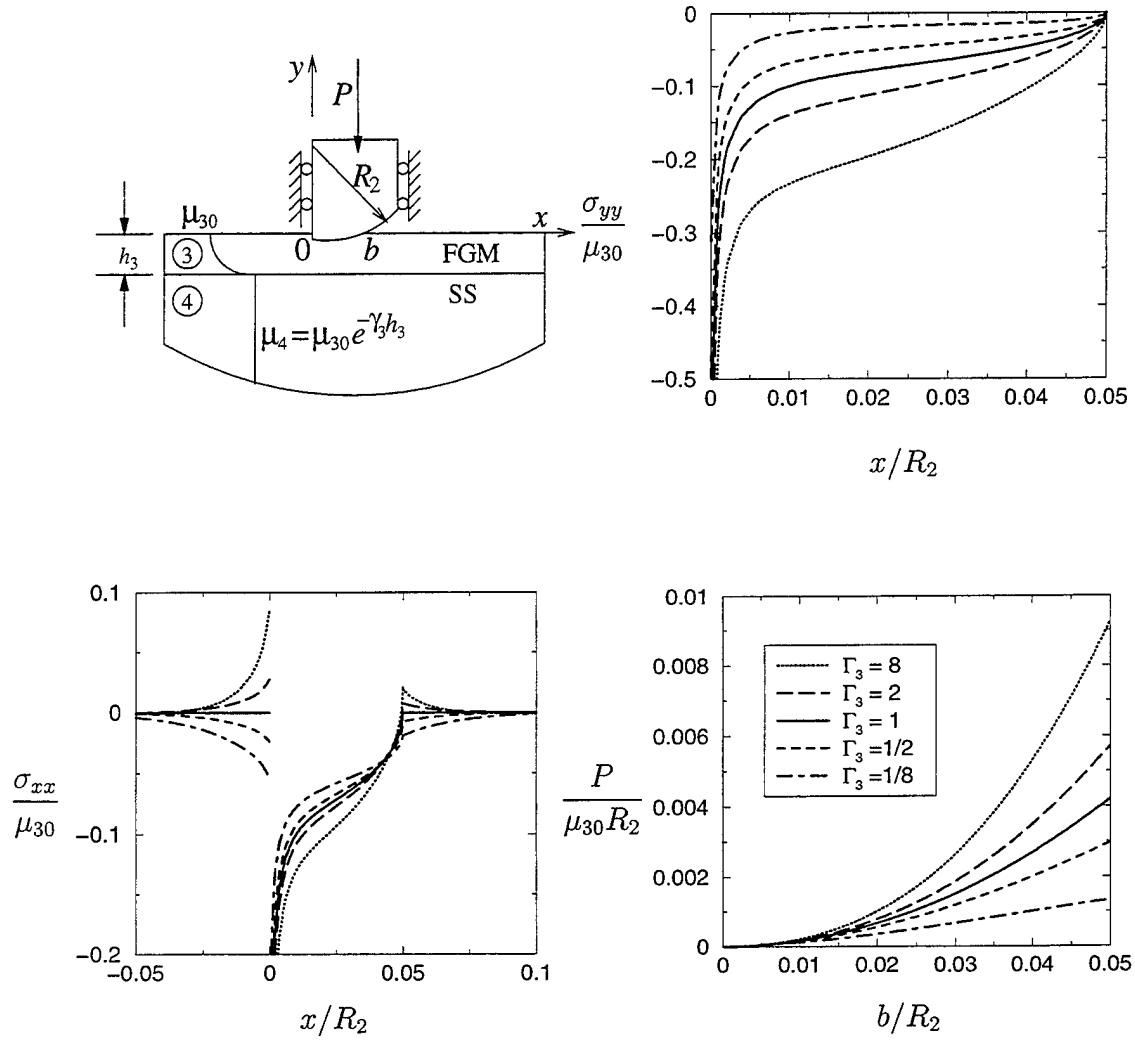

Figure 5.24: Stress distribution on the surface of an FGM coating loaded by a rigid semi-circular stamp for various values of the stiffness ratio, $\Gamma_3 = \mu_4/\mu_{30}$, $b/R_2 = 0.05$, $R_2/h_3 = 20$, $\eta = 0.0$.

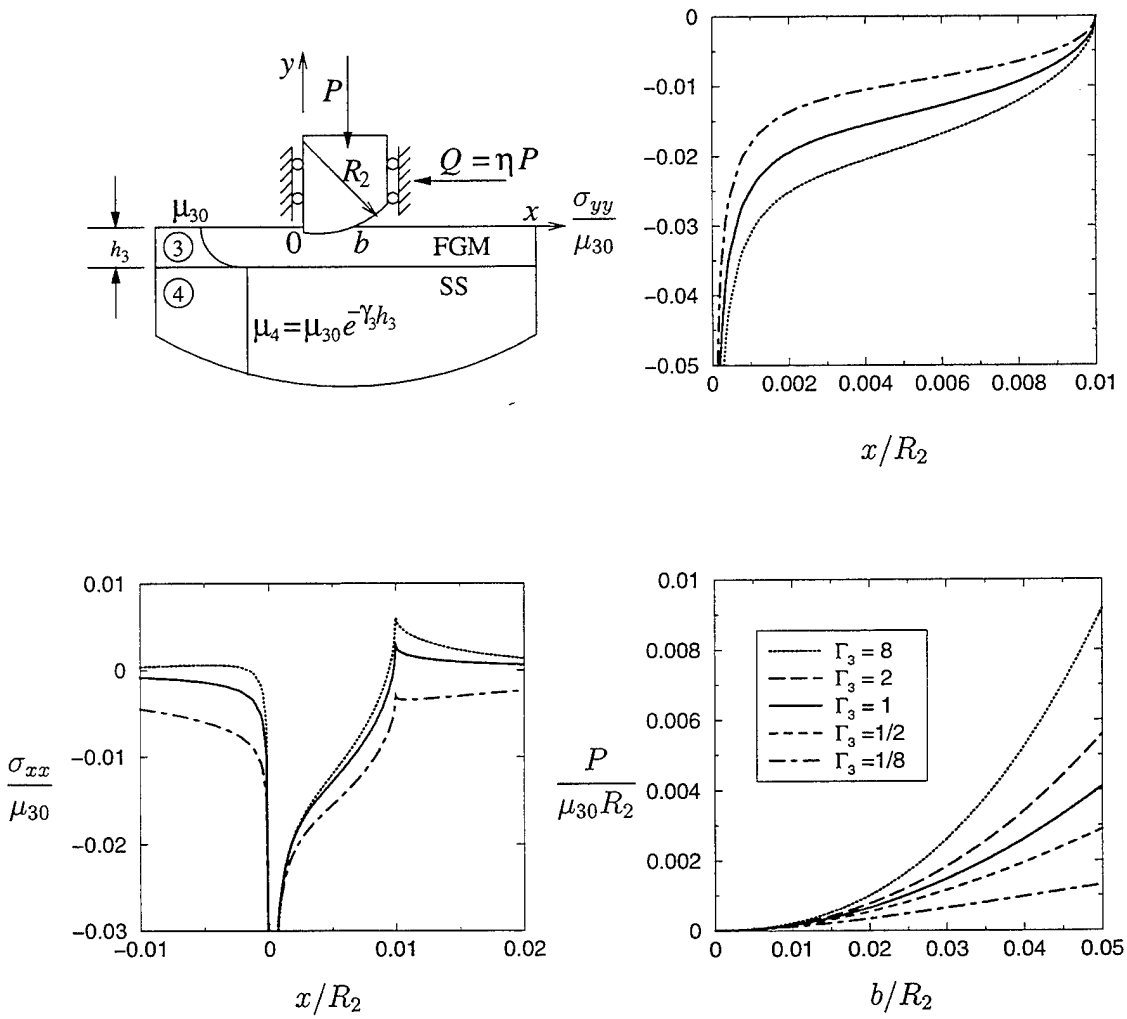

Figure 5.25: Stress distribution on the surface of an FGM coating loaded by a rigid semi-circular stamp for various values of the stiffness ratio, $\Gamma_3 = \mu_4/\mu_{30}$, $b/R_2 = 0.01$, $R_2/h_3 = 20$, $\eta = 0.1$.

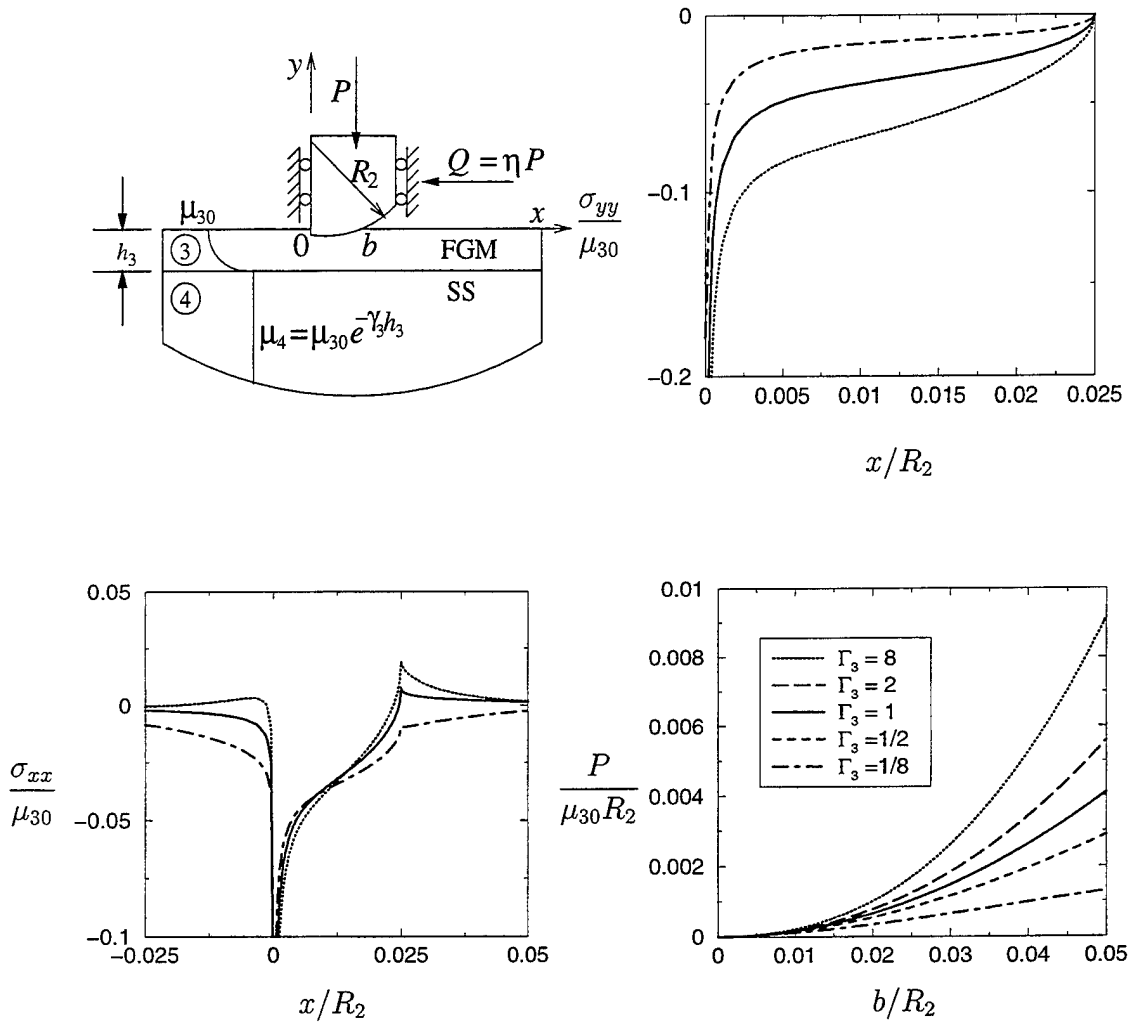

Figure 5.26: Stress distribution on the surface of an FGM coating loaded by a rigid semi-circular stamp for various values of the stiffness ratio, $\Gamma_3 = \mu_4/\mu_{30}$, $b/R_2 = 0.025$, $R_2/h_3 = 20$, $\eta = 0.1$.

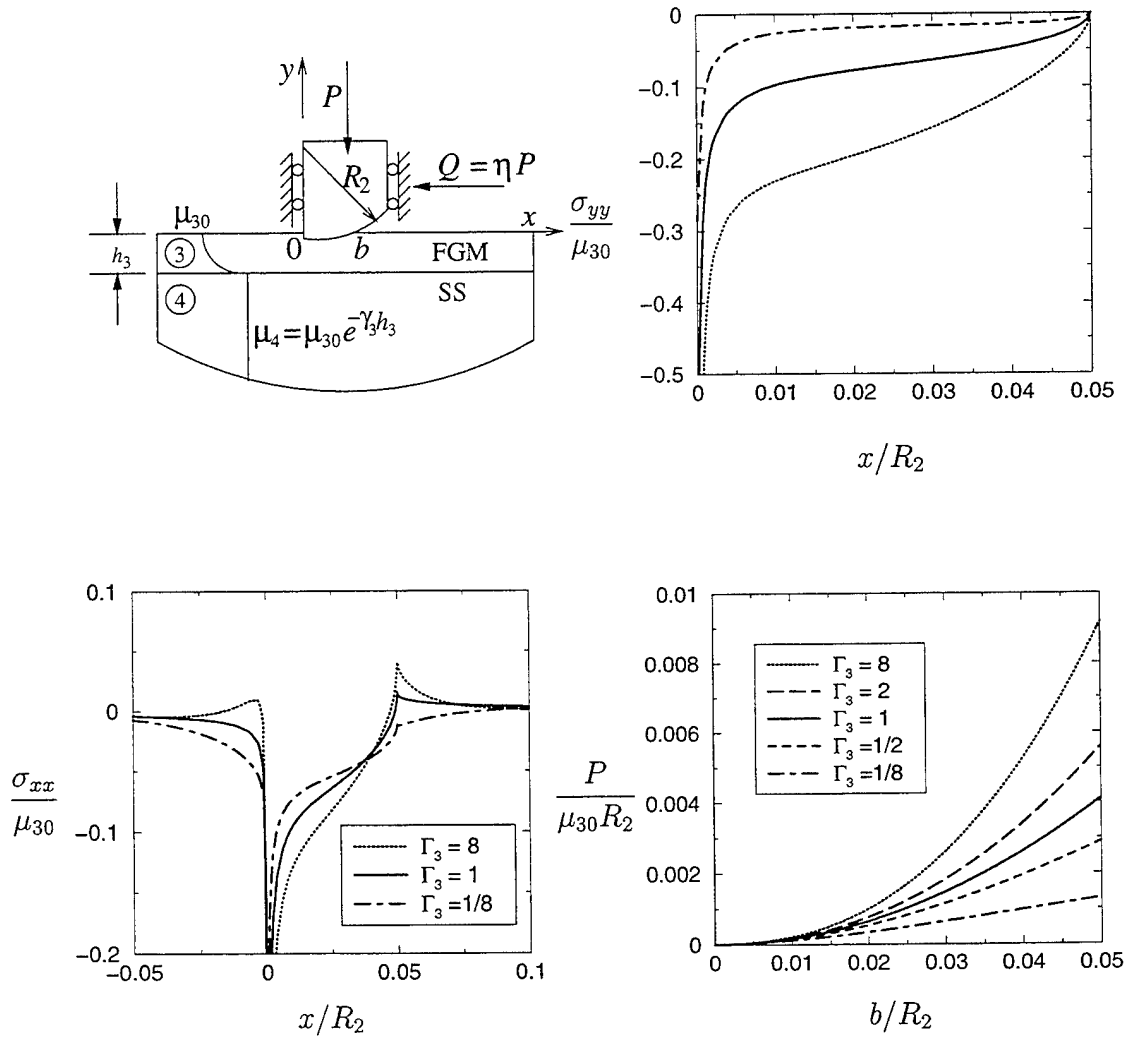

Figure 5.27: Stress distribution on the surface of an FGM coating loaded by a rigid semi-circular stamp for various values of the stiffness ratio, $\Gamma_3 = \mu_4/\mu_{30}$, $b/R_2 = 0.05$, $R_2/h_3 = 20$, $\eta = 0.1$.

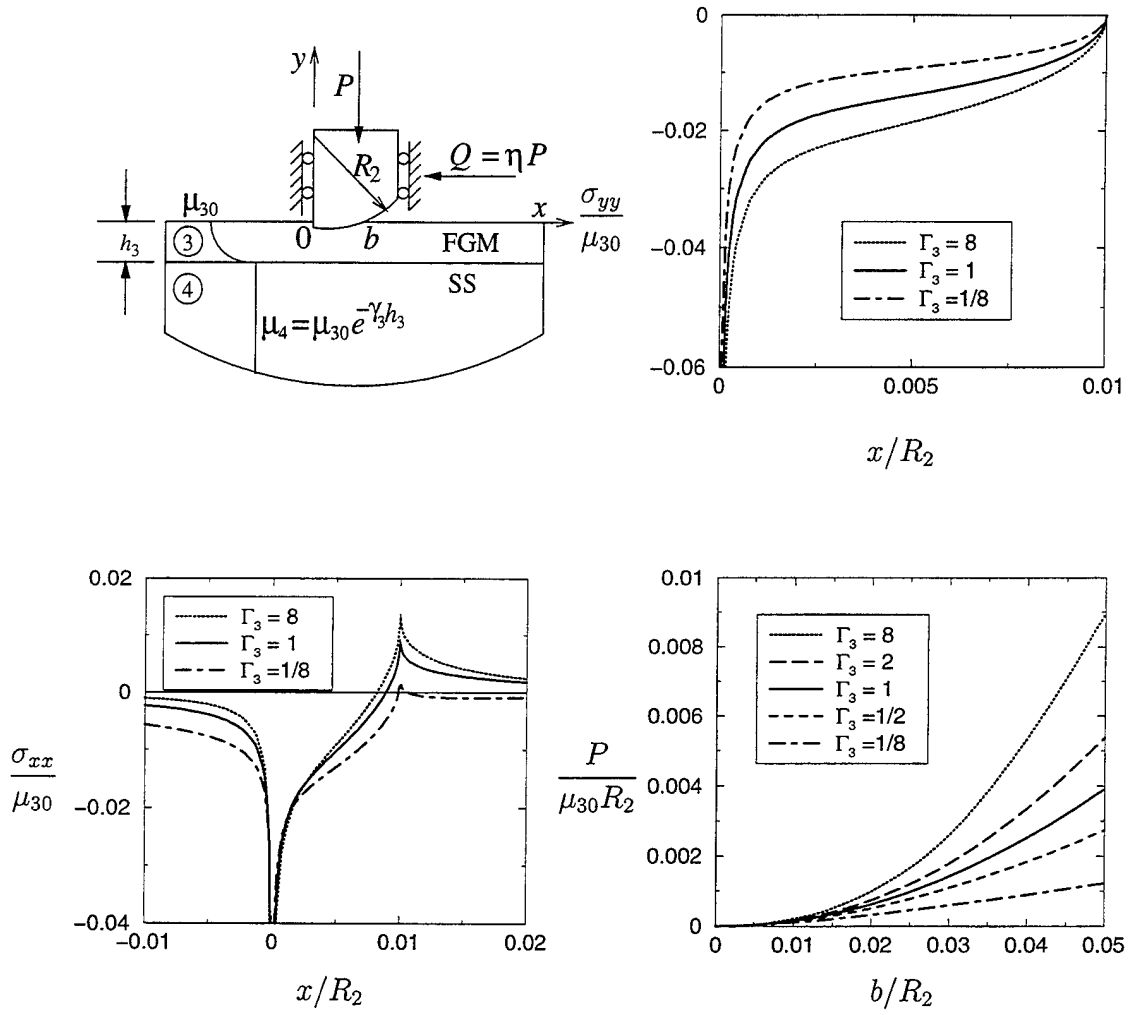

Figure 5.28: Stress distribution on the surface of an FGM coating loaded by a rigid semi-circular stamp for various values of the stiffness ratio, $\Gamma_3 = \mu_4/\mu_{30}$, $b/R_2 = 0.01$, $R_2/h_3 = 20$, $\eta = 0.3$.

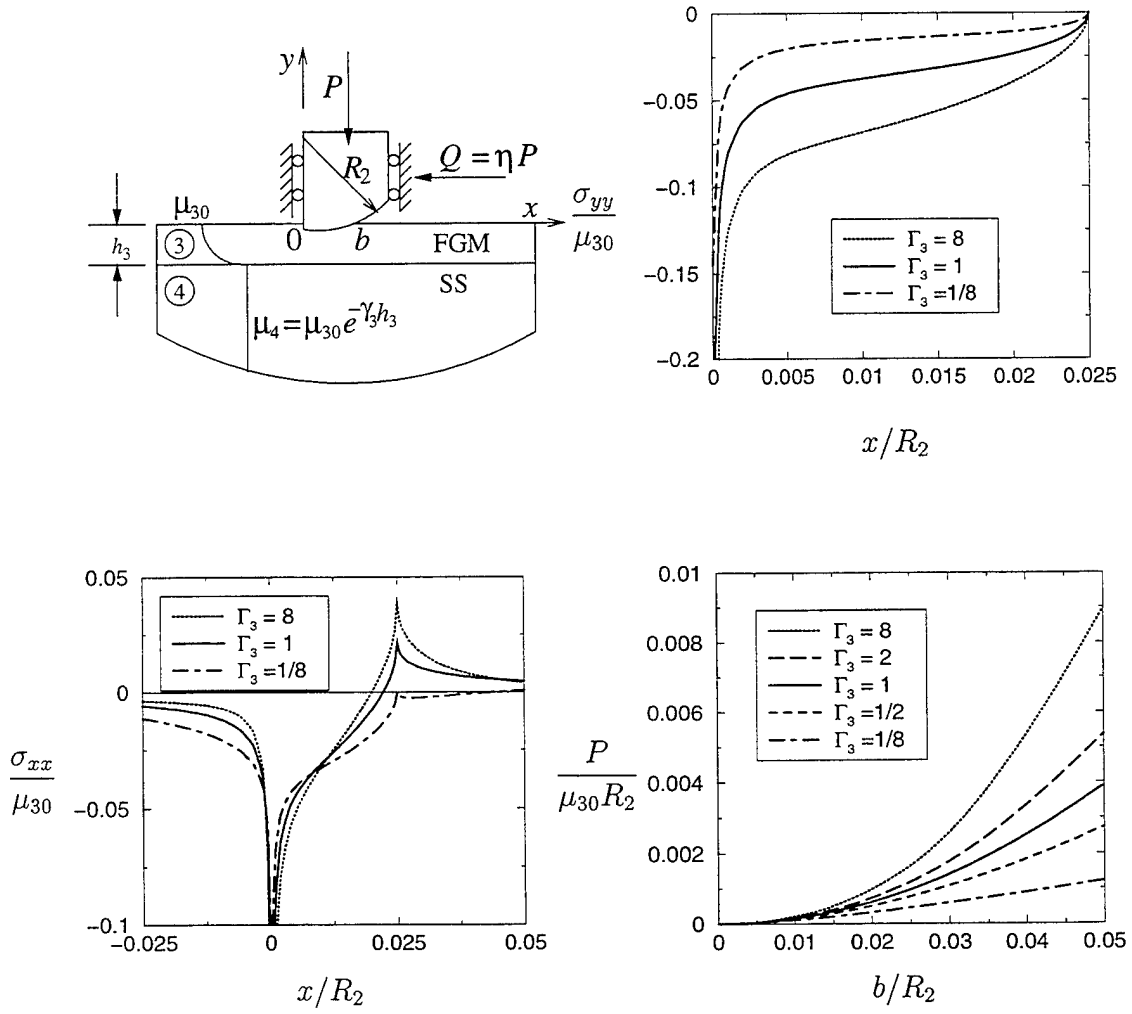

Figure 5.29: Stress distribution on the surface of an FGM coating loaded by a rigid semi-circular stamp for various values of the stiffness ratio, $\Gamma_3 = \mu_4/\mu_{30}$, $b/R_2 = 0.025$, $R_2/h_3 = 20$, $\eta = 0.3$.

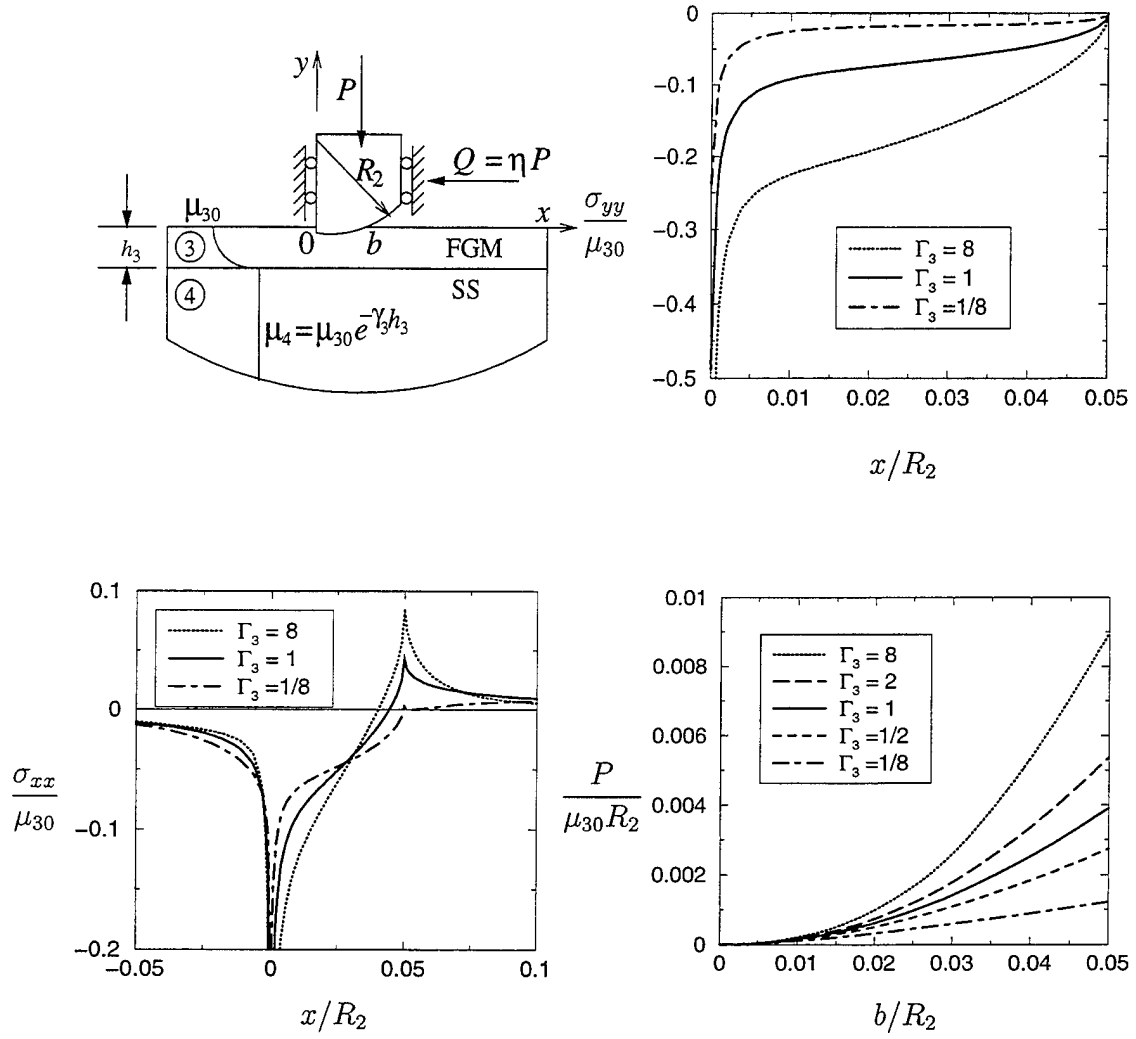

Figure 5.30: Stress distribution on the surface of an FGM coating loaded by a rigid semi-circular stamp for various values of the stiffness ratio, $\Gamma_3 = \mu_4/\mu_{30}$, $b/R_2 = 0.05$, $R_2/h_3 = 20$, $\eta = 0.3$.

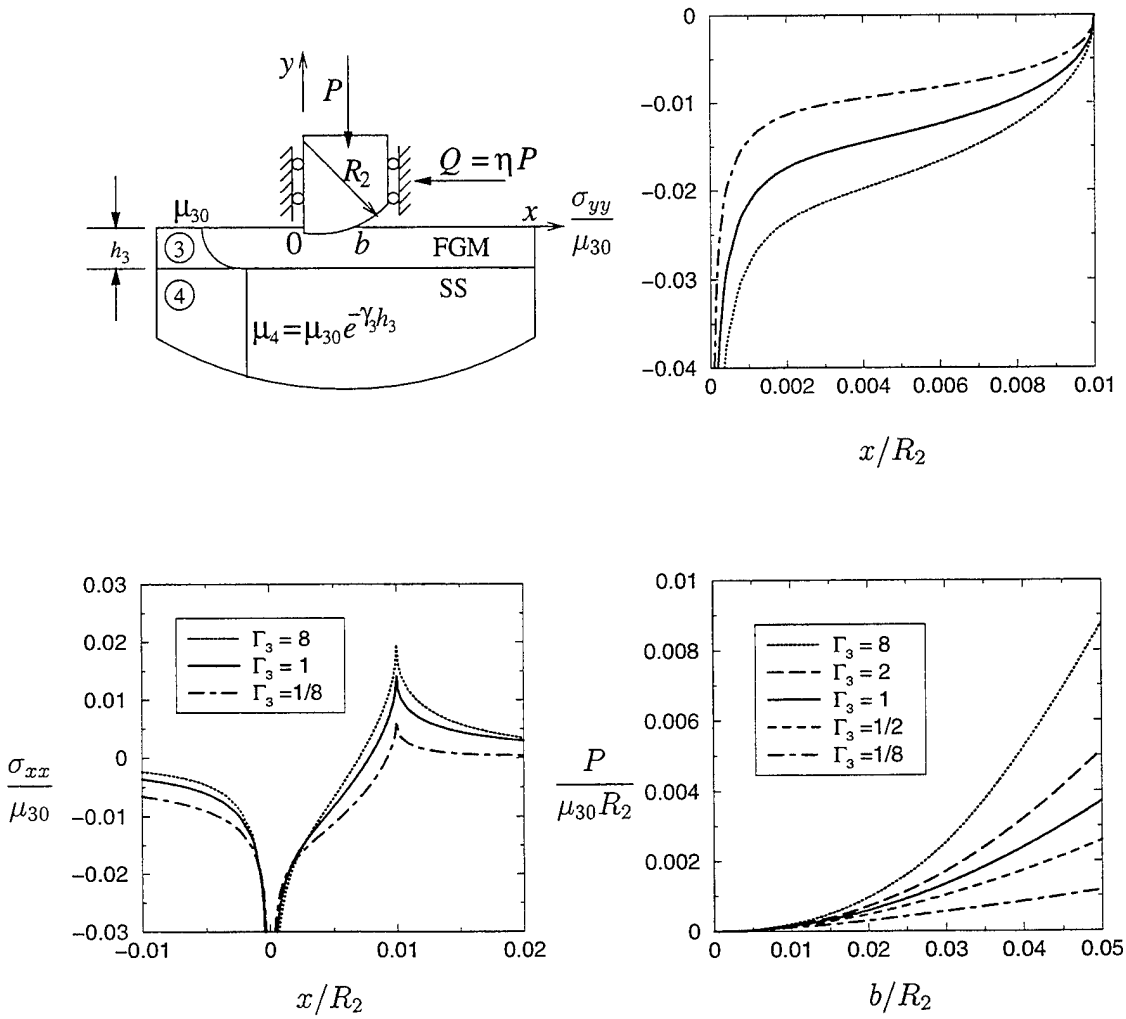

Figure 5.31: Stress distribution on the surface of an FGM coating loaded by a rigid semi-circular stamp for various values of the stiffness ratio, $\Gamma_3 = \mu_4/\mu_{30}$, $b/R_2 = 0.01$, $R_2/h_3 = 20$, $\eta = 0.5$.

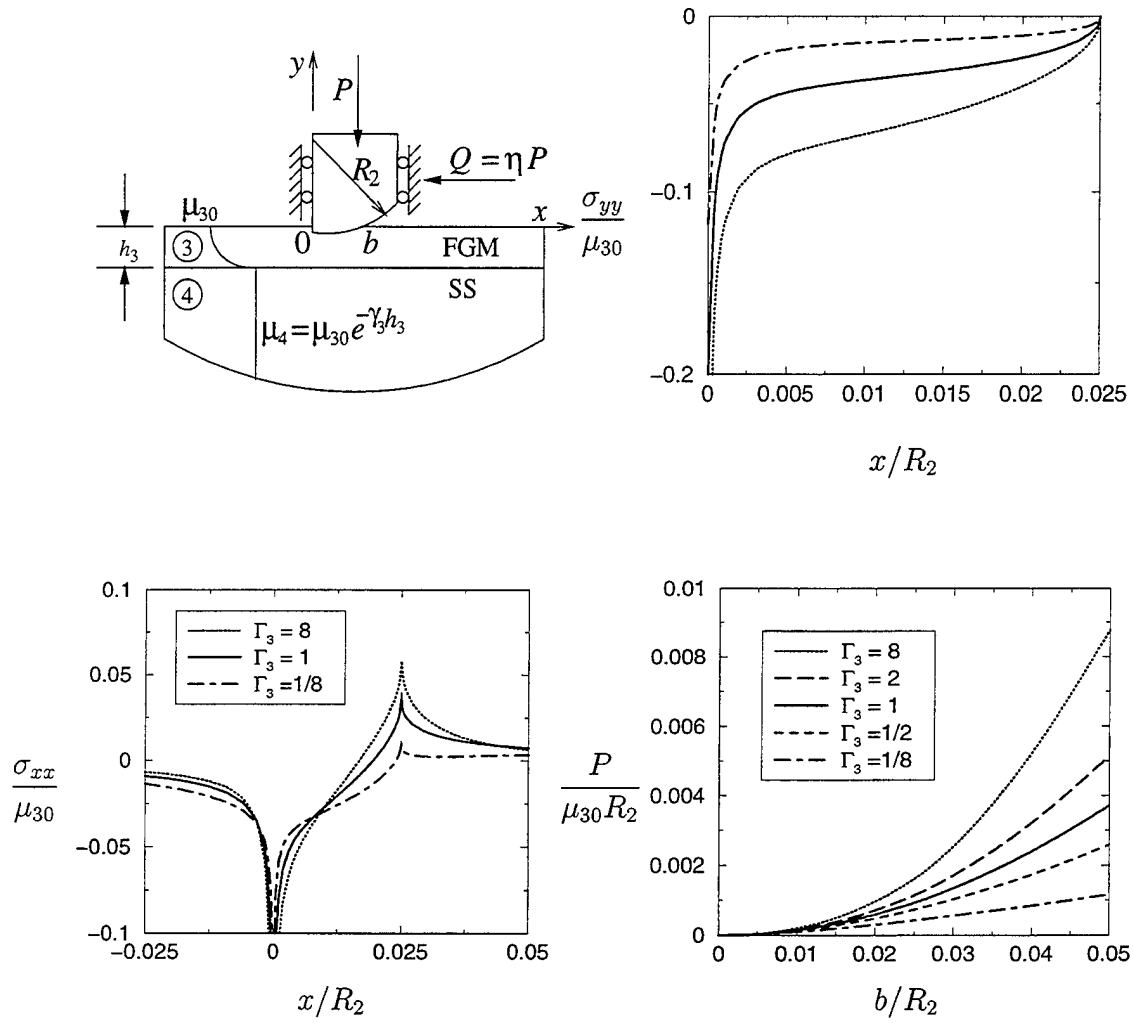

Figure 5.32: Stress distribution on the surface of an FGM coating loaded by a rigid semi-circular stamp for various values of the stiffness ratio, $\Gamma_3 = \mu_4/\mu_{30}$, $b/R_2 = 0.025$, $R_2/h_3 = 20$, $\eta = 0.5$.

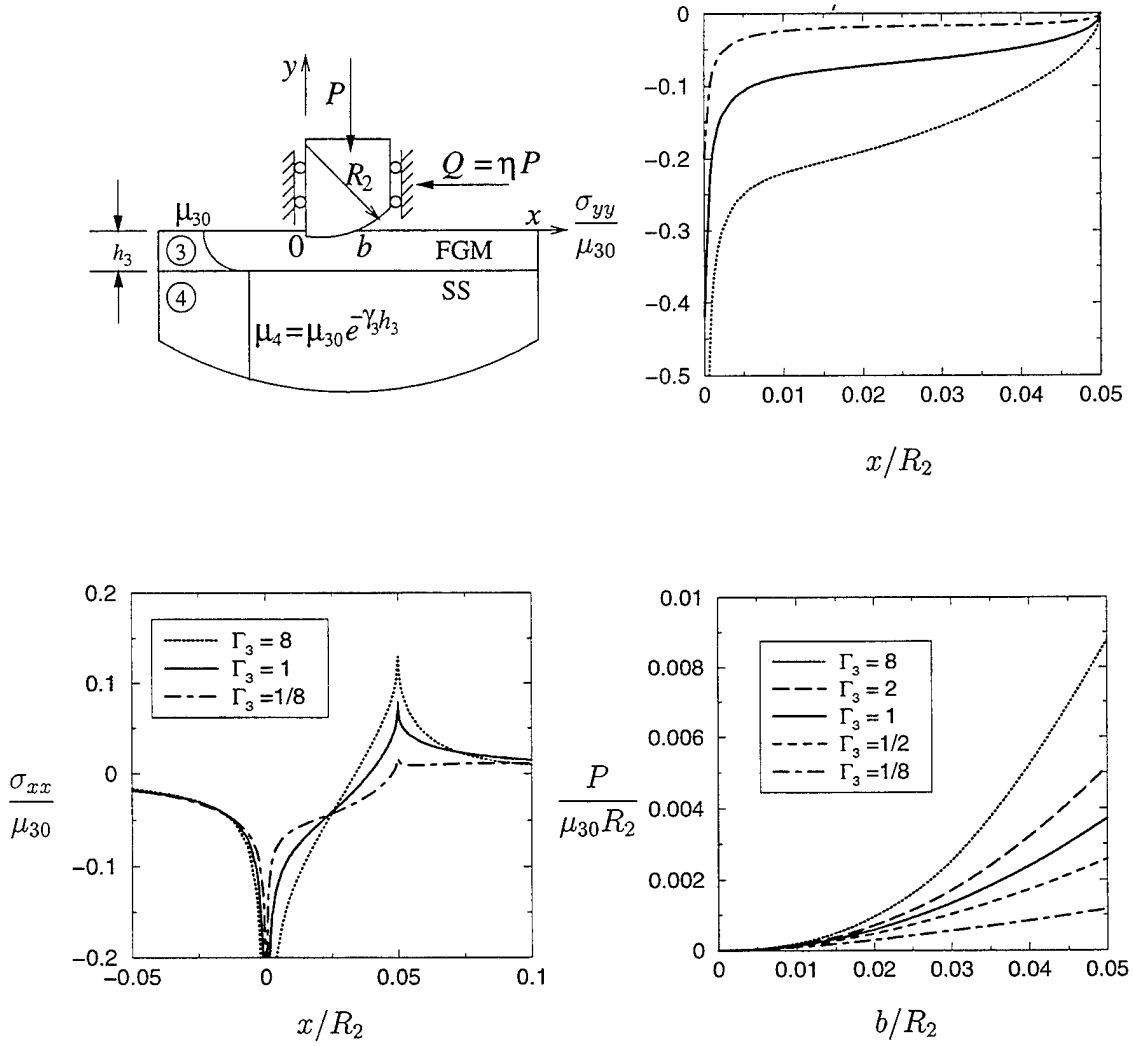

Figure 5.33: Stress distribution on the surface of an FGM coating loaded by a rigid semi-circular stamp for various values of the stiffness ratio, $\Gamma_3 = \mu_4/\mu_{30}$, $b/R_2 = 0.05$, $R_2/h_3 = 20$, $\eta = 0.5$.

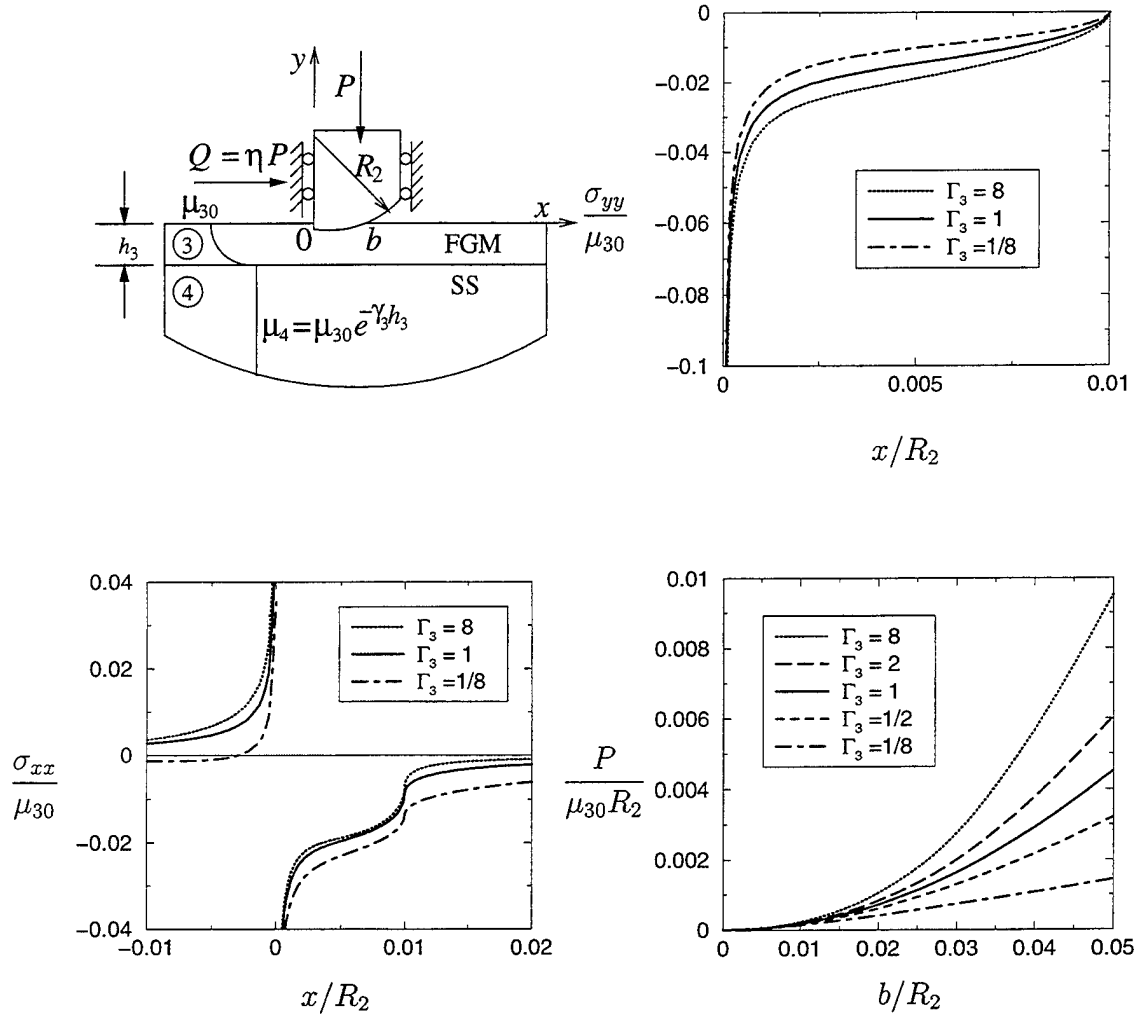

Figure 5.34: Stress distribution on the surface of an FGM coating loaded by a rigid semi-circular stamp for various values of the stiffness ratio, $\Gamma_3 = \mu_4/\mu_{30}$, $b/R_2 = 0.01$, $R_2/h_3 = 20$, $\eta = 0.3$.

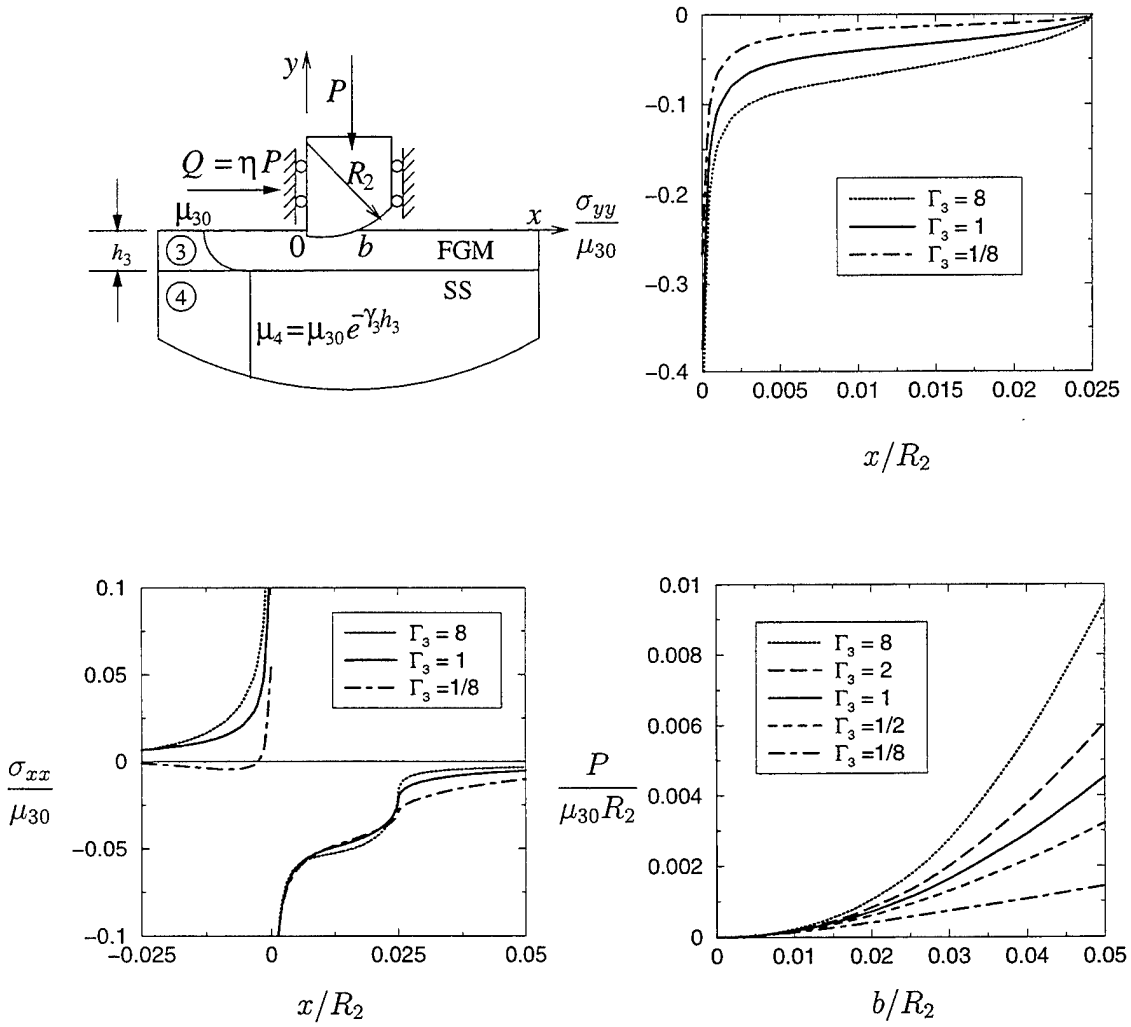

Figure 5.35: Stress distribution on the surface of an FGM coating loaded by a rigid semi-circular stamp for various values of the stiffness ratio, $\Gamma_3 = \mu_4/\mu_{30}$, $b/R_2 = 0.025$, $R_2/h_3 = 20$, $\eta = 0.3$.

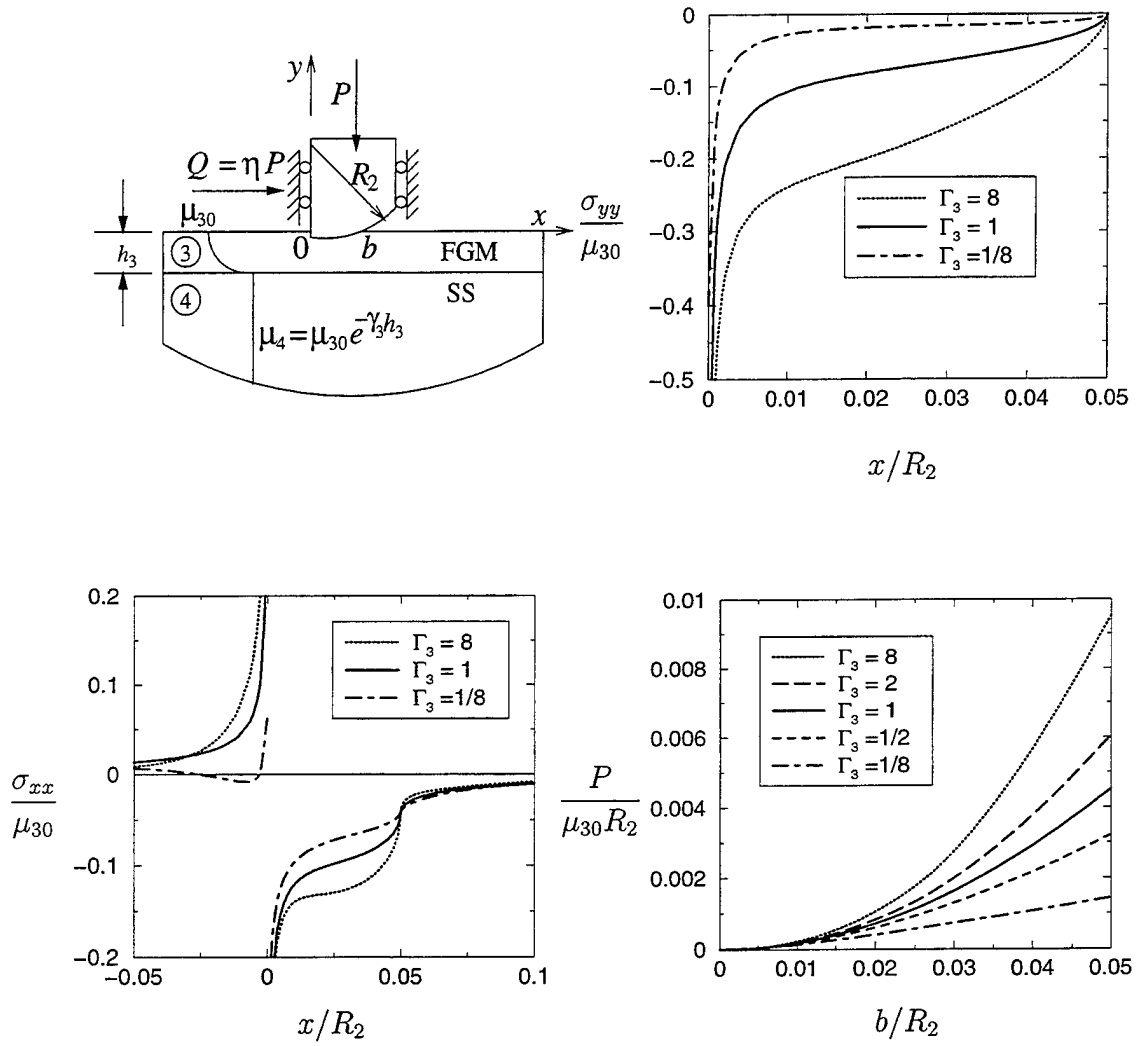

Figure 5.36: Stress distribution on the surface of an FGM coating loaded by a rigid semi-circular stamp for various values of the stiffness ratio, $\Gamma_3 = \mu_4/\mu_{30}$, $b/R_2 = 0.05$, $R_2/h_3 = 20$, $\eta = 0.3$.

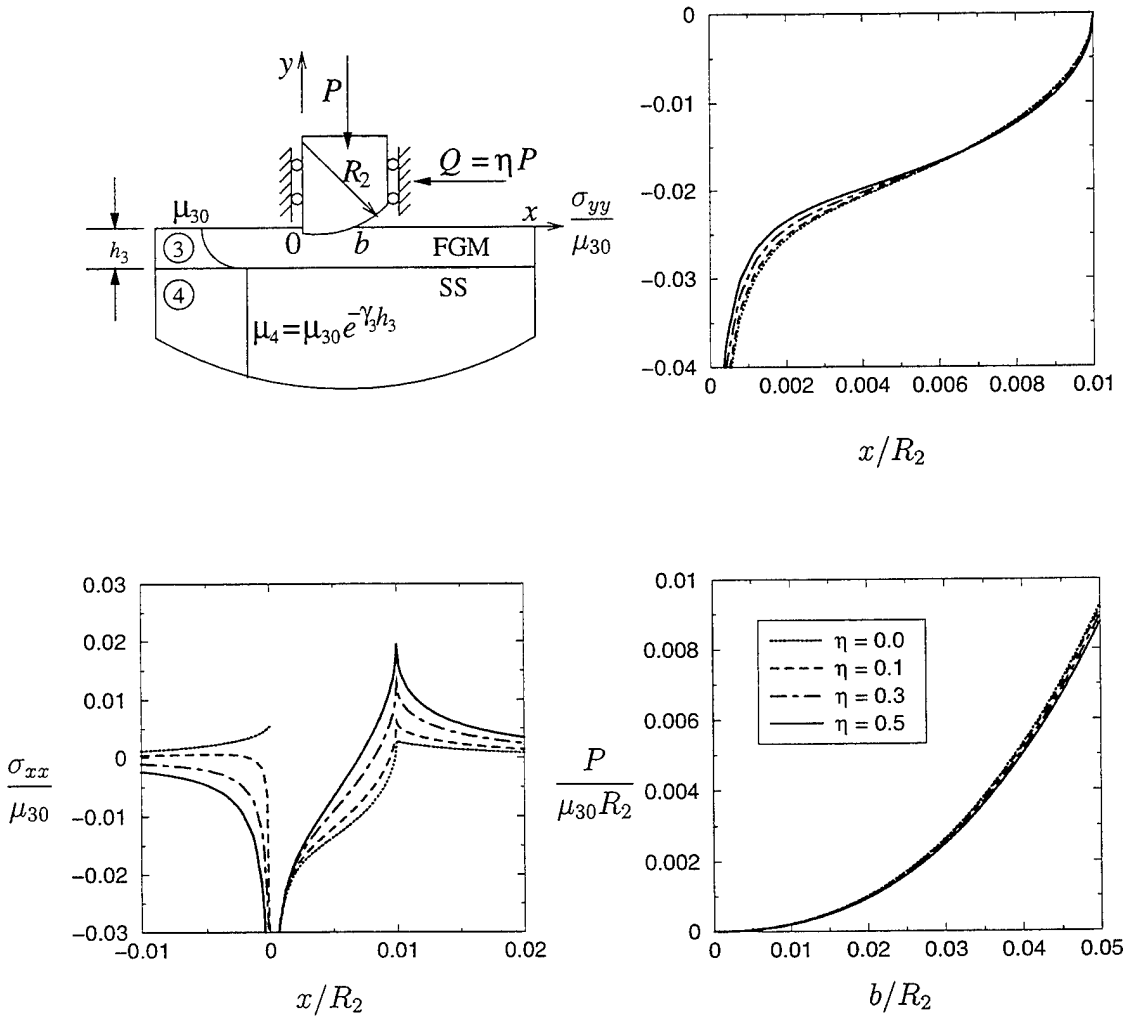

Figure 5.37: Stress distribution on the surface of an FGM coating loaded by a rigid semi-circular stamp for various values of the coefficient of friction, η, $\Gamma_3 = \mu_4/\mu_{30} = 8$, $b/R_2 = 0.01$, $R_2/h_3 = 20$.

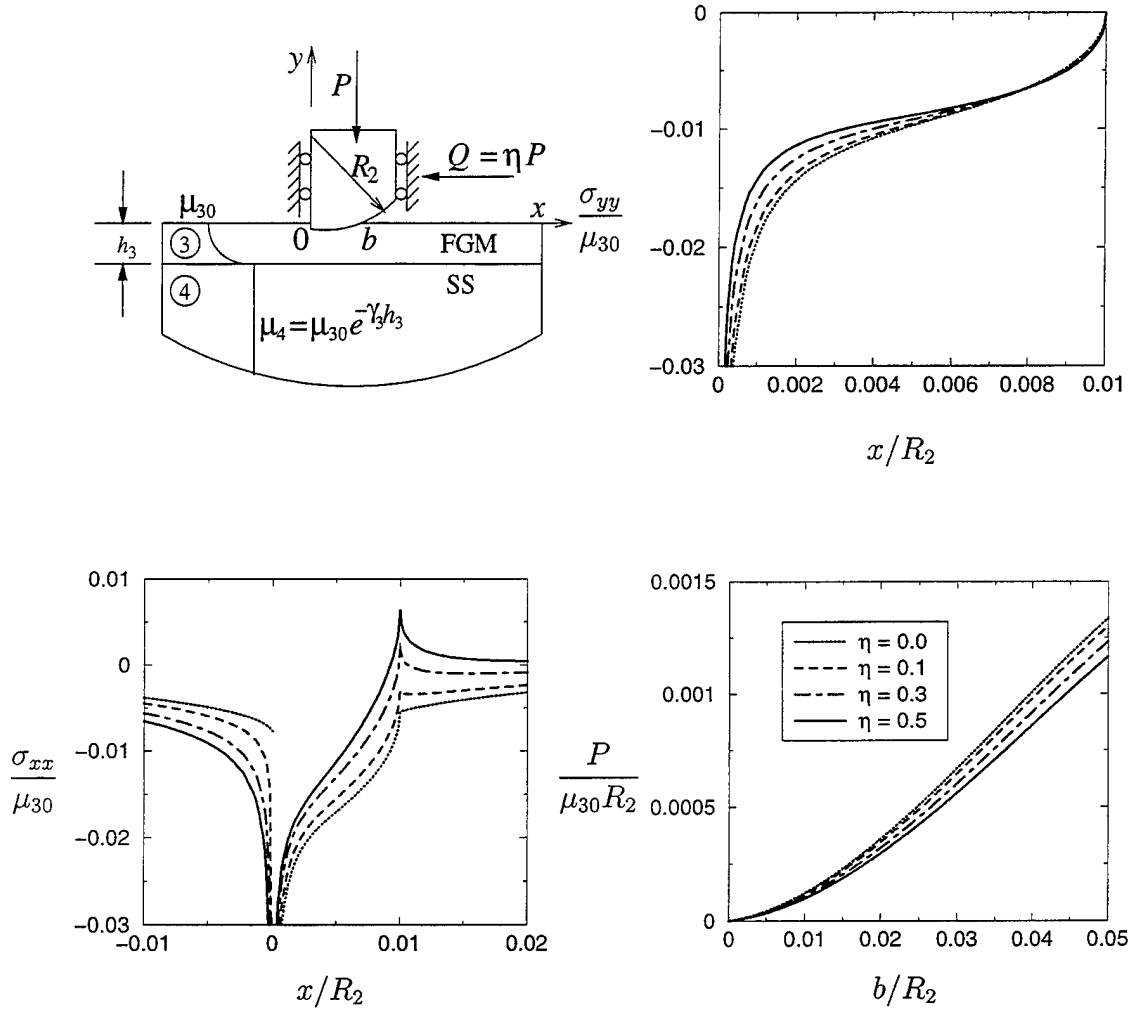

Figure 5.38: Stress distribution on the surface of an FGM coating loaded by a rigid semi-circular stamp for various values of the coefficient of friction, η, $\Gamma_3 = \mu_4/\mu_{30} = 1/8$, $b/R_2 = 0.01$, $R_2/h_3 = 20$.

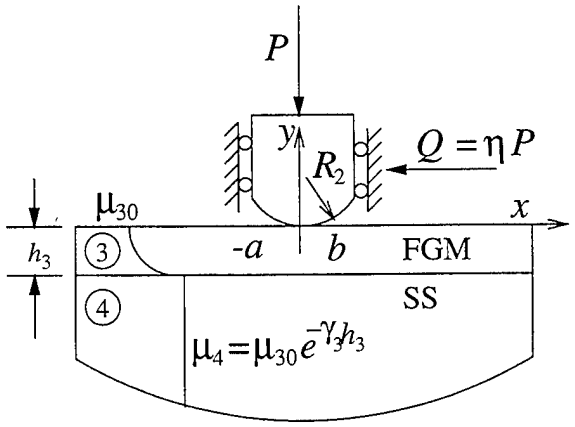

Figure 5.39: Geometry of the cylindrical stamp problem

5.4 The Cylindrical Stamp

The cylindrical stamp problem is described in Fig. 5.39. Again, for small values of b/R_2 and a/R_2 we can approximate the surface of the cylindrical stamp by a parabola. Therefore, the displacement in y direction and its derivative become

$$v_3(x,0) = -v_{30} + \frac{x^2}{2R_2}, \tag{5.119}$$

$$\frac{\partial}{\partial x} v_3(x,0) = \frac{x}{R_2}. \tag{5.120}$$

Letting

$$\begin{aligned} \sigma_{3yy}(t,0) &= -p(t), \qquad \sigma_{3xy}(t,0) = -\eta p(t), \qquad -a < t < b, \\ \sigma_{3yy}(t,0) &= \sigma_{3xy}(t,0) = 0 \qquad\qquad\qquad t < a, t > b, \end{aligned} \tag{5.121}$$

and using the relations (4.17)-(4.23) integral equation (4.3) and the equilibrium equation (4.12) become

$$Ap(x) + \frac{1}{\pi}\int_{-a}^{b}\left[-\frac{1}{t-x} + k_{31}(t,x) + \eta k_{32}(t,x)\right] p(t)dt = f_3(x), \tag{5.122}$$

$$\int_{-a}^{b} p(t)dt = P, \tag{5.123}$$

where

$$A = \omega_3 \eta, \tag{5.124}$$

$$f_3(x) = \lambda_3 \frac{x}{R_2}, \tag{5.125}$$

$$\lambda_3 = \frac{4\mu_{30}}{1+\kappa_3}, \tag{5.126}$$

$$\omega_3 = \frac{\kappa_3 - 1}{\kappa_3 + 1}. \tag{5.127}$$

In order to solve the integral equation the limits of integration have to be normalized from $(-a, b)$ to $(-1, 1)$. Now setting

$$t = t^* R_2, \tag{5.128}$$

$$x = x^* R_2, \tag{5.129}$$

$$b = b^* R_2, \tag{5.130}$$

$$a = a^* R_2, \tag{5.131}$$

$$p(t) = p^*(t^*), \tag{5.132}$$

$$k_{31}(t,x) = \frac{1}{R_2} k_{31}^*(t^*, x^*), \tag{5.133}$$

$$k_{32}(t,x) = \frac{1}{R_2} k_{32}^*(t^*, x^*), \tag{5.134}$$

$$f_3(x) = f_3^*(x^*), \tag{5.135}$$

(5.122) and (5.123) can be written as

$$Ap^*(x^*) + \frac{B}{\pi} \int_{-a^*}^{b^*} \frac{p^*(t^*)}{t^* - x^*} dt^* + \frac{1}{\pi} \int_{-a^*}^{b^*} \left[k_{31}^*(t^*, x^*) + \eta k_{32}^*(t^*, x^*) \right] p^*(t^*) dt^* = f_3^*(x^*), \tag{5.136}$$

$$\int_{-a^*}^{b^*} p^*(t^*) dt^* = \frac{P}{R_2}. \tag{5.137}$$

Further normalizing the integration limits from $(-a^*, b^*)$ to $(-1, 1)$ by the following change of variables

$$t^* = \frac{b^*+a^*}{2}s + \frac{b^*-a^*}{2}, \qquad -1 < s < 1 \tag{5.138}$$

$$x^* = \frac{b^*+a^*}{2}r + \frac{b^*-a^*}{2}, \qquad -1 < r < 1 \tag{5.139}$$

$$p^*(t^*) = \frac{\lambda_3}{2}\phi(s), \tag{5.140}$$

$$k_{31}^*(t^*, x^*) = \frac{2}{b^*+a^*}\widehat{k}_{31}(s, r), \tag{5.141}$$

$$k_{32}^*(t^*, x^*) = \frac{2}{b^*+a^*}\widehat{k}_{32}(s, r), \tag{5.142}$$

$$f_3^*(x^*) = \widehat{f}_3(r), \tag{5.143}$$

the integral equation and the equilibrium equation become

$$A\phi(r) + \frac{1}{\pi}\int_{-1}^{1}\left[-\frac{1}{s-r} + \widehat{k}_{31}(s, r) + \eta\widehat{k}_{32}(s, r)\right]\phi(s)ds = \widehat{f}_3(r), \tag{5.144}$$

$$\int_{-1}^{1}\phi(s)ds = \frac{4}{b^*+a^*}\frac{P}{\lambda_3 R_2}, \tag{5.145}$$

where

$$\hat{f}_3(r) = (b^*+a^*)\,r + (b^*-a^*)\,. \tag{5.146}$$

Since there are smooth contacts at both ends $x = -a$ and $x = b$, from the physics of the problem we must require that both α and β be positive.

If $\eta > 0$ from equations (4.48) and (4.49) we have

$$\alpha = N + \frac{\theta}{\pi}, \quad \Longrightarrow \quad N = 0, \tag{5.147}$$

$$\beta = M - \frac{\theta}{\pi}, \quad \Longrightarrow \quad M = 1, \tag{5.148}$$

and if $\eta < 0$ from equations (4.56) and (4.57)

$$\alpha = N - \frac{\theta}{\pi}, \quad \Longrightarrow \quad N = 1, \tag{5.149}$$

$$\beta = M + \frac{\theta}{\pi}, \quad \Longrightarrow \quad M = 0. \tag{5.150}$$

Table 5.10: Values of α and β for the index, $\kappa_0 = -1$

η	α	β
-0.3	0.5272	0.4728
-0.1	0.5091	0.4909
0	0.5000	0.5000
0.1	0.4909	0.5091
0.3	0.4728	0.5272

The index of the integral equation is defined by

$$\kappa_0 = -(\alpha + \beta) = -(N + M) = -1. \tag{5.151}$$

α and β then becomes

$$\begin{aligned} \eta > 0: &\quad \alpha = \theta/\pi, &\quad \beta = 1 - \theta/\pi, \\ \eta = 0: &\quad \alpha = 0.5, &\quad \beta = 0.5, \\ \eta < 0: &\quad \alpha = 1 - \theta/\pi, &\quad \beta = \theta/\pi, \end{aligned} \tag{5.152}$$

where

$$\theta = \arctan \left| \frac{1}{A} \right|. \tag{5.153}$$

In Table 5.10 some values of the α and β are given for various values of η.

Assuming a solution of the form

$$\phi(s) = w(s) \sum_{0}^{\infty} c_n P_n^{(\alpha,\beta)}(s), \tag{5.154}$$

$$w(s) = (1-s)^{\alpha} (1+s)^{\beta}, \tag{5.155}$$

defining

$$\widehat{\phi}(s) = w(s)\sum_{0}^{\infty}\widehat{c}_n P_n^{(\alpha,\beta)}(s), \tag{5.156}$$

$$P^* = \frac{P}{\mu_{30}R_2}, \tag{5.157}$$

$$\widehat{c}_n = \frac{c_n}{\sqrt{P^*}}, \tag{5.158}$$

$$\widehat{b} = \frac{b^*}{\sqrt{P^*}}, \tag{5.159}$$

$$\widehat{a} = \frac{a^*}{\sqrt{P^*}}, \tag{5.160}$$

$$\widehat{x} = \frac{x^*}{\sqrt{P^*}}, \tag{5.161}$$

and Using the orthogonality of the Jacobi polynomials, the equilibrium equation (5.145) becomes

$$\widehat{c}_0\theta_0 = \frac{\kappa_3 + 1}{\widehat{b} + \widehat{a}}, \tag{5.162}$$

where, from (A.8)

$$\theta_0 = \frac{2\pi\alpha(1-\alpha)}{\sin\pi\alpha}. \tag{5.163}$$

Considering the property of Jacobi Polynomials (A.6), letting

$$\mathcal{K}_{3n}(r) = \frac{1}{\pi}\int_{-1}^{1}\left[\widehat{k}_{31}(s,r) + \eta\widehat{k}_{32}(s,r)\right] w(s)P_n^{(\alpha,\beta)}(s)ds, \tag{5.164}$$

and truncating the series at $N-1$, (5.144) can be written as

$$\sum_{0}^{N-1}\widehat{c}_n\left[\frac{2}{\sin\pi\alpha}P_{n-\kappa}^{(-\alpha,-\beta)}(r) + \mathcal{K}_{3n}(r)\right] = (r+1)\widehat{b} + (r-1)\widehat{a}. \tag{5.165}$$

Since $\kappa_0 = -1$, the consistency condition becomes

$$\int_{-1}^{1}\left[\widehat{f}(r) - \frac{1}{\pi}\int_{-1}^{1}\left[\widehat{k}_{31}(s,r) + \eta\widehat{k}_{32}(s,r)\right]\phi(s)\right]\frac{dr}{w(r)} = 0, \tag{5.166}$$

From equation (5.144) it may be observed that

$$\begin{aligned}
&\widehat{f}_3(r) - \frac{1}{\pi}\int_{-1}^{1}\left[\widehat{k}_{31}(s,r) + \eta\widehat{k}_{32}(s,r)\right]\phi(s)ds \\
&= A\phi(r) - \frac{1}{\pi}\int_{-1}^{1}\frac{\phi(s)}{s-r}dr \\
&= \sum_{0}^{\infty} c_n\left[Aw(r)P_n^{(\alpha,\beta)}(r) - \frac{1}{\pi}\int_{-1}^{1}\frac{w(s)P_n^{(\alpha,\beta)}(s)}{s-r}ds\right] \\
&= \frac{2^{-\kappa_0}}{\sin\pi\alpha}\sum_{0}^{\infty} c_n P_{n-\kappa_0}^{(-\alpha,-\beta)}(r). \qquad (5.167)
\end{aligned}$$

Integrating (5.167) from -1 to 1 and using the orthogonality we find

$$\begin{aligned}
&\int_{-1}^{1}\left[\widehat{f}_3(r) - \frac{1}{\pi}\int_{-1}^{1}\left[\widehat{k}_{31}(s,r) + \eta\widehat{k}_{32}(s,r)\right]\phi(s)ds\right]\frac{dr}{w(r)} \\
&= \frac{2^{-\kappa_0}}{\sin\pi\alpha}\sum_{0}^{\infty} c_n^*\int_{-1}^{1}\frac{P_{n+1}^{(-\alpha,-\beta)}(s)ds}{w(s)} = 0. \qquad (5.168)
\end{aligned}$$

Therefore the consistency condition is automatically satisfied.

In (5.165) we have $N+2$ unknowns ($\widehat{c}_0, \widehat{c}_1, ..., \widehat{c}_{N-1}, \widehat{a}, \widehat{b}$). An additional equation can be obtained from the consistency condition(see [46]). Since equation (5.165) is satisfied for $N+1$ values of r_j, an equation corresponding to one of the r_j's can be used to determine $\widehat{b}$. We first express equation (5.165) in the following form

$$F(r_j) - (r_j+1)\widehat{b} = (r_j-1)\widehat{a} \qquad j = 1..N+1, \qquad (5.169)$$

where

$$F(r_j) = \sum_{0}^{N-1} c_n^*\left[\frac{2}{\sin\pi\alpha}P_{n+1}^{(-\alpha,-\beta)}(r_j) + \mathcal{K}_{3n}(r_j)\right], \qquad j = 1..N+1. \qquad (5.170)$$

The collocation points are obtained from

$$P_{n+1}^{(\alpha-1,\beta-1)}(r_j) = 0, \qquad j = 1..N+1. \qquad (5.171)$$

The system of equations may then be expressed as

$$\begin{bmatrix} F_0(r_1) & . & F_{N-1}(r_1) & -(r_1+1) \\ F_0(r_2) & . & F_{N-1}(r_2) & -(r_2+1) \\ . & . & . & . \\ . & . & . & . \\ . & . & . & . \\ . & . & . & . \\ . & . & . & . \\ F_0(r_N) & . & F_{N-1}(r_N) & -(r_N+1) \\ F_0(r_{N+1}) & . & F_{N-1}(r_{N+1}) & -(r_{N+1}+1) \end{bmatrix} \begin{Bmatrix} \widehat{c}_0 \\ \widehat{c}_1 \\ . \\ . \\ . \\ . \\ . \\ \widehat{c}_{N-1} \\ \widehat{b} \end{Bmatrix} = \begin{Bmatrix} (r_1-1) \\ (r_2-1) \\ . \\ . \\ . \\ . \\ . \\ (r_N-1) \\ (r_{N+1}-1) \end{Bmatrix} \widehat{a}. \tag{5.172}$$

Equation (5.172) can be solved by using a suitable iterative technique. In the iterative procedure, we guess $\widehat{a}$ first, then calculate the $N+1$ unknowns ($\widehat{c}_0, \widehat{c}_1, ..., \widehat{c}_{N-1}, \widehat{b}$). With the calculated $\widehat{b}$ and $\widehat{c}_0$ we can determine the new $\widehat{a}$ by using the equilibrium equation (5.162), as follows:

$$\widehat{a} = \frac{\kappa^- + 1}{\widehat{c}_0 \theta_0} - \widehat{b}. \tag{5.173}$$

Iteration continuous until we have the same old and new $\widehat{a}$. Once $\widehat{a}$ and $\widehat{b}$ are obtained, the dimensionless load P^* can be calculated for a given value of the contact length $(a^* + b^*)$ as

$$P^* = \frac{P}{\mu_{30} R_2} = \left(\frac{a^* + b^*}{\widehat{a} + \widehat{b}} \right)^2. \tag{5.174}$$

Similarly, the ends of the contact length and c_n's can be found from

$$a^* = \widehat{a}\sqrt{P^*}, \tag{5.175}$$

$$b^* = \widehat{b}\sqrt{P^*}, \tag{5.176}$$

$$c_n = \widehat{c}_n\sqrt{P^*}. \tag{5.177}$$

From (5.132) and (5.140),the nondimensional contact stresses can then be obtained as

$$\frac{\sigma_{3yy}(x^*,0)}{\mu_{30}} = \frac{\sigma(x^*)}{\mu_{30}} = -\frac{2}{1+\kappa_3} w(r) \sum_0^\infty c_n P_n^{(\alpha,\beta)}(r), \tag{5.178}$$

where

$$r = \frac{2x^* - b^* + a^*}{b^* + a^*}.$$

Defining

$$\sigma_{xx}(x^*,0) = \frac{\lambda_3}{2}\psi(r),$$

the in-plane stresses, $\sigma_{3xx}(x^*,0)$ can be found by using equation (4.74):

$$\sigma_{3xx}(x^*,0) = \sigma(x^*) + \frac{2\eta}{\pi}\int_{-a^*}^{b^*} \frac{\sigma(t^*)}{t^*-x^*}dt^* - \frac{2}{\pi}\int_{-a^*}^{b^*} \left[k_{42}^*(t^*,x^*) + \eta k_{41}^*(t^*,x^*)\right]\sigma(t^*)\,dt^*.$$

Using equations (5.132) and (5.140) we find

$$\sigma_{3xx}(x^*,0) = \frac{\lambda_3}{2}\left[-\phi(r) - \frac{2\eta}{\pi}\int_{-1}^{1}\frac{\phi(s)}{s-r}dt + \frac{2}{\pi}\int_{-1}^{1}\left[\widehat{k}_{42}(s,r) + \eta\widehat{k}_{41}(s,r)\right]\phi(s)\,ds\right].$$

Therefore,

$$\psi(r) = -\phi(r) - \frac{2\eta}{\pi}\int_{-1}^{1}\frac{\phi(s)}{s-r}dt + \frac{2}{\pi}\int_{-1}^{1}\left[\widehat{k}_{42}(s,r) + \eta\widehat{k}_{41}(s,r)\right]\phi(s)\,ds$$

and the nondimensional in-plane streses $\sigma_{3xx}(x^*,0)$ becomes

$$\frac{\sigma_{3xx}(x^*,0)}{\mu_{30}} = \frac{2}{\kappa_3+1}\psi(r).$$

Figure 5.40-5.42 give the stress distribution and the load versus contact length curves of an FGM coating loaded by a cylindrical stamp for various values of the stiffness ratio, $\Gamma_3 = \mu_4/\mu_{30}$ in the case of no friction and $(b+a)/R_2 = 0.01, 0.03, 0.05$, respectively. The contact pressure σ_{yy} is bounded at both ends of the stamp $x = a$, $x = b$. The stress σ_{yy} is symmetic and is greater for the stiffening coating $\Gamma_3 = 7$

than for the softening coating $\Gamma_3 = 1/7$. It is observed that the in-plane stress σ_{xx} at both ends of the stamp are tensile for the stiffening FGM coating, zero for the homogeneous coating and compressive for the softening FGM coating. The load versus contact length relation for the homogeneous coating is parabolic. For the same applied load the contact length increases as Γ_3 decreases. Also the contact stresses increase as contact length increases or the radius of the stamp decreses.

Figure 5.43-5.55 give the stress distribution and the load versus contact length curves of an FGM coating loaded by a cylindrical stamp for various values of the stiffness ratio, $\Gamma_3 = \mu_4/\mu_{30}$ and coefficent of friction $\eta = 0.1, 0.3, 0.5$. The stress σ_{yy} is not symmetric anymore but slanted or concentrated towards the trailing edge of the contact region. For the same contact length, σ_{yy} on the surface of the stiffening coating is always greater than σ_{yy} on the surface of the softening coating. Note that the maximum tensile stress σ_{xx} occur at the trailing edge of the contact area. When we compare the magnitudes of σ_{xx} at $x = b$ we conclude that they are greater for the stiffening coating (e.g. $\Gamma_3 = 7$) than for the softening coating(e.g. $\Gamma_3 = 1/7$). For the homogeneous case the σ_{xx} stresses lies between the stiffening and the softening cases. Also as we increase the load the contact length increases and in return the contact stresses increase as well. This is also true if we decrease the radius of the cylindrical stamp, R_2.

Next we investigate the behaviour of the contact stresses as we fix the stiffness ratio Γ_3 and vary the coefficient of friction η(see Figures 5.54 and 5.55). For the stiffening coating in Figure 5.54, as we increase the coefficient of friction η, the in-plane stress σ_{xx} at the trailing edge $x = b$ increases sharply. This a big concern from the point of view of the fretting mechanics of bolted joints used in aircraft and other structures. The peak stress at the trailing edge would serve as a crack initiator. And we can easily observe that the initial crack growth direction from the surface is

perpendicular to the surface. That is because when maximum tensile σ_{xx} occur at the trailing edge the other two components of the stress are zero. There is no significant change in σ_{yy} other than the contact zone are shifted towards to the trailing edge as η increases. Finally there is almost no change inthe load versus contact length curves as we increase η.

Although, the effect of friction on the trends of the contact stresses at the surface of the softening coating in Figure 5.55 are almost the same as the stiffening one, but the magnitude of these stresses are considerably lower. And in some cases for $\Gamma_3 < 1$, there is no in-plane tensile σ_{xx}.

The influence of the parameter χ_3 on the contact stresses is shown in Figures 5.56 and 5.57. And the effect of the thickness of the FGM coating on the contact stresses is depicted in Figures 5.58 and 5.59.

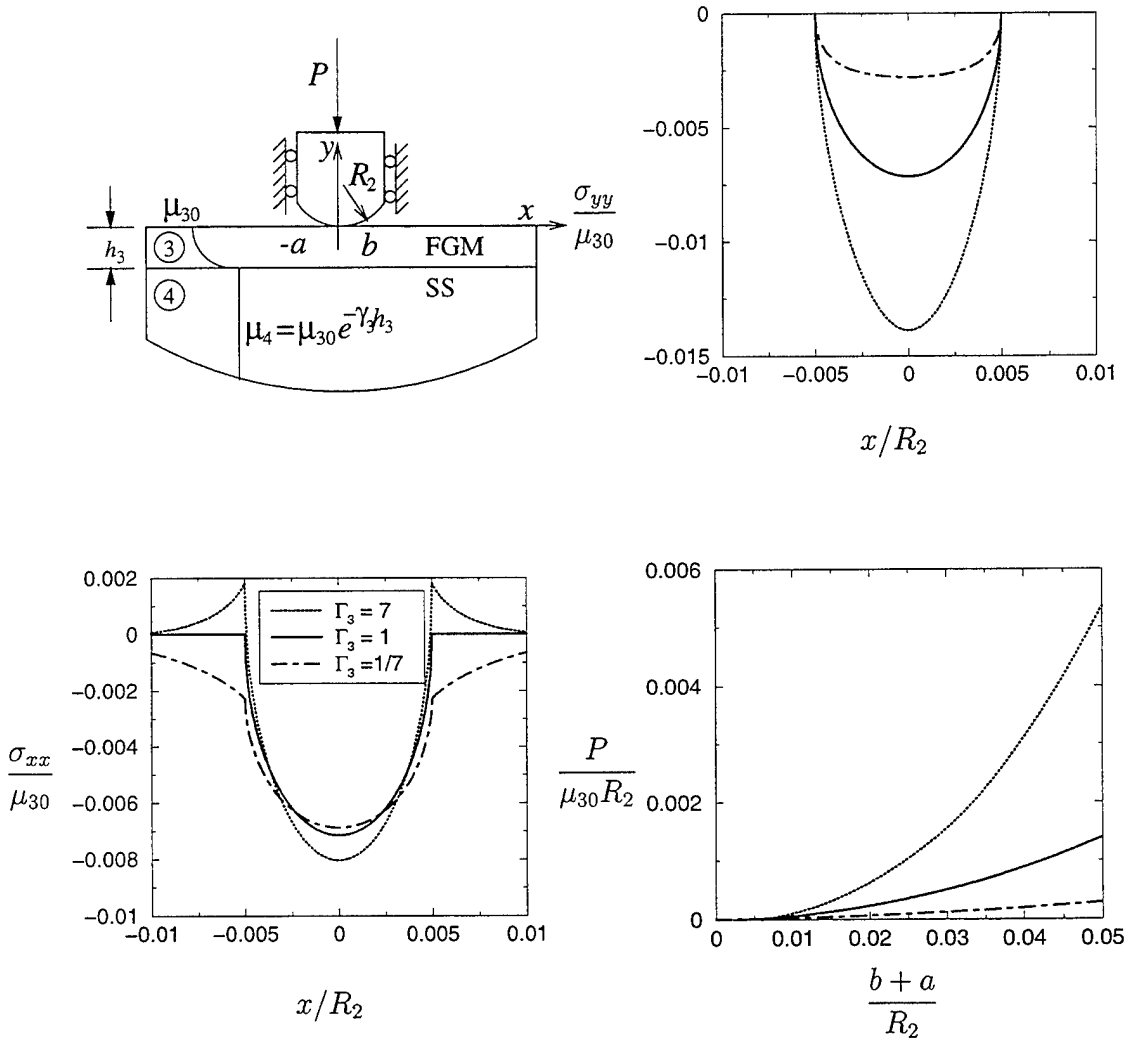

Figure 5.40: Stress distribution on the surface of an FGM coating loaded by a rigid cylindrical stamp for various values of the stiffness ratio, $\Gamma_3 = \mu_4/\mu_{30}$, $(b+a)/R_2 = 0.01$, $R_2/h_3 = 100$, $\eta = 0.0$.

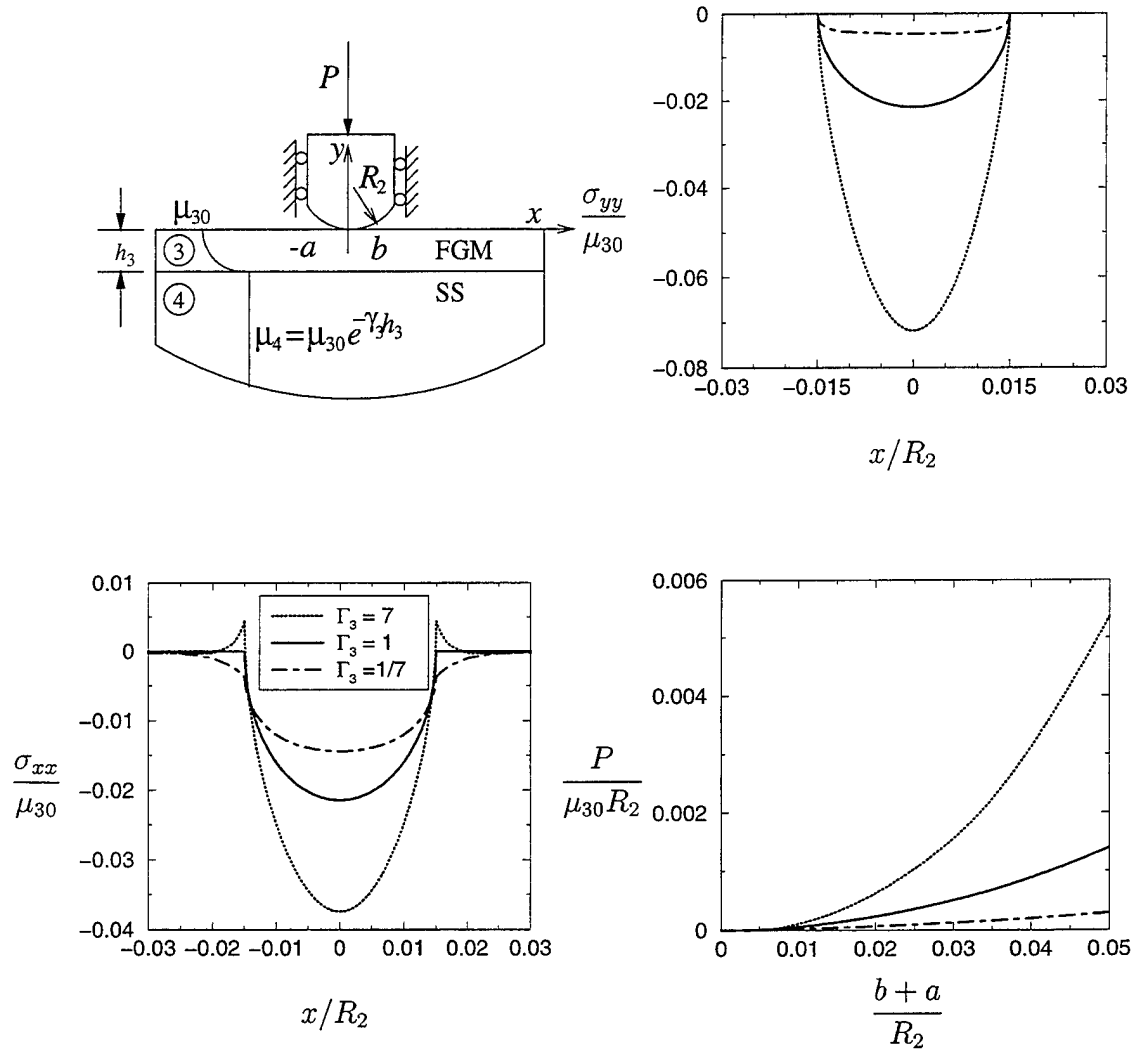

Figure 5.41: Stress distribution on the surface of an FGM coating loaded by a rigid cylindrical stamp for various values of the stiffness ratio, $\Gamma_3 = \mu_4/\mu_{30}$, $(b+a)/R_2 = 0.03$, $R_2/h_3 = 100$, $\eta = 0.0$.

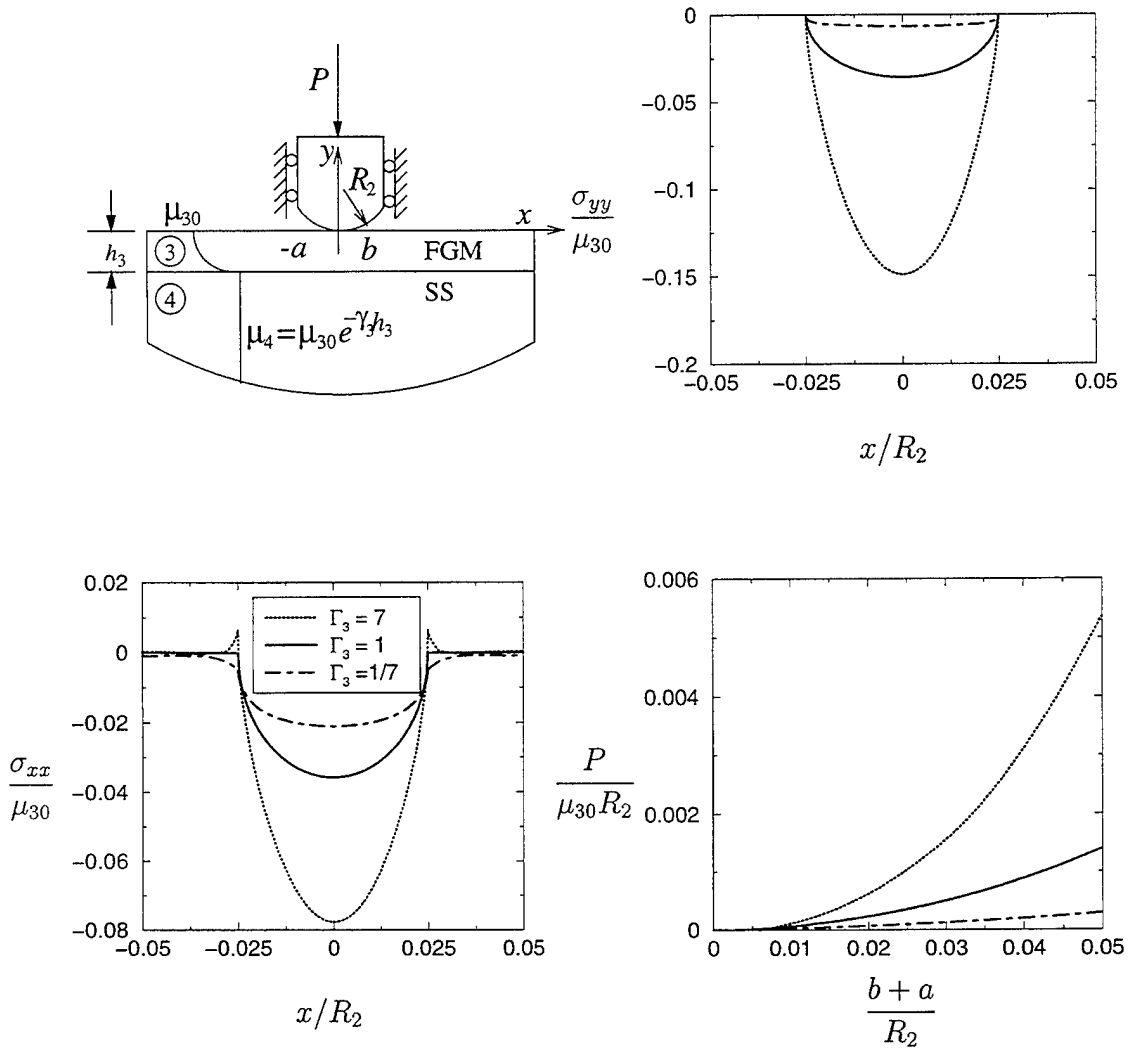

Figure 5.42: Stress distribution on the surface of an FGM coating loaded by a rigid cylindrical stamp for various values of the stiffness ratio, $\Gamma_3 = \mu_4/\mu_{30}$, $(b+a)/R_2 = 0.05$, $R_2/h_3 = 100$, $\eta = 0.0$.

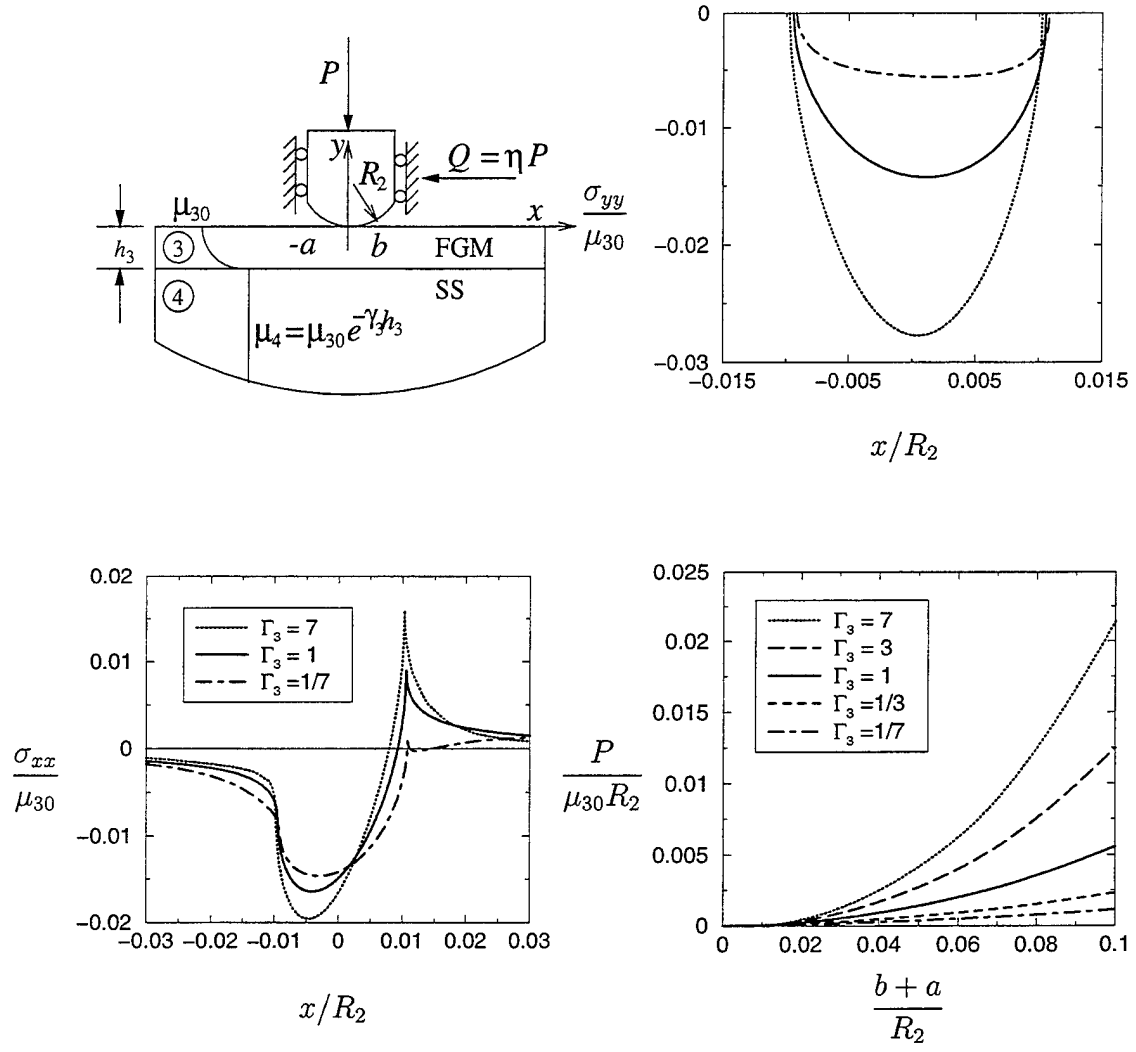

Figure 5.43: Stress distribution on the surface of an FGM coating loaded by a rigid cylindrical stamp for various values of the stiffness ratio, $\Gamma_3 = \mu_4/\mu_{30}$, $(b+a)/R_2 = 0.02$, $R_2/h_3 = 50$, $\eta = 0.3$.

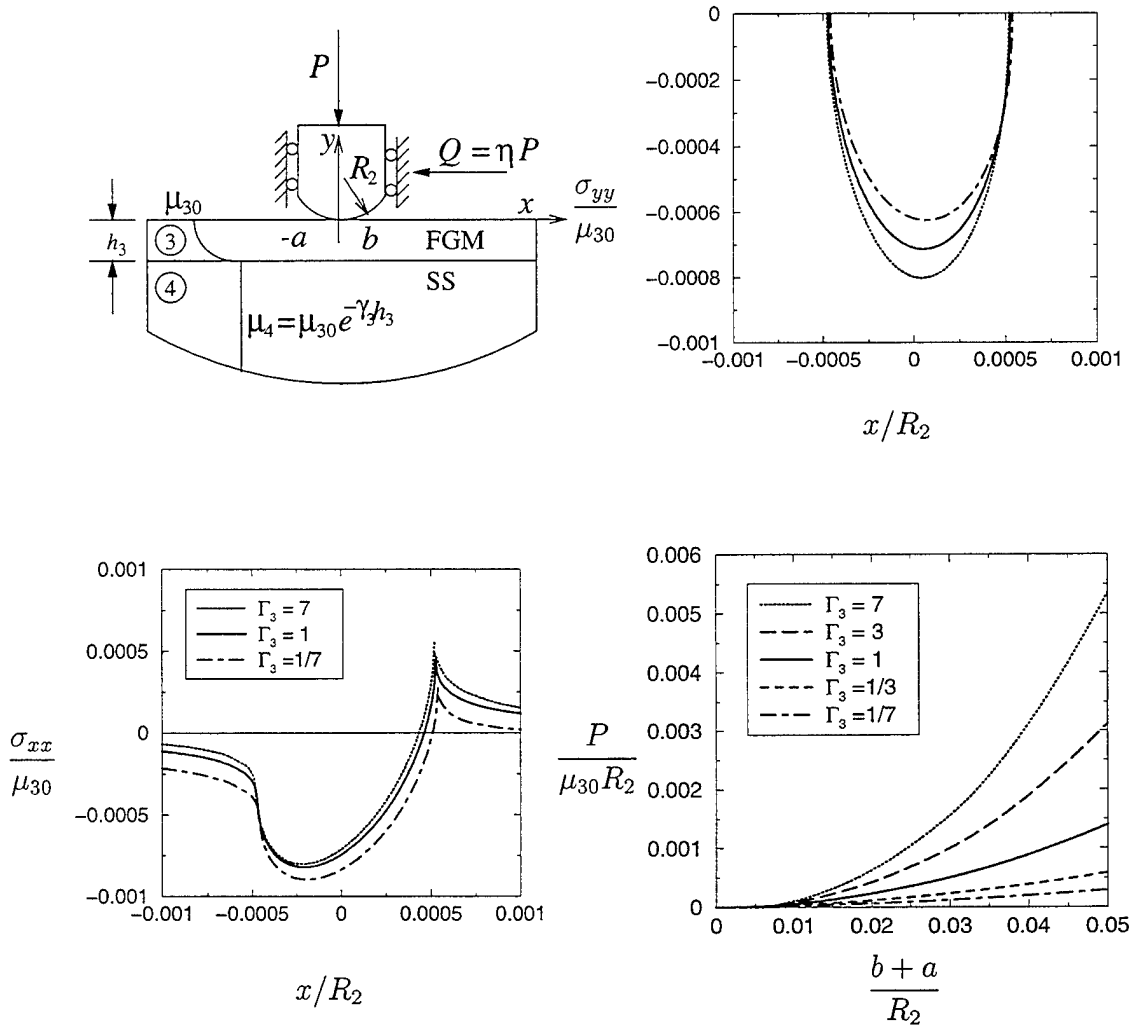

Figure 5.44: Stress distribution on the surface of an FGM coating loaded by a rigid cylindrical stamp for various values of the stiffness ratio, $\Gamma_3 = \mu_4/\mu_{30}$, $(b+a)/R_2 = 0.001$, $R_2/h_3 = 100$, $\eta = 0.3$.

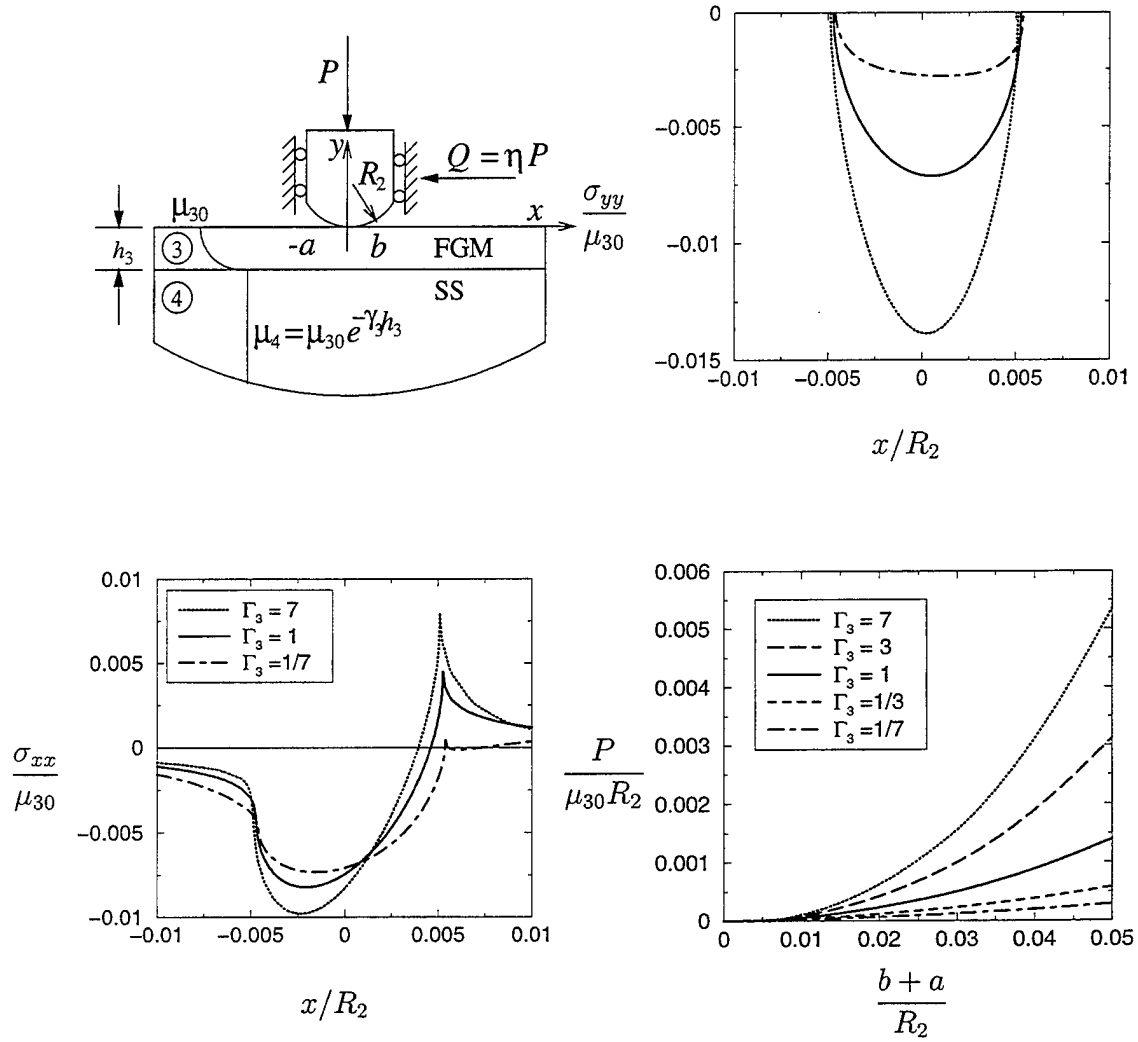

Figure 5.45: Stress distribution on the surface of an FGM coating loaded by a rigid cylindrical stamp for various values of the stiffness ratio, $\Gamma_3 = \mu_4/\mu_{30}$, $(b+a)/R_2 = 0.01$, $R_2/h_3 = 100$, $\eta = 0.3$.

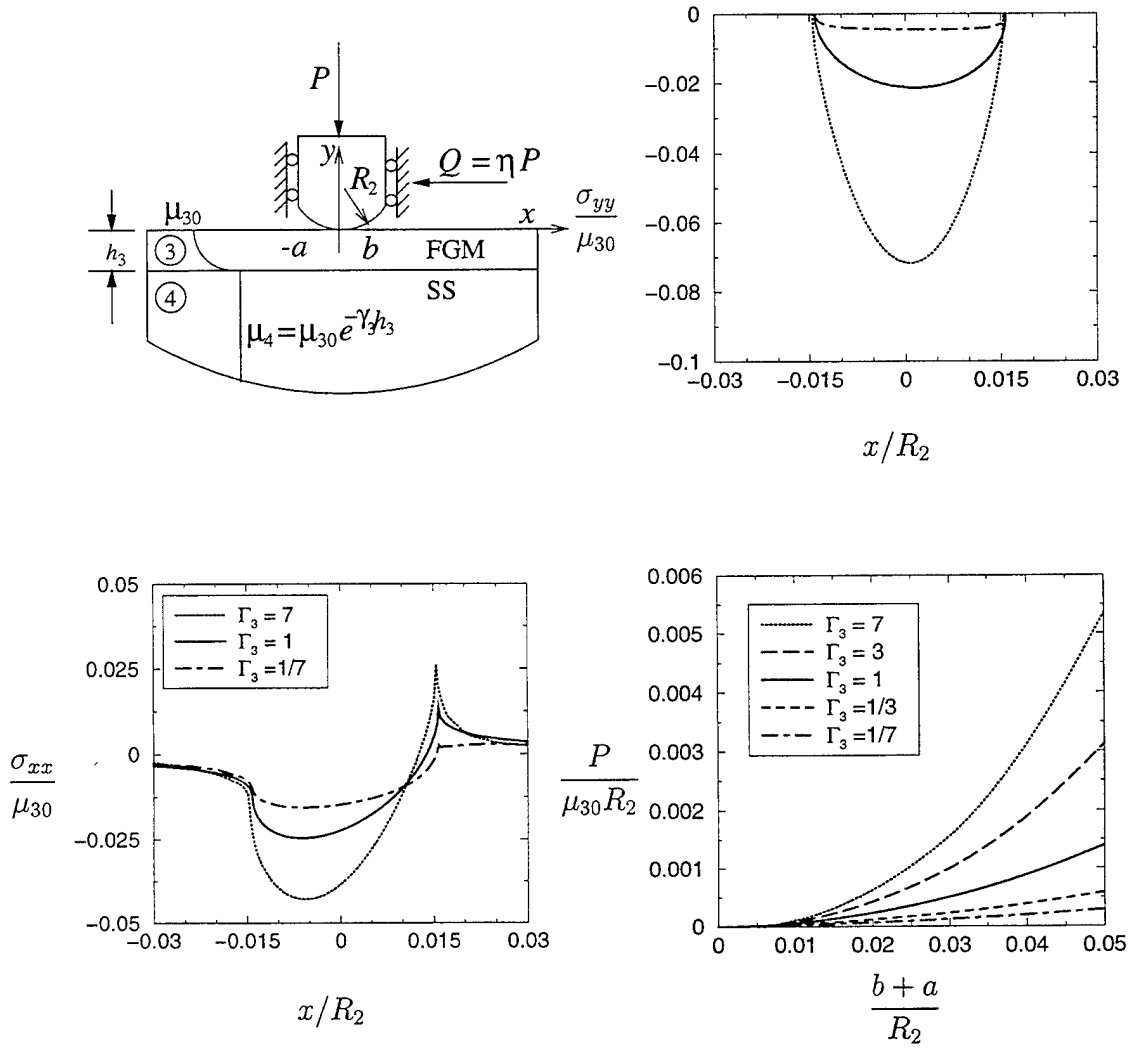

Figure 5.46: Stress distribution on the surface of an FGM coating loaded by a rigid cylindrical stamp for various values of the stiffness ratio, $\Gamma_3 = \mu_4/\mu_{30}$, $(b+a)/R_2 = 0.03$, $R_2/h_3 = 100$, $\eta = 0.3$.

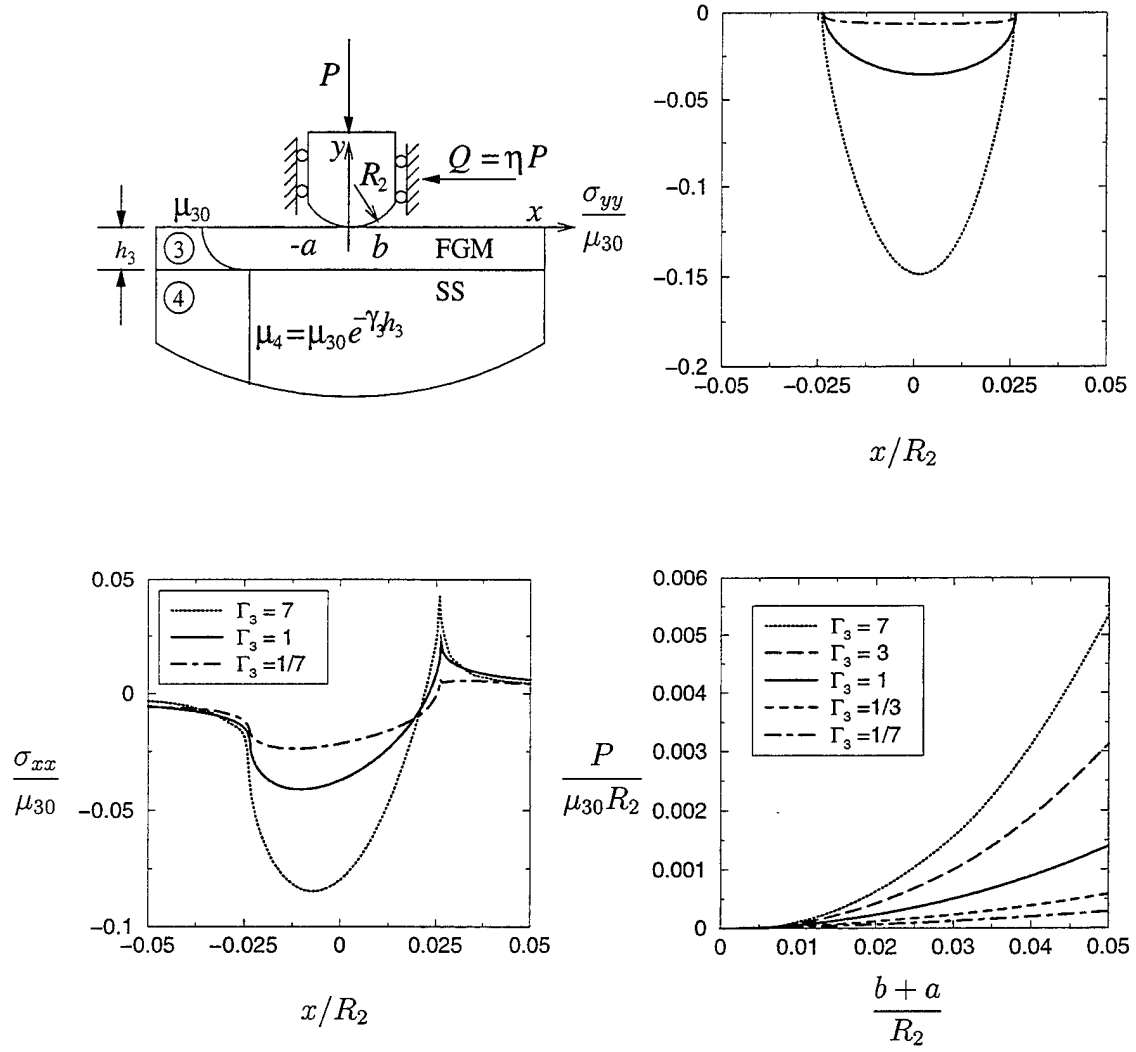

Figure 5.47: Stress distribution on the surface of an FGM coating loaded by a rigid cylindrical stamp for various values of the stiffness ratio, $\Gamma_3 = \mu_4/\mu_{30}$, $(b+a)/R_2 = 0.05$, $R_2/h_3 = 100$, $\eta = 0.3$.

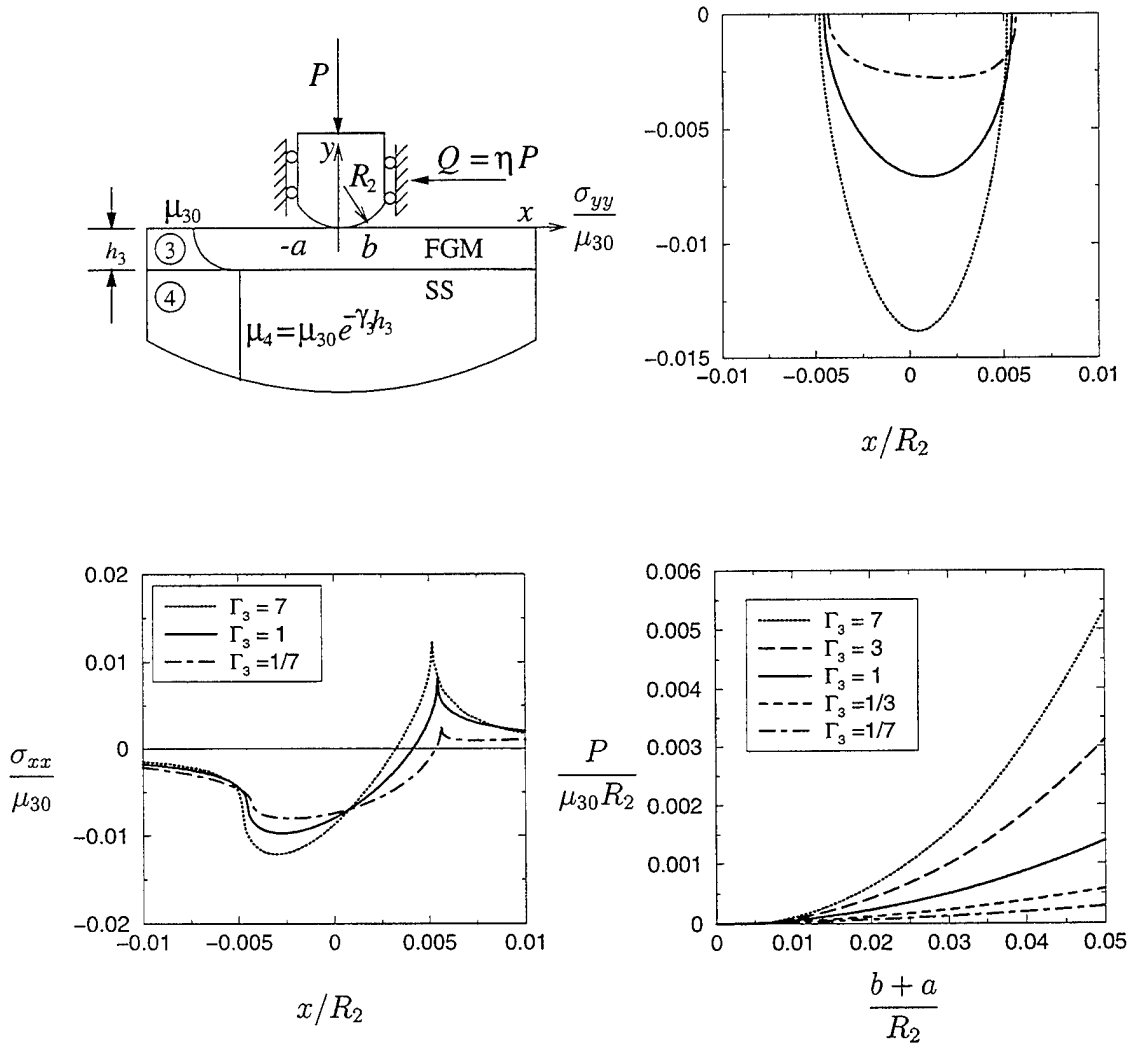

Figure 5.48: Stress distribution on the surface of an FGM coating loaded by a rigid cylindrical stamp for various values of the stiffness ratio, $\Gamma_3 = \mu_4/\mu_{30}$, $(b+a)/R_2 = 0.01$, $R_2/h_3 = 100$, $\eta = 0.5$.

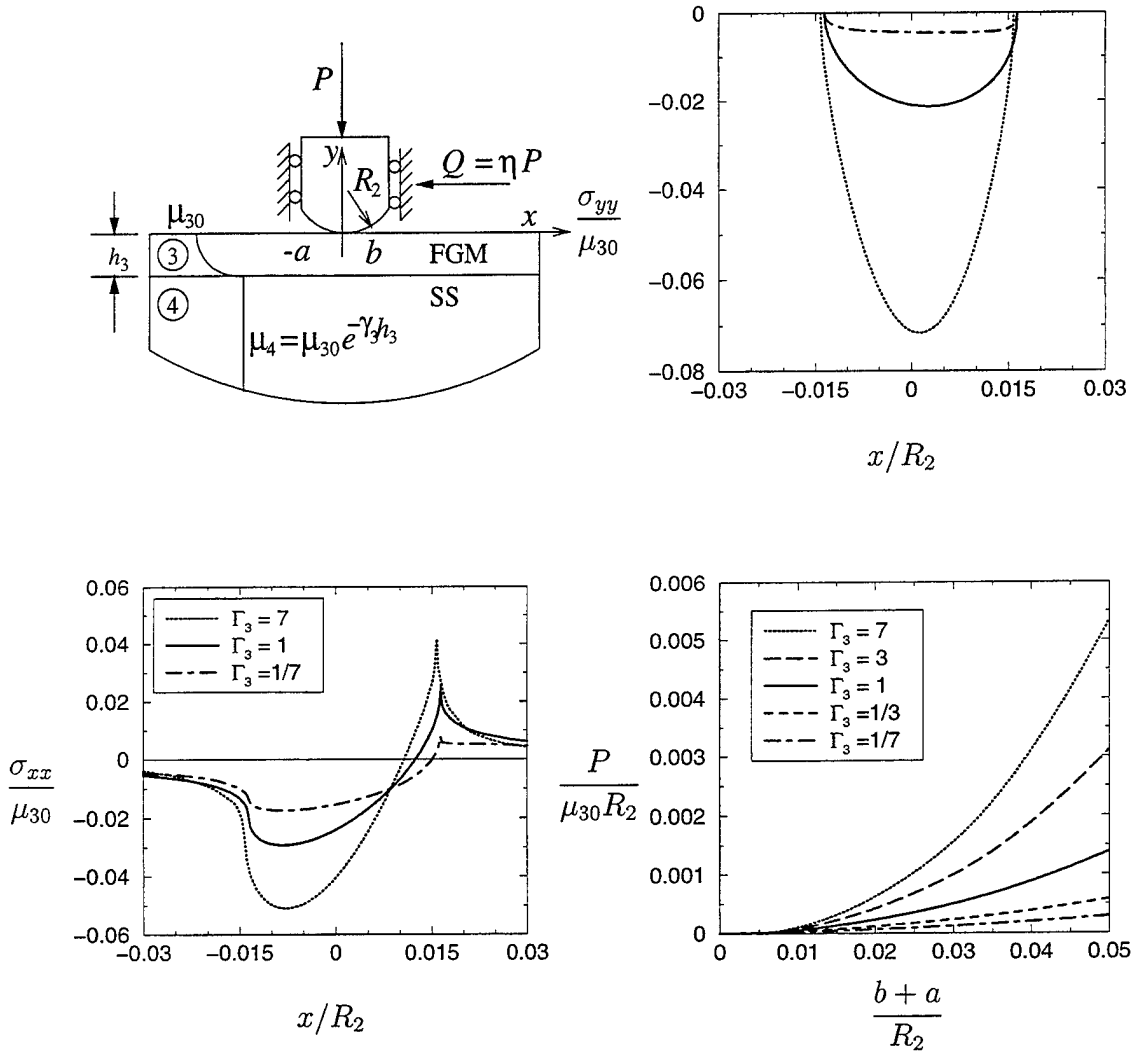

Figure 5.49: Stress distribution on the surface of an FGM coating loaded by a rigid cylindrical stamp for various values of the stiffness ratio, $\Gamma_3 = \mu_4/\mu_{30}$, $(b+a)/R_2 = 0.03$, $R_2/h_3 = 100$, $\eta = 0.5$.

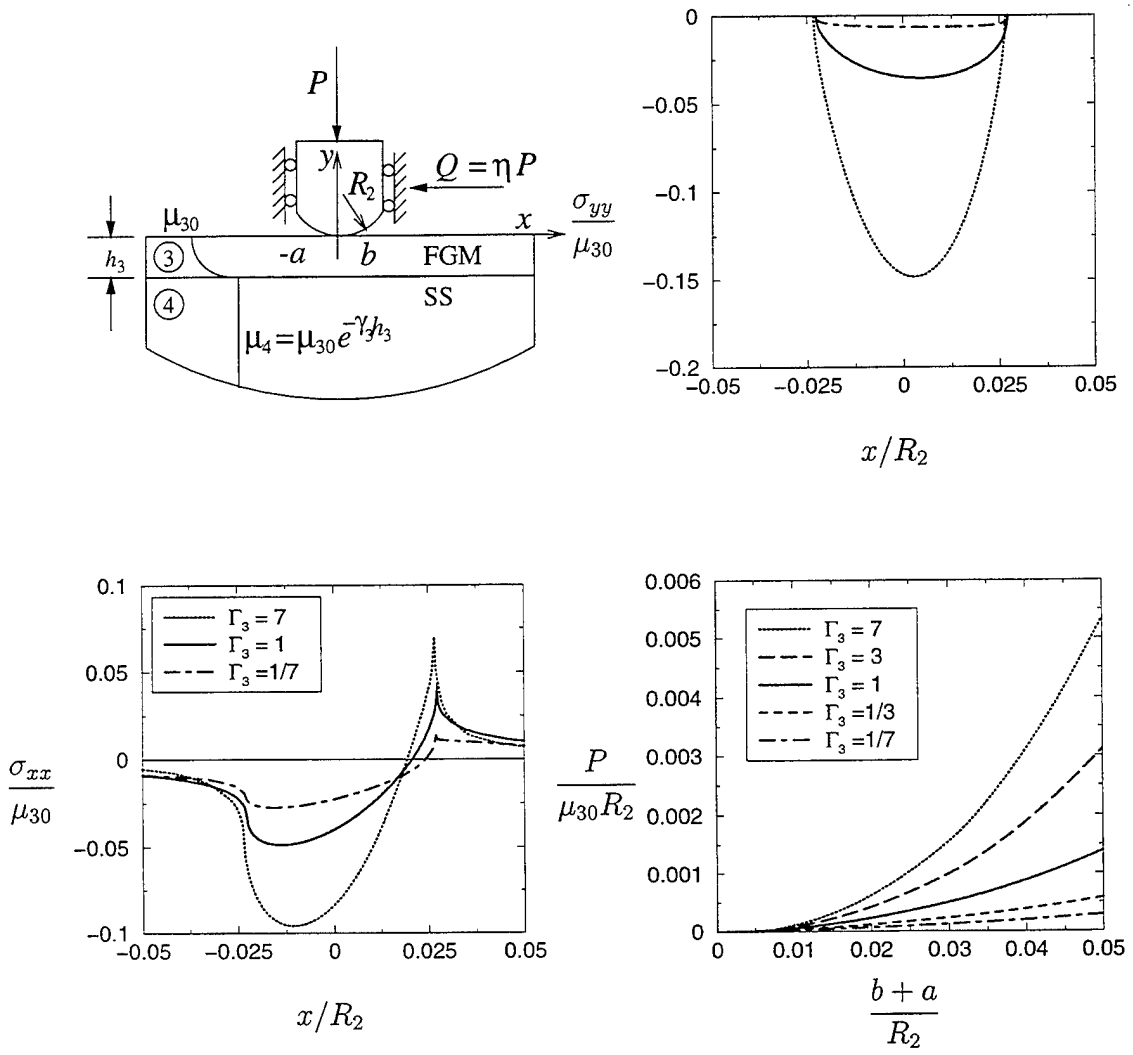

Figure 5.50: Stress distribution on the surface of an FGM coating loaded by a rigid cylindrical stamp for various values of the stiffness ratio, $\Gamma_3 = \mu_4/\mu_{30}$, $(b+a)/R_2 = 0.05$, $R_2/h_3 = 100$, $\eta = 0.5$.

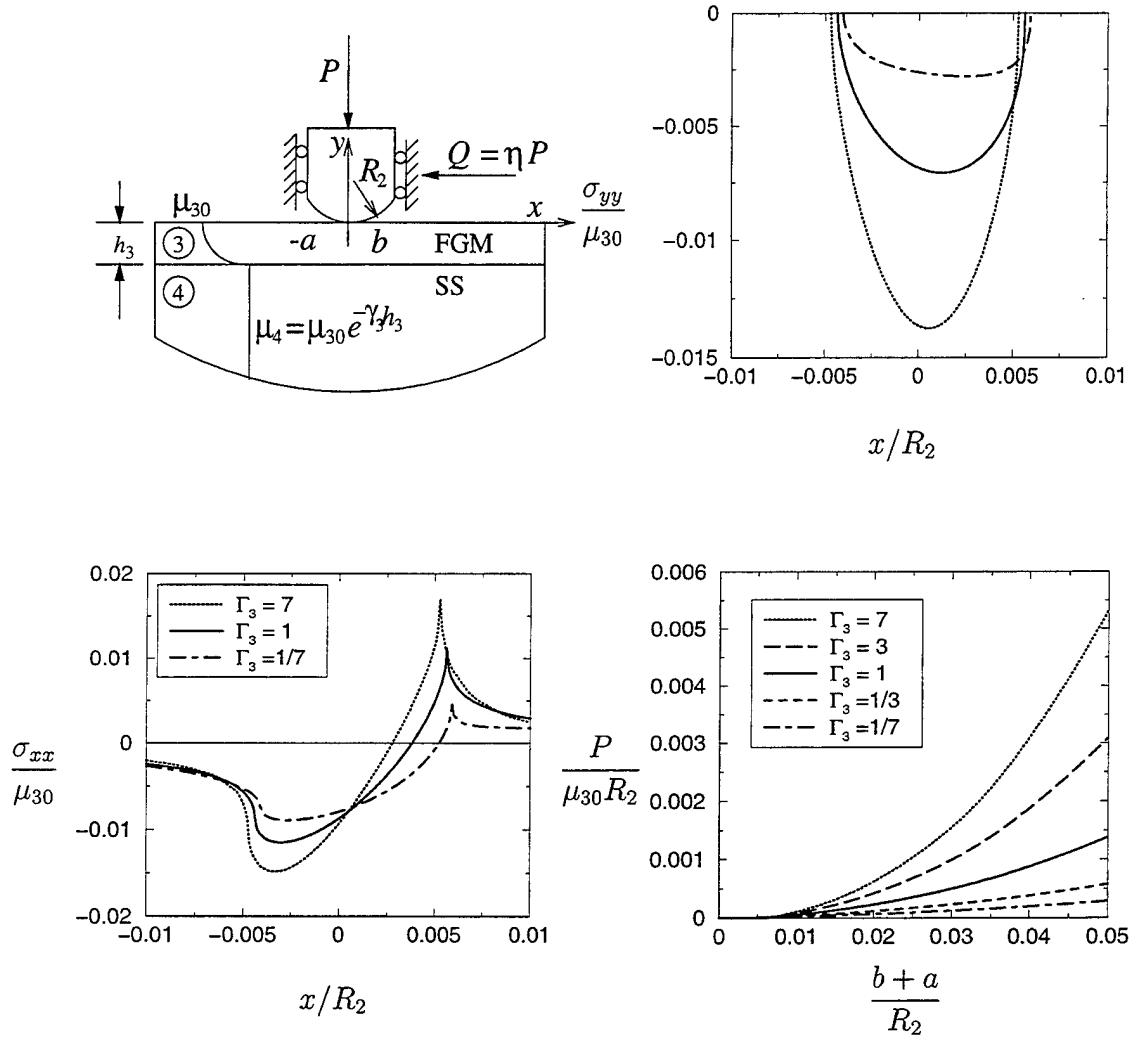

Figure 5.51: Stress distribution on the surface of an FGM coating loaded by a rigid cylindrical stamp for various values of the stiffness ratio, $\Gamma_3 = \mu_4/\mu_{30}$, $(b+a)/R_2 = 0.01$, $R_2/h_3 = 100$, $\eta = 0.7$.

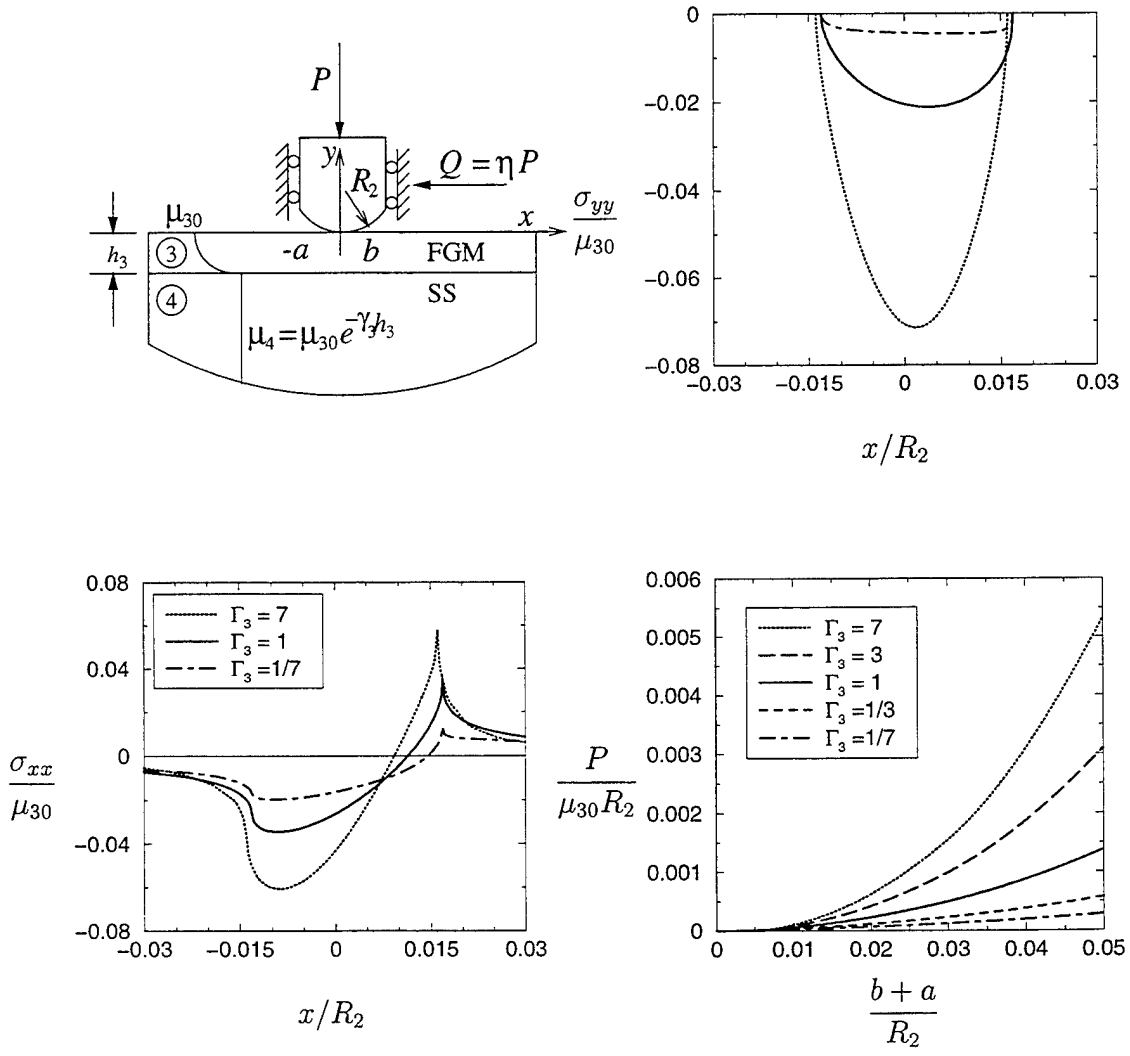

Figure 5.52: Stress distribution on the surface of an FGM coating loaded by a rigid cylindrical stamp for various values of the stiffness ratio, $\Gamma_3 = \mu_4/\mu_{30}$, $(b+a)/R_2 = 0.03$, $R_2/h_3 = 100$, $\eta = 0.7$.

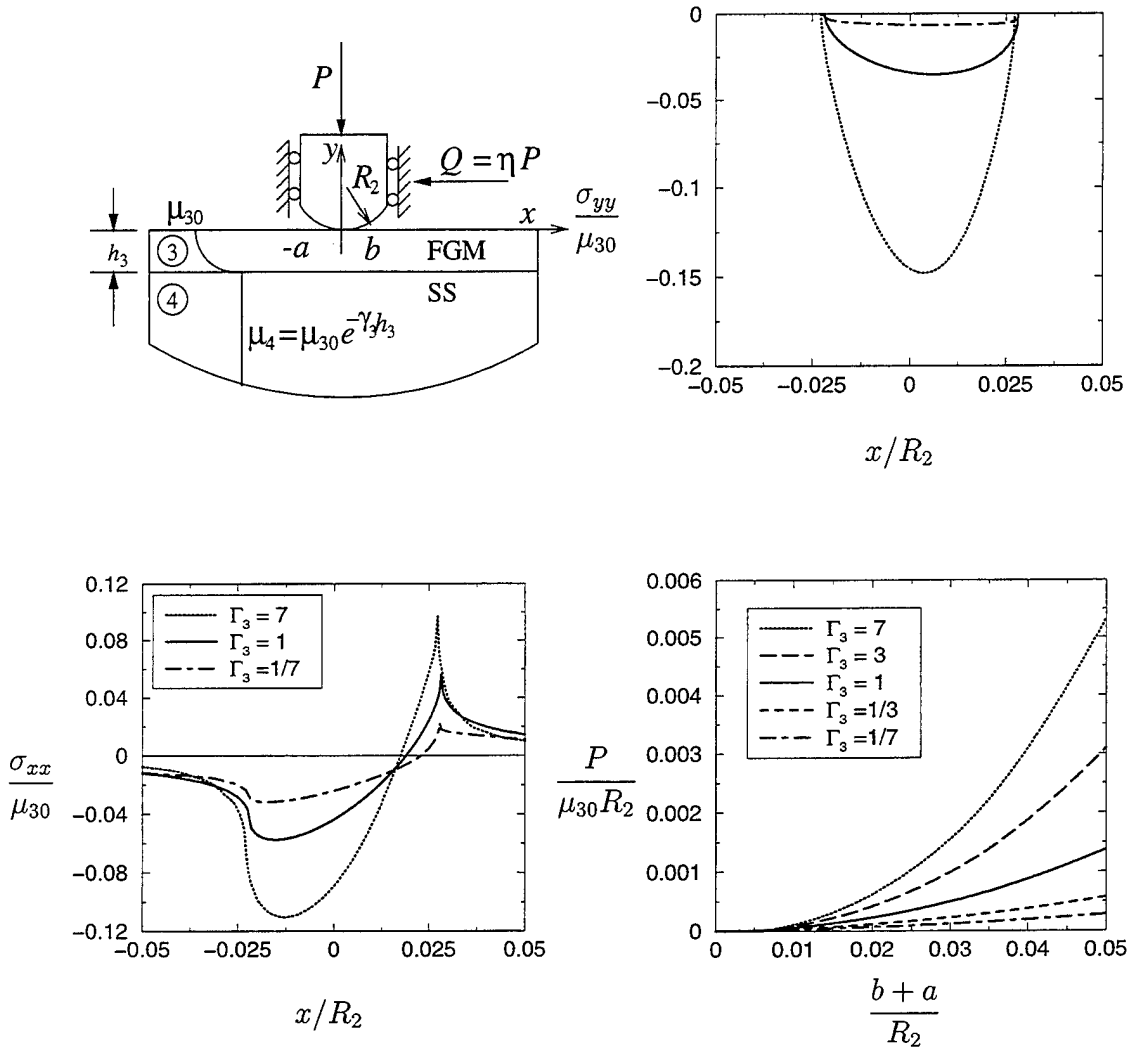

Figure 5.53: Stress distribution on the surface of an FGM coating loaded by a rigid cylindrical stamp for various values of the stiffness ratio, $\Gamma_3 = \mu_4/\mu_{30}$, $(b+a)/R_2 = 0.05$, $R_2/h_3 = 100$, $\eta = 0.7$.

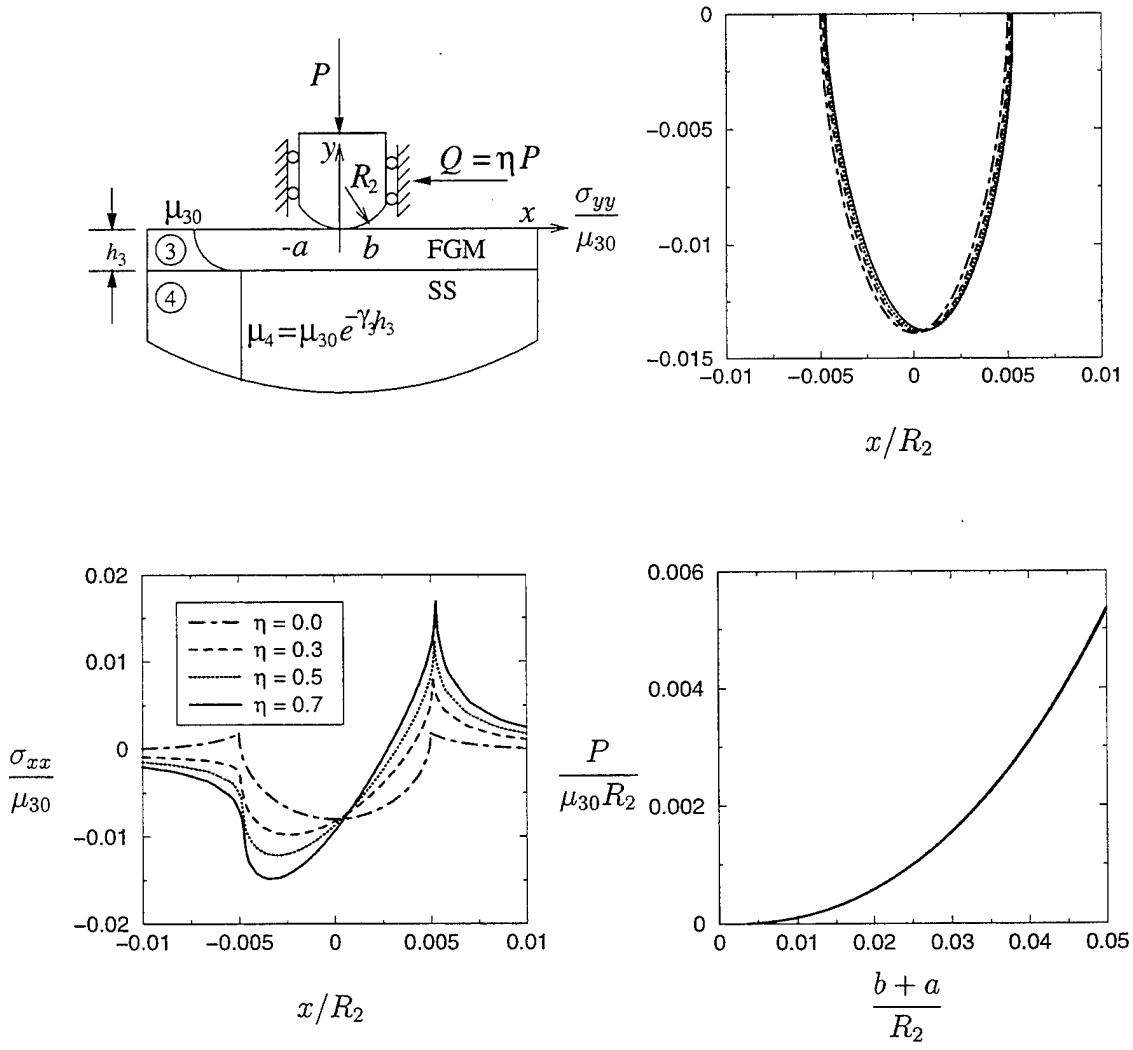

Figure 5.54: Stress distribution on the surface of an FGM coating loaded by a rigid cylindrical stamp for various values of the coefficient of friction, η, $\Gamma_3 = \mu_4/\mu_{30} = 7$, $(b+a)/R_2 = 0.01$, $R_2/h_3 = 100$.

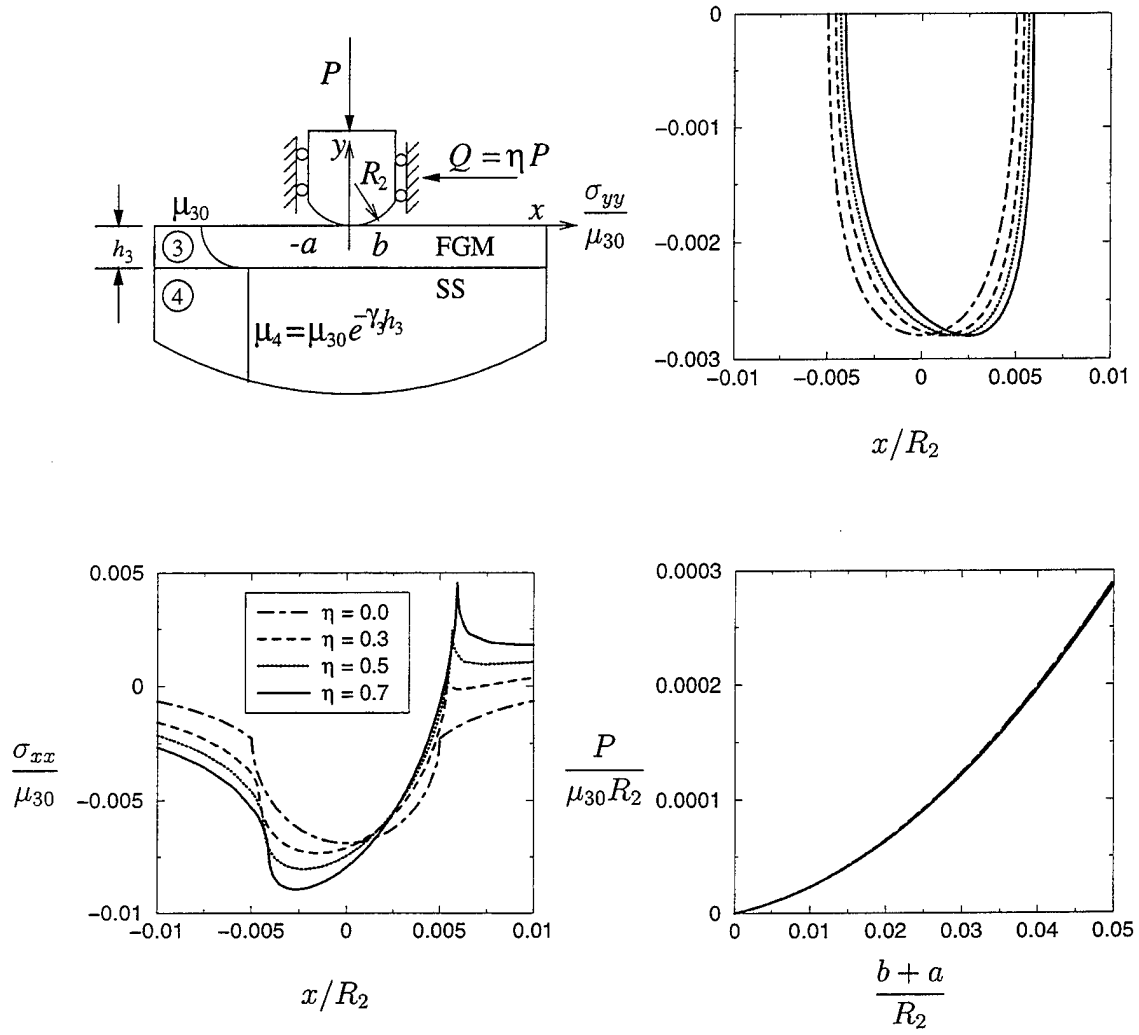

Figure 5.55: Stress distribution on the surface of an FGM coating loaded by a rigid cylindrical stamp for various values of the coefficient of friction, η, $\Gamma_3 = \mu_4/\mu_{30} = 1/7$, $(b+a)/R_2 = 0.01$, $R_2/h_3 = 100$.

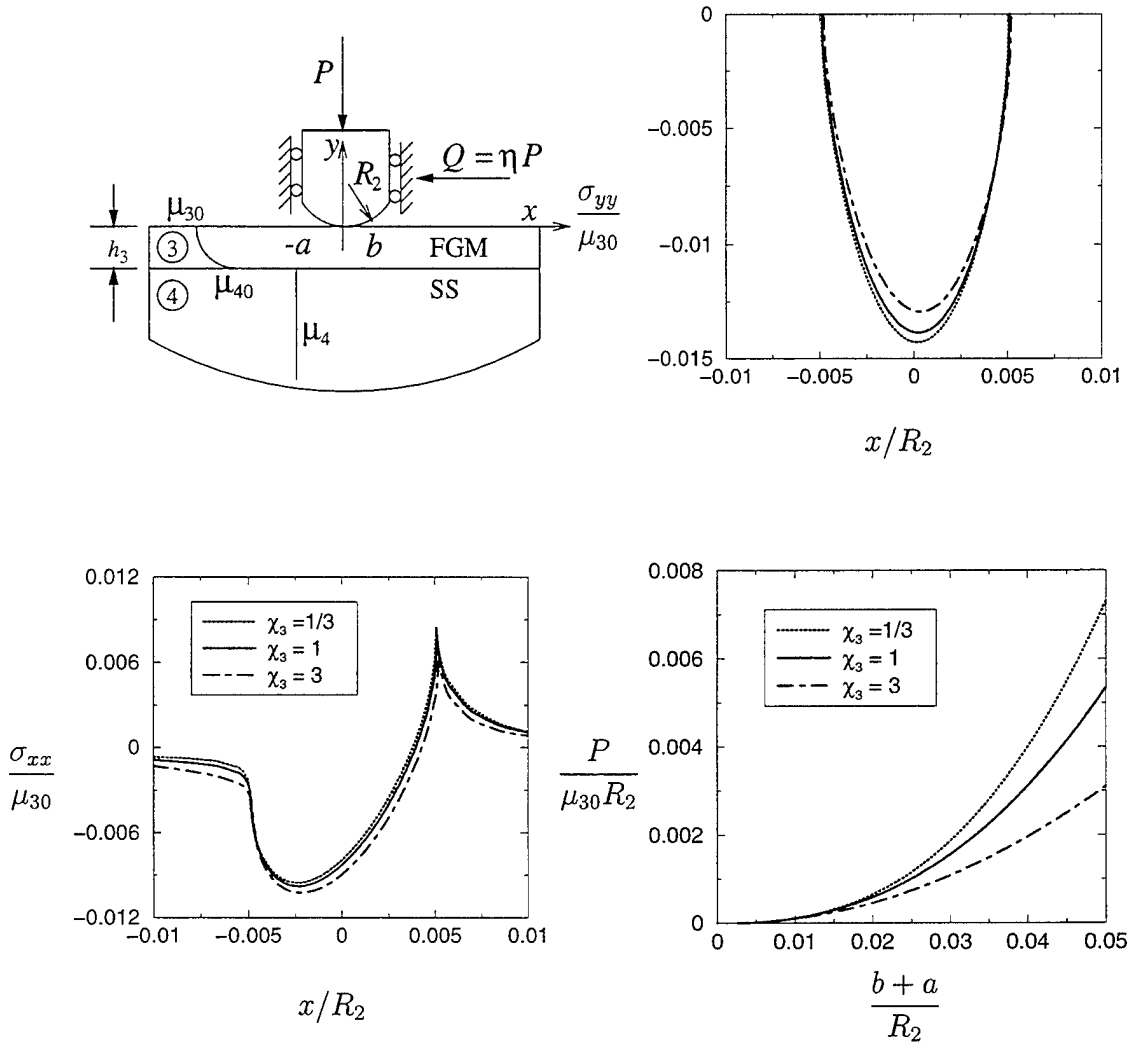

Figure 5.56: Stress distribution on the surface of an FGM coating loaded by a rigid cylindrical stamp for various values of the stiffness ratio, $\chi_3 = \mu_{40}/\mu_4$, $\Gamma_3 = \mu_{40}/\mu_{30} = 7$, $(b+a)/R_2 = 0.01$, $R_2/h_3 = 100$, $\eta = 0.3$.

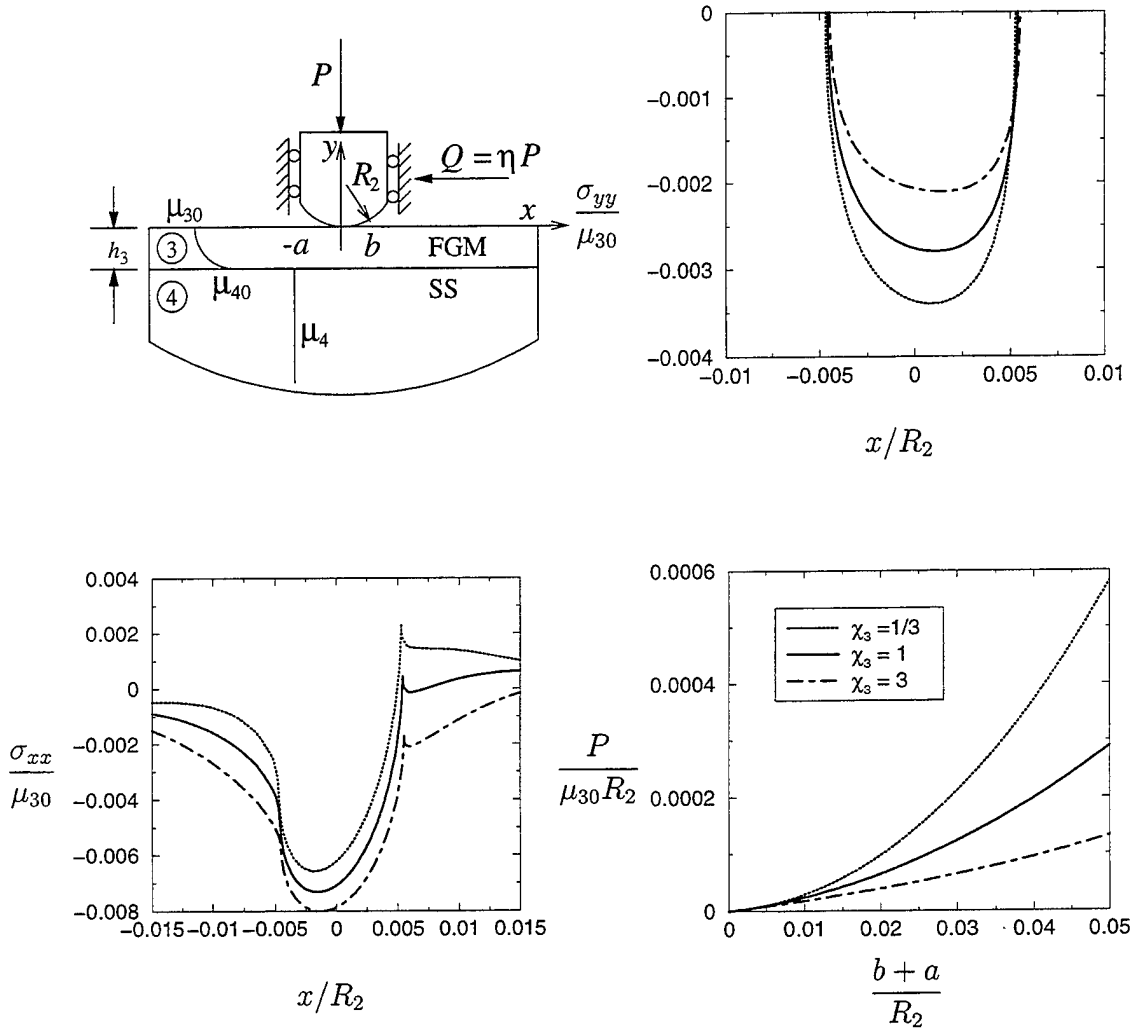

Figure 5.57: Stress distribution on the surface of an FGM coating loaded by a rigid cylindrical stamp for various values of the stiffness ratio, $\chi_3 = \mu_{40}/\mu_4$, $\Gamma_3 = \mu_{40}/\mu_{30} = 1/7$, $(b+a)/R_2 = 0.01$, $R_2/h_3 = 100$, $\eta = 0.3$.

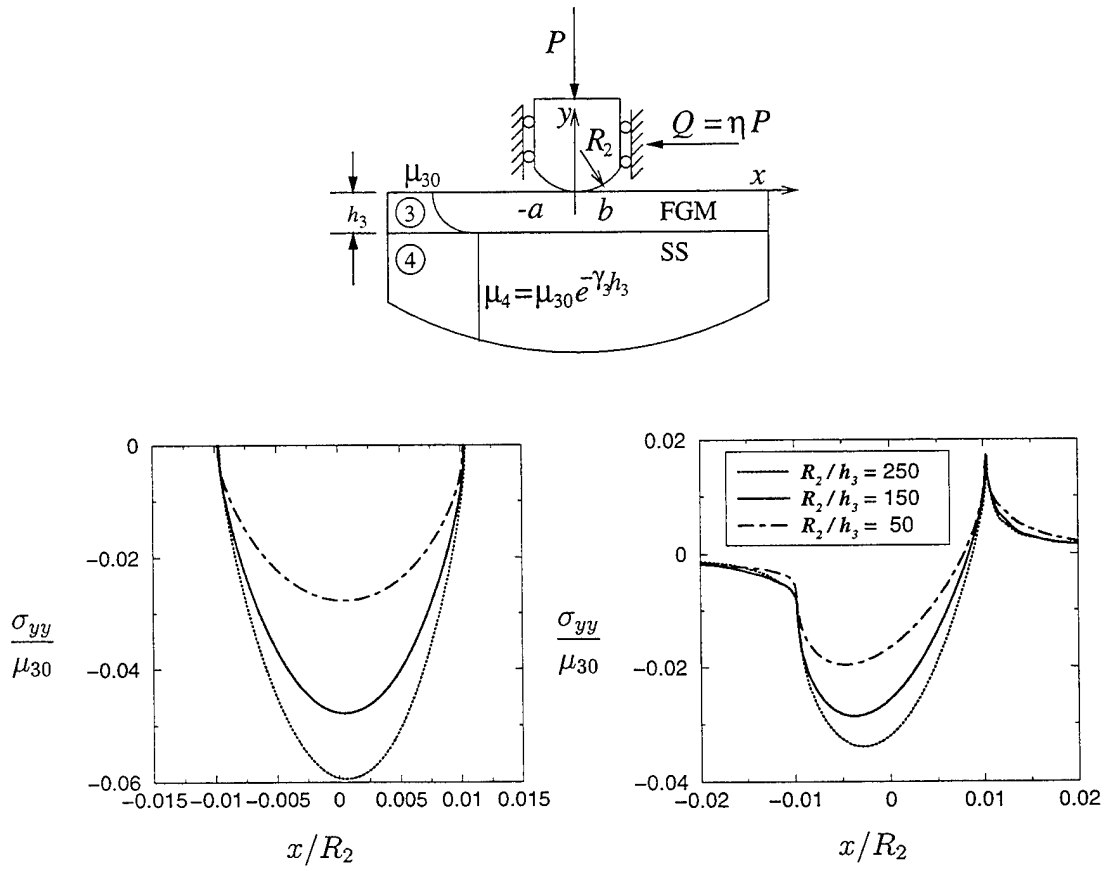

Figure 5.58: Stress distribution on the surface of an FGM coating loaded by a cylindrical stamp for various values of the thickness of the coating, $\Gamma_3 = \mu_{40}/\mu_{30} = 7$, $(b+a)/R_2 = 0.02$, $\eta = 0.3$.

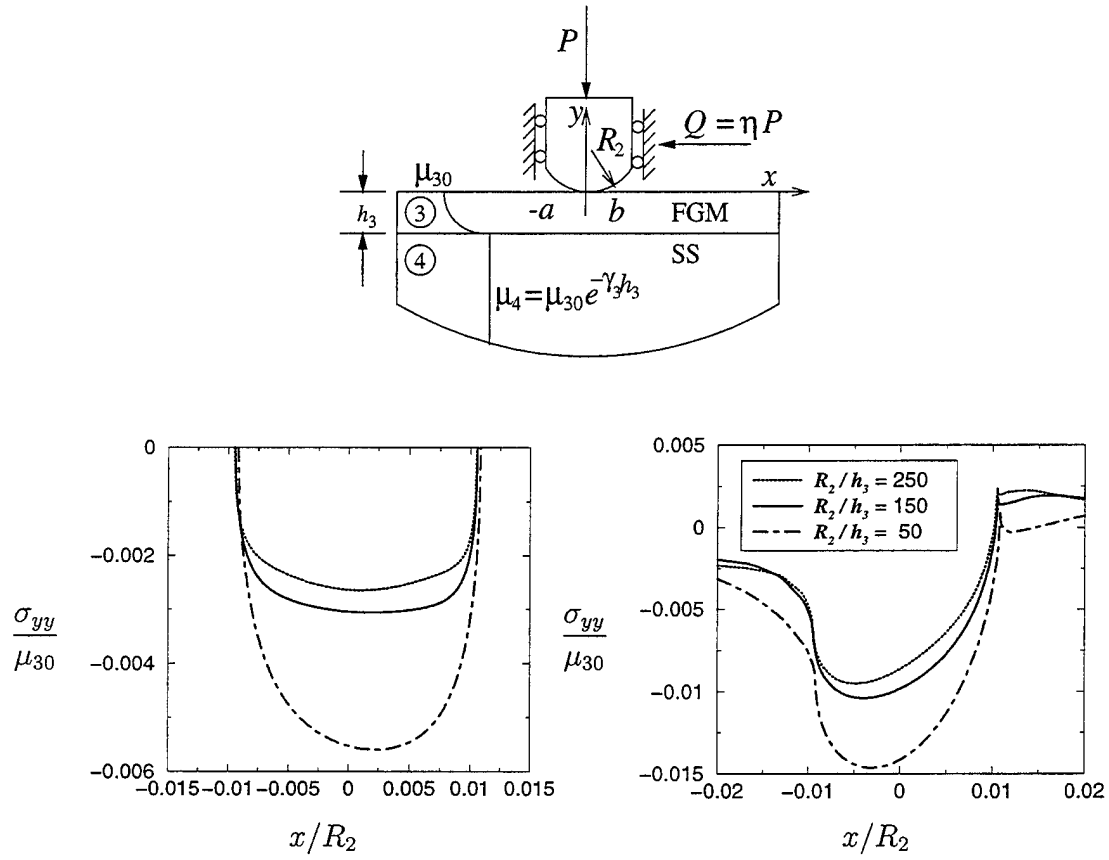

Figure 5.59: Stress distribution on the surface of an FGM coating loaded by a cylindrical stamp for various values of the thickness of the coating, $\Gamma_3 = \mu_{40}/\mu_{30} = 1/7$, $(b+a)/R_2 = 0.02$, $\eta = 0.3$.

Chapter 6

Contact Problems for two Deformable Solids

6.1 Contacting Solids with Positive Curvatures

In the load-transfer components shown in Fig.1.2, it will be assumed that the contacting solids locally have shallow curvatures(that is, the contact zone size $(b+a)$ is "small" compared to R_1 and R_2). Thus, in formulating the problem one may make the standard Hertzian assumption to the effect that the Green's functions for the concentrated surface tractions in a cylindrical medium may be approximated by that of a half plane. The contacting solids consist of dissimilar homogeneous materials coated by graded elastic layers of known thickness. Locally the solids will be represented by circular cylinders with positive/negative (Fig.1.2a) or positive/positive (Fig.1.2b) curvatures. The problem will be considered with or without friction. The main calculated quantities will again be the contact stresses and the load versus the contact zone size curves.

The general equations of the surface displacement derivatives for the upper and

lower media may be written as

$$\omega_3\eta p(x)+\frac{1}{\pi}\int_{-a}^{b}\left[-\frac{1}{t-x}+k_{31}(t,x)+\eta k_{32}(t,x)\right]p(t)dt = f_3(x), \quad (6.1)$$

$$\omega_2\eta p(x)+\frac{1}{\pi}\int_{-a}^{b}\left[\frac{1}{t-x}+k_{11}(t,x)+\eta k_{12}(t,x)\right]p(t)dt = f_2(x), \quad (6.2)$$

$$-\omega_3 p(x)+\frac{1}{\pi}\int_{-a}^{b}\left[-\frac{\eta}{t-x}+\eta k_{41}(t,x)+k_{42}(t,x)\right]p(t)dt = g_3(x), \quad (6.3)$$

$$-\omega_2 p(x)+\frac{1}{\pi}\int_{-a}^{b}\left[\frac{\eta}{t-x}+\eta k_{21}(t,x)+k_{22}(t,x)\right]p(t)dt = g_2(x), \quad (6.4)$$

where

$$f_3(x) = \lambda_3\frac{\partial}{\partial x}v_3(x,0), \quad (6.5)$$

$$f_2(x) = \lambda_2\frac{\partial}{\partial x}v_2(x,0), \quad (6.6)$$

$$g_3(x) = \lambda_3\frac{\partial}{\partial x}u_3(x,0), \quad (6.7)$$

$$g_2(x) = \lambda_2\frac{\partial}{\partial x}u_2(x,0), \quad (6.8)$$

$$\lambda_3 = \frac{4\mu_{30}}{\kappa_3+1}, \quad (6.9)$$

$$\lambda_2 = \frac{4\mu_{20}}{\kappa_2+1}, \quad (6.10)$$

$$\omega_3 = \frac{\kappa_3-1}{\kappa_3+1}, \quad (6.11)$$

$$\omega_2 = \frac{\kappa_2-1}{\kappa_2+1}, \quad (6.12)$$

$$k_{11}(t,x) = -\frac{4}{(\kappa_2+1)}\int_0^\infty \Phi_{11}(\alpha)\sin\alpha(t-x)d\alpha, \quad (6.13)$$

$$k_{12}(t,x) = -\frac{4}{(\kappa_2+1)}\int_0^\infty \Phi_{12}(\alpha)\cos\alpha(t-x)d\alpha, \quad (6.14)$$

$$k_{21}(t,x) = -\frac{4}{(\kappa_2+1)}\int_0^\infty \Phi_{21}(\alpha)\sin\alpha(t-x)d\alpha, \quad (6.15)$$

$$k_{22}(t,x) = -\frac{4}{(\kappa_2+1)}\int_0^\infty \Phi_{22}(\alpha)\cos\alpha(t-x)d\alpha, \quad (6.16)$$

$$k_{31}(t,x) = -\frac{4}{(\kappa_3+1)}\int_0^\infty \Phi_{31}(\alpha)\sin\alpha(t-x)d\alpha, \tag{6.17}$$

$$k_{32}(t,x) = -\frac{4}{(\kappa_3+1)}\int_0^\infty \Phi_{32}(\alpha)\cos\alpha(t-x)d\alpha, \tag{6.18}$$

$$k_{41}(t,x) = -\frac{4}{(\kappa_3+1)}\int_0^\infty \Phi_{41}(\alpha)\sin\alpha(t-x)d\alpha, \tag{6.19}$$

$$k_{42}(t,x) = -\frac{4}{(\kappa_3+1)}\int_0^\infty \Phi_{42}(\alpha)\cos\alpha(t-x)d\alpha. \tag{6.20}$$

By using equations (6.1) and (6.2), the displacement gradients for the upper and for the lower media can be expressed as

$$\frac{\partial}{\partial x}v_2(x,0) = \frac{\omega_2}{\lambda_2}\eta p(x) + \frac{1}{\lambda_2\pi}\int_{-a}^{b}\left[\frac{1}{t-x} + k_{11}(t,x) + \eta k_{12}(t,x)\right]p(t)dt, \tag{6.21}$$

$$\frac{\partial}{\partial x}v_3(x,0) = \frac{\omega_3}{\lambda_3}\eta p(x) + \frac{1}{\lambda_3\pi}\int_{-a}^{b}\left[-\frac{1}{t-x} + k_{31}(t,x) + \eta k_{32}(t,x)\right]p(t)dt \tag{6.22}$$

Subtracting (6.21) from (6.22) we have

$$\begin{aligned}\frac{\partial}{\partial x}v_3(x,0) - \frac{\partial}{\partial x}v_2(x,0) = &-\left[\frac{\omega_2}{\lambda_2} - \frac{\omega_3}{\lambda_3}\right]\eta p(x) \\ &-\left[\frac{1}{\lambda_2} + \frac{1}{\lambda_3}\right]\frac{1}{\pi}\int_{-a}^{b}\frac{p(t)}{t-x}dt \\ &-\frac{1}{\lambda_2\pi}\int_{-a}^{b}\left[k_{11}(t,x) + \eta k_{12}(t,x)\right]p(t)dt \\ &+\frac{1}{\lambda_3\pi}\int_{-a}^{b}\left[k_{31}(t,x) + \eta k_{32}(t,x)\right]p(t)dt.\end{aligned} \tag{6.23}$$

The displacement derivatives are related to the curvatures as follows:

$$\frac{\partial}{\partial x}v_2(x,0) = -\frac{x}{R_1}, \tag{6.24}$$

$$\frac{\partial}{\partial x}v_3(x,0) = +\frac{x}{R_2}. \tag{6.25}$$

Subtracting (6.24) from (6.25) we obtain

$$\frac{\partial}{\partial x}v_3(x,0) - \frac{\partial}{\partial x}v_2(x,0) = \frac{x}{R}, \tag{6.26}$$

where

$$\frac{1}{R} = \frac{1}{R_1} + \frac{1}{R_2} = \frac{1}{R_2}\left(1 + \frac{R_2}{R_1}\right) = \frac{R^*}{R_2}, \tag{6.27}$$

$$R^* = 1 + \chi, \tag{6.28}$$

$$\chi = \frac{R_2}{R_1}. \tag{6.29}$$

If we define

$$C = \frac{\omega_3}{\lambda_3} - \frac{\omega_2}{\lambda_2} = \frac{\kappa_3 - 1}{4\mu_{30}} - \frac{\kappa_2 - 1}{4\mu_{20}} = \frac{C^*}{\mu_{30}}, \tag{6.30}$$

$$D = \frac{1}{\lambda_3} + \frac{1}{\lambda_2} = \frac{\kappa_3 + 1}{4\mu_{30}} + \frac{\kappa_2 + 1}{4\mu_{20}} = \frac{D^*}{\mu_{30}}, \tag{6.31}$$

$$C^* = \frac{(\kappa_3 - 1) - (\kappa_2 - 1)\Gamma}{4}, \tag{6.32}$$

$$D^* = \frac{(\kappa_3 + 1) + (\kappa_2 + 1)\Gamma}{4}, \tag{6.33}$$

$$A^* = \frac{C}{D} = \frac{(\kappa_3 - 1) - (\kappa_2 - 1)\Gamma}{(\kappa_3 + 1) + (\kappa_2 + 1)\Gamma}, \tag{6.34}$$

$$\Gamma = \frac{\mu_{30}}{\mu_{20}}, \tag{6.35}$$

and use (6.24)-(6.35), the integral equation (6.23) and the equilibrium equation becomes

$$\begin{aligned} \frac{\mu_{30} R^* x}{D^* R_2} = {} & A^* \eta p(x) - \frac{1}{\pi}\int_{-a}^{b} \frac{p(t)}{t - x} dt \\ & - \frac{1}{D\lambda_2}\frac{1}{\pi}\int_{-a}^{b} \left[k_{11}(t,x) + \eta k_{12}(t,x)\right] p(t) dt \\ & + \frac{1}{D\lambda_3}\frac{1}{\pi}\int_{-a}^{b} \left[k_{31}(t,x) + \eta k_{32}(t,x)\right] p(t) dt, \end{aligned} \tag{6.36}$$

$$\int_{-a}^{b} p(t) dt = P, \tag{6.37}$$

where

$$D\lambda_2 = \left[\frac{\kappa_2 + 1}{4\mu_{20}} + \frac{\kappa_3 + 1}{4\mu_{30}}\right]\frac{4\mu_{20}}{\kappa_2 + 1} = 1 + \frac{\kappa_3 + 1}{(\kappa_2 + 1)\Gamma}, \tag{6.38}$$

$$D\lambda_3 = \left[\frac{\kappa_2 + 1}{4\mu_{20}} + \frac{\kappa_3 + 1}{4\mu_{30}}\right]\frac{4\mu_{30}}{\kappa_3 + 1} = 1 + \frac{\kappa_2 + 1}{\kappa_3 + 1}\Gamma. \tag{6.39}$$

In order to solve the integral equation (6.36) the limits of integration have to be normalized. Now setting

$$t = t^* R_2, \tag{6.40}$$

$$x = x^* R_2, \tag{6.41}$$

$$b = b^* R_2, \tag{6.42}$$

$$a = a^* R_2, \tag{6.43}$$

$$p(t) = p^*(t^*), \tag{6.44}$$

$$k_{11}(t,x) = \frac{1}{R_2} k_{11}^*(t,x), \tag{6.45}$$

$$k_{12}(t,x) = \frac{1}{R_2} k_{12}^*(t,x), \tag{6.46}$$

$$k_{31}(t,x) = \frac{1}{R_2} k_{31}^*(t,x), \tag{6.47}$$

$$k_{32}(t,x) = \frac{1}{R_2} k_{32}^*(t,x), \tag{6.48}$$

equation (6.36) and (6.37) become

$$\begin{aligned} \frac{\mu_{30} R^* x^*}{D^*} &= A^* \eta p^*(x^*) - \frac{1}{\pi} \int_{-a^*}^{b^*} \frac{p^*(t^*)}{t^* - x^*} dt^* \\ &\quad - \frac{1}{D\lambda_2} \frac{1}{\pi} \int_{-a^*}^{b^*} \left[k_{11}^*(t^*, x^*) + \eta k_{12}^*(t^*, x^*) \right] p^*(t^*) dt^* \\ &\quad + \frac{1}{D\lambda_3} \frac{1}{\pi} \int_{-a^*}^{b^*} \left[k_{31}^*(t^*, x^*) + \eta k_{32}^*(t^*, x^*) \right] p^*(t^*) dt^*, \end{aligned} \tag{6.49}$$

$$\int_{-a^*}^{b^*} p^*(t^*) dt^* = \frac{P}{R_2}. \tag{6.50}$$

Further normalizing the integration limits from $(-a^*, b^*)$ to $(-1, 1)$ by using the

following change of variables

$$t^* = \frac{b^*+a^*}{2}s + \frac{b^*-a^*}{2}, \qquad -1<s<1 \tag{6.51}$$

$$x^* = \frac{b^*+a^*}{2}r + \frac{b^*-a^*}{2}, \qquad -1<r<1 \tag{6.52}$$

$$p^*(t^*) = \frac{\mu_{30}R^*}{2D^*}\phi(s), \tag{6.53}$$

$$k_{11}^*(t^*,x^*) = \frac{2}{b^*+a^*}\widehat{k}_{11}(s,r), \tag{6.54}$$

$$k_{12}^*(t^*,x^*) = \frac{2}{b^*+a^*}\widehat{k}_{12}(s,r), \tag{6.55}$$

$$k_{31}^*(t^*,x^*) = \frac{2}{b^*+a^*}\widehat{k}_{31}(s,r), \tag{6.56}$$

$$k_{32}^*(t^*,x^*) = \frac{2}{b^*+a^*}\widehat{k}_{32}(s,r), \tag{6.57}$$

the integral equation and the equilibrium equation become

$$\begin{aligned} & A\phi(r) - \frac{1}{\pi}\int_{-1}^{1}\frac{\phi(s)}{s-r}ds \\ & -\frac{1}{D\lambda_2}\frac{1}{\pi}\int_{-a^*}^{b^*}\left[\widehat{k}_{11}(s,r)+\eta\widehat{k}_{12}(s,r)\right]\phi(s)ds \\ & +\frac{1}{D\lambda_3}\frac{1}{\pi}\int_{-a^*}^{b^*}\left[\widehat{k}_{31}(s,r)+\eta\widehat{k}_{32}(s,r)\right]\phi(s)ds \\ = \; & (b^*+a^*)\,r + (b^*-a^*)\,, \end{aligned} \tag{6.58}$$

$$\int_{-1}^{1}\phi(s)ds = \frac{4}{b^*+a^*}\frac{D^*P}{R^*\mu_{30}R_2}, \tag{6.59}$$

where

$$A = A^*\eta = \eta\frac{(\kappa_3-1)-(\kappa_2-1)\,\Gamma}{(\kappa_3+1)+(\kappa_2+1)\,\Gamma}. \tag{6.60}$$

α and β for this problem becomes

$$\begin{aligned} \eta>0: \quad & \alpha=\theta/\pi, && \beta=1-\theta/\pi, \\ \eta=0: \quad & \alpha=0.5, && \beta=0.5, \\ \eta<0: \quad & \alpha=1-\theta/\pi, && \beta=\theta/\pi, \end{aligned} \tag{6.61}$$

where

$$\theta = \arctan\left|\frac{1}{A}\right|. \tag{6.62}$$

Therefore the index of the problem becomes

$$\kappa_0 = -(\alpha+\beta) = -1. \tag{6.63}$$

Assuming a solution of the form

$$\phi(s) = w(s)\sum_0^\infty c_n P_n^{(\alpha,\beta)}(s), \tag{6.64}$$

$$w(s) = (1-s)^\alpha (1+s)^\beta, \tag{6.65}$$

defining

$$\widehat{\phi}(s) = w(s)\sum_0^\infty \widehat{c}_n P_n^{(\alpha,\beta)}(s), \tag{6.66}$$

$$P^* = \frac{P}{\mu_{30}R_2}, \tag{6.67}$$

$$\widehat{c}_n = \frac{c_n}{\sqrt{P^*}}, \tag{6.68}$$

$$\widehat{b} = \frac{b^*}{\sqrt{P^*}}, \tag{6.69}$$

$$\widehat{a} = \frac{a^*}{\sqrt{P^*}}, \tag{6.70}$$

$$\widehat{x} = \frac{x^*}{\sqrt{P^*}}, \tag{6.71}$$

and using the orthogonality of the Jacobi polynomials, the equilibrium equation (6.59) becomes

$$\widehat{c}_0\theta_0 = \frac{4}{\widehat{b}+\widehat{a}}\frac{D^*}{R^*}, \tag{6.72}$$

where, from (A.8)

$$\theta_0 = \frac{2\pi\alpha(1-\alpha)}{\sin\pi\alpha}. \tag{6.73}$$

Considering the property of Jacobi Polynomials (A.6) and letting

$$\mathcal{K}_{1n}(r) = \frac{1}{\pi}\int_{-1}^{1}\left[\widehat{k}_{11}(s,r)+\eta\widehat{k}_{12}(s,r)\right]w(s)P_n^{(\alpha,\beta)}(s)ds, \tag{6.74}$$

$$\mathcal{K}_{3n}(r) = \frac{1}{\pi}\int_{-1}^{1}\left[\widehat{k}_{31}(s,r)+\eta\widehat{k}_{32}(s,r)\right]w(s)P_n^{(\alpha,\beta)}(s)ds, \tag{6.75}$$

after truncating the series at $N-1$ (6.58) can be written as

$$\sum_{0}^{N-1}\widehat{c}_n\left[\frac{2}{\sin\pi\alpha}P_{n-\kappa_0}^{(-\alpha,-\beta)}(r)-\frac{1}{D\lambda_2}\mathcal{K}_{1n}(r)+\frac{1}{D\lambda_3}\mathcal{K}_{3n}(r)\right]=(r+1)\widehat{b}+(r-1)\widehat{a}, \tag{6.76}$$

The consistency condition is again automatically satisfied. The solution procedure is identical to that of the cylindrical stamp.

The nondimensional contact stresses can then be obtained as

$$\frac{\sigma_{3yy}(x^*,0)}{\mu_{30}}=\frac{\sigma(x^*)}{\mu_{30}}=-\frac{R^*}{2D^*}w(r)\sum_{0}^{\infty}c_nP_n^{(\alpha,\beta)}(r), \tag{6.77}$$

where

$$r=\frac{2x^*-b^*+a^*}{b^*+a^*}. \tag{6.78}$$

the in-plane stresses, $\sigma_{3xx}(x^*,0)$ can be found by using equation (4.74). as follows:

$$\begin{aligned}\sigma_{3xx}(x^*,0) &= \sigma(x^*)+\frac{2\eta}{\pi}\int_{-a^*}^{b^*}\frac{\sigma(t^*)}{t^*-x^*}dt^*-\frac{2}{\pi}\int_{-a^*}^{b^*}\left[k_{42}^*(t^*,x^*)+\eta k_{41}^*(t^*,x^*)\right]\sigma(t^*)\,dt^*\\ &= -p(x^*)-\frac{2\eta}{\pi}\int_{-a^*}^{b^*}\frac{p(t^*)}{t^*-x^*}dt^*+\frac{2}{\pi}\int_{-a^*}^{b^*}\left[k_{42}^*(t^*,x^*)+\eta k_{41}^*(t^*,x^*)\right]p(t^*)\,dt^*\\ &= \frac{\mu_{30}R^*}{2D^*}\psi(r)\end{aligned} \tag{6.79}$$

where

$$\psi(r)=-\phi(r)-\frac{2\eta}{\pi}\int_{-1}^{1}\frac{\phi(s)}{s-r}dt+\frac{2}{\pi}\int_{-1}^{1}\left[\widehat{k}_{22}(s,r)+\eta\widehat{k}_{21}(s,r)\right]\phi(s)\,ds \tag{6.80}$$

The nondimensional in-plane streses $\sigma_{3xx}(x^*,0)$ then becomes

$$\frac{\sigma_{3xx}(x^*,0)}{\mu_{30}}=\frac{R^*}{2D^*}\psi(r) \tag{6.81}$$

Figure 6.1 - 6.3 give the stress distribution and the load versus contact length curves for two elastic cylinders with frictional contact $\eta = 0.3$. The ratio of the radius of curvatures R_2/R_1 is 5 and the stiffness of the surface of the upper cylinder is two times that of the lower one and both cylinders have the same coating thickness. The normalized contact length is varied between 0.01 to 0.05. The severe contact stresses occur when both cylinders have stiffening coatings on the stiff substrate namely $\Gamma_2 = \Gamma_3 = 7$, wheras in the case of softening coating on the soft substrate $\Gamma_2 = \Gamma_3 = 1/7$ the contact stresses are relatively lower. If both cylinders are homogeneous that is $\Gamma_2 = \Gamma_3 = 1$ the contact stresses lie between the previous two cases. The stress σ_{yy} is almost symmetric since $\alpha = 0.4909$ and $\beta = 0.5091$ for this combination($\eta = 0.3$). It is obvius that if the stiffness of the surface of the upper cylinder goes to infinity or becomes rigid α and β approaches to 0.4728 and 0.5272 respectively. And if we take $R_2/R_1 = 0$ the results for this case reduces to the rigid cylinder cases of chapter 5.

For the same combination of material properties we investigate the behaviour of the stresses as we increase the coefficient of friction from 0.3 to 0.7 in Figures 6.4 - 6.6. The effect of increasing friction is to increase the contact stresses. The stress σ_{yy} is slightly slanted towards the trailing edge of the contact region. Note also that the peak value of the in-plane σ_{xx} stress at the trailing edge increases with increasing stiffness Γ_2 and Γ_3.

Next we fix the stiffness ratio of the lower cylinder Γ_3 at 7, 3, 1/3 and 1/7 and vary the stiffness ratio of the upper cylinder Γ_2 in Figures 6.7 - 6.10, respectively. Note that the coefficient of friction is 0.3 and $\mu_{30}/\mu_{20} = 0.5$. The maximum in-plane tensile stress σ_{xx} occurs again at the trailing edge and becomes higher as Γ_2 increases. As the stiffness ratio of the lower cylinder decreases the contact stresses also decrease.

In Figures 6.11 - 6.17 μ_{30}/μ_{20} is taken to be 2. With $\eta = 0.3$, $\alpha = 0.5091$ and $\beta = 0.4909$ this is the opposite of the case when $\mu_{30}/\mu_{20} = 0.5$. The effect of the

stiffness ratio on the contact stresses can be seen in Figures 6.11 - 6.13. In These figures $\Gamma_2 = \Gamma_3$ and the coefficient of friction is taken to be 0.7. The contact stress distribution on the surface of an FGM coating for various values of the stiffness ratio of the upper cylinder Γ_2 is given in Figures 6.14 - 6.17.

6.2 The Case of Negative Curvature

For the problem described in Figure 1.2 the only difference will be in the right hand side and the curvature of the lower half plane (see (6.25)), that is

$$\frac{\partial}{\partial x} v_2(x,0) = \frac{x}{R_1}, \tag{6.82}$$

Thus the right hand side of the integral equation becomes

$$\frac{\partial}{\partial x} v_3(x,0) - \frac{\partial}{\partial x} v_2(x,0) = \frac{x}{R}, \tag{6.83}$$

where

$$\begin{aligned} \frac{1}{R} &= \frac{1}{R_2} - \frac{1}{R_1} = \frac{R^*}{R_2}, \\ R^* &= 1 + \chi, \\ \chi &= -\frac{R_2}{R_1}. \end{aligned} \tag{6.84}$$

Note that $R_2 < R_1$. and the range of χ is $(-1 < \chi < 0)$.

Figures 6.18 - 6.20 give the stress distribution and the load versus contact length curves for two elastic cylinders with frictional contact $\eta = 0.3$ and $\mu_{30}/\mu_{20} = 0.5$. The radius of curvature of the outer cylinder, R_1 is 5 times the radius of the inner cylinder R_2. The contact stresses are much lower than the configuration seen in Figures 6.1 - 6.3. The effect of increasing friction on the contact stresses can be seen in Figures 6.21 - 6.23.

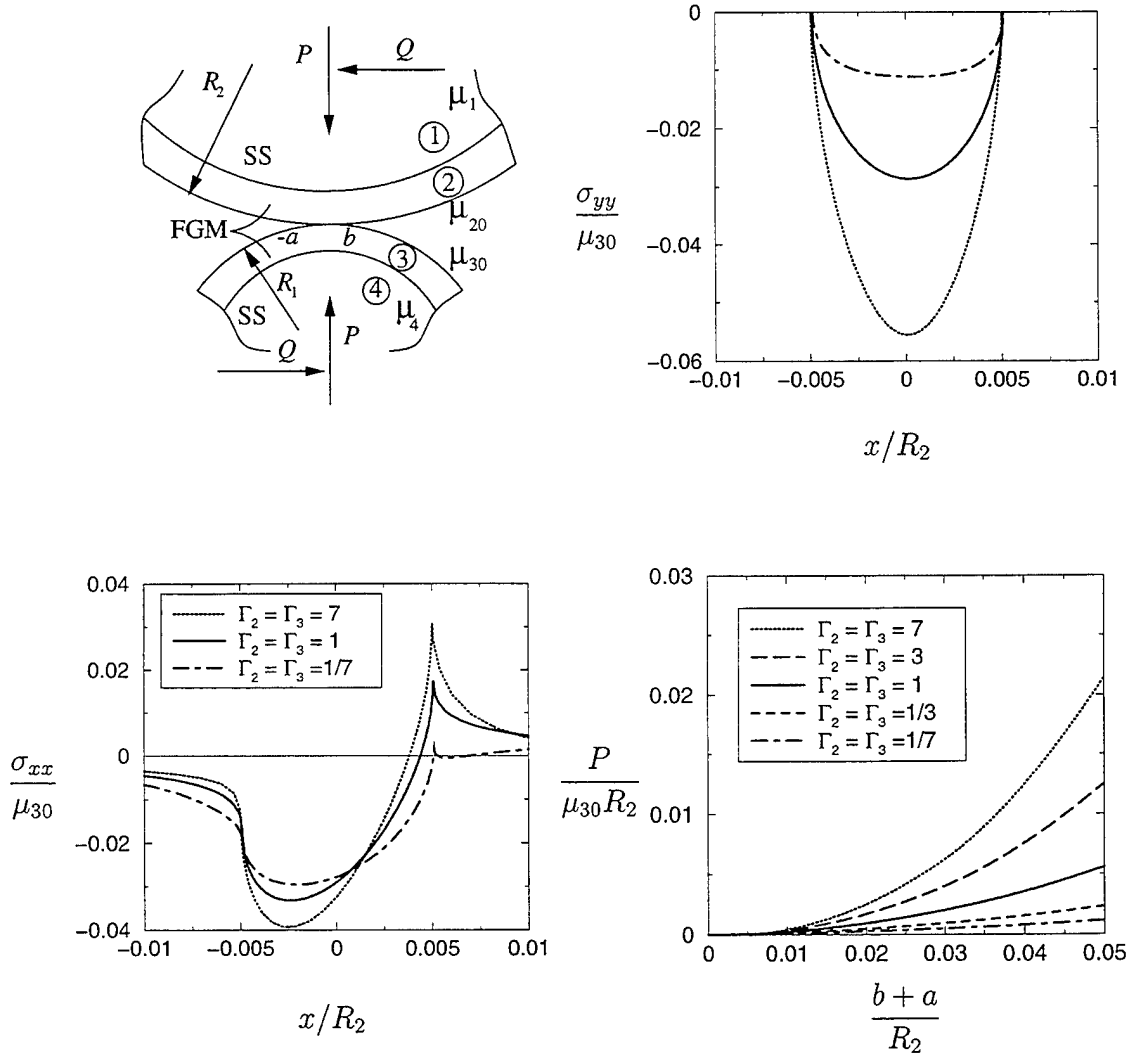

Figure 6.1: Stress distribution on the surface of an FGM coating for various values of the stiffness ratio $\Gamma_2 = \mu_1/\mu_{20}$, $\Gamma_3 = \mu_4/\mu_{30}$, $\mu_{30}/\mu_{20} = 0.5$, $R_2/R_1 = 5.0$, $(b+a)/R_2 = 0.01$, $R_2/h_3 = 100$, $h_2/h_3 = 1$, $\eta = 0.3$.

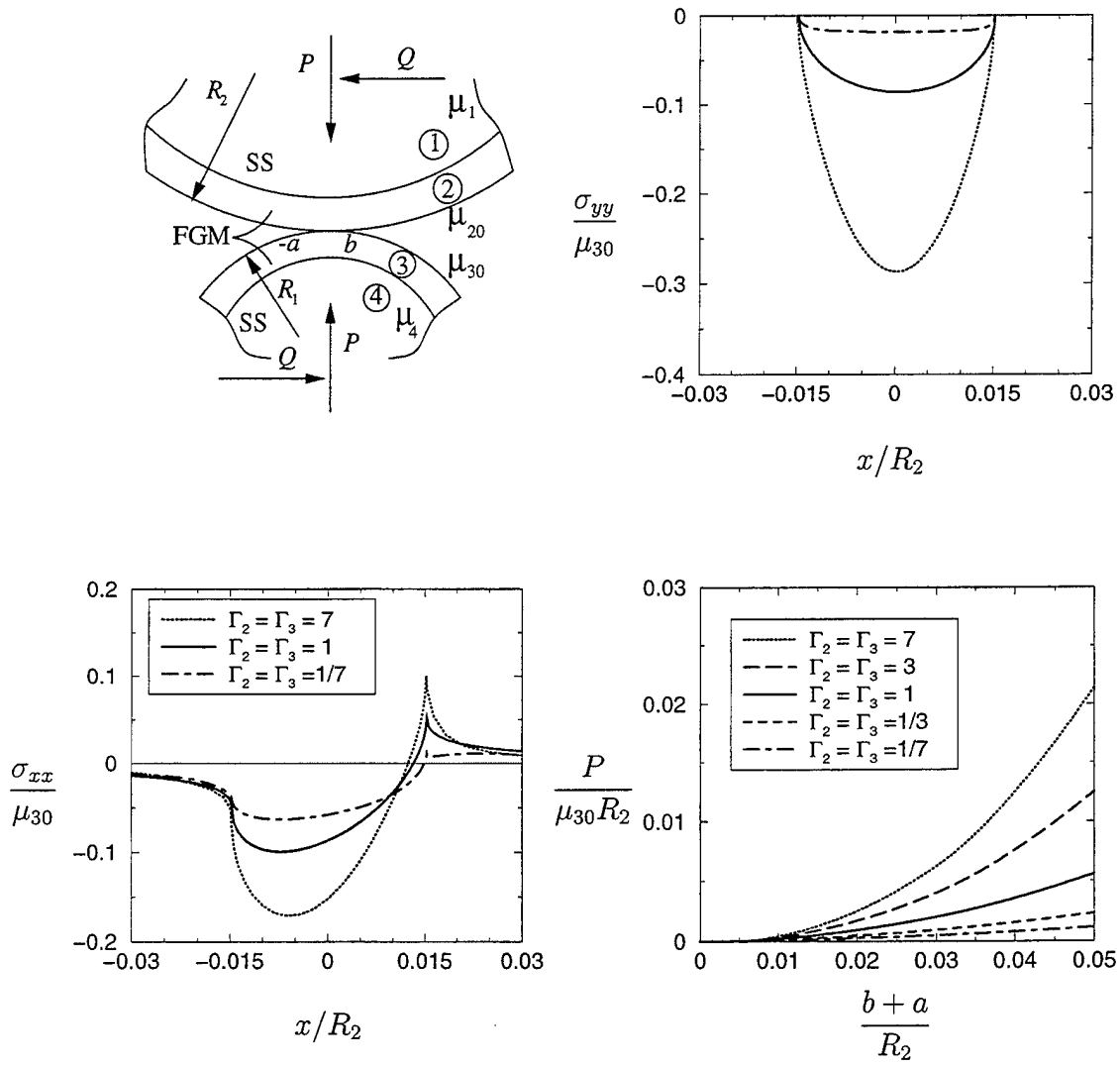

Figure 6.2: Stress distribution on the surface of an FGM coating for various values of the stiffness ratio $\Gamma_2 = \mu_1/\mu_{20}$, $\Gamma_3 = \mu_4/\mu_{30}$, $\mu_{30}/\mu_{20} = 0.5$, $R_2/R_1 = 5.0$, $(b+a)/R_2 = 0.03$, $R_2/h_3 = 100$, $h_2/h_3 = 1$, $\eta = 0.3$.

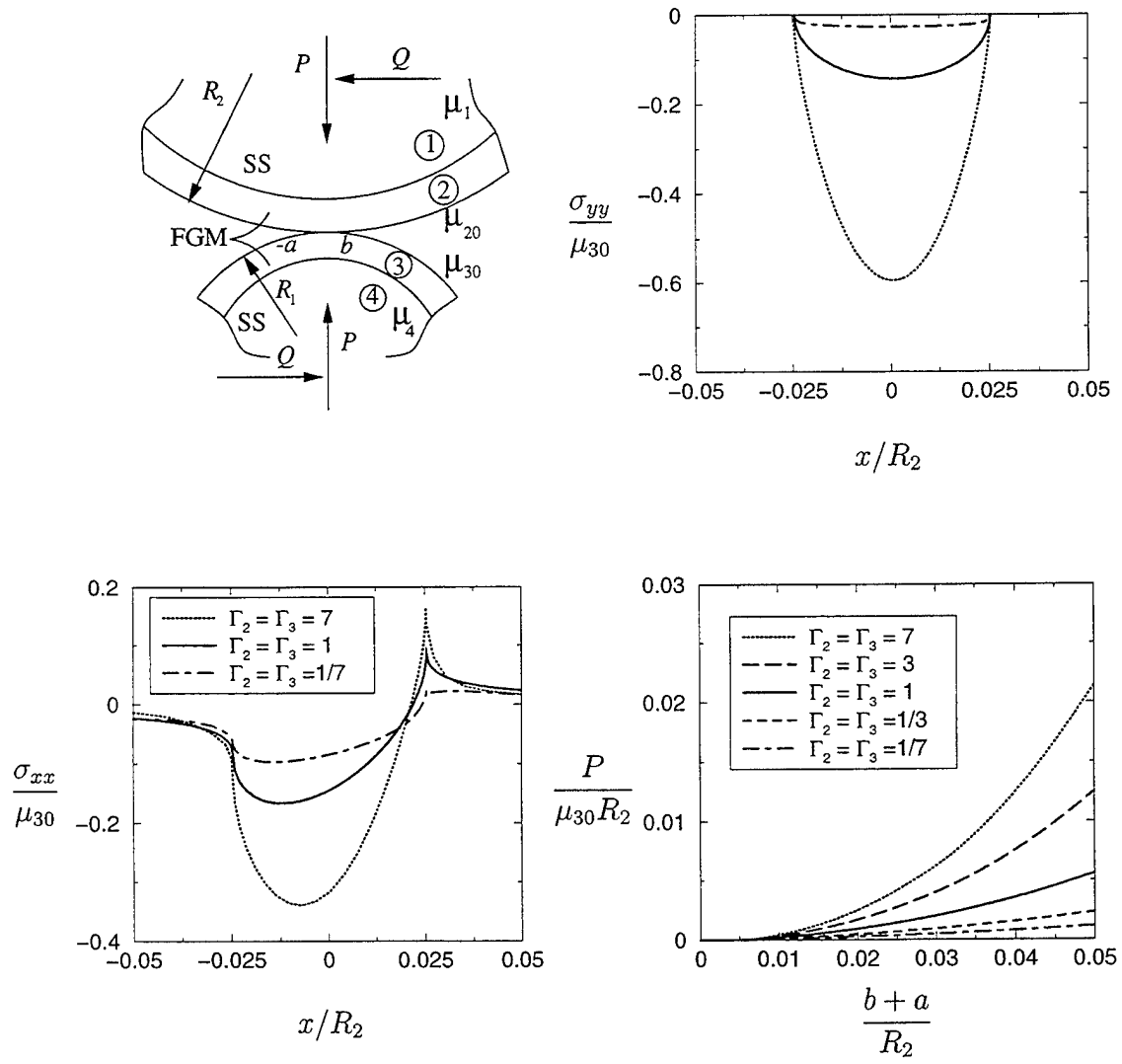

Figure 6.3: Stress distribution on the surface of an FGM coating for various values of the stiffness ratio $\Gamma_2 = \mu_1/\mu_{20}$, $\Gamma_3 = \mu_4/\mu_{30}$, $\mu_{30}/\mu_{20} = 0.5$, $R_2/R_1 = 5.0$, $(b+a)/R_2 = 0.05$, $R_2/h_3 = 100$, $h_2/h_3 = 1$, $\eta = 0.3$.

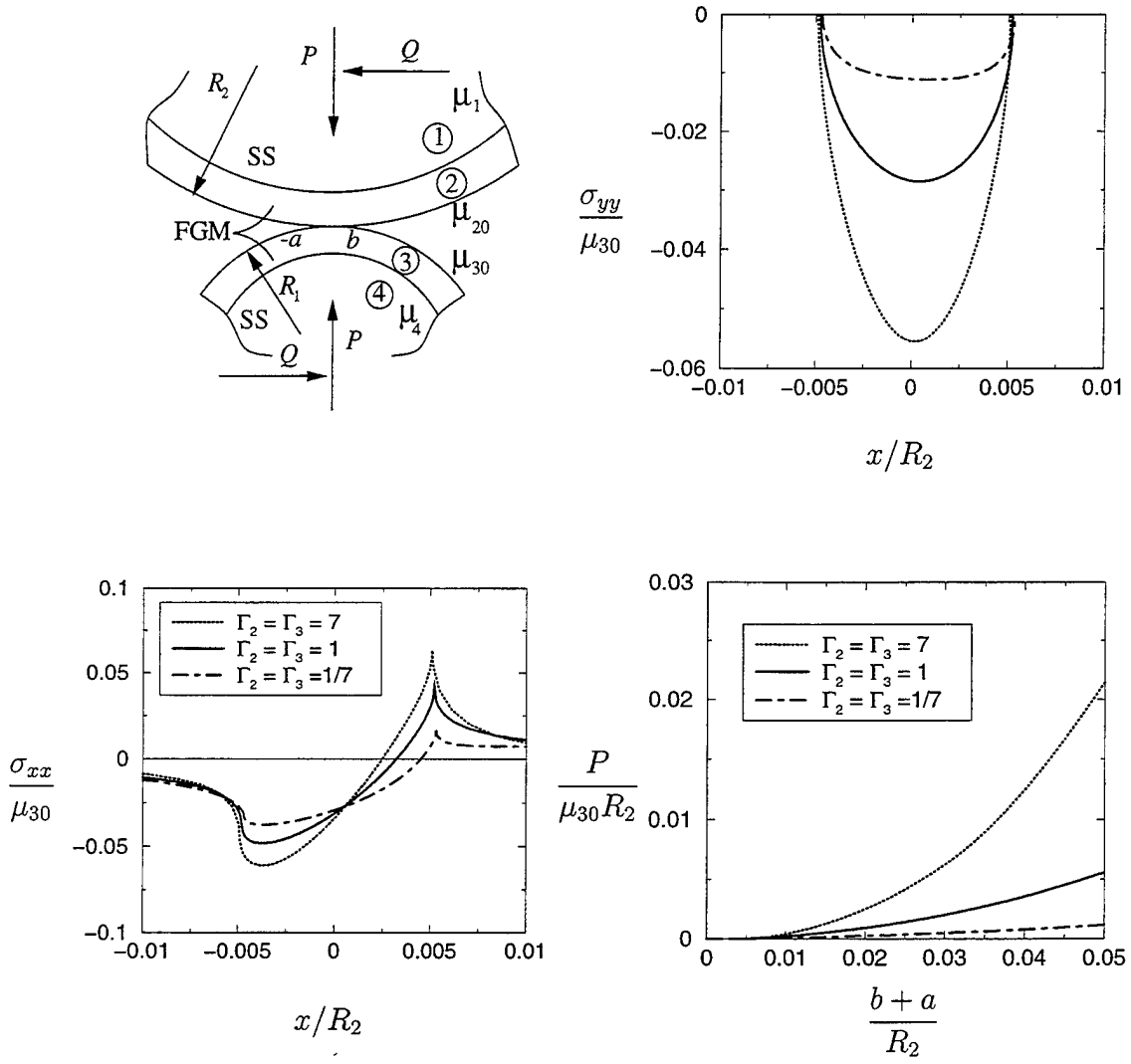

Figure 6.4: Stress distribution on the surface of an FGM coating for various values of the stiffness ratio $\Gamma_2 = \mu_1/\mu_{20}$, $\Gamma_3 = \mu_4/\mu_{30}$, $\mu_{30}/\mu_{20} = 0.5$, $R_2/R_1 = 5.0$, $(b+a)/R_2 = 0.01$, $R_2/h_3 = 100$, $h_2/h_3 = 1$, $\eta = 0.7$.

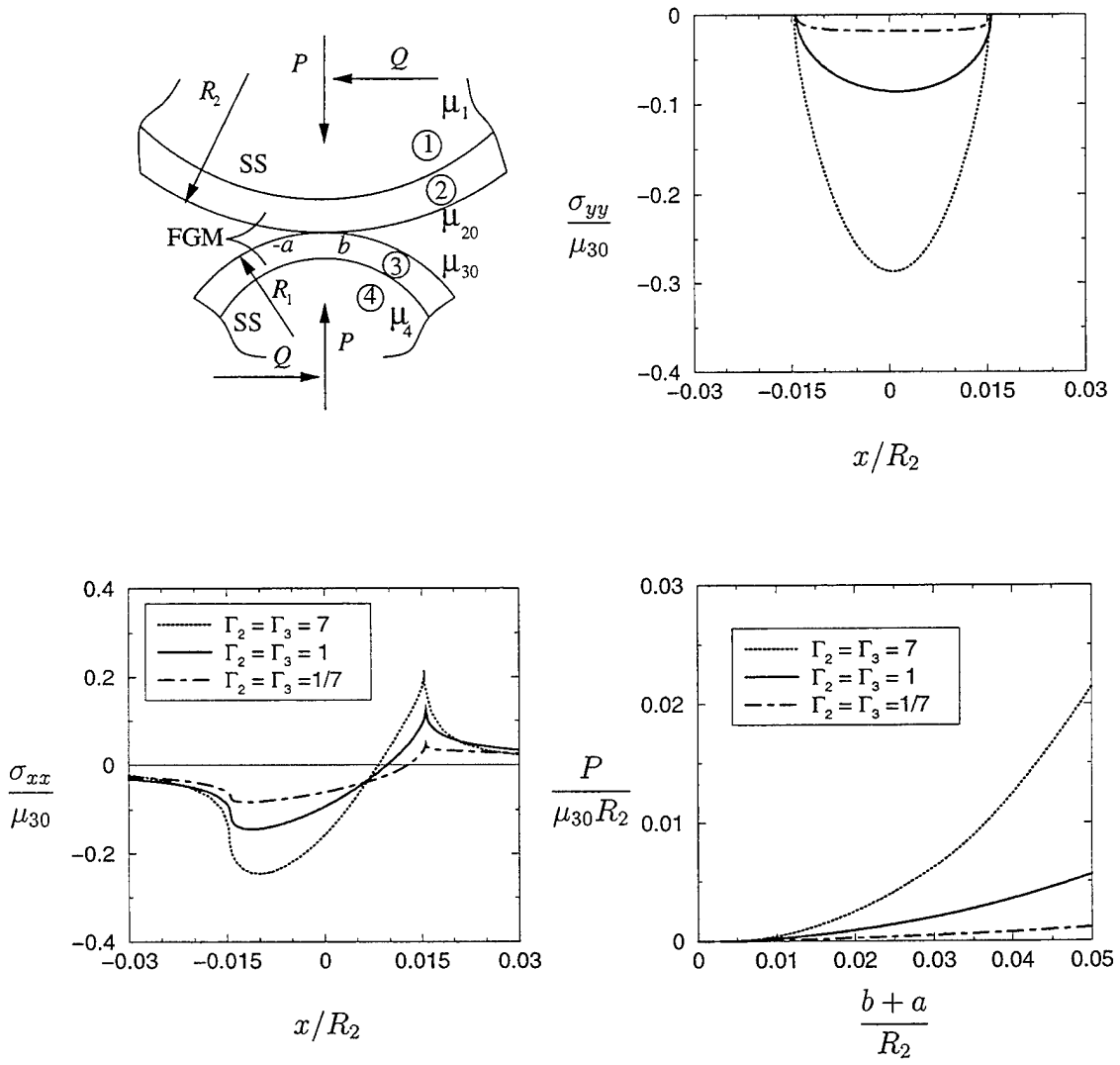

Figure 6.5: Stress distribution on the surface of an FGM coating for various values of the stiffness ratio $\Gamma_2 = \mu_1/\mu_{20}$, $\Gamma_3 = \mu_4/\mu_{30}$, $\mu_{30}/\mu_{20} = 0.5$, $R_2/R_1 = 5.0$, $(b+a)/R_2 = 0.03$, $R_2/h_3 = 100$, $h_2/h_3 = 1$, $\eta = 0.7$.

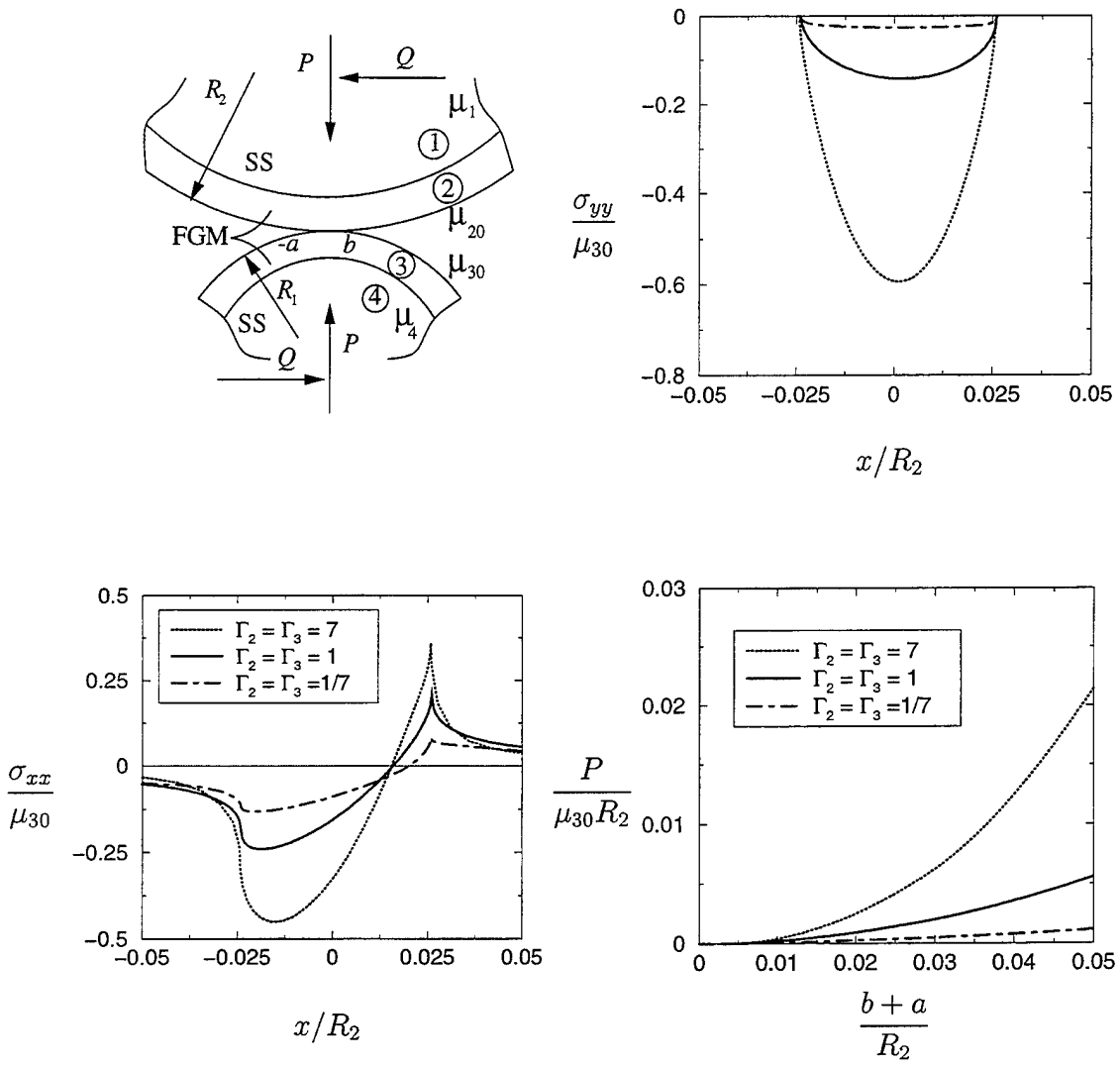

Figure 6.6: Stress distribution on the surface of an FGM coating for various values of the stiffness ratio $\Gamma_2 = \mu_1/\mu_{20}$, $\Gamma_3 = \mu_4/\mu_{30}$, $\mu_{30}/\mu_{20} = 0.5$, $R_2/R_1 = 5.0$, $(b+a)/R_2 = 0.05$, $R_2/h_3 = 100$, $h_2/h_3 = 1$, $\eta = 0.7$.

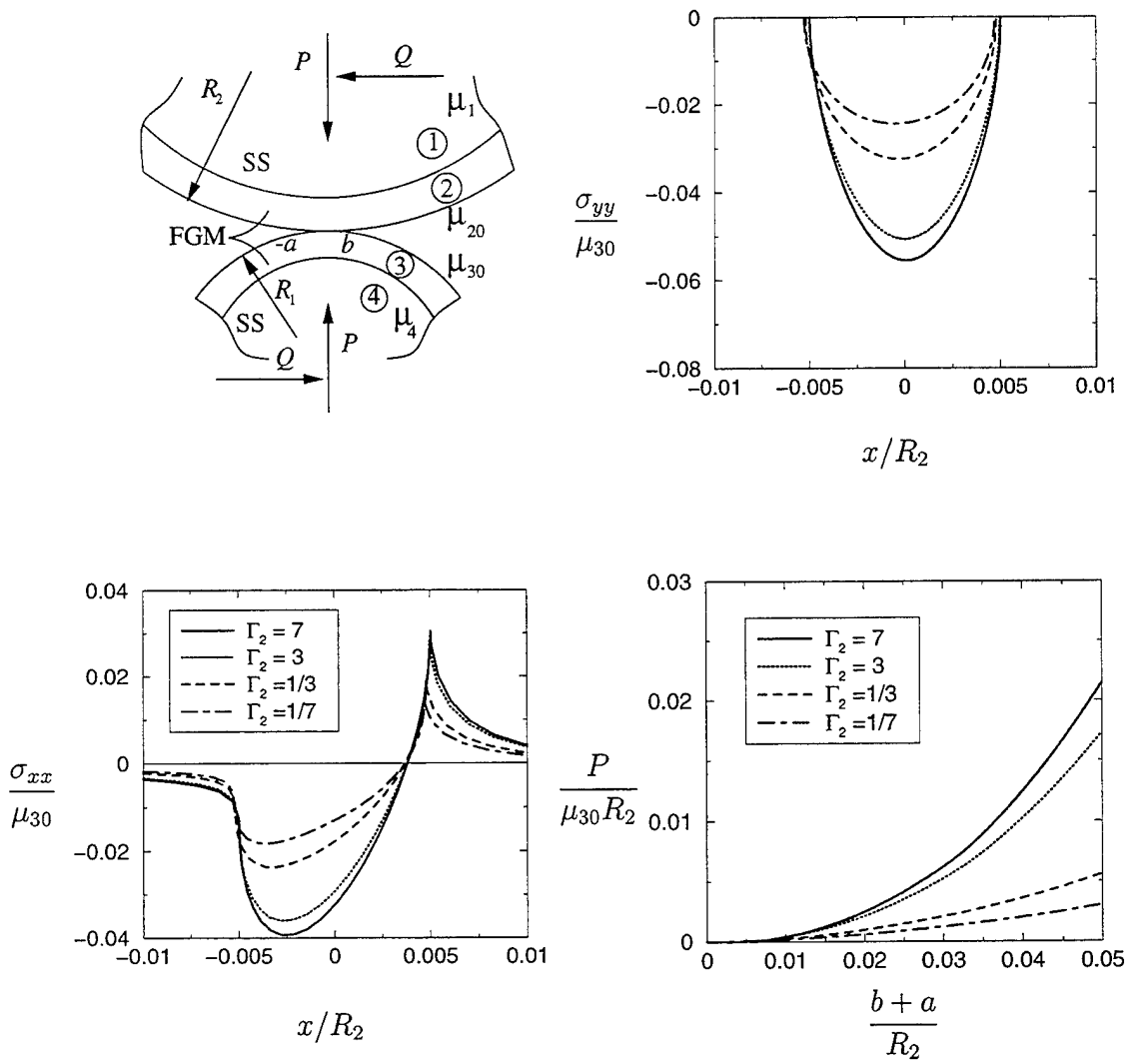

Figure 6.7: Stress distribution on the surface of an FGM coating for various values of the stiffness ratio $\Gamma_2 = \mu_1/\mu_{20}$, $\Gamma_3 = \mu_4/\mu_{30} = 7$, $\mu_{30}/\mu_{20} = 0.5$, $R_2/R_1 = 5.0$, $(b+a)/R_2 = 0.01$, $R_2/h_3 = 100$, $h_2/h_3 = 1$, $\eta = 0.3$.

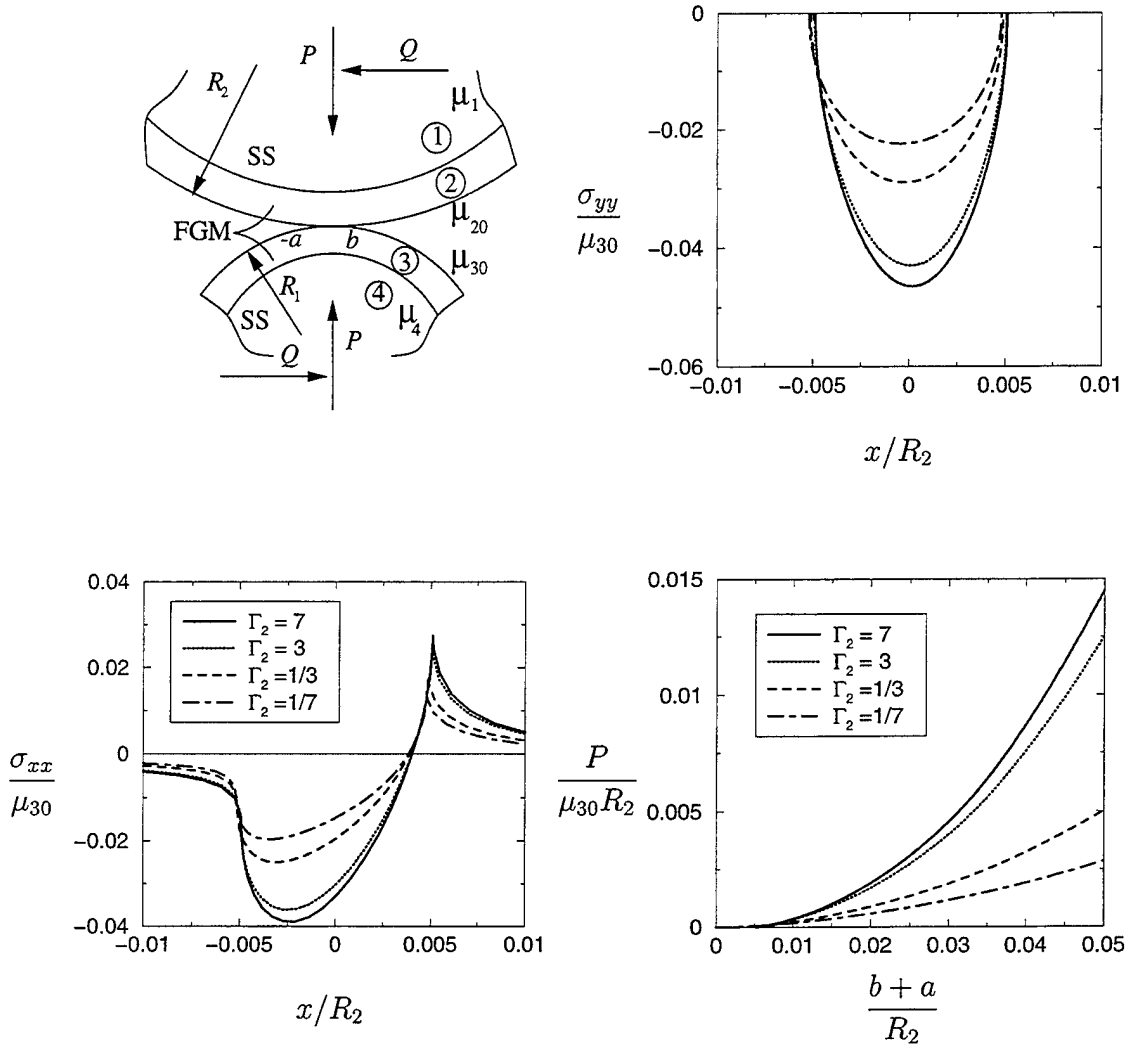

Figure 6.8: Stress distribution on the surface of an FGM coating for various values of the stiffness ratio $\Gamma_2 = \mu_1/\mu_{20}$, $\Gamma_3 = \mu_4/\mu_{30} = 3$, $\mu_{30}/\mu_{20} = 0.5$, $R_2/R_1 = 5.0$, $(b+a)/R_2 = 0.01$, $R_2/h_3 = 100$, $h_2/h_3 = 1$, $\eta = 0.3$.

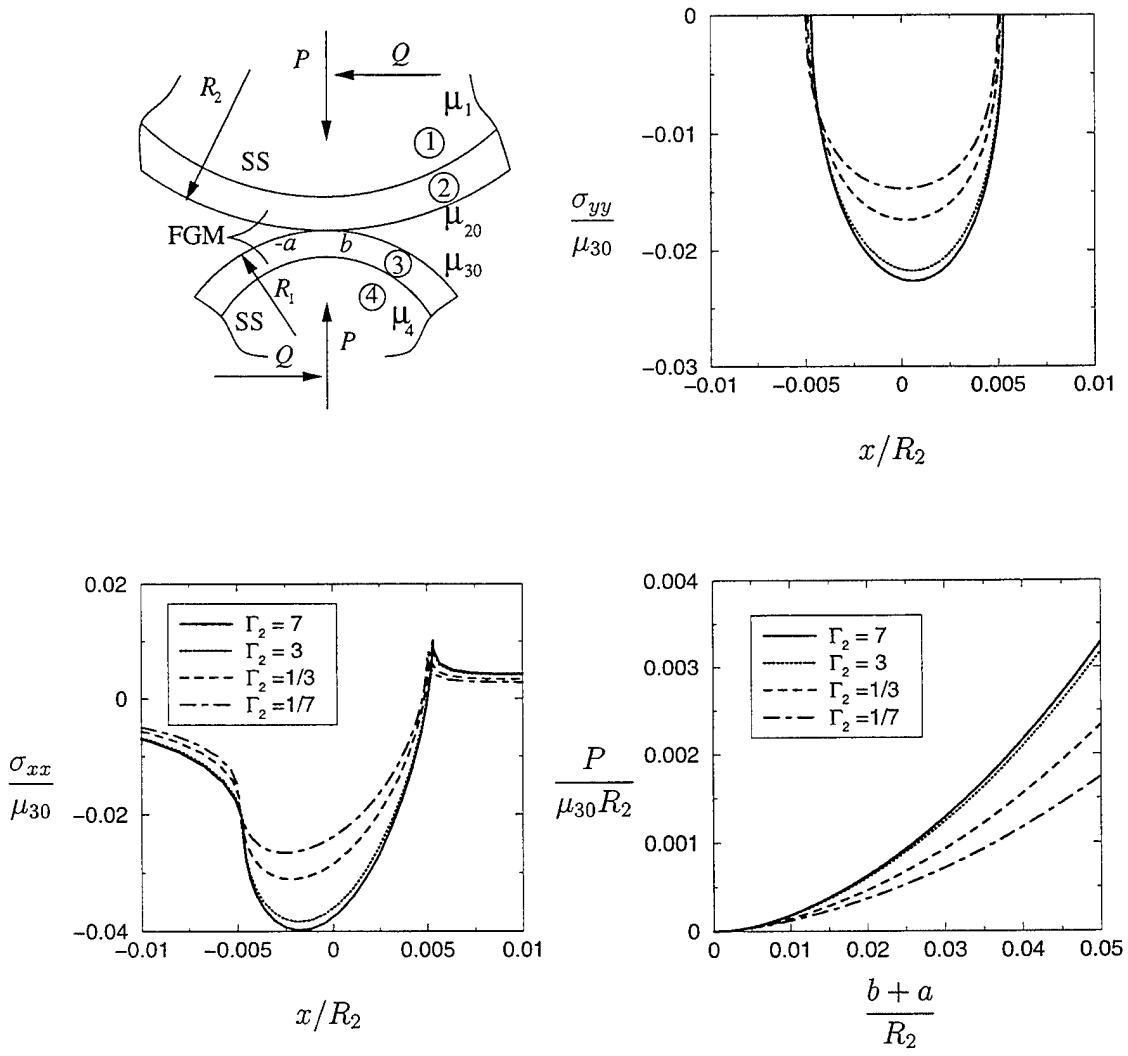

Figure 6.9: Stress distribution on the surface of an FGM coating for various values of the stiffness ratio $\Gamma_2 = \mu_1/\mu_{20}$, $\Gamma_3 = \mu_4/\mu_{30} = 1/3$, $\mu_{30}/\mu_{20} = 0.5$, $R_2/R_1 = 5.0$, $(b+a)/R_2 = 0.01$, $R_2/h_3 = 100$, $h_2/h_3 = 1$, $\eta = 0.3$.

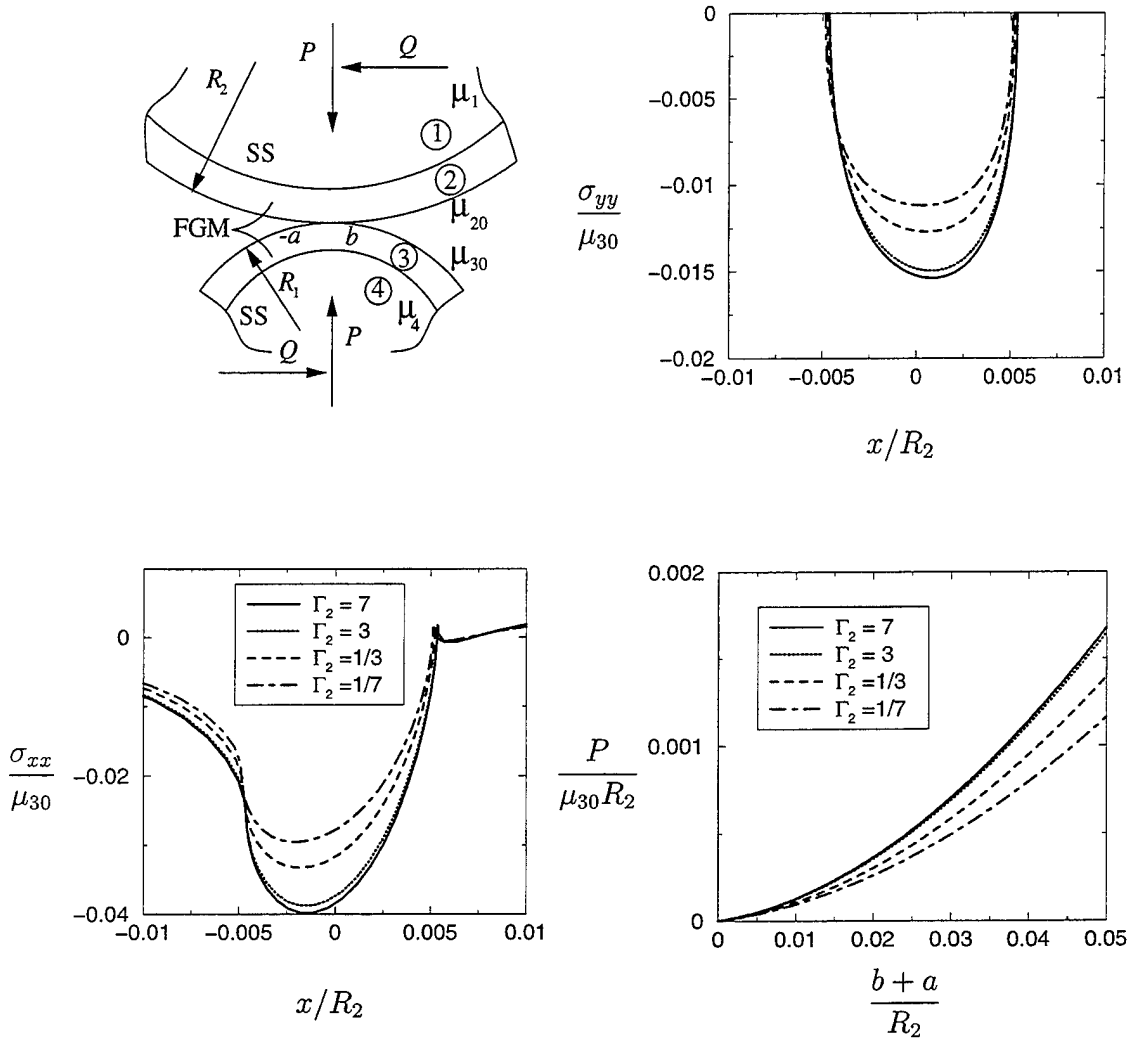

Figure 6.10: Stress distribution on the surface of an FGM coating for various values of the stiffness ratio $\Gamma_2 = \mu_1/\mu_{20}$, $\Gamma_3 = \mu_4/\mu_{30} = 1/7$, $\mu_{30}/\mu_{20} = 0.5$, $R_2/R_1 = 5.0$, $(b+a)/R_2 = 0.01$, $R_2/h_3 = 100$, $h_2/h_3 = 1$, $\eta = 0.3$.

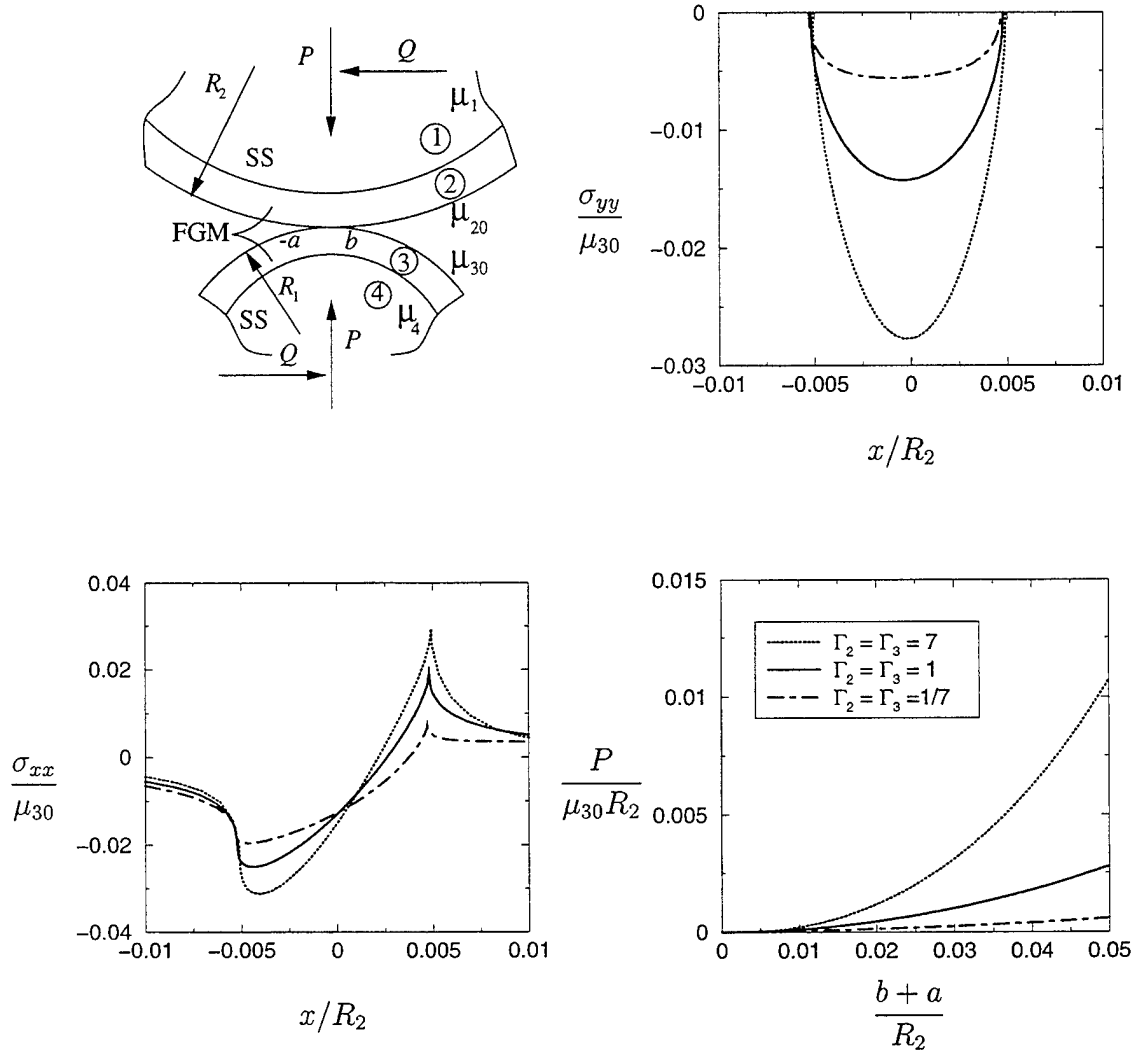

Figure 6.11: Stress distribution on the surface of an FGM coating for various values of the stiffness ratio $\Gamma_2 = \mu_1/\mu_{20}$, $\Gamma_3 = \mu_4/\mu_{30}$, $\mu_{30}/\mu_{20} = 2.0$, $R_2/R_1 = 5.0$, $(b+a)/R_2 = 0.01$, $R_2/h_3 = 100$, $h_2/h_3 = 1$, $\eta = 0.7$.

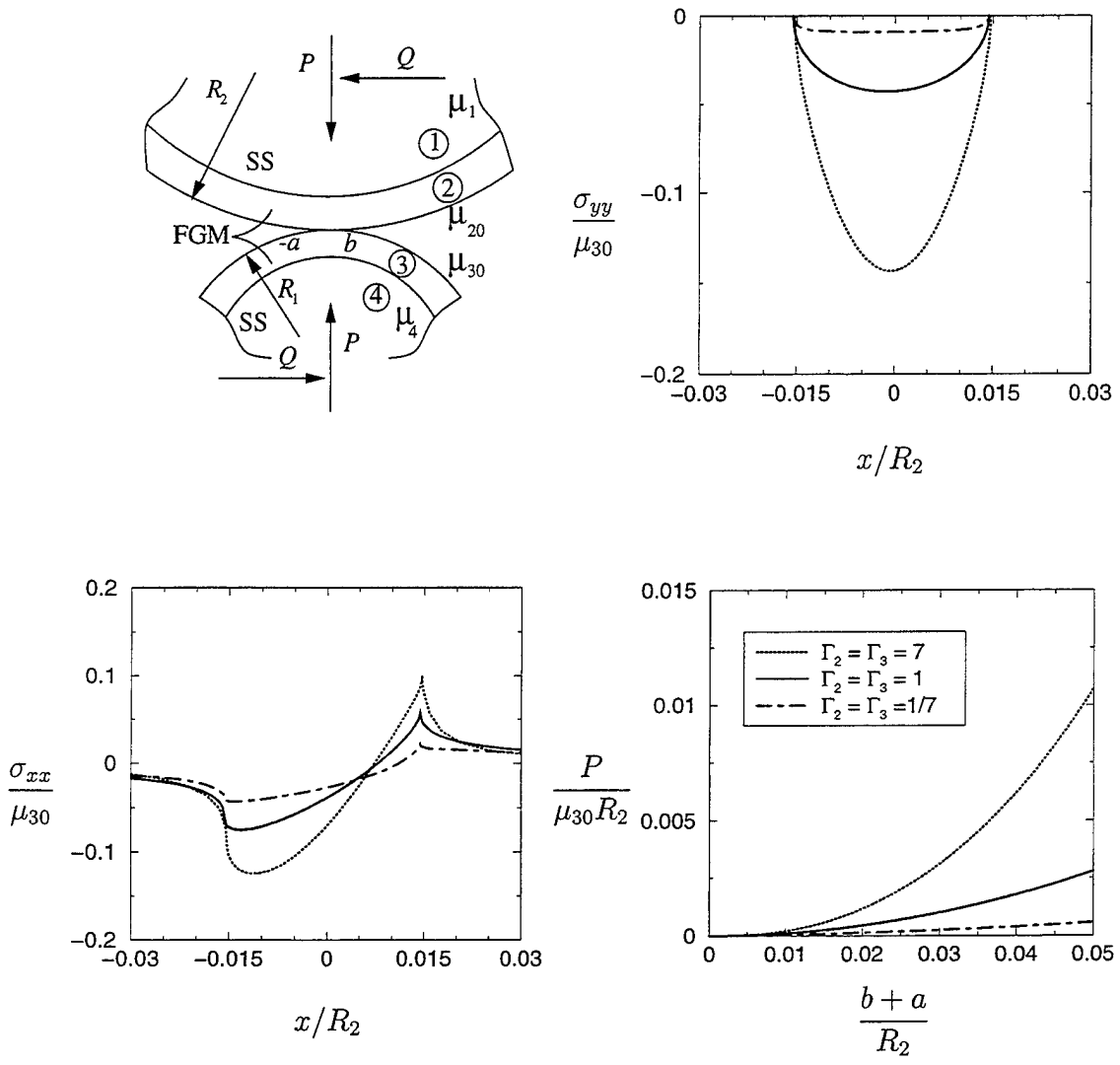

Figure 6.12: Stress distribution on the surface of an FGM coating for various values of the stiffness ratio $\Gamma_2 = \mu_1/\mu_{20}$, $\Gamma_3 = \mu_4/\mu_{30}$, $\mu_{30}/\mu_{20} = 2.0$, $R_2/R_1 = 5.0$, $(b+a)/R_2 = 0.03$, $R_2/h_3 = 100$, $h_2/h_3 = 1$, $\eta = 0.7$.

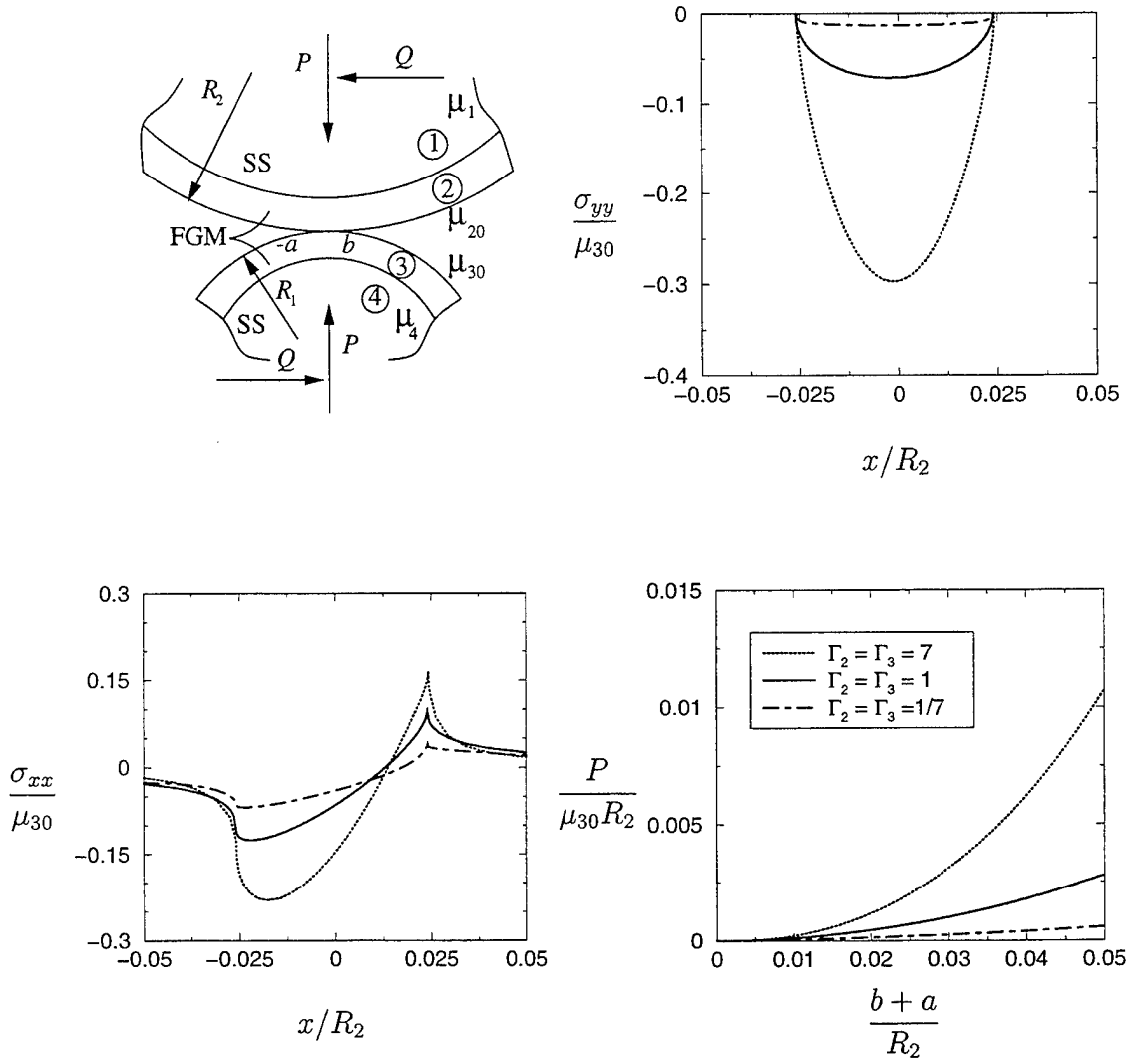

Figure 6.13: Stress distribution on the surface of an FGM coating for various values of the stiffness ratio $\Gamma_2 = \mu_1/\mu_{20}$, $\Gamma_3 = \mu_4/\mu_{30}$, $\mu_{30}/\mu_{20} = 2.0$, $R_2/R_1 = 5.0$, $(b+a)/R_2 = 0.05$, $R_2/h_3 = 100$, $h_2/h_3 = 1$, $\eta = 0.7$.

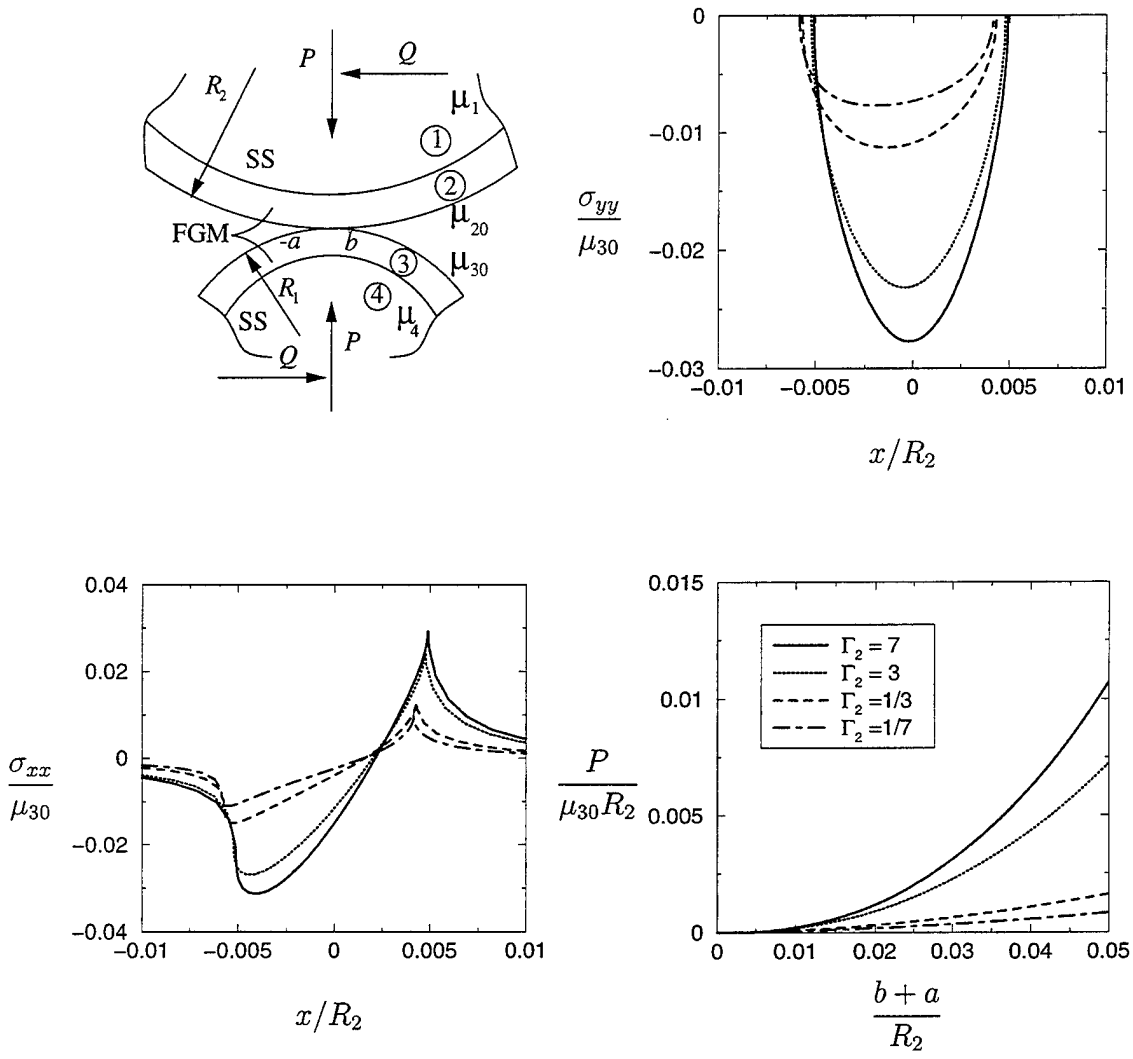

Figure 6.14: Stress distribution on the surface of an FGM coating for various values of the stiffness ratio $\Gamma_2 = \mu_1/\mu_{20}$, $\Gamma_3 = \mu_4/\mu_{30} = 7$, $\mu_{30}/\mu_{20} = 2.0$, $R_2/R_1 = 5.0$, $(b+a)/R_2 = 0.01$, $R_2/h_3 = 100$, $h_2/h_3 = 1$, $\eta = 0.7$.

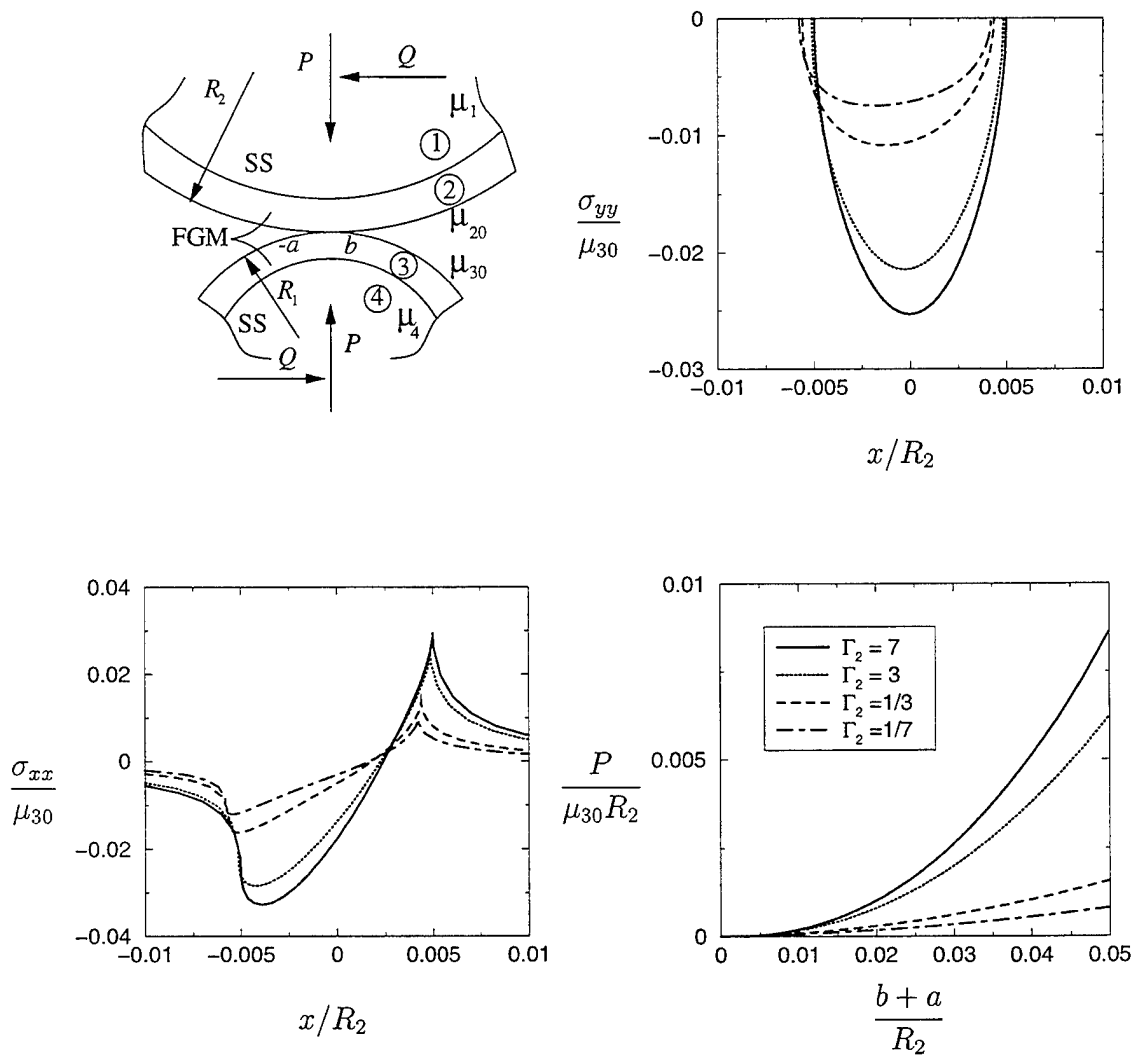

Figure 6.15: Stress distribution on the surface of an FGM coating for various values of the stiffness ratio $\Gamma_2 = \mu_1/\mu_{20}$, $\Gamma_3 = \mu_4/\mu_{30} = 3$, $\mu_{30}/\mu_{20} = 2.0$, $R_2/R_1 = 5.0$, $(b+a)/R_2 = 0.01$, $R_2/h_3 = 100$, $h_2/h_3 = 1$, $\eta = 0.7$.

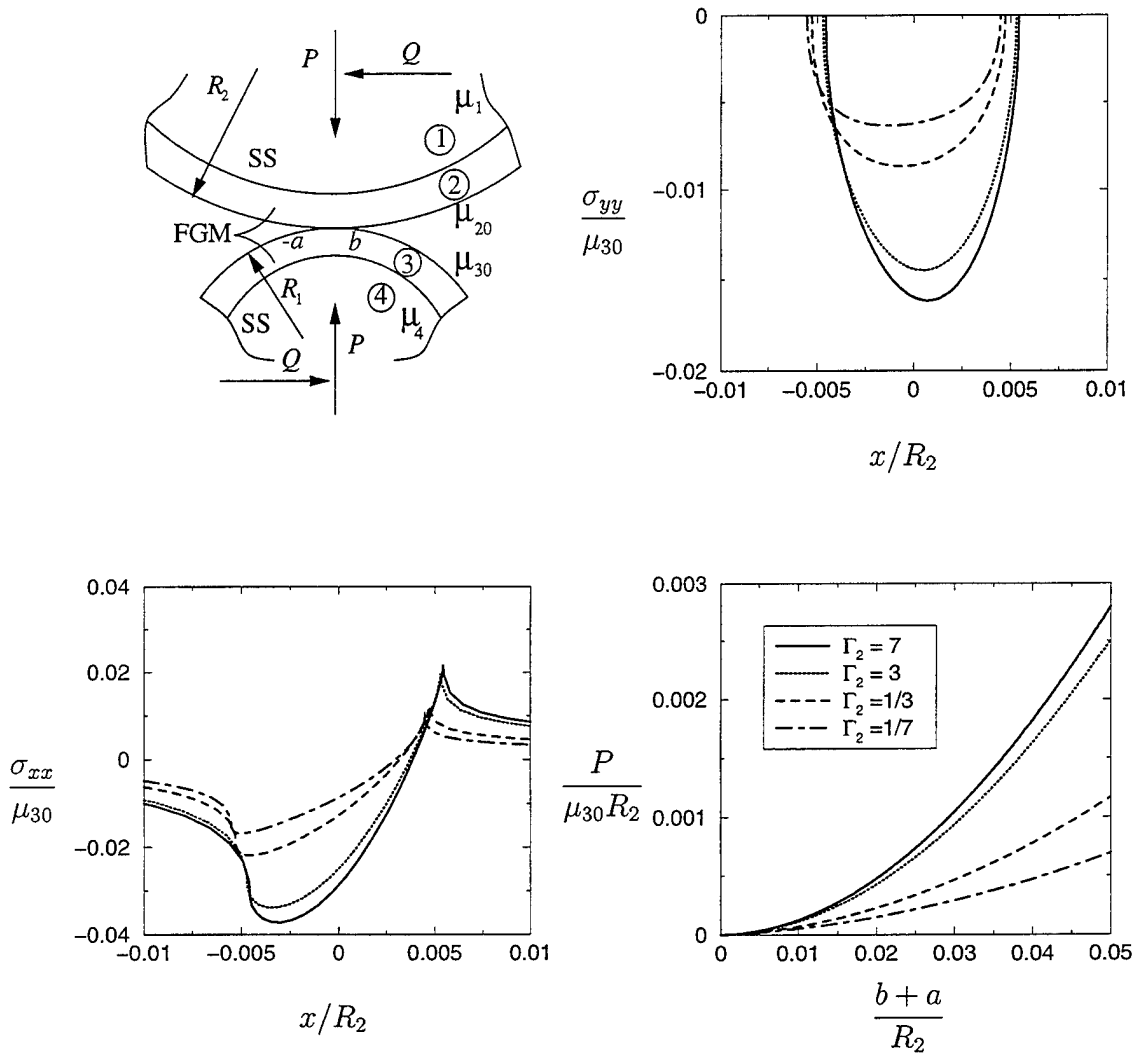

Figure 6.16: Stress distribution on the surface of an FGM coating for various values of the stiffness ratio $\Gamma_2 = \mu_1/\mu_{20}$, $\Gamma_3 = \mu_4/\mu_{30} = 1/3$, $\mu_{30}/\mu_{20} = 2.0$, $R_2/R_1 = 5.0$, $(b+a)/R_2 = 0.01$, $R_2/h_3 = 100$, $h_2/h_3 = 1$, $\eta = 0.7$.

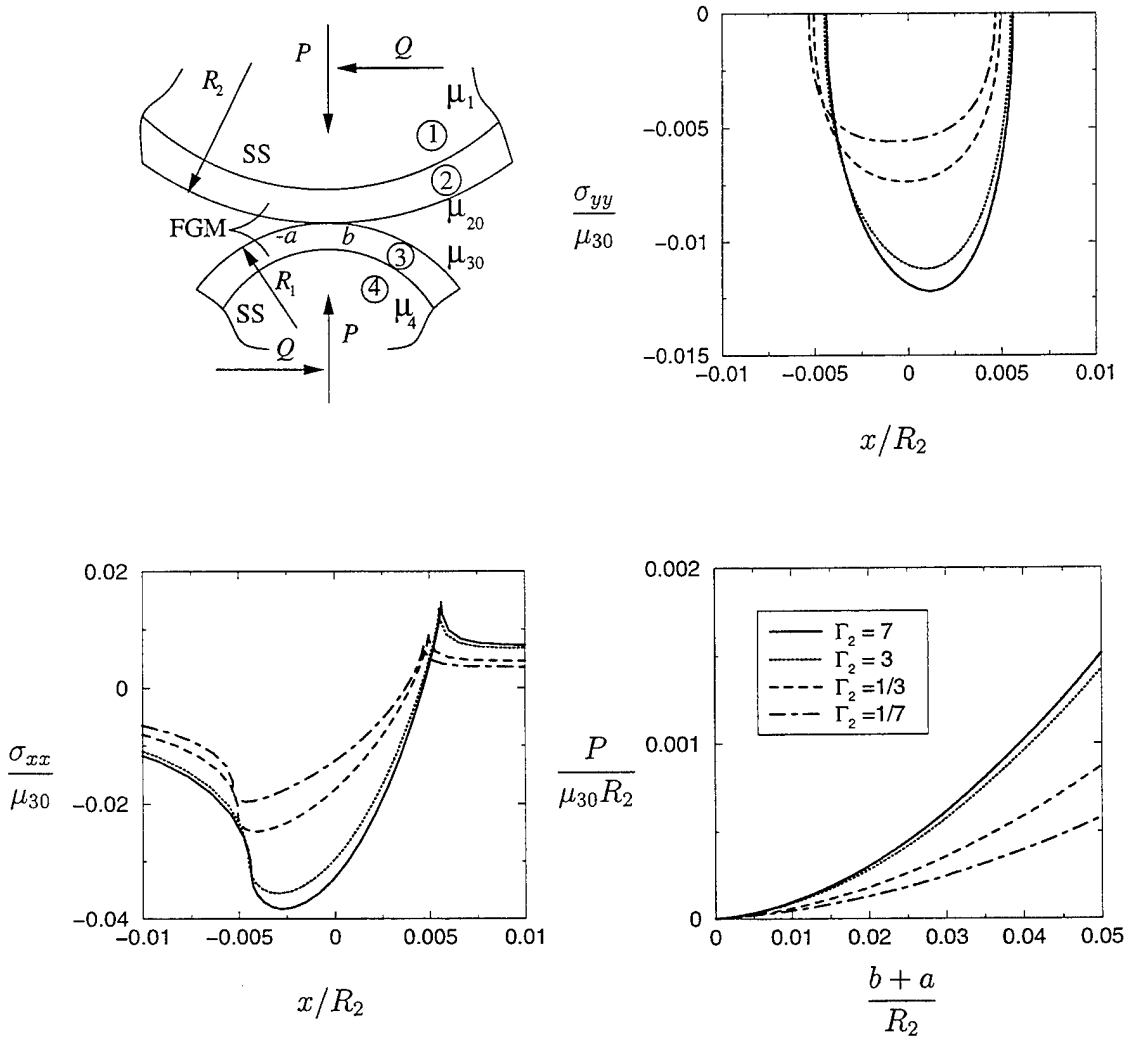

Figure 6.17: Stress distribution on the surface of an FGM coating for various values of the stiffness ratio $\Gamma_2 = \mu_1/\mu_{20}$, $\Gamma_3 = \mu_4/\mu_{30} = 1/7$, $\mu_{30}/\mu_{20} = 2.0$, $R_2/R_1 = 5.0$, $(b+a)/R_2 = 0.01$, $R_2/h_3 = 100$, $h_2/h_3 = 1$, $\eta = 0.7$.

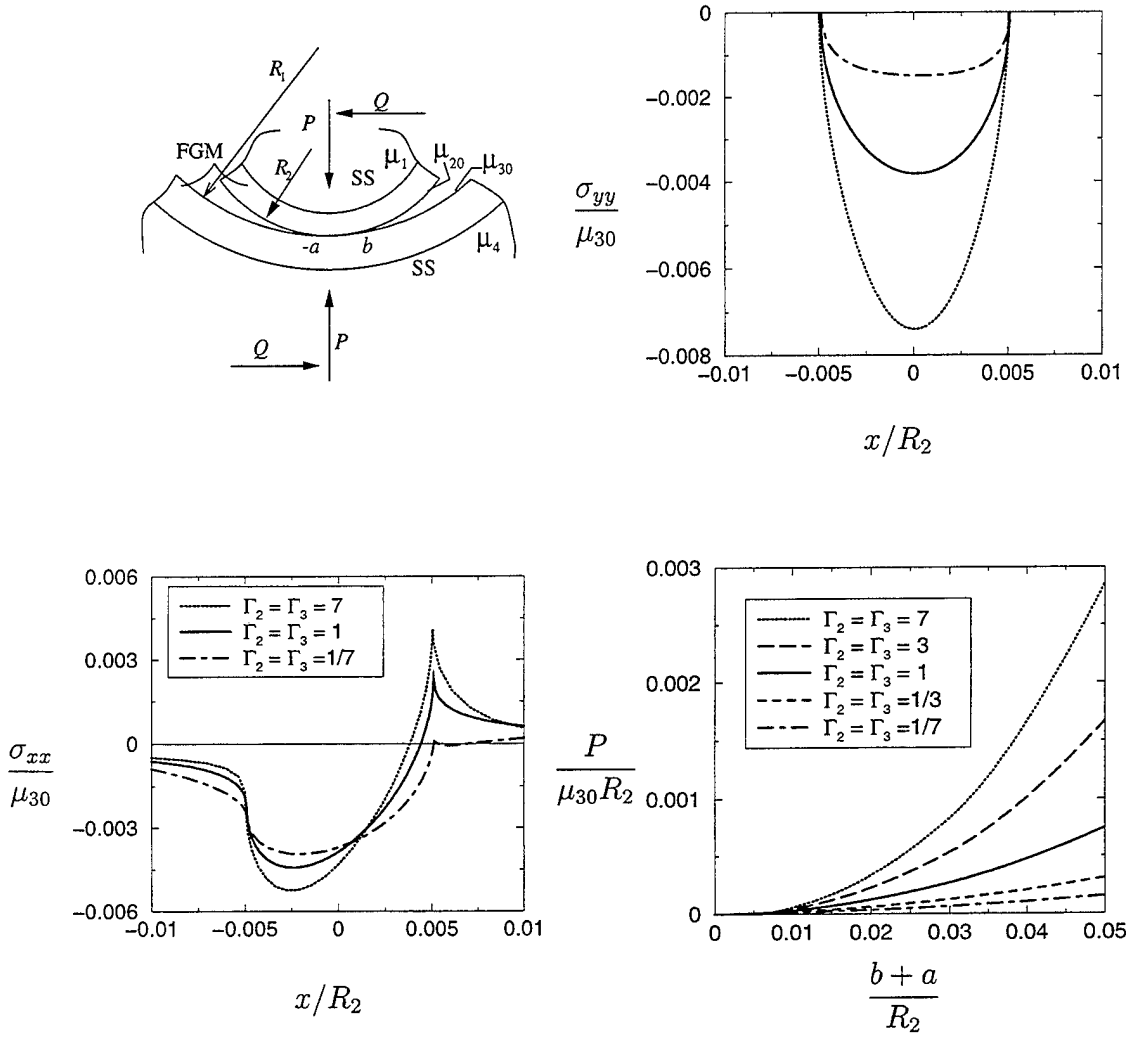

Figure 6.18: Stress distribution on the surface of an FGM coating for various values of the stiffness ratio $\Gamma_2 = \mu_1/\mu_{20}$, $\Gamma_3 = \mu_4/\mu_{30}$, $\mu_{30}/\mu_{20} = 0.5$, $R_2/R_1 = 0.2$, $(b+a)/R_2 = 0.01$, $R_2/h_3 = 100$, $h_2/h_3 = 1$, $\eta = 0.3$.

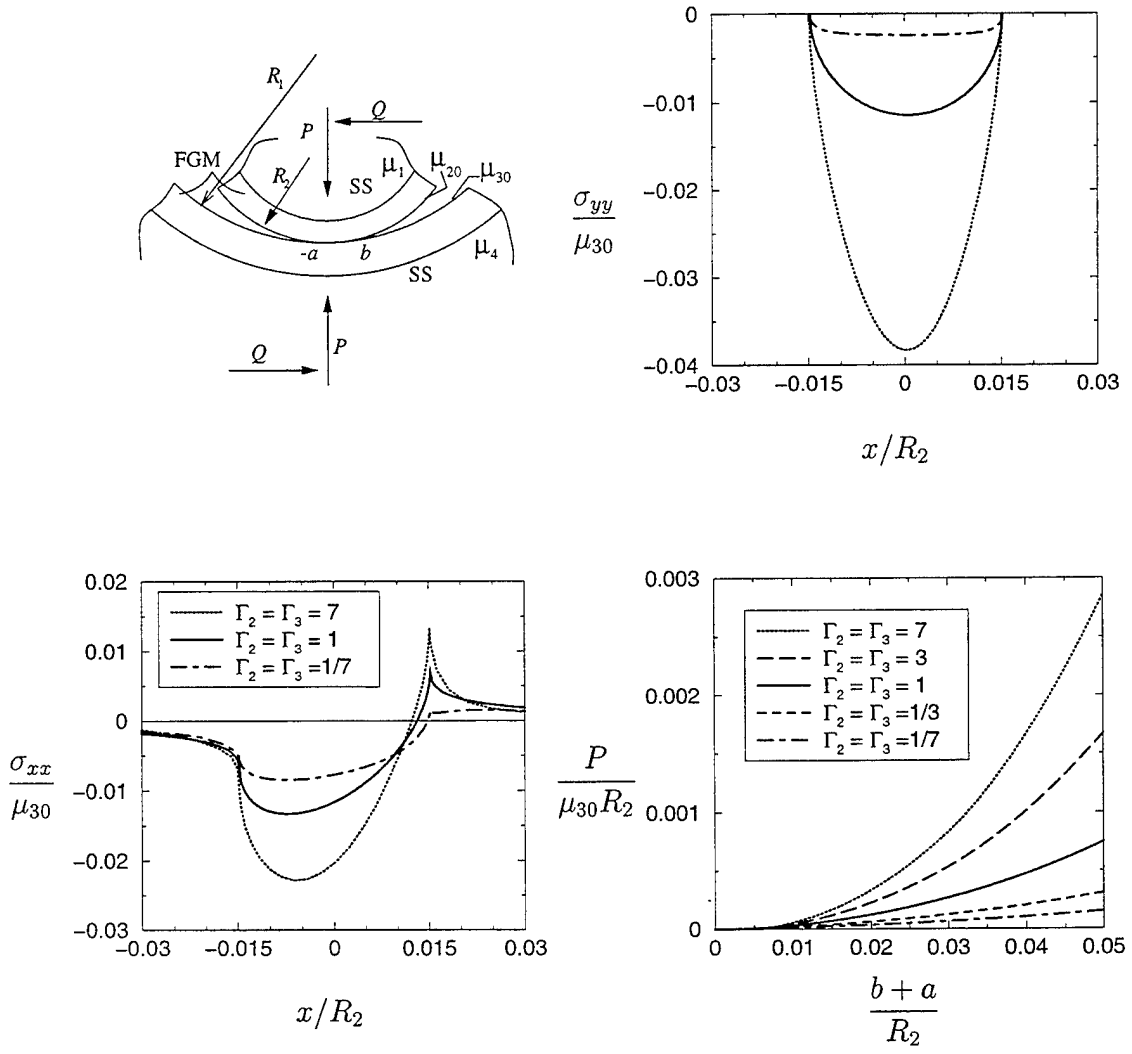

Figure 6.19: Stress distribution on the surface of an FGM coating for various values of the stiffness ratio $\Gamma_2 = \mu_1/\mu_{20}$, $\Gamma_3 = \mu_4/\mu_{30}$, $\mu_{30}/\mu_{20} = 0.5$, $R_2/R_1 = 0.2$, $(b+a)/R_2 = 0.03$, $R_2/h_3 = 100$, $h_2/h_3 = 1$, $\eta = 0.3$.

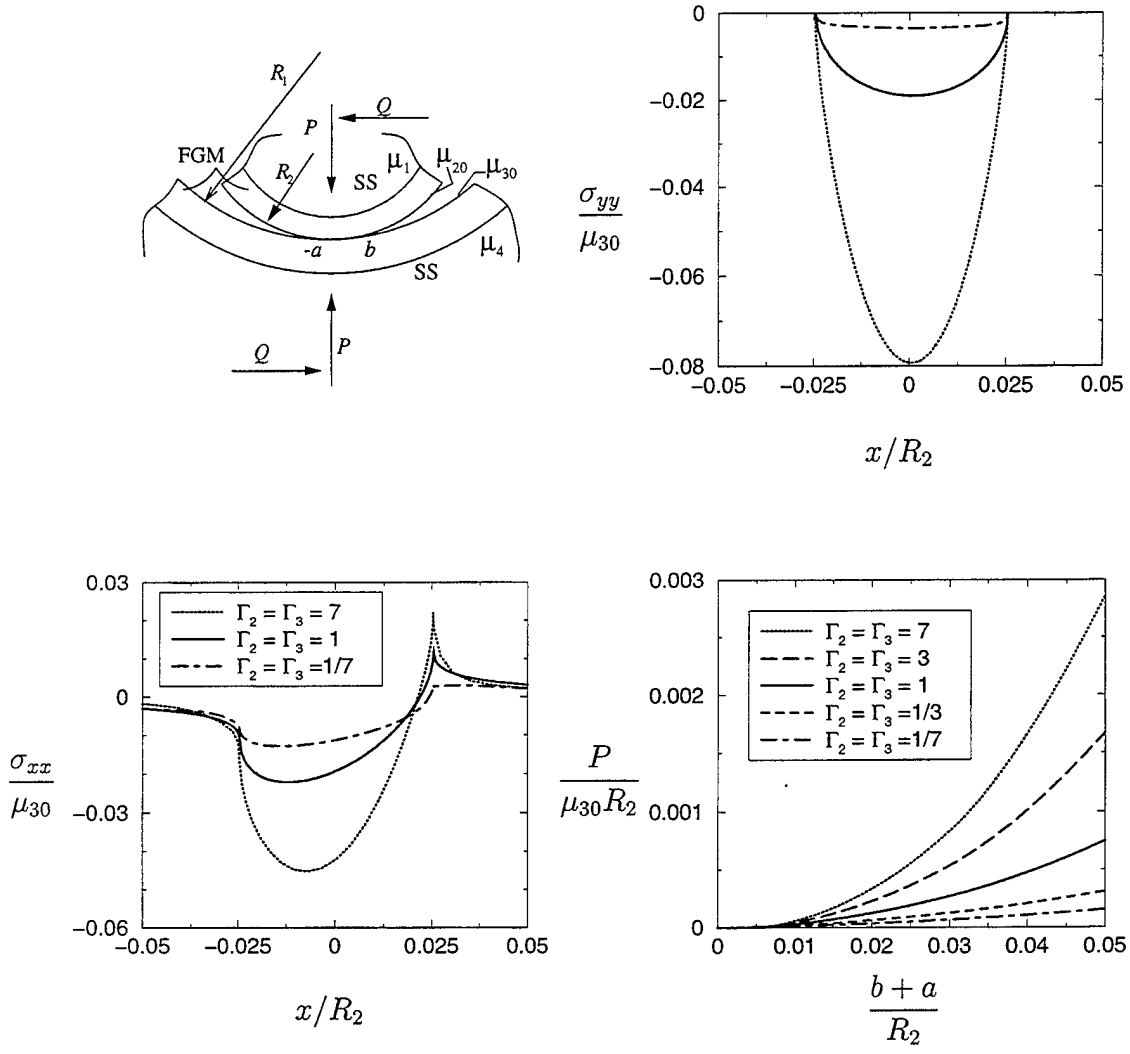

Figure 6.20: Stress distribution on the surface of an FGM coating for various values of the stiffness ratio $\Gamma_2 = \mu_1/\mu_{20}$, $\Gamma_3 = \mu_4/\mu_{30}$, $\mu_{30}/\mu_{20} = 0.5$, $R_2/R_1 = 0.2$, $(b+a)/R_2 = 0.05$, $R_2/h_3 = 100$, $h_2/h_3 = 1$, $\eta = 0.3$.

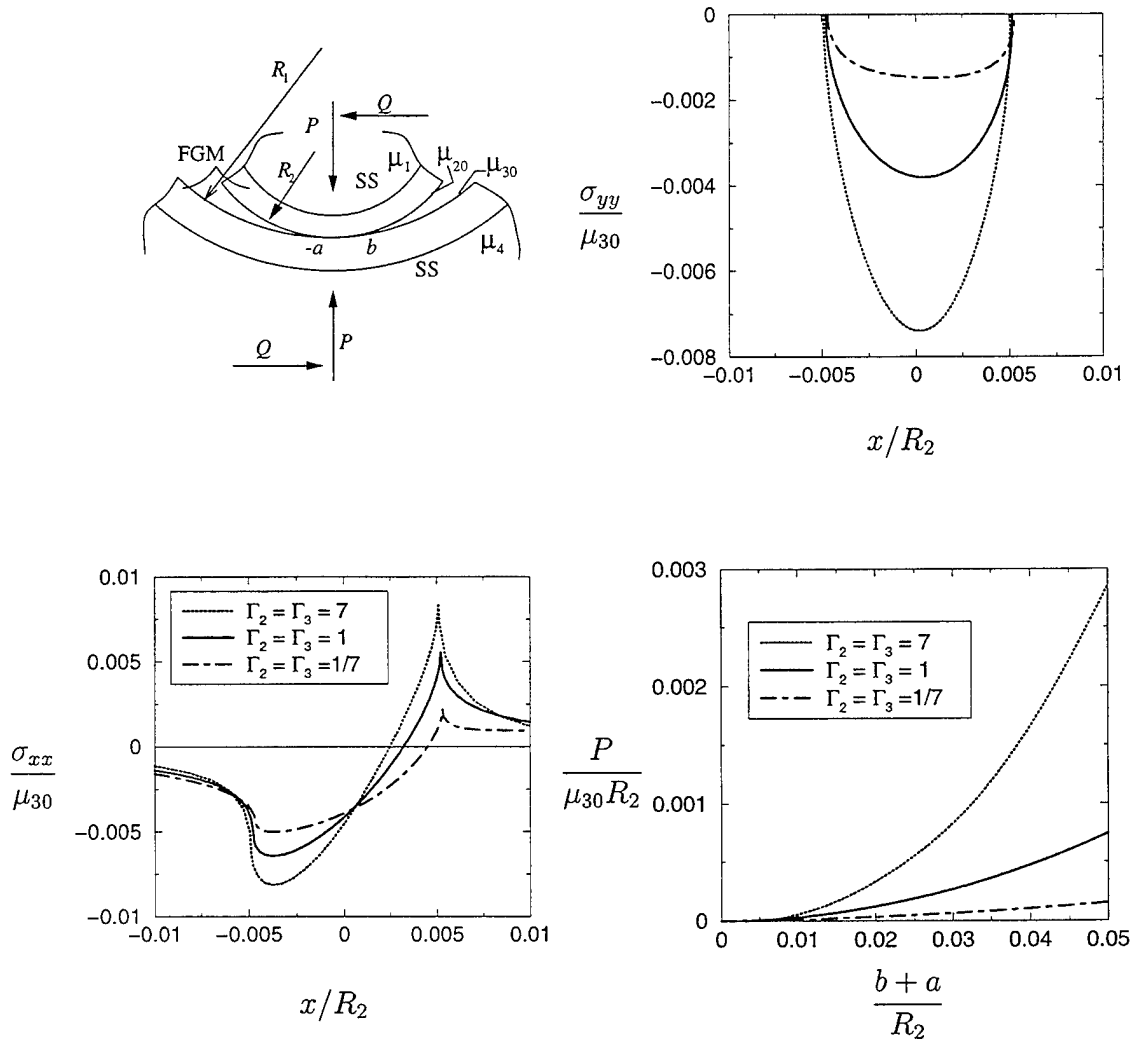

Figure 6.21: Stress distribution on the surface of an FGM coating for various values of the stiffness ratio $\Gamma_2 = \mu_1/\mu_{20}$, $\Gamma_3 = \mu_4/\mu_{30}$, $\mu_{30}/\mu_{20} = 0.5$, $R_2/R_1 = 0.2$, $(b+a)/R_2 = 0.01$, $R_2/h_3 = 100$, $h_2/h_3 = 1$, $\eta = 0.7$.

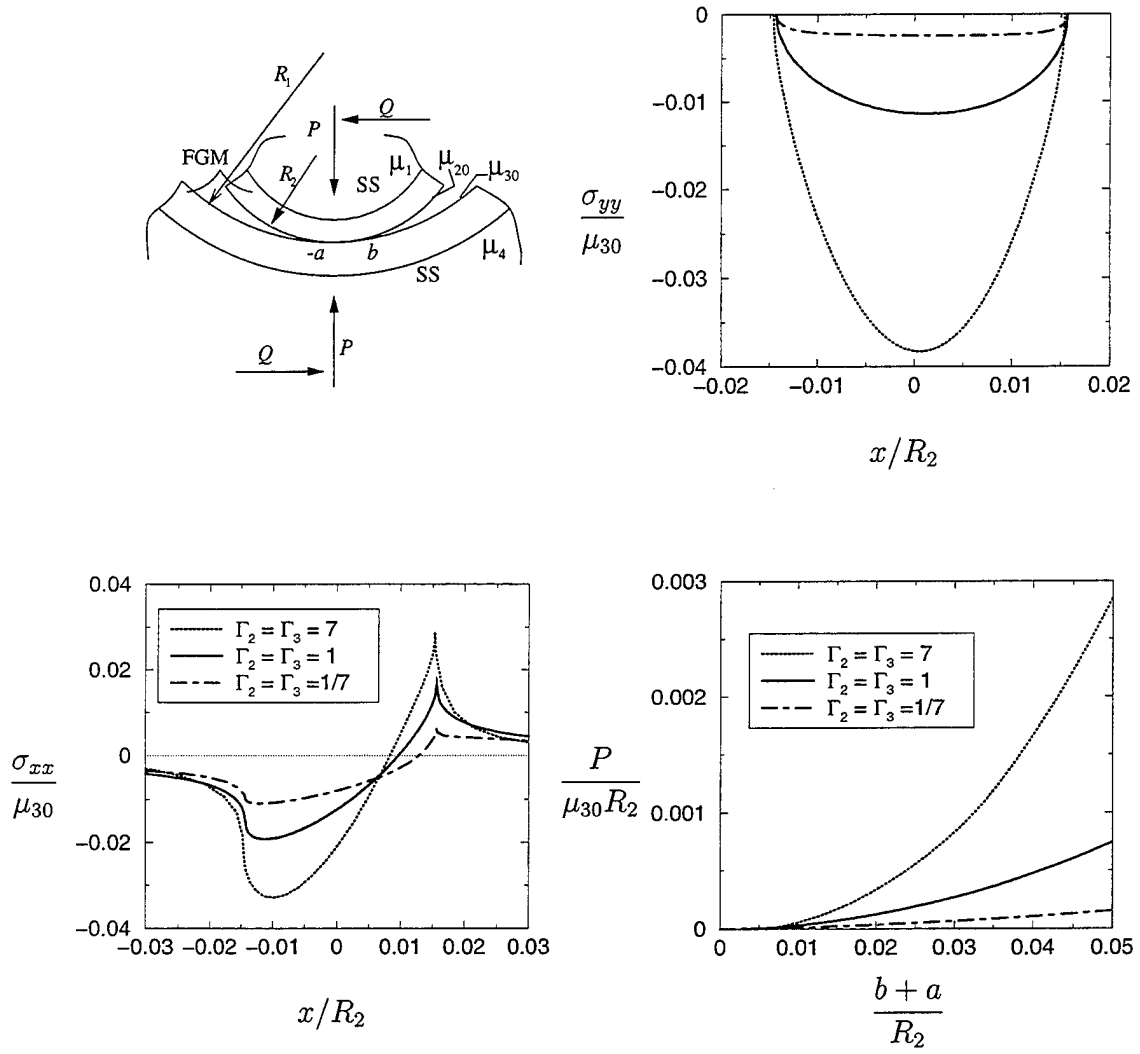

Figure 6.22: Stress distribution on the surface of an FGM coating for various values of the stiffness ratio $\Gamma_2 = \mu_1/\mu_{20}$, $\Gamma_3 = \mu_4/\mu_{30}$, $\mu_{30}/\mu_{20} = 0.5$, $R_2/R_1 = 0.2$, $(b+a)/R_2 = 0.03$, $R_2/h_3 = 100$, $h_2/h_3 = 1$, $\eta = 0.7$.

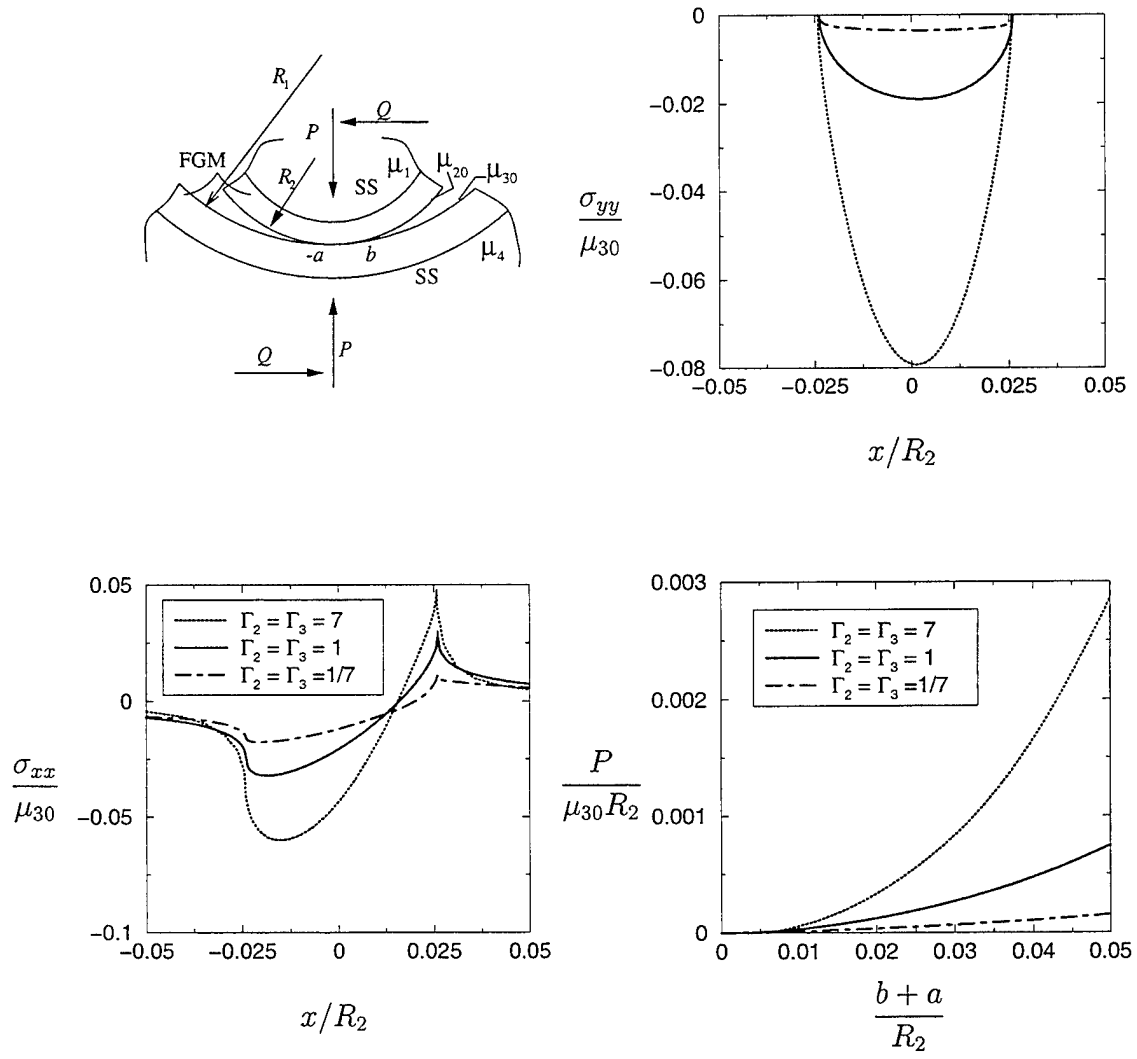

Figure 6.23: Stress distribution on the surface of an FGM coating for various values of the stiffness ratio $\Gamma_2 = \mu_1/\mu_{20}$, $\Gamma_3 = \mu_4/\mu_{30}$, $\mu_{30}/\mu_{20} = 0.5$, $R_2/R_1 = 0.2$, $(b+a)/R_2 = 0.05$, $R_2/h_3 = 100$, $h_2/h_3 = 1$, $\eta = 0.7$.

Chapter 7

Conclusions

In this study, two classes of problems are investigated, namely; the contact problems for rigid stamps and the contact problems in elastic load transfer components. The main calculated quantities are the contact stresses, the in-plane stress component on the surface, the load versus the contact length relations and, where applicable, the stress intensity factors. The contact problem of an FGM coating under an elastic/rigid stamp is examined first by reducing the governing equations to a system of ordinary differential equations by using the Fourier Integral transformation technique. The resulting integral equation is solved numerically. The parameters used in this study are the non-homogeneity parameters, $\gamma_3 h_3$ and $\gamma_2 h_2$, the coefficient of friction, η and various length parameters. Different stamp profiles are used for the application of the load P, and the shear load,Q. The latter is related to the normal load by the Coulomb theory for friction.

After solving the half space problem the Green's functions necessary for the solution of the contact problem in load transfer components are obtained. A parametric study is performed to find the influence of coefficient of friction, material property grading and surface shear modulus of upper/lower or inner/outer cylinders on the stress distribution.

We may summarize the results obtained from this study as follows:

1) For the flat stamp, in the case of no friction, stiffening coating gives tensile in-plane stress σ_{xx}at both ends of the contact whereas for the softening coating σ_{xx} is compressive everywhere along the surface. In the presence of friction, σ_{xx} is tensile for $x > a$, becomes unbounded for $x \to a$ and is compressive for $x < a$, $x = a$ being the trailing edge of the contact region. The in-plane infinite tensile stress at the trailing edge may cause crack initiation. Also as the coefficient of friction increases, the magnitude of the in-plane and contact stresses increase.

2) For the triangular stamp, it is found that σ_{xx} on the surface is tensile outside the contact region for stiffening coating ($\Gamma_3 > 1$) and no friction. There is a linear relationship between the load versus the contact length for the homogeneous half plane. In the presence of friction, σ_{xx} is tensile for $x > b$ for the stiffening coating where b is the trailing end. As the stiffness of the substrate increases with respect to the stiffness of coating at the surface (i.e. for $\Gamma_3 > 1$), the magnitude of σ_{yy} increases. As the coefficient of friction increases the peak stress at the trailing edge of the contact region also increases.

3) For the semicircular stamp, the behavior of the contact stresses were similar to the triangular stamp case. However, there is a parabolic relationship between the load versus the contact length for the homogeneous half plane(i.e., for $\gamma_3 = 0$). When the direction of the applied force Q is reversed as in Figure 5.34, singular tensile stress $\sigma_{xx}$is generated at the trailing edge of the contact. Stress intensity factors increase as the stiffness of the coating increases.

4) For the cylindrical stamp, it is observed that the positive σ_{xx} arises at both ends of the contact for the stiffening coating($\Gamma_3 > 0$) and no friction. At the trailing edge of the contact, σ_{xx} assumes its maximum value. These stresses are important from the fretting mechanics point of view since they can lead to fretting fatigue of

the component if a cyclic loading is applied. The stress σ_{yy} is again slanted towards the trailing edge. As the contact length increases the contact stresses increase in a parabolic manner. Also an increase in the coefficient of friction gave rise to the higher peak stresses at the trailing edge. The contact stresses are relatively low for the softening coating($\Gamma_3 < 1$).

5) For the two deformable elastic cylinders, the maximum of the tensile stress σ_{xx} occurs at the trailing edge of the contact region when both of the cylinders have a stiffening FGM coating . However, these stresses are minimized if both of the cylinders have a softening FGM coating($\Gamma_2 < 1$, $\Gamma_3 < 1$). Various combinations of the properties of cylinders are used and the contact stresses and the load versus the contact length relations are presented. The load versus contact length relations are approximately parabolic. For the negative radius of curvatures in load transfer components such as bearings, the contact stresses are much lower than that for the positive radius of curvature case such as gears. The contact stresses show the same behavior but are smaller in magnitude.

Bibliography

[1] Hirano, T., Yamada, T., Teraki, J., Niino, M., Kumakawa, A., "A study of functionally gradient material design for a thrust chamber", *Proceedings of the 16th International Symposium on Space Technology and Science,* Sapporo, Japan, May 1988.

[2] Marumatsu, K., Kawasaki, A., Taya, M. and Watanabe R., *FGM '90*, p.53, FGM Forum, Sendai, Japan, 1990.

[3] Kawasaki A. and Watanabe R., *FGM '90*, p. 197, FGM Forum, Sendai, Japan, 1990.

[4] Ilschner, B., and Cherradi, N., eds., *Proc. of the Third Int. Symp. on Structural and Functional Gradient Materials*, Presses Polytechniques et Universitaires Romands, Lausanne, Switzerland, 1995.

[5] Kaysser, W. A., *Proc. of the Fifth Int. Symp. on Structural and Functional Gradient Materials*, New Town Hall, Dresden, Germany, 1998.

[6] Sampath, S., Herman, H., Shimoda, N. and Saito, T., *MRS Bulletin*, p. 27, January 1995.

[7] Kurihara, K., Sasaki, K., Kawarada, M., "Adhesion Improvement of diomond films", *FGM '90,* pp.65-69, 1990.

[8] Yamanouchi, M., Koizumi, M., Hirai, T. and Shiota, I., eds. FGM-90, *Proc. of the First Int. Symp. on Functionally Gradient Materials*, FGM Forum, Sendai, Japan, 1990.

[9] Holt, J.B., Koizumi, M., Hirai, T. and Munir, Z. A., eds., *Proc. of the Second Int. Symp. on Functionally Gradient Materials*, Ceramic Transactions, Vol. 34, American Ceramic Society, Westerville, OH, 1993

[10] Bamberger, E.N., Averbach, B. L., Pearson, P. K., Vanpelt, S. and Price, J., Improved fatigue life bearing development, Final Report, AFWAL-7R-89-2012, Wright Patterson AFB, OH, June 1989.

[11] Jamal, T., Nimmagadda, R. and Bunshah, R. F., *Thin Solid Films*, 73 (1980) 245

[12] Hochman, R. F., Erdemir, A., Dolan, F.J. and Thom, R. C., *J. Vac. Sci. Technol.* A, 36 (1985) 2348

[13] Kustas,F. M., Misra, M. S., Shepard, D. F. and Froechtenigt, J.F., *Surf. Coat. Techol.*, 48 (1991) 115

[14] Wei, R., Wilbur, P.J. and Kustas, F. M., *J. Tribol.*, 114 (1992) 298

[15] Lee, W. Y., Bae, Y. W., Berndt, C. C., Erdogan, F., Lee, Y. D. and Mustasim, Z., Advanced Turbine Systems - Materials Workshop, Charleston, SC, Feb. 13-14, 1996.

[16] Hertz H. (1882). On the contact of elastic Solids. *J. Reine Angewandte Mathematic.*92, 156-171

[17] Harding, J. W., and Sneddon, I. N., "The Elastic Stresses Produced by the Indentation of the Plane Surface of a Semi-infinite Elastic Sokid by a Rigid

Punch", *Proceedings of the Cambridge Philosophical Society,* Vol 41, 1945, pp.16-26.

[18] Galin, L. A.(1961) *Contact problems in the Theory of Elasticity*(translated by H. Moss). North Caroline State College, Raleigh.

[19] Rostovtsev, N. A. (1961) An integral equation encountered in the problem of a rigid foundation bearing on nonhomogeneous soil.*PMM* 25, 164-168.

[20] Rostovtsev, N. A. (1964) On the theory of elasticity of a nonhomogeneous medium. *PMM* 28, 601-611.

[21] Willis, J. R. (1966) Hertzian contact of anisotropic bodies. *J. Mech. Phys. Solids* 14, 163-176.

[22] Willis, J. R. (1967) Hertzian contact of anisotropic bodies. *J. Mech. Phys. Solids* 15, 331-339

[23] Sneddon, I. N., and Hill, R., *Progress in Solid Mechanics*, Vol. 1, North-Holland Publishing Company, Amsterdam, 1960, pp. 410-413.

[24] Muskhelishvili, N. I., *Some basic Problems of the Mathematical Theory of Elasticity.* Noordhoff, Groningen, The Netherlands(1963).

[25] Ufliand, Ia S., *Survey of Articles on the Application of Integral Transforms in the Theory of Elasticity.* North Carolina State Translation Series, Raleigh, N. C., 1965

[26] R. D. Miller, Variation of line pressure and rolling speed with indentation of covered rollers. *Br. J. app. Phys.* 15, 1423-1435(1964).

[27] Sneddon, I. N., *Fourier Transforms*, McGraw-Hill, 1951.

[28] Wu, T. S., and Chiu, Y. P., "On the Contact Problems of Layered Elastic Bodies ", *Quarterly Journal of Applied Mathematics*, Vol. 25, 1967, pp. 233-242.

[29] Pao, Y. C., Wu, T. S., and Chiu, Y. P., "Bounds on the Maximum Contact Stress of an Indented Elastic Layer ", *Journal of Applied Mechanics*, Vol. 38, Transactions of the ASME, 1971, pp. 608-614.

[30] Kasmalkar, M. B., M. S. Thesis, Lehigh University, 1993

[31] Ratwani, M., and Erdogan, F., "On the Plane Contact Problem for a Frictionless Elastic Layer ", *Journal of Solids and Structures*, Vol. 9, 1973, pp. 921-936.

[32] Civelek, M. B., and Erdogan, F., "The Axisymmetric Double Contact Problem for a Frictionless Elastic Layer", *International Journal of Solids and Structures*, Vol. 10, 1974, pp. 639-659.

[33] Oden, J. T. and Martins, J. A. C., "Models and Computational Methods for Dynamic Friction Phenomena", *Comput. Meth. appl. Mech. Engng*, Vol. 52, 1985, pp. 527-634.

[34] Tabor, D., "Friction-the Present State of Our Understanding", *J. Lubr. Technol.*, Vol. 103, 1981, pp.169-179.

[35] Chan, S. K., Tuba, I. S., "A Finite Element Method for Contact Problems of Solid Bodies-Part I. Theory and Validation", *Int. J. Mech. Sci.*, Vol. 13, 1971, pp. 519-530.

[36] Tsuta T, and Yamaji S., *Finite Element Analysis of Contact Problems. Theory and Practice in Finite Element Structural Analysis.* University of Tokyo Press, Japan, 1973.

[37] Ohte, S., "Finite Element Analysis of Elastic Contact Problems", *Bull. JSME*, Vol. 16, 1973, pp.797-804.

[38] Lindeman, R. A., "Finite Element Computer Program for the Solution of Non-linear Axisymmetric Contact Problem with Interference Fits", *Rep.* TR-3148, Naval Weapons Lab., Virginia, 1974.

[39] Bakırtaş, I., "The Problem of a Rigid Punch on a Non-homogeneous Elastic Half Space", *Int. J. Engng. Sci.*, Vol 18, 1980, pp. 597-610.

[40] Bakırtaş, I, *Solution of Certain Elasticity Problems for a Medium with Varying Modulus of Elasticity.* Ph. D. Dissertation, Istanbul, Istanbul Technical University(1977) (in Turkish).

[41] Guler, M. A. *The Problem of a Rigid Punch with Friction on a Graded Elastic Medium*, M. S. Thesis, Lehigh University, 1996.

[42] Ghizetti, A and Ossicini A, Quadrature Formulae, 1970

[43] Muskhelishvili, N. L., *Singular Integral equations*, P. Noordhoff, Groningen, The Netherlands,1953.

[44] Erdogan, F., and Gupta, G. D.," On the Numerical Solution of Singular Integral Equations ", *Quarterly of Applied Mathematics,* Vol. 29. 1972, pp. 525-534.

[45] Kaya, A.C., and Erdogan, F., "On the Solution of Integral Equation with a Generalized Cauchy Kernel", *Quarterly of Applied Mathematics*, Vol. xiv, pp. 455-469,1987

[46] Erdogan, F., Gupta, G. D., and Cook, T. S., "Numerical Solution of Singular Integral Equations," *Method of Analysis and Solution of Crack Problems*, G.C. Sih (ed.), Noordhoff Int. Publ., Leyden(1973) 368-425.

[47] Tricomi, F.G., *Integral Equations,* Interscience, New York (1957)

[48] Szegö, G., *Orthogonal Polynomials*, Colloquium Publications, 23,Am. Math. Soc.(1939)

[49] Abramowitz, M. and Stegun, I. A., *Handbook of Mathematical Functions, National Bureu of Standards, Applied Mathematics Series*, 1964.

[50] Stroud, A. H. and Secrest, D., *Gaussian Quadrature Formulas.* Prentice-Hall, New York, 1966

Appendix A

Some Useful properties of Jacobi Polynomials

For $\kappa_0 = (-1, 0, 1)$ the following relation can be written(see Tricomi [47], Szegö [48])

$$\begin{aligned} & \frac{1}{\pi}\int_{-1}^{1}\frac{w(t)P_n^{(\alpha,\beta)}(t)}{t-x}dt \\ = \; & \cot\pi\alpha w(x)P_n^{(\alpha,\beta)}(x) \\ & -\frac{2^{\alpha+\beta}\Gamma(\alpha)\Gamma(n+\beta+1)}{\pi\Gamma(n+\alpha+\beta+1)}F\left(n+1,-n-\alpha-\beta,1-\alpha,\frac{1-x}{2}\right), \\ -1 \; < \; & x<1, \qquad \Re(\alpha)>-1, \qquad \Re(\beta)>-1, \\ \alpha+\beta \; = \; & -\kappa_0, \qquad \Re(\alpha)\neq(0,1,\ldots). \end{aligned} \tag{A.1}$$

By observing that

$$P_{n-\kappa}^{(-\alpha,-\beta)}(x) = \frac{\Gamma(n-\kappa-\alpha+1)}{\Gamma(n-\kappa+1)\Gamma(1-\alpha)}F\left(n+1,-n+\kappa,1-\alpha,\frac{1-x}{2}\right), \tag{A.2}$$

and substituting $\kappa_0 = -(\alpha+\beta)$ into (A.2) yields

$$F\left(n+1,-n+\kappa_0,1-\alpha,\frac{1-x}{2}\right) = \frac{\Gamma(n+\alpha+\beta+1)\Gamma(1-\alpha)}{\Gamma(n+\beta+1)}P_{n-\kappa_0}^{(-\alpha,-\beta)}(x). \tag{A.3}$$

By substituting now (A.3) back into (A.1), we obtain

$$\begin{aligned} & \frac{1}{\pi}\int_{-1}^{1}\frac{w(t)P_n^{(\alpha,\beta)}(t)}{t-x}dt \\ = \; & \frac{\cos\pi\alpha}{\sin\pi\alpha}w(x)P_n^{(\alpha,\beta)}(x) - 2^{-\kappa_0}\frac{\Gamma(\alpha)\Gamma(1-\alpha)}{\pi}P_{n-\kappa_0}^{(-\alpha,-\beta)}(x). \qquad \text{(A.4)} \\ -1 \; < \; & x < 1 \end{aligned}$$

Note also that

$$\Gamma(\alpha)\Gamma(1-\alpha) = \frac{\pi}{\sin\pi\alpha}. \qquad \text{(A.5)}$$

Equation (A.1) further reduces to

$$AP_n^{(\alpha,\beta)}(r)w(r) + \frac{B}{\pi}\int_{-1}^{1}\frac{P_n^{(\alpha,\beta)}(s)w(s)}{(s-r)}ds = -2^{-\kappa_0}\frac{B}{sin\pi\alpha}P_{n-\kappa_0}^{(-\alpha,-\beta)}(r),$$
$$-1 \; < \; r < 1, \qquad \Re(\alpha) > -1, \qquad \Re(\beta) > -1, \qquad \Re(\alpha) \neq (0,1,...,). \qquad \text{(A.6)}$$

The Orthogonality relation can be written as

$$\int_{-1}^{1} P_n^{(\alpha,\beta)}(t)\, P_j^{(\alpha,\beta)}(t)\, w(t)\, dt = \begin{cases} 0 & n \neq j \\ \theta_j^{(\alpha,\beta)} & n = j \end{cases} \qquad j = 0,1,2,..., \qquad \text{(A.7)}$$

where

$$\theta_0^{(\alpha,\beta)} = \int_{-1}^{1} w(t)\, dt = \frac{2^{\alpha+\beta+1}\Gamma(\alpha+1)\Gamma(\beta+1)}{\Gamma(\alpha+\beta+2)}, \qquad \text{(A.8)}$$

$$\theta_j^{(\alpha,\beta)} = \frac{2^{\alpha+\beta+1}\Gamma(j+\alpha+1)\Gamma(j+\beta+1)}{(2j+\alpha+\beta+1)\, j!\Gamma(j+\alpha+\beta+1)}. \qquad \text{(A.9)}$$

Rodrigues formula is given as

$$w^{(\alpha,\beta)}(t)\, P_n^{(\alpha,\beta)}(t) = -\frac{(-1)^n}{2^n n!}\frac{d^n}{dt^n}\left[w^{(\alpha+n,\beta+n)}(t)\right], \qquad n = 0,1,2,... \qquad \text{(A.10)}$$

$$w^{(\alpha,\beta)}(t)\, P_n^{(\alpha,\beta)}(t) = -\frac{1}{2n}\frac{d}{dt}\left[w^{(\alpha+1,\beta+1)}P_{n-1}^{(\alpha+1,\beta+1)}(t)\right]. \qquad \text{(A.11)}$$

The following recurrence relation is given in [42]

$$P_{n+1}^{(\alpha,\beta)}(x)P_n^{(\alpha,\beta)}(y) - P_{n+1}^{(\alpha,\beta)}(y)P_n^{(\alpha,\beta)}(x) = (x-y)\frac{\theta_n^{(\alpha,\beta)}}{A_n^{(\alpha,\beta)}}\sum_{k=0}^{n}\frac{P_k^{(\alpha,\beta)}(x)P_k^{(\alpha,\beta)}(y)}{\theta_k^{(\alpha,\beta)}}, \tag{A.12}$$

where

$$A_n^{(\alpha,\beta)} = \frac{2\,(n+1)\,(\alpha+\beta+n+1)}{(\alpha+\beta+2n+1)\,(\alpha+\beta+2n+2)}, \tag{A.13}$$

where θ_n is given in (A.8)

Appendix B

Calculation of some useful integrals

We will examine the evaluation of the following integral

$$\int_{-1}^{1} \frac{(z-1)^{\alpha}(1+z)^{\beta}}{z-r} dz, \qquad \alpha+\beta=1, \qquad -\infty < r < \infty \tag{B.1}$$

In the complex plane, since

$$\lim_{z\to\infty} \frac{z^{\alpha+\beta+1}}{z-z_0} = \infty,$$

we will start with the following contour integral

$$\oint_C f(z)dz, \tag{B.2}$$

where

$$f(z) = \frac{(z-1)^{\alpha}(1+z)^{\beta}}{(z-z_0)(1-\lambda z)}, \tag{B.3}$$

in which

$$\lim_{z\to\infty} \frac{(z-1)^{\alpha}(1+z)^{\beta}}{(z-z_0)(1-\lambda z)} = -\frac{1}{\lambda}, \tag{B.4}$$

is finite, and therefore

$$\int_{-1}^{1} \frac{(z-1)^{\alpha}(1+z)^{\beta}}{z-r} dz = \lim_{\lambda\to 0} \int_{-1}^{1} \frac{(z-1)^{\alpha}(1+z)^{\beta}}{(z-r)(1-\lambda z)} dz. \tag{B.5}$$

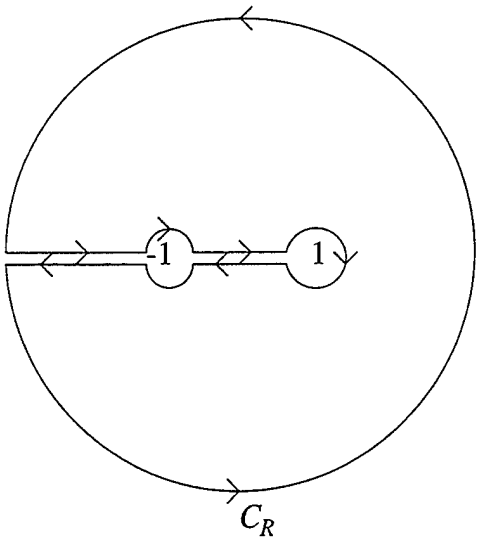

Figure B.1: The contour used in evaluating the integral in B.2

and ($z = z_0$ and $z = 1/\lambda$) are the singular points of the integral (B.2) within C, C being the contour shown in Figure B.1 and it is assumed that z_0 is outside the cut plane $[-1, 1]$. According to Cauchy's theorem on residues , we have

$$\oint_C f(z)\,dz = 2\pi i \sum Res f(z)\Big|_{z=z_k}, \tag{B.6}$$

where

$$\begin{aligned}\oint_C f(z)\,dz &= \oint_{\Gamma_1+C_{\varepsilon_1}+L_1+C_{\varepsilon_2}+L_2+C_{\varepsilon_3}+\Gamma_2+C_R} f(z)\,dz \\ &= \left\{\int_{\Gamma_1} + \oint_{C_{\varepsilon_1}} + \int_{L_1} + \oint_{C_{\varepsilon_2}} + \int_{L_2} + + \int_{\Gamma_2} + \oint_{C_R}\right\} f(z)\,dz. \end{aligned} \tag{B.7}$$

Since

$$\lim_{z\to 1}(z-1)\,f(z) = \lim_{z\to -1}(z+1)\,f(z) = 0,$$

from the Jordan's lemma, it can be shown that the contour integrals along C_{ε_1}, C_{ε_2}, vanishes, i.e,

$$\oint_{C_{\varepsilon_1}} f(z)\,dz = \oint_{C_{\varepsilon_2}} f(z)\,dz = 0, \tag{B.8}$$

Further, since

$$\lim_{z\to\infty} zf(z) = -\frac{1}{\lambda}, \tag{B.9}$$

we find that

$$\oint_{C_R} f(z)\,dz = -\frac{2\pi}{\lambda}i. \tag{B.10}$$

Also the line integrals,

$$\int_{\Gamma_1} f(z)\,dz = -\int_{\Gamma_2} f(z)\,dz. \tag{B.11}$$

If $\varepsilon \to 0$ and $R \to \infty$ from (B.8) (B.10) (B.11) and (B.7)

$$\int_{L_1} f(z)\,dz + \int_{L_2} f(z)\,dz = 2\pi i \sum Res + \frac{2\pi}{\lambda}i. \tag{B.12}$$

For the evaluation of the line integrals of equation (B.12), we define

$$z+1 = \rho_1 e^{i\theta_1}, \tag{B.13}$$

$$z-1 = \rho_2 e^{i\theta_2}, \tag{B.14}$$

where

$$\rho_1 = s+1, \tag{B.15}$$

$$\rho_2 = 1-s, \tag{B.16}$$

$$\theta_1 = \begin{cases} 0 & s \in L_1 \\ 0 & s \in L_2 \end{cases}, \tag{B.17}$$

$$\theta_2 = \begin{cases} \pi & s \in L_1 \\ -\pi & s \in L_2 \end{cases}. \tag{B.18}$$

Using (B.15)-(B.18) the line integrals on L_1 and L_2 becomes

$$\int_{L_1} f(z)\,dz = \int_{-1}^{1} \frac{\rho_2^{\alpha}\rho_1^{\beta}e^{\pi i\alpha}}{(s-z_0)(1-\lambda s)}ds, \tag{B.19}$$

$$\int_{L_2} f(z)\,dz = \int_{1}^{-1} \frac{\rho_2^{\alpha}\rho_1^{\beta}e^{-\pi i\alpha}}{(s-z_0)(1-\lambda s)}ds. \tag{B.20}$$

From (B.19) and (B.20) it can be shown that

$$\int_{L_1} f(z)\,dz + \int_{L_2} f(z)\,dz = 2i\sin\pi\alpha \int_{-1}^{1} \frac{(1-s)^{\alpha}(1+s)^{\beta}}{(s-z_0)(1-\lambda s)}ds. \tag{B.21}$$

Residues at $z = z_0$ and $z = 1/\lambda$ can be calculated as

$$Res \quad f(z)|_{z=z_0} = \frac{(z_0-1)^{\alpha}(1+z_0)^{\beta}}{(1-\lambda z_0)}, \tag{B.22}$$

$$Res \quad f(z)|_{z=\frac{1}{\lambda}} = -\frac{1}{\lambda}\frac{(1-\lambda)^{\alpha}(1+\lambda)^{\beta}}{1-\lambda z_0}. \tag{B.23}$$

Using (B.12), (B.21), (B.22), (B.23), It can be shown that

$$\begin{aligned} 2i\sin\pi\alpha \int_{-1}^{1} \frac{(1-s)^{\alpha}(1+s)^{\beta}\,ds}{(s-z_0)(1-\lambda s)} &= 2\pi i\frac{(z_0-1)^{\alpha}(1+z_0)^{\beta}}{(1-\lambda z_0)} \\ &\quad +2\pi i\left[\frac{1-\lambda z_0-(1-\lambda)^{\alpha}(1+\lambda)^{\beta}}{\lambda(1-\lambda z_0)}\right] \end{aligned} \tag{B.24}$$

Taking the limit of equation (B.24) as $\lambda \to 0$ it may easily be shown that

$$\int_{-1}^{1} \frac{(1-s)^{\alpha}(1+s)^{\beta}}{(s-z_0)}ds = \frac{\pi}{\sin\pi\alpha}\left[(z_0-1)^{\alpha}(1+z_0)^{\beta}+\alpha-\beta-z_0\right], \qquad \alpha+\beta=1. \tag{B.25}$$

In order to evaluate the following integral on line $L = [-1, 1]$,

$$\int_L \frac{\phi(s)}{s-r}ds, \tag{B.26}$$

where

$$\phi(t) = (1-t)^{\alpha}(1+t)^{\beta}. \tag{B.27}$$

we consider the following sectionally holomorphic function

$$\Phi(z) = \frac{1}{2\pi i}\int_L \frac{\phi(t)}{t-z}dt, \tag{B.28}$$

where

$$\Phi(z) = \frac{1}{2i\sin\pi\alpha}\left[(z-1)^{\alpha}(z+1)^{\beta} + \alpha - \beta - z\right]. \tag{B.29}$$

From the Plemelj formulas we have

$$\Phi^{+}(r) - \Phi^{-}(r) = \phi(r), \tag{B.30}$$

$$\Phi^{+}(r) + \Phi^{-}(r) = \frac{1}{\pi i}\int_L \frac{\phi(s)}{s-r}ds. \tag{B.31}$$

In order to find $\Phi^{+}(r)$ and $\Phi^{-}(r)$ first, observe that

$$\left[(z-1)^{\alpha}(z+1)^{\beta}\right]^{+} = (1-r)^{\alpha}(r+1)^{\beta}e^{\pi i\alpha}, \tag{B.32}$$

$$\left[(z-1)^{\alpha}(z+1)^{\beta}\right]^{-} = (1-r)^{\alpha}(r+1)^{\beta}e^{-\pi i\alpha}. \tag{B.33}$$

So that $\Phi^{+}(r)$ and $\Phi^{-}(r)$ becomes

$$\Phi^{+}(r) = \frac{1}{2i\sin\pi\alpha}\left[(1-r)^{\alpha}(r+1)^{\beta}e^{\pi i\alpha} - r + \alpha - \beta\right], \tag{B.34}$$

$$\Phi^{-}(r) = \frac{1}{2i\sin\pi\alpha}\left[(1-r)^{\alpha}(r+1)^{\beta}e^{-\pi i\alpha} - r + \alpha - \beta\right]. \tag{B.35}$$

Therefore using (B.31) , (B.34), and (B.35) for $\alpha+\beta=1$ we obtained

$$\int_L \frac{(1-s)^{\alpha}(1+s)^{\beta}}{s-r}ds = \frac{\pi}{\sin\pi\alpha}\left[(1-r)^{\alpha}(r+1)^{\beta}\cos\pi\alpha - r + \alpha - \beta\right], \qquad -1 < r < 1. \tag{B.36}$$

One may easily evaluate the integral for $r > 1$ and $r < -1$ by using equation (B.25) as follows:

$$\int_L \frac{(1-s)^\alpha (1+s)^\beta}{s-r} ds = \frac{\pi}{\sin \pi\alpha} \left[(r-1)^\alpha (r+1)^\beta - r + \alpha - \beta \right], \qquad r > 1, \quad \text{(B.37)}$$

$$\int_L \frac{(1-s)^\alpha (1+s)^\beta}{s-r} ds = \frac{\pi}{\sin \pi\alpha} \left[-(1-r)^\alpha (-1-r)^\beta - r + \alpha - \beta \right], \qquad r < -1. \quad \text{(B.38)}$$

In summary, for $\alpha > 0, \beta > 0$ and $\alpha + \beta = 1$

$$\int_{-1}^{1} \frac{(1-s)^\alpha (1+s)^\beta}{s-r} = \frac{\pi}{\sin \pi\alpha} \begin{cases} \left[-(-r+1)^\alpha (-r-1)^\beta - r + \alpha - \beta \right], & -\infty < r < -1, \\ \left[(1-r)^\alpha (1+r)^\beta \cos \pi\alpha - r + \alpha - \beta \right], & -1 < r < 1, \\ \left[(r-1)^\alpha (r+1)^\beta - r + \alpha - \beta \right], & 1 < r < \infty. \end{cases} \quad \text{(B.39)}$$

A similar analysis can be carried out for the evaluation of for $\alpha > 0, \beta < 0$ and $\alpha + \beta = 0$

$$\int_{-1}^{1} \frac{(1-s)^\alpha (1+s)^\beta}{s-r} = \frac{\pi}{\sin \pi\alpha} \begin{cases} \left[(-r+1)^\alpha (-r-1)^\beta - 1 \right], & -\infty < r < -1, \\ \left[(1-r)^\alpha (1+r)^\beta \cos \pi\alpha - 1 \right], & -1 < r < 1, \\ \left[(r-1)^\alpha (r+1)^\beta - 1 \right], & 1 < r < \infty, \end{cases} \quad \text{(B.40)}$$

and for $\alpha < 0, \beta < 0$ and $\alpha + \beta = -1$

$$\int_{-1}^{1} \frac{(1-s)^\alpha (1+s)^\beta}{s-r} = \frac{\pi}{\sin \pi\alpha} \begin{cases} \left[-(-r+1)^\alpha (-r-1)^\beta \right], & -\infty < r < -1, \\ \left[(1-r)^\alpha (1+r)^\beta \cos \pi\alpha \right], & -1 < r < 1, \\ \left[(r-1)^\alpha (r+1)^\beta \right], & 1 < r < \infty. \end{cases} \quad \text{(B.41)}$$

Evaluation of the following integral

$$L_n(x) = \int_{-1}^{1} \frac{P_n^{(\alpha,\beta)}(t)\, w(t)\, dt}{t-x}, \qquad -\infty < x < \infty, \tag{B.42}$$

where

$$w(t) = (1-t)^{\alpha}(1+t)^{\beta}, \tag{B.43}$$

will now be examined.

Multiplying (B.42) with $P_{n+1}^{(\alpha,\beta)}(x)$, we have

$$P_{n+1}^{(\alpha,\beta)}(x)\, L_n(x) = \int_{-1}^{1} \frac{P_{n+1}^{(\alpha,\beta)}(x)\, P_n^{(\alpha,\beta)}(t)\, w(t)\, dt}{t-x}, \tag{B.44}$$

also we can write the following relation

$$P_n^{(\alpha,\beta)}(x)\, L_{n+1}(x) = \int_{-1}^{1} \frac{P_n^{(\alpha,\beta)}(x)\, P_{n+1}^{(\alpha,\beta)}(t)\, w(t)\, dt}{t-x}. \tag{B.45}$$

If we subtract (B.45) from (B.44) we have

$$\begin{aligned} & P_{n+1}^{(\alpha,\beta)}(x)\, L_n(x) - P_n^{(\alpha,\beta)}(x)\, L_{n+1}(x) \\ = & \int_{-1}^{1} \frac{w(t)}{(t-x)} \left[P_{n+1}^{(\alpha,\beta)}(x)\, P_n^{(\alpha,\beta)}(t) - P_n^{(\alpha,\beta)}(x)\, P_{n+1}^{(\alpha,\beta)}(t) \right] dt. \end{aligned} \tag{B.46}$$

Using the following relation

$$\begin{aligned} & P_{n+1}^{(\alpha,\beta)}(x)\, L_n(x) - P_n^{(\alpha,\beta)}(x)\, L_{n+1}(x) \\ = & \int_{-1}^{1} \frac{w(t)}{(t-x)} (x-t) \frac{h_n}{A_n} \sum_{0}^{n} \frac{P_k^{(\alpha,\beta)}(x) P_k^{(\alpha,\beta)}(t)}{h_k} dt \\ = & -\frac{h_n}{A_n} \sum_{0}^{n} \frac{P_k^{(\alpha,\beta)}(x)}{h_k} \int_{-1}^{1} P_0^{(\alpha,\beta)}(t)\, P_k^{(\alpha,\beta)}(t) w(t)\, dt \end{aligned} \tag{B.47}$$

by observing that

$$\int_{-1}^{1} P_0^{(\alpha,\beta)}(t)\, P_k^{(\alpha,\beta)}(t) w(t)\, dt = \theta_0, \tag{B.48}$$

we obtain

$$P_{n+1}^{(\alpha,\beta)}(x) L_n(x) - P_n^{(\alpha,\beta)}(x) L_{n+1}(x) = -\frac{h_n}{A_n} \frac{P_0^{(\alpha,\beta)}(x)}{h_0} \theta_0, \tag{B.49}$$

or

$$P_{n+1}^{(\alpha,\beta)}(x) L_n(x) - P_n^{(\alpha,\beta)}(x) L_{n+1}(x) = -\frac{h_n}{A_n} \frac{\theta_0}{h_0}. \tag{B.50}$$

Finally the recurrence relation is

$$L_{n+1}(x) = \frac{1}{P_n^{(\alpha,\beta)}(x)} \left[P_{n+1}^{(\alpha,\beta)}(x) L_n(x) + \frac{h_n}{A_n} \frac{\theta_0}{h_0} \right], \tag{B.51}$$

where for $\alpha > 0, \beta > 0$ and $\alpha + \beta = 1$

$$\begin{aligned} L_0(r) &= \int_{-1}^{1} \frac{w(s)\,ds}{s-r} = \int_{-1}^{1} \frac{(1-s)^\alpha (1+s)^\beta}{s-r} \\ &= \frac{\pi}{\sin \pi\alpha} \begin{cases} -(-r+1)^\alpha (-r-1)^\beta - r + \alpha - \beta, & -\infty < r < -1, \\ (1-r)^\alpha (1+r)^\beta \cos \pi\alpha - r + \alpha - \beta, & -1 < r < 1, \\ (r-1)^\alpha (r+1)^\beta - r + \alpha - \beta, & 1 < r < \infty, \end{cases} \end{aligned} \tag{B.52}$$

and for $\alpha > 0, \beta < 0$ and $\alpha + \beta = 0$,

$$L_0(r) = \frac{\pi}{\sin \pi\alpha} \begin{cases} (-r+1)^\alpha (-r-1)^\beta - 1, & -\infty < r < -1, \\ (1-r)^\alpha (1+r)^\beta \cos \pi\alpha - 1, & -1 < r < 1, \\ (r-1)^\alpha (r+1)^\beta - 1, & 1 < r < \infty, \end{cases} \tag{B.53}$$

and for $\alpha < 0, \beta < 0$ and $\alpha + \beta = -1$,

$$L_0(r) = \frac{\pi}{\sin \pi\alpha} \begin{cases} -(-r+1)^\alpha (-r-1)^\beta, & -\infty < r < -1, \\ (1-r)^\alpha (1+r)^\beta \cos \pi\alpha, & -1 < r < 1, \\ (r-1)^\alpha (r+1)^\beta, & 1 < r < \infty. \end{cases} \tag{B.54}$$

Appendix C

The Contact Problem for Homogeneous Solids

C.1 Formulation of the problem

For the plane contact problem under consideration shown in Figure C.1 the Hooke's law can be written as

$$\sigma_{xx}(x,y) = \frac{\mu_0}{\kappa-1}\left[(\kappa+1)\frac{\partial u}{\partial x}+(3-\kappa)\frac{\partial v}{\partial y}\right], \tag{C.1}$$

$$\sigma_{yy}(x,y) = \frac{\mu_0}{\kappa-1}\left[(3-\kappa)\frac{\partial u}{\partial x}+(\kappa+1)\frac{\partial v}{\partial y}\right], -\infty < y < 0 \tag{C.2}$$

$$\sigma_{xy}(x,y) = \mu_0\left[\frac{\partial u}{\partial y}+\frac{\partial v}{\partial x}\right], \tag{C.3}$$

where $\kappa = 3-4\nu$ for plane strain and $\kappa = (3-\nu)/(1+\nu)$ for the generalized plane stress conditions. The governing equations are the equilibrium equations which in the absence of body forces can be written as

$$\frac{\partial \sigma_{xx}}{\partial x}+\frac{\partial \sigma_{xy}}{\partial y} = 0, \tag{C.4}$$

$$\frac{\partial \sigma_{xy}}{\partial x}+\frac{\partial \sigma_{yy}}{\partial y} = 0. \tag{C.5}$$

Substituting stresses from equations (C.1)-(C.3) into equations of equilibrium (C.4)-(C.5), we obtain the Navier's equations as follows

$$(\kappa+1)\frac{\partial^2 u}{\partial x^2}+(\kappa-1)\frac{\partial^2 u}{\partial y^2}+2\frac{\partial^2 v}{\partial x\partial y} = 0, \tag{C.6}$$

$$(\kappa+1)\frac{\partial^2 v}{\partial y^2}+(\kappa-1)\frac{\partial^2 v}{\partial x^2}+2\frac{\partial^2 u}{\partial x\partial y} = 0. \tag{C.7}$$

To solve the Navier's equations we define the Fourier transforms of the two displacement components, $u(x,y)$ and $v(x,y)$, as

$$F(\alpha,y) = \int_{-\infty}^{\infty} u(x,y)e^{-i\alpha x}dx, \tag{C.8}$$

$$G(\alpha,y) = \int_{-\infty}^{\infty} v(x,y)e^{-i\alpha x}dx. \tag{C.9}$$

The functions $u(x,y)$ and $v(x,y)$ are given by the following inverse transforms;

$$u(x,y) = \frac{1}{2\pi}\int_{-\infty}^{\infty} F(\alpha,y)e^{i\alpha x}d\alpha, \tag{C.10}$$

$$v(x,y) = \frac{1}{2\pi}\int_{-\infty}^{\infty} G(\alpha,y)e^{i\alpha x}d\alpha. \tag{C.11}$$

Substituting (C.10)-(C.11) into (C.6)-(C.7) yields the following system of differential equations with constant coefficients.

$$(\kappa-1)\frac{d^2F}{dy^2}-(\kappa+1)\alpha^2F+2i\alpha\frac{dG}{dy} = 0, \tag{C.12}$$

$$(\kappa+1)\frac{d^2G}{dy^2}-(\kappa-1)\alpha^2G+2i\alpha\frac{dF}{dy} = 0. \tag{C.13}$$

Assuming a solution of the form

$$F(\alpha,y) = A(\alpha)e^{my}, \tag{C.14}$$

$$G(\alpha,y) = B(\alpha)e^{my}, \tag{C.15}$$

we obtain the solution of (C.12) and (C.13) as

$$F(\alpha,y) = [A_1(\alpha)+A_2(\alpha)y]\,e^{|\alpha|y}+[A_3(\alpha)+A_4(\alpha)y]\,e^{-|\alpha|y}, \tag{C.16}$$

$$G(\alpha,y) = [B_1(\alpha)+B_2(\alpha)y]\,e^{|\alpha|y}+[B_3(\alpha)+B_4(\alpha)y]\,e^{-|\alpha|y}, \tag{C.17}$$

where $m_j, (j = 1, \ldots, 4)$ satisfies the following characteristic equation

$$(m^2 - \alpha^2)^2 = 0, \tag{C.18}$$

yielding

$$m_1 = m_2 = |\alpha|, \tag{C.19}$$

$$m_3 = m_4 = -|\alpha|. \tag{C.20}$$

Since the displacements have to be bounded as $y \to -\infty$, we require $A_3 = A_4 = B_3 = B_4 = 0$. Therefore equations (C.16) and (C.17) become

$$F(\alpha, y) = [A_1(\alpha) + A_2(\alpha)y]\, e^{|\alpha|y}, \tag{C.21}$$

$$G(\alpha, y) = [B_1(\alpha) + B_2(\alpha)y]\, e^{|\alpha|y}. \tag{C.22}$$

The functions $A_j(\alpha)$, $B_j(\alpha)$ $(j = 1, 2)$ are unknown functions and are not independent. The relationship between them can be found by using equation (C.12) or (C.13):

$$B_1(\alpha) = -i\frac{|\alpha|}{\alpha}A_1(\alpha) + \frac{i}{\alpha}\kappa A_2(\alpha), \tag{C.23}$$

$$B_2(\alpha) = -i\frac{|\alpha|}{\alpha}A_2(\alpha). \tag{C.24}$$

The equations (C.21) and (C.22) then become

$$F(\alpha, y) = [A_1(\alpha) + A_2(\alpha)y]\, e^{|\alpha|y}, \tag{C.25}$$

$$G(\alpha, y) = \left[-i\frac{|\alpha|}{\alpha}A_1(\alpha) + \frac{i}{\alpha}\left(-|\alpha|\, y + \kappa\right) A_2(\alpha)\right] e^{|\alpha|y}. \tag{C.26}$$

Now substituting (C.10) and (C.11) into (C.2) and (C.3) we have

$$\sigma_{yy}(x, y) = \frac{\mu_0}{\kappa - 1}\frac{1}{2\pi}\int_{-\infty}^{\infty}\left[(3 - \kappa)(i\alpha)F + (\kappa + 1)\frac{\partial G}{\partial y}\right] e^{i\alpha x} d\alpha, \tag{C.27}$$

$$\sigma_{xy}(x, y) = \mu_0\frac{1}{2\pi}\int_{-\infty}^{\infty}\left[\frac{\partial F}{\partial y} + (i\alpha)G\right] e^{i\alpha x} d\alpha. \tag{C.28}$$

Taking the inverse transform of (C.27) and (C.28) we find

$$(3-\kappa)(i\alpha)F(\alpha,y)+(\kappa+1)\frac{\partial G}{\partial y}(\alpha,y) = \frac{\kappa-1}{\mu_0}\int_{-\infty}^{\infty}\sigma_{yy}(t,y)e^{-i\alpha t}dt, \quad \text{(C.29)}$$

$$\frac{\partial F}{\partial y}(\alpha,y)+(i\alpha)G(\alpha,y) = \frac{1}{\mu_0}\int_{-\infty}^{\infty}\sigma_{xy}(t,y)e^{-i\alpha t}dt. \quad \text{(C.30)}$$

Defining the contact stresses

$$\sigma_{yy}(x,0) = \sigma(x), \quad \text{(C.31)}$$

$$\sigma_{xy}(x,0) = \tau(x), \quad \text{(C.32)}$$

the Fourier transforms of the tractions on the boundary become

$$P(\alpha)=\int_{-\infty}^{\infty}\sigma(t)e^{-i\alpha t}dt, \quad \text{(C.33)}$$

$$Q(\alpha)=\int_{-\infty}^{\infty}\tau(t)e^{-i\alpha t}dt, \quad \text{(C.34)}$$

and substituting F and G from (C.25) and (C.26) into equations (C.29) and (C.30) we have

$$\begin{bmatrix} -2i\alpha & i\frac{\alpha}{|\alpha|}(\kappa+1) \\ 2|\alpha| & -(\kappa-1) \end{bmatrix} \begin{Bmatrix} A_1(\alpha) \\ A_2(\alpha) \end{Bmatrix} = \frac{1}{\mu_0}\begin{Bmatrix} P(\alpha) \\ Q(\alpha) \end{Bmatrix}. \quad \text{(C.35)}$$

Thus, the unknowns $A_1(\alpha)$ and $A_{21}(\alpha)$ become

$$A_1(\alpha) = \frac{1}{\mu_0\Delta}\begin{vmatrix} P(\alpha) & i\frac{\alpha}{|\alpha|}(\kappa+1) \\ Q(\alpha) & -(\kappa-1) \end{vmatrix},$$

$$= \frac{\kappa-1}{4\mu_0 i\alpha}P(\alpha)+\frac{\kappa+1}{4\mu_0|\alpha|}Q(\alpha), \quad \text{(C.36)}$$

$$A_2(\alpha) = \frac{1}{\mu_0\Delta}\begin{vmatrix} -2i\alpha & P(\alpha) \\ 2|\alpha| & Q(\alpha) \end{vmatrix},$$

$$= -\frac{i|\alpha|}{2\mu_0\alpha}P(\alpha)+\frac{1}{2\mu_0}Q(\alpha), \quad \text{(C.37)}$$

where

$$\Delta = -4i\alpha. \tag{C.38}$$

C.2 The displacement gradients on the surface

Taking the x derivative of equations (C.10) and (C.11) we have

$$\begin{aligned}
\lim_{y\to 0}\frac{\partial v(x,y)}{\partial x} &= \lim_{y\to 0}\frac{1}{2\pi}\int_{-\infty}^{\infty} i\alpha G(\alpha,y)e^{i\alpha x}d\alpha, \\
&= \lim_{y\to 0}\frac{1}{2\pi}\int_{-\infty}^{\infty}\left[|\alpha|\,A_1(\alpha)-(-|\alpha|\,y+\kappa)\,A_2(\alpha)\right]e^{|\alpha|y}e^{i\alpha x}d\alpha, \qquad \text{(C.39)} \\
\lim_{y\to 0}\frac{\partial u(x,y)}{\partial x} &= \lim_{y\to 0}\frac{1}{2\pi}\int_{-\infty}^{\infty} i\alpha F(\alpha,y)e^{i\alpha x}d\alpha, \\
&= \lim_{y\to 0}\frac{1}{2\pi}\int_{-\infty}^{\infty}\left[A_1(\alpha)+A_2(\alpha)\,y\right]e^{|\alpha|y}e^{i\alpha x}d\alpha. \qquad \text{(C.40)}
\end{aligned}$$

Substituting (C.36) and (C.37) into (C.39) and (C.40) we obtain

$$\begin{aligned}
\lim_{y\to 0} 2\pi\frac{\partial}{\partial x}v(x,y) &= \int_{-\infty}^{\infty} K_{11}(x,y,t)\sigma(t)dt+\int_{-\infty}^{\infty} K_{12}(x,y,t)\tau(t)dt, \qquad \text{(C.41)} \\
\lim_{y\to 0} 2\pi\frac{\partial}{\partial x}u(x,y) &= \int_{-\infty}^{\infty} K_{21}(x,y,t)\tau(t)dt+\int_{-\infty}^{\infty} K_{22}(x,y,t)\sigma(t)dt, \qquad \text{(C.42)}
\end{aligned}$$

where

$$\begin{aligned}
K_{11}(x,y,t) &= \lim_{y\to 0}\int_{-\infty}^{\infty}\left[i\frac{\alpha}{|\alpha|}\frac{\kappa+1}{4\mu_0}-\frac{i\alpha}{2\mu_0}y\right]e^{|\alpha|y}e^{-i\alpha(t-x)}d\alpha, \qquad \text{(C.43)} \\
K_{12}(x,y,t) &= \lim_{y\to 0}\int_{-\infty}^{\infty}\left[-\frac{\kappa-1}{4\mu_0}+\frac{|\alpha|\,y}{2\mu_0}\right]e^{|\alpha|y}e^{-i\alpha(t-x)}d\alpha, \qquad \text{(C.44)} \\
K_{21}(x,y,t) &= \lim_{y\to 0}\int_{-\infty}^{\infty}\left\{i\frac{\alpha}{|\alpha|}\frac{\kappa+1}{4\mu_0}+\frac{i\alpha}{2\mu_0}y\right\}e^{|\alpha|y}e^{-i\alpha(t-x)}d\alpha, \qquad \text{(C.45)} \\
K_{22}(x,y,t) &= \lim_{y\to 0}\int_{-\infty}^{\infty}\left\{\frac{\kappa-1}{4\mu_0}+\frac{|\alpha|\,y}{2\mu_0}\right\}e^{|\alpha|y}e^{-i\alpha(t-x)}d\alpha. \qquad \text{(C.46)}
\end{aligned}$$

Using the following relations

$$\int_{-\infty}^{+\infty} i\frac{|\alpha|}{\alpha}e^{|\alpha|y}e^{-i\alpha(t-x)}d\alpha = \frac{2(t-x)}{(t-x)^2+y^2} \qquad y<0, \tag{C.47}$$

$$\int_{-\infty}^{+\infty} e^{|\alpha|y}e^{-i\alpha(t-x)}d\alpha = -\frac{2y}{(t-x)^2+y^2} \qquad y<0, \tag{C.48}$$

$$\int_{-\infty}^{+\infty} i\alpha e^{|\alpha|y}e^{-i\alpha(t-x)}d\alpha = -\frac{4(t-x)y^2}{\left[(t-x)^2+y^2\right]^2}, \qquad y<0 \tag{C.49}$$

$$\int_{-\infty}^{+\infty} |\alpha|\, y e^{|\alpha|y}e^{-i\alpha(t-x)}d\alpha = -\frac{2\left[(t-x)^2-y^2\right]y}{\left[(t-x)^2+y^2\right]^2}, \qquad y<0. \tag{C.50}$$

equations (C.41) and (C.42) become

$$\begin{aligned}\lim_{y\to 0} 2\pi\frac{\partial}{\partial x}v(x,y) &= \lim_{y\to 0}\frac{\kappa+1}{4\mu_0}\int_{-\infty}^{\infty}\frac{2(t-x)}{(t-x)^2+y^2}\sigma(t)dt \\ &\quad + \lim_{y\to 0}\frac{\kappa-1}{4\mu_0}\int_{-\infty}^{\infty}\frac{2y}{(t-x)^2+y^2}\tau(t)dt,\end{aligned} \tag{C.51}$$

$$\begin{aligned}\lim_{y\to 0} 2\pi\frac{\partial}{\partial x}u(x,y) &= \lim_{y\to 0}\frac{\kappa+1}{4\mu_0}\int_{-\infty}^{\infty}\frac{2(t-x)}{(t-x)^2+y^2}\tau(t)dt \\ &\quad - \lim_{y\to 0}\frac{\kappa-1}{4\mu_0}\int_{-\infty}^{\infty}\frac{2y}{(t-x)^2+y^2}\sigma(t)dt.\end{aligned} \tag{C.52}$$

Using

$$\lim_{y\to 0^-}\frac{t-x}{(t-x)^2+y^2} = \frac{1}{t-x}, \tag{C.53}$$

$$\lim_{y\to 0^-}\frac{y}{(t-x)^2+y^2} = -\pi\delta(t-x), \tag{C.54}$$

equations (C.51) and (C.52) become

$$2\pi\frac{\partial}{\partial x}v(x,0) = \frac{\kappa+1}{2\mu_0}\int_{-\infty}^{\infty}\frac{\sigma(t)}{t-x}dt - \frac{\kappa-1}{2\mu_0}\pi\tau(x), \tag{C.55}$$

$$2\pi\frac{\partial}{\partial x}u(x,0) = \frac{\kappa+1}{2\mu_0}\int_{-\infty}^{\infty}\frac{\tau(t)}{t-x}dt + \frac{\kappa-1}{2\mu_0}\pi\sigma(x). \tag{C.56}$$

Modifying equations (C.55) and (C.56), we find

$$-\omega\tau(x) + \frac{1}{\pi}\int_{-\infty}^{\infty}\frac{\sigma(t)}{t-x}dt = f(x) \tag{C.57}$$

$$\omega\sigma(x) + \frac{1}{\pi}\int_{-\infty}^{\infty}\frac{\tau(t)}{t-x}dt = g(x) \tag{C.58}$$

where

$$f(x) = \lambda \frac{\partial}{\partial x} v(x,0), \tag{C.59}$$

$$g(x) = \lambda \frac{\partial}{\partial x} u(x,0), \tag{C.60}$$

$$\omega = \frac{\kappa - 1}{\kappa + 1}, \tag{C.61}$$

$$\lambda = \frac{4\mu_0}{\kappa + 1}. \tag{C.62}$$

C.3 The in-plane stress σ_{xx}

Once the contact stresses $\sigma(x)$ and $\tau(x)$ are determined we can find the in-plane stress, $\sigma_{xx}(x,0)$. The strains in y and z direction can be written as

$$\epsilon_{yy} = \frac{1}{E}\left[\sigma_{yy} - \nu(\sigma_{xx} + \sigma_{zz})\right], \tag{C.63}$$

$$\epsilon_{zz} = \frac{1}{E}\left[\sigma_{zz} - \nu(\sigma_{xx} + \sigma_{yy})\right]. \tag{C.64}$$

Under plane strain conditions($\epsilon_{zz} = 0$) the stress in z direction becomes

$$\sigma_{zz} = \nu(\sigma_{xx} + \sigma_{yy}). \tag{C.65}$$

Substituting this stress back into equation (C.63) we have

$$\epsilon_{yy}(x,y) = \frac{1-\nu^2}{E}\sigma_{yy}(x,y) - \frac{\nu(1+\nu)}{E}\sigma_{xx}(x,y). \tag{C.66}$$

For Plane strain case we have

$$\nu = \frac{3-\kappa}{4},$$

$$E = 2\mu_0(1+\nu).$$

Thus, equation (C.66) becomes

$$\epsilon_{yy}(x,0) = \frac{\partial}{\partial y} v(x,0) = \frac{\kappa+1}{8\mu_0}\sigma_{yy}(x,0) - \frac{3-\kappa}{8\mu_0}\sigma_{xx}(x,0). \tag{C.67}$$

Substituting $\frac{\partial}{\partial x}u(x,0)$ and $\frac{\partial}{\partial y}v(x,0)$ from equations (C.57) and (C.58) into equation (C.1) we obtain

$$\begin{aligned}\sigma_{xx}(x,0) &= \sigma_{yy}(x,0) + \frac{2}{\pi}\int_{-\infty}^{\infty}\frac{\sigma_{xy}(t,0)}{t-x}dt, \qquad \text{(C.68)}\\ &= \sigma(x) + \frac{2}{\pi}\int_{-\infty}^{\infty}\frac{\tau(t)}{t-x}dt.\end{aligned}$$

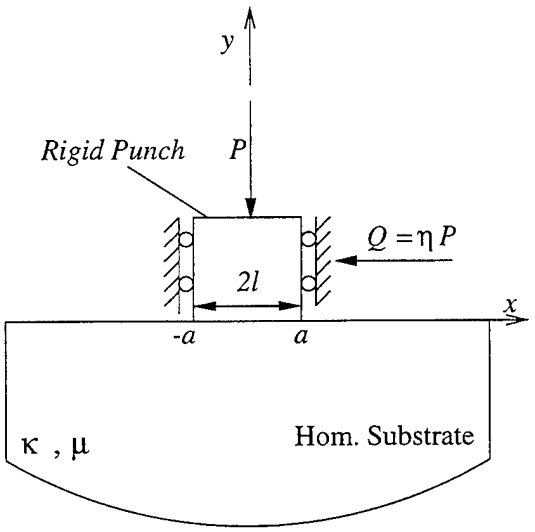

Figure C.1: Geometry of flat punch on a homogeneous medium

C.4 Flat Stamp

The problem geometry can be seen in Figure C.1. Using the following tractions on the boundary

$$\sigma_{yy}(x,0) = -p(x), \qquad \sigma_{xy}(x,0) = -\eta p(x), \qquad -a < x < a, \tag{C.69}$$

$$\sigma_{yy}(x,0) = \sigma_{xy}(x,0) = 0, \qquad |x| > a, \tag{C.70}$$

equation (C.57) becomes

$$Ap(x) + \frac{B}{\pi}\int_{-a}^{a}\frac{p(t)}{t-x}dt = \lambda\frac{\partial}{\partial x}v(x,0), \tag{C.71}$$

where

$$A = \frac{\kappa-1}{\kappa+1}\eta, \tag{C.72}$$

$$B = -1, \tag{C.73}$$

$$\lambda = \frac{4\mu_0}{\kappa+1}, \tag{C.74}$$

$$\frac{\partial}{\partial x}v(x,0) = 0. \tag{C.75}$$

The equilibrium equation for this profile can be written as

$$\int_{-a}^{a} p(t)dt = P. \tag{C.76}$$

In order to solve the integral equation the limits of integration have to be normalized. Now setting

$$t = as, \qquad -1 < s < 1, \tag{C.77}$$

$$x = ar, \qquad -1 < r < 1, \tag{C.78}$$

$$p(t) = p^*(s). \tag{C.79}$$

and substituting (C.77)-(C.79) into (C.71) the integral equation of the problem becomes

$$Ap^*(r) + \frac{B}{\pi}\int_{-1}^{1} \frac{p^*(s)\,ds}{s-r} = 0, \qquad -1 < r < 1. \tag{C.80}$$

Defining

$$p^*(s) = 2\sigma_0\phi(s), \tag{C.81}$$

where

$$\sigma_0 = \frac{P}{2a}, \tag{C.82}$$

the integral equation (C.80) and the equilibrium equation (C.76) become

$$A\phi(r) + \frac{B}{\pi}\int_{-1}^{1} \frac{\phi(s)ds}{s-r} = 0, \qquad -1 < r < 1, \tag{C.83}$$

$$\int_{-1}^{1} \phi(s)ds = 1. \tag{C.84}$$

The index of the integral equation is defined by

$$\kappa_0 = -(\alpha+\beta) = -(N+M) = 1, \tag{C.85}$$

where α and β are found to be

$$\begin{aligned} \eta > 0: &\quad \alpha = -1 + \theta/\pi, \quad \beta = -\theta/\pi, \\ \eta = 0: &\quad \alpha = -0.5, \qquad \beta = -0.5, \\ \eta < 0: &\quad \alpha = -\theta/\pi, \qquad \beta = -1 + \theta/\pi, \end{aligned} \tag{C.86}$$

$$\theta = \arctan \left| \frac{\kappa + 1}{\eta (\kappa - 1)} \right|. \tag{C.87}$$

Now assuming a solution of the form

$$\phi(s) = \sum_0^\infty c_n w(s) P_n^{(\alpha,\beta)}(s), \qquad w(s) = (1-s)^\alpha (1+s)^\beta, \tag{C.88}$$

equation (C.83) may be expressed as

$$\sum_0^\infty c_n \left[A w(r) P_n^{(\alpha,\beta)}(r) + \frac{B}{\pi} \int_{-1}^{1} \frac{w(s) P_n^{(\alpha,\beta)}(s) \phi(s) ds}{s - r} \right] = 0, \qquad -1 < r < 1. \tag{C.89}$$

Using the property of Jacobi Polynomials in Appendix (A) equation (A.6), (C.89) becomes

$$\sum_0^N c_n \left[\frac{1}{\sin \pi\alpha} P_{n-1}^{(-\alpha,-\beta)}(r) \right] = 0, \tag{C.90}$$

From the orthogonality of the Jacobi polynomials we can see that equation (C.88) has only one unknown coefficient c_0. Therefore from equation (C.88)

$$\phi(s) = c_0 (1-s)^\alpha (1+s)^\beta. \tag{C.91}$$

c_0 has to be determined from the equilibrium equation (C.84). Using the orthogonality of Jacobi Polynomials given in equation (A.7), (C.84) becomes

$$c_0 \theta_0 = 1, \tag{C.92}$$

where (for $\alpha + \beta = -1$) θ_0 is given by equation (A.8)

$$\begin{aligned} \theta_0 &= \int_{-1}^{1} w(t)\, dt = \frac{2^{\alpha+\beta+1} \Gamma(\alpha+1) \Gamma(\beta+1)}{\Gamma(\alpha+\beta+2)}, \\ &= -\frac{\pi}{\sin \pi\alpha}. \end{aligned} \tag{C.93}$$

Therefore from (C.92) and (C.93) the only nonzero coefficient may be obtained as

$$c_0 = -\frac{\sin \pi\alpha}{\pi}. \tag{C.94}$$

Thus from (C.91) $\phi(s)$ becomes

$$\phi(s) = -\frac{\sin \pi\alpha}{\pi}(1-s)^{\alpha}(1+s)^{\beta}. \tag{C.95}$$

Substituting $\phi(s)$ from (C.95) into (C.81) we can find the pressure distribution in normalized coordinates as

$$\begin{aligned} p^*(s) &= 2\sigma_0\phi(s), \\ &= -\frac{2\sigma_0 \sin \pi\alpha}{\pi}(1-s)^{\alpha}(1+s)^{\beta}. \end{aligned} \tag{C.96}$$

Or in physical coordinates from (C.69), $p(x)$ becomes

$$p(x) = -\frac{2\sigma_0 \sin \pi\alpha}{\pi}\left(1-\frac{x}{a}\right)^{\alpha}\left(1+\frac{x}{a}\right)^{\beta}. \tag{C.97}$$

The pressure distribution can be obtained in dimensionless form by using (C.97) and (C.69)

$$\frac{\sigma_{yy}(x,0)}{\sigma_0} = \frac{2\sin \pi\alpha}{\pi}\left(1-\frac{x}{a}\right)^{\alpha}\left(1+\frac{x}{a}\right)^{\beta}. \tag{C.98}$$

The stress component $\sigma_{xx}(x,0)$ stresses can be found by using equation (C.68). Since $\sigma_{yy}(x,0)$ is zero outside the contact region (i.e, $-a < x < a$) (C.68) can be written as

$$\sigma_{xx}(x,0) = \begin{cases} \sigma_{yy}(x,0) + \dfrac{2}{\pi}\displaystyle\int_{-a}^{a}\frac{\sigma_{xy}(t,0)}{t-x}dt & -a < x < a, \\ \dfrac{2}{\pi}\displaystyle\int_{-a}^{a}\frac{\sigma_{xy}(t,0)}{t-x}dt & |x| > a. \end{cases} \tag{C.99}$$

Defining

$$\sigma_{xx}(x,0) = -2\sigma_0 q(r), \tag{C.100}$$

and substituting $\sigma_{xy}(t,0)$ from (C.69) and using (C.79), (C.84)and (C.95), equation (C.99) may be expressed as

$$q(r) = \begin{cases} \phi(r) + \dfrac{2\eta}{\pi}\displaystyle\int_{-1}^{1} \frac{\phi(s)}{s-r} ds, & -1 < r < 1, \\ \dfrac{2\eta}{\pi}\displaystyle\int_{-1}^{1} \frac{\phi(s)}{s-r} ds, & |r| > 1, \end{cases} \tag{C.101}$$

Substituting $\phi(r)$ into (C.101)

$$q(r) = \begin{cases} c_0 w(r) + \dfrac{2\eta}{\pi} c_0 L_0(r), & -1 < r < 1, \\ \dfrac{2\eta}{\pi} c_0 L_0(r), & |r| > 1, \end{cases} \tag{C.102}$$

where $L_0(r)$ is given in Appendix (B) equation (B.54)

$$L_0(r) = \frac{\pi}{\sin \pi\alpha} \begin{cases} -(-r+1)^{\alpha}(-r-1)^{\beta}, & -\infty < r < -1, \\ (1-r)^{\alpha}(1+r)^{\beta} \cos \pi\alpha, & -1 < r < 1, \\ (r-1)^{\alpha}(r+1)^{\beta}, & 1 < r < \infty. \end{cases}$$

C.4.1 Stress intensity factors

Mode I stress intensity factors at the ends of the stamp for a homogeneous medium can be defined as

$$k_1(a) = \lim_{x \to a} \frac{p(x)}{2^{\beta}(a-x)^{\alpha}} = \frac{2\sigma_0}{a^{\alpha}} c_0, \tag{C.103}$$

$$k_1(-a) = \lim_{x \to -a} \frac{p(x)}{2^{\alpha}(x+a)^{\beta}} = \frac{2\sigma_0}{a^{\beta}} c_0. \tag{C.104}$$

Defining the nondimensional stress intensity factors as

$$k_1^*(a) = \frac{a^{\alpha}}{2\sigma_0} k_1(a) = c_0,$$

$$k_1^*(-a) = \frac{a^{\beta}}{2\sigma_0} k_1(-a) = c_0,$$

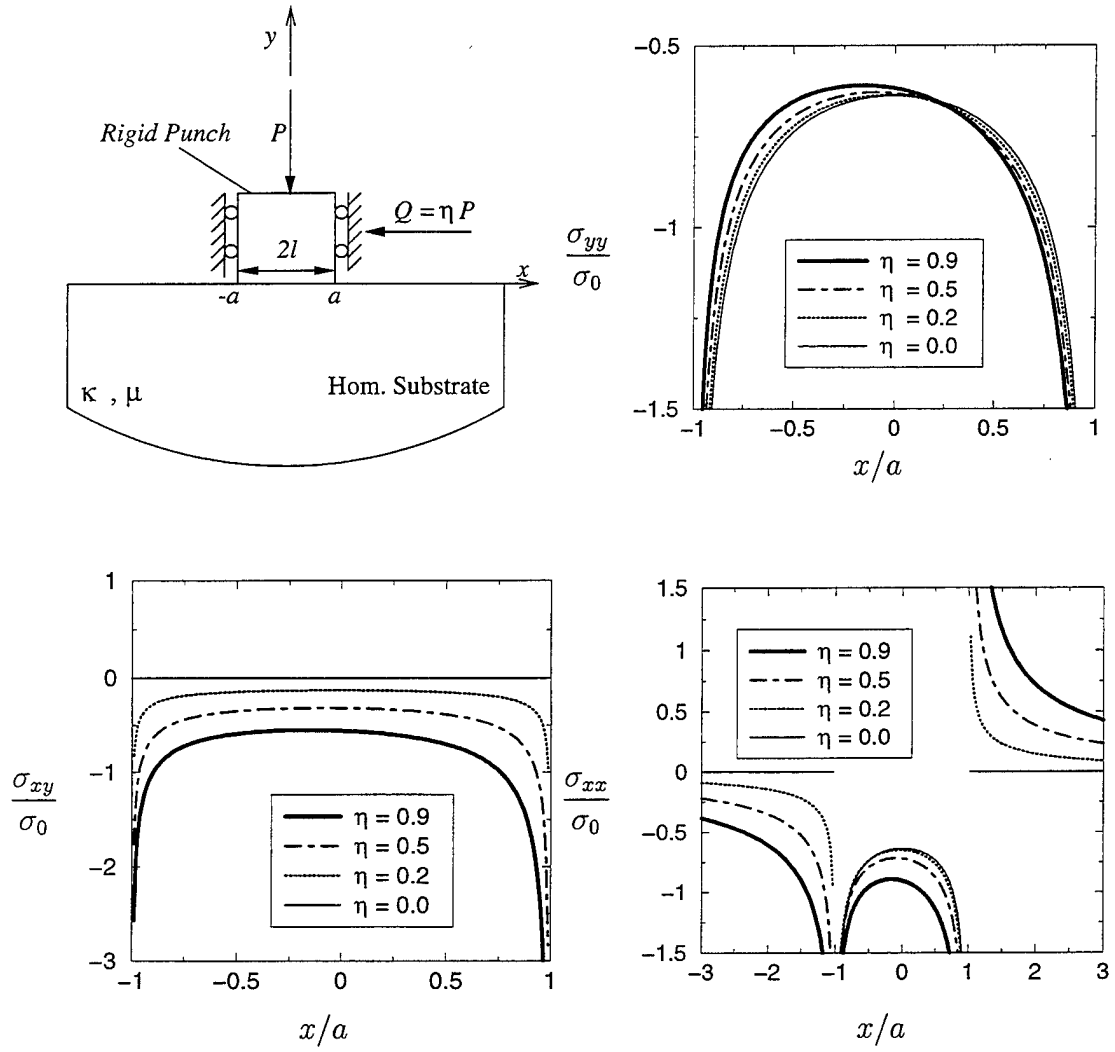

Figure C.2: Stress distribution under frictional contact, $\sigma_0 = \dfrac{P}{2a}$ for the homogeneous flat punchproblem

for the frictionless case α and β become $-1/2$ and c_0 becomes $1/\pi$, therefore equations (C.103) and (C.104) become

$$k_1(a) = k_1(-a) = \frac{2}{\pi}\sigma_0\sqrt{a} = \frac{P}{\pi\sqrt{a}}. \tag{C.105}$$

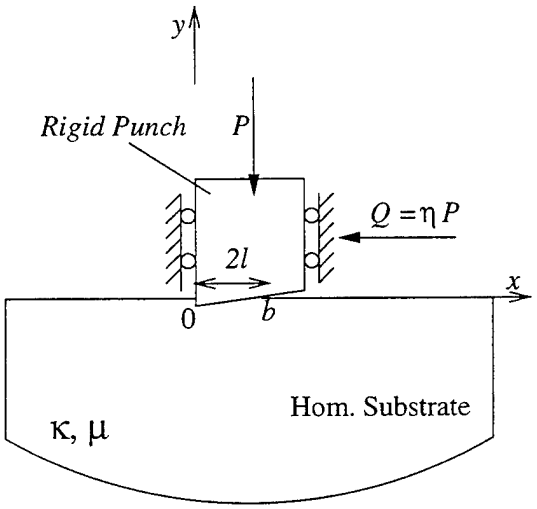

Figure C.3: The Geometry of the triangular punch

C.5 Triangular Stamp

The problem geometry can be seen in Figure C.3. Using the following tractions on the boundary

$$\sigma_{yy}(x,0) = -p(x), \qquad \sigma_{xy}(x,0) = -\eta p(x), \qquad 0 < x < b, \tag{C.106}$$

$$\sigma_{yy}(x,0) = \sigma_{xy}(x,0) = 0, \qquad x < 0, \quad x > b, \tag{C.107}$$

equation (C.57) becomes

$$Ap(x) + \frac{B}{\pi}\int_0^b \frac{p(t)}{t-x}dt = \lambda\frac{\partial}{\partial x}v(x,0), \tag{C.108}$$

where

$$A = \frac{\kappa-1}{\kappa+1}\eta, \tag{C.109}$$

$$B = -1, \tag{C.110}$$

$$\lambda = \frac{4\mu_0}{\kappa+1}, \tag{C.111}$$

$$\frac{\partial}{\partial x}v(x,0) = m. \tag{C.112}$$

The equilibrium equation for this profile can be written as

$$\int_0^b p(t)dt = P. \tag{C.113}$$

In order to solve the integral equation the limits of integration have to be normalized. Now setting

$$t = \frac{b}{2}(s+1), \qquad -1 < s < 1, \tag{C.114}$$

$$x = \frac{b}{2}(r+1), \qquad -1 < r < 1, \tag{C.115}$$

$$p(t) = \lambda m \phi(s). \tag{C.116}$$

and substituting (C.114)-(C.116) into (C.108) the integral equation of the problem becomes

$$A\phi(r) + \frac{B}{\pi}\int_{-1}^{1} \frac{\phi(s)}{s-r} ds = 1. \tag{C.117}$$

The index of the integral equation is defined by

$$\kappa_0 = -(\alpha+\beta) = -(N+M) = 0, \tag{C.118}$$

where α and β is found to be

$$\begin{aligned} \eta > 0: &\quad \alpha = \theta/\pi, &\quad \beta = -\theta/\pi, \\ \eta = 0: &\quad \alpha = 0.5, &\quad \beta = -0.5, \\ \eta < 0: &\quad \alpha = 1-\theta/\pi, &\quad \beta = -1+\theta/\pi, \end{aligned} \tag{C.119}$$

$$\theta = \arctan\left|\frac{\kappa+1}{\eta(\kappa-1)}\right|. \tag{C.120}$$

Now assuming a solution of the form

$$\phi(s) = \sum_0^\infty c_n w(s) P_n^{(\alpha,\beta)}(s), \qquad w(s) = (1-s)^\alpha (1+s)^\beta, \tag{C.121}$$

equation (C.117) may be expressed as

$$\sum_{0}^{\infty} c_n \left[Aw(r) P_n^{(\alpha,\beta)}(r) + \frac{B}{\pi} \int_{-1}^{1} \frac{w(s) P_n^{(\alpha,\beta)}(s) \phi(s) ds}{s-r} \right] = 1, \qquad -1 < r < 1. \tag{C.122}$$

Using the property of Jacobi Polynomials (A.6), (C.122) becomes

$$\sum_{0}^{N} c_n \left[\frac{1}{\sin \pi\alpha} P_n^{(-\alpha,-\beta)}(r) \right] = 1, \tag{C.123}$$

In this problem, after the application of a given load, one end of the contact region(i.e. b) is unknown. However for a given value of the contact length (i.e., b), equation (C.123) gives $N+1$ equations for $N+1$ unknowns ($c_0, c_1, ..., c_N$).

Expanding right hand side of equation (C.123) into a series of Jacobi polynomials $P_n^{(-\alpha,-\beta)}$, we can write the following equation

$$\frac{1}{\sin \pi\alpha} \sum_{0}^{N} c_n P_n^{(-\alpha,-\beta)}(r) = P_0^{(-\alpha,-\beta)}(r). \tag{C.124}$$

Comparing right hand side and left hand side of equation (C.124), we can see that we just have one nonzero coefficient

$$c_0 = \sin \pi\alpha. \tag{C.125}$$

Thus $\phi(s)$ becomes

$$\phi(s) = c_0 w(s) = \sin \pi\alpha \, (1-s)^{\alpha} (1+s)^{\beta}. \tag{C.126}$$

By using (C.114)-(C.116) the equilibrium equation (C.113) may be expressed as

$$\int_{-1}^{1} \phi(s) \, ds = \frac{2P}{\lambda m b}. \tag{C.127}$$

Inserting $\phi(s)$ from equation (C.126) into (C.127) and using the orthogonality of Jacobi Polynomials in Appendix (A.7), we have

$$c_0 \theta_0 = \frac{2P}{\lambda m b} \tag{C.128}$$

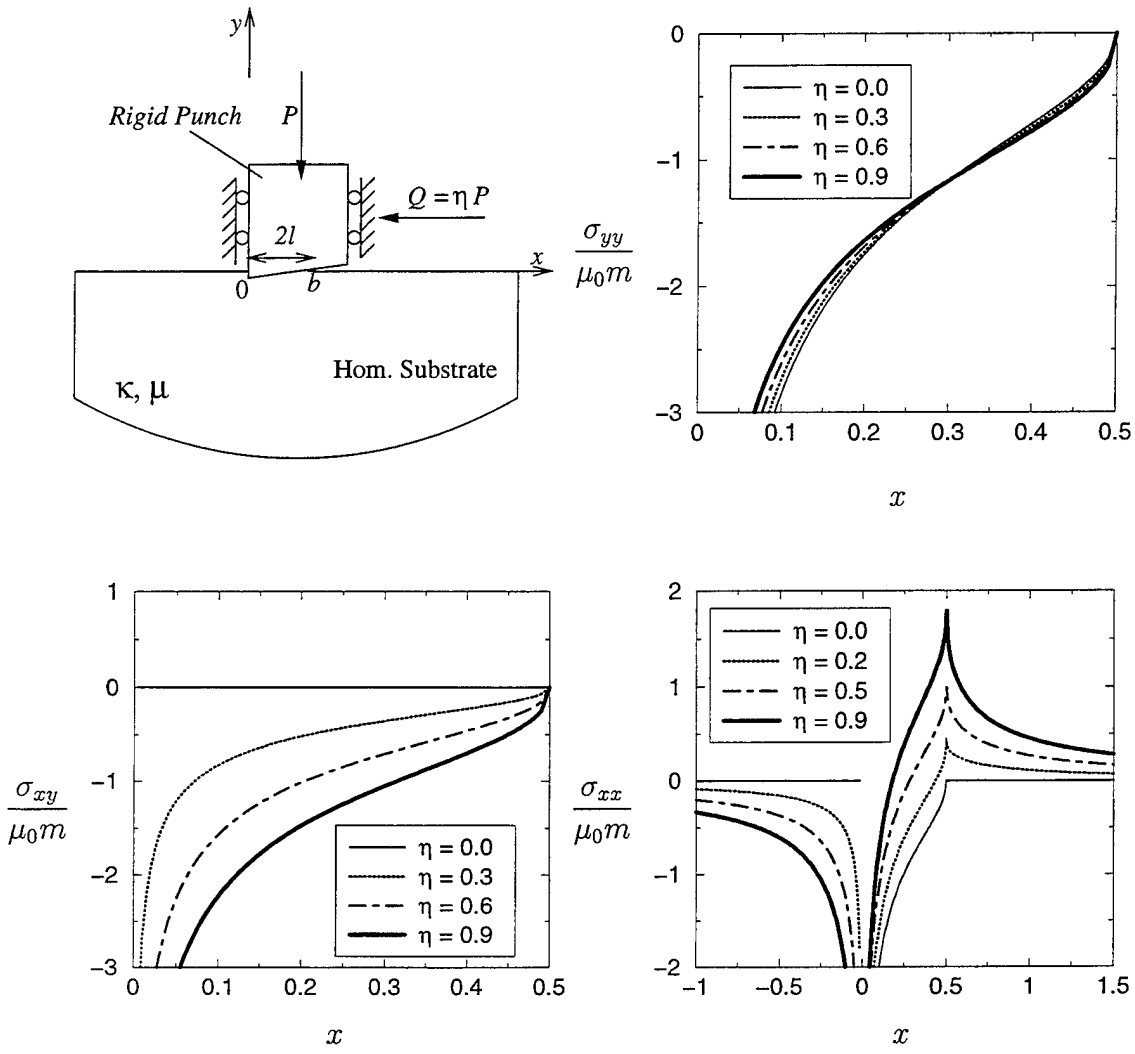

Figure C.4: Stress distribution on the surface of a homogeneous medium under a triangular punch for various values of the friction coefficient, η

For the frictionless case $\alpha = 1/2$ and $\beta = -1/2$ and c_0 becomes 1, therefore equations (C.103) and (C.104) become

$$k_1^*(0) = \frac{k_1(0)}{\mu_0 m\sqrt{b}} = \frac{4}{\kappa + 1}. \tag{C.142}$$

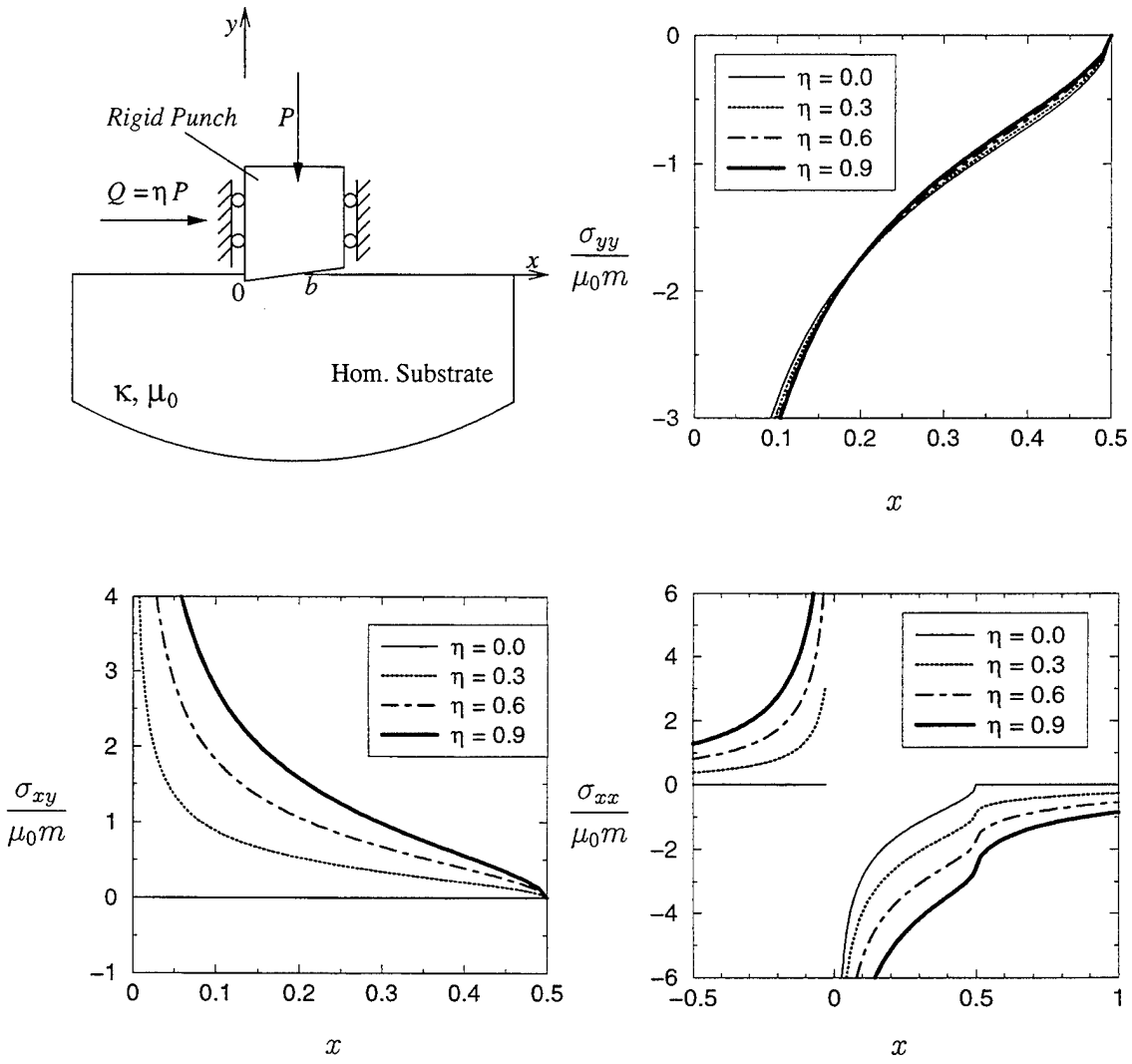

Figure C.5: Stress distribution on the surface of a homogeneous medium under a triangular punch for various values of the friction coefficient, η

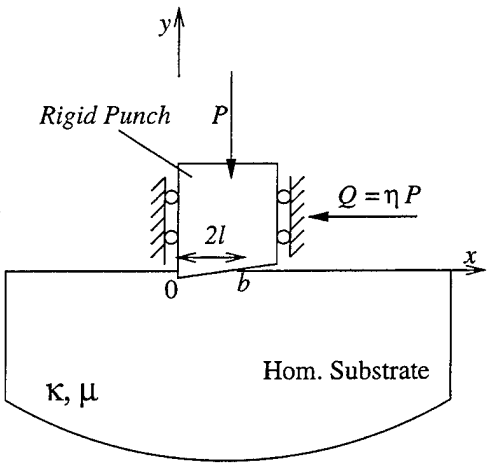

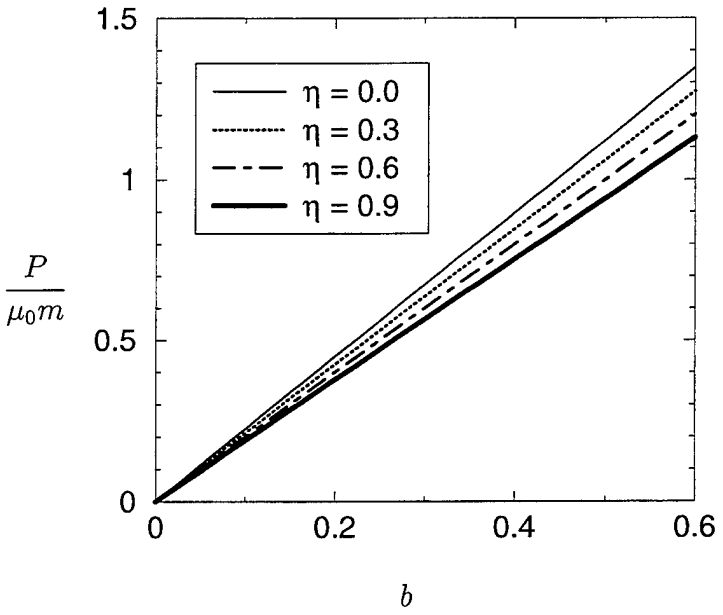

Figure C.6: The load versus the contact length for a homogeneous medium under a triangular punch for various values of the friction coefficient, η

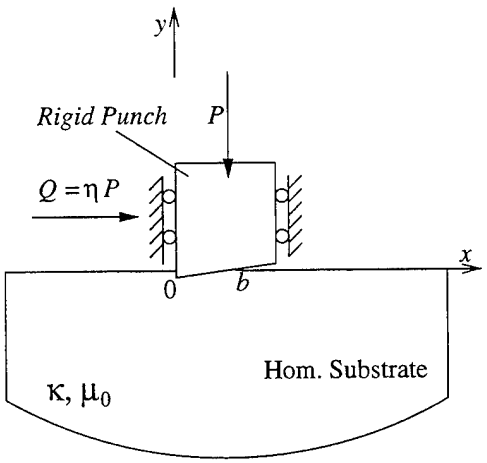

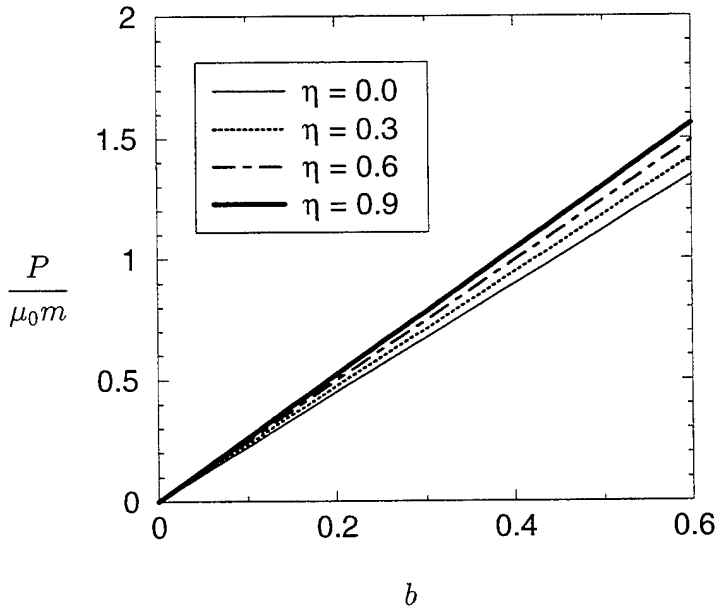

Figure C.7: The load versus the contact length for a homogeneous medium under a triangular punch for various values of the friction coefficient, η

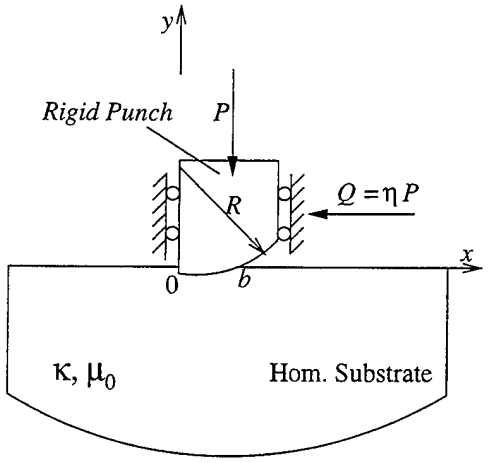

Figure C.8: Geomety of the semi-cirular punch problem for the homogeneous medium

C.6 The Semi-circular punch

The problem geometry can be seen in Figure C.8. Using the following tractions on the boundary

$$\sigma_{yy}(x,0) = -p(x), \qquad \sigma_{xy}(x,0) = -\eta p(x), \qquad 0 < x < b, \tag{C.143}$$

$$\sigma_{yy}(x,0) = \sigma_{xy}(x,0) = 0, \qquad x < 0, \quad x > b. \tag{C.144}$$

equation (C.57) becomes

$$Ap(x) + \frac{B}{\pi}\int_0^b \frac{p(t)}{t-x}dt = \lambda\frac{\partial}{\partial x}v(x,0), \qquad 0 < x < b, \tag{C.145}$$

where

$$A = \frac{\kappa-1}{\kappa+1}\eta, \tag{C.146}$$

$$B = -1, \tag{C.147}$$

$$\lambda = \frac{4\mu_0}{\kappa+1}, \tag{C.148}$$

$$\frac{\partial}{\partial x}v(x,0) = \frac{x}{R}, \tag{C.149}$$

and the equilibrium equation becomes

$$\int_0^b p(t)dt = P. \tag{C.150}$$

In order to solve the integral equation the limits of integration have to be normalized. Now setting

$$t = t^* R, \tag{C.151}$$

$$x = x^* R, \tag{C.152}$$

$$b = b^* R, \tag{C.153}$$

$$p(t) = p^*(t^*), \tag{C.154}$$

(C.145) can be written as

$$Ap^*(x^*) + \frac{B}{\pi}\int_0^{b^*} \frac{p^*(t^*)}{t^* - x^*}dt^* = \lambda x^*, \tag{C.155}$$

Further normalizing the integration limit from $(0, b^*)$ to $(-1, 1)$ by the following change of variables

$$t^* = \frac{b^*}{2}(s+1), \qquad -1 < s < 1 \tag{C.156}$$

$$x^* = \frac{b^*}{2}(r+1), \qquad -1 < r < 1 \tag{C.157}$$

$$p^*(t^*) = \lambda\frac{b^*}{2}\phi(s), \tag{C.158}$$

one obtains

$$A\phi(r) + \frac{B}{\pi}\int_{-1}^{1} \frac{\phi(s)ds}{s-r} = f(r), \qquad -1 < r < 1. \tag{C.159}$$

where

$$f(r) = r + 1.$$

Now assuming a solution of the form

$$\phi(s) = \sum_0^\infty c_n w(s) P_n^{(\alpha,\beta)}(s). \tag{C.160}$$

where

$$w(s) = (1-s)^{\alpha}(1+s)^{\beta},$$

equation (C.159) may be expressed as

$$\sum_{0}^{\infty} c_n \left[Aw(r)P_n^{(\alpha,\beta)}(r) + \frac{B}{\pi}\int_{-1}^{1} \frac{w(s)P_n^{(\alpha,\beta)}(s)\phi(s)ds}{s-r} \right] = f(r), \qquad -1 < r < 1. \tag{C.161}$$

Using the property of Jacobi Polynomials in Appendix (A) equation (A.6), (C.161) becomes

$$\sum_{0}^{N} c_n \left[\frac{1}{\sin \pi\alpha} P_n^{(-\alpha,-\beta)}(r) \right] = f(r), \tag{C.162}$$

where κ_0 is the index of the problem which is

$$\kappa_0 = -(\alpha+\beta) = 0.$$

In this problem, after the application of a given load, one end of the contact length(i.e. b^*) is unknown. However for a given value of the contact zone (i.e., b^*), equation (C.162) gives $N+1$ equations for $N+1$ unknowns. Expanding right hand side of equation (C.162) into a series of Jacobi polynomials $P_n^{(-\alpha,-\beta)}$ and observing that $\beta = -\alpha$, we find

$$r+1 = P_1^{(-\alpha,-\beta)}(r) + (1+\alpha)\,P_0^{(-\alpha,-\beta)}(r). \tag{C.163}$$

Therefore

$$\frac{1}{\sin \pi\alpha} \sum_{0}^{N} c_n P_n^{(-\alpha,-\beta)}(r) = P_1^{(-\alpha,-\beta)}(r) + (1+\alpha)\,P_0^{(-\alpha,-\beta)}(r). \tag{C.164}$$

Comparing right hand side and left hand side of equation (C.164), we have only two nonzero coefficients

$$c_0 = (1+\alpha)\sin \pi\alpha, \tag{C.165}$$

$$c_1 = \sin \pi\alpha. \tag{C.166}$$

Therefore, $\phi(s)$ becomes

$$\begin{aligned}\phi(s) &= w(s)\sum_{n=0}^{1} c_n P_n^{(\alpha,\beta)}(s), \\ &= w(s)\sin\pi\alpha\left[1+2\alpha+s\right]. \end{aligned} \tag{C.167}$$

Using (C.158) the equilibrium equation (C.150) may be expressed as

$$\int_{-1}^{1}\phi(s)\,ds = \frac{4}{b^{*2}}\frac{P}{\lambda R}. \tag{C.168}$$

Using the orthogonality of the Jacobi Polynomials (C.168) becomes

$$c_0\theta_0 = \frac{4}{b^{*2}}\frac{P}{\lambda R}. \tag{C.169}$$

In this case $\alpha+\beta=0$, and θ_0 becomes

$$\begin{aligned}\theta_0 &= \int_{-1}^{1} w(t)\,dt = \frac{2^{\alpha+\beta+1}\Gamma(\alpha+1)\Gamma(\beta+1)}{\Gamma(\alpha+\beta+2)}, \\ &= \frac{2\pi\alpha}{\sin\pi\alpha}. \end{aligned} \tag{C.170}$$

The load versus the contact length relation may be obtained by substituting c_0 and θ_0 into equation (C.169)

$$P^* = \frac{P}{\mu_0 R} = \frac{2\pi\alpha(1+\alpha)}{\kappa+1}b^{*2}. \tag{C.171}$$

Then the pressure distribution, $p^*(t^*)$ becomes

$$\begin{aligned}p^*(t^*) &= \frac{\lambda}{2}b^*\phi(s), \\ &= \frac{2\mu_0}{\kappa+1}b^*\left(\frac{b^*-t^*}{t^*}\right)^{\alpha}\sum_{n=0}^{1} c_n P_n^{(\alpha,\beta)}\left(\frac{2t^*}{b^*}-1\right), \\ &= \frac{4\mu_0}{\kappa+1}b^*\left(\frac{b^*-t^*}{t^*}\right)^{\alpha}\sin\pi\alpha\left[\alpha+\frac{t^*}{b^*}\right]. \end{aligned} \tag{C.172}$$

Using equation (C.143) and (C.154) the nondimensional pressure distribution becomes

$$\frac{\sigma_{yy}(x^*,0)}{\mu_0} = -\frac{4}{\kappa+1}b^*\left(\frac{b^*-x^*}{x^*}\right)^{\alpha}\sin\pi\alpha\left[\alpha+\frac{x^*}{b^*}\right] \tag{C.173}$$

The stress $\sigma_{xx}(x,0)$ can be found by using equation (C.68). Since $\sigma_{yy}(x,0)$ is zero outside the contact region (i.e $0<x<b$) (C.68) can be written as

$$\sigma_{xx}(x,0)=\begin{cases}\sigma_{yy}(x,0)+\dfrac{2}{\pi}\displaystyle\int_0^b\frac{\sigma_{xy}(t,0)}{t-x}dt & 0<x<b,\\ \dfrac{2}{\pi}\displaystyle\int_0^b\frac{\sigma_{xy}(t,0)}{t-x}dt & x\notin[0,b],\end{cases} \tag{C.174}$$

Defining

$$\sigma_{xx}(x,0)=-\lambda\frac{b^*}{2}q\left(r\right), \tag{C.175}$$

and substituting $\sigma_{xy}(t,0)$ from (C.143) and using (C.154), (C.158)and (C.167), equation (C.174) for the region $0<x<b$ may be expressed as

$$q\left(r\right)=\begin{cases}\phi(r)+\dfrac{2\eta}{\pi}\displaystyle\int_{-1}^1\frac{\phi(s)ds}{s-r}ds, & -1<r<1,\\ \dfrac{2\eta}{\pi}\displaystyle\int_{-1}^1\frac{\phi(s)ds}{s-r}ds, & |r|>1.\end{cases} \tag{C.176}$$

Substituting $\phi(r)$ into (C.176) we find

$$\frac{\sigma_{xx}(x,0)}{\mu_0}=\frac{4}{\kappa+1}\begin{cases}-\dfrac{b^*}{2}w(r)\displaystyle\sum_{n=0}^1c_nP_n^{(\alpha,\beta)}(r)-\frac{b^*\eta}{\pi}\sum_{n=0}^1c_nL_n\left(r\right), & -1<r<1,\\ -\dfrac{b^*\eta}{\pi}\displaystyle\sum_{n=0}^1c_nL_n\left(r\right), & |r|>1,\end{cases} \tag{C.177}$$

where $L_0\left(r\right)$ and $L_1\left(r\right)$ are obtained from appendix B equation (B.51) and (B.53)

$$L_0\left(r\right)=\frac{\pi}{\sin\pi\alpha}\begin{cases}-\left(-r+1\right)^\alpha\left(-r-1\right)^\beta-1, & -\infty<r<-1,\\ \left(1-r\right)^\alpha\left(1+r\right)^\beta\cos\pi\alpha-1, & -1<r<1,\\ \left(r-1\right)^\alpha\left(r+1\right)^\beta-1, & 1<r<\infty,\end{cases} \tag{C.178}$$

$$L_1\left(r\right)=P_1^{(\alpha,\beta)}\left(r\right)L_0\left(r\right)+\frac{2\pi\alpha}{\sin\pi\alpha}. \tag{C.179}$$

C.6.1 The Stress intensity factor

Expressing the pressure distribution in physical coordinates

$$\begin{aligned} p(x) &= \frac{\lambda}{2} b^* \phi(r), \\ &= \frac{2\mu_0}{\kappa+1} b^* \left(\frac{b-x}{x}\right)^{\alpha} \sum_{n=0}^{1} c_n P_n^{(\alpha,\beta)} \left(\frac{2x}{b} - 1\right), \end{aligned} \tag{C.180}$$

the mode I stress intensity factors at the end ($x = 0$) of the punch for a homogeneous medium can be defined as

$$\begin{aligned} k_1(0) &= \lim_{x\to 0} x^{\alpha} p(x), \\ &= \frac{2\mu_0 b^*}{\kappa+1} b^{\alpha} \sum_{n=0}^{1} c_n P_n^{(\alpha,\beta)} (-1), \\ &= \frac{4\mu_0 b^*}{\kappa+1} b^{\alpha} \alpha \sin \pi\alpha. \end{aligned} \tag{C.181}$$

Or in nondimensional form

$$\begin{aligned} k_1^*(0) &= \frac{k_1(0)}{\mu_0 b^{\alpha}}, \\ &= \frac{2b^*}{\kappa+1} \sum_{n=0}^{1} c_n P_n^{(\alpha,\beta)} (-1), \\ &= \frac{4\alpha \sin \pi\alpha}{\kappa+1} b^*. \end{aligned} \tag{C.182}$$

For the frictionless case $\alpha = 1/2$ and $\beta = -1/2$ and , the stress intensity factor becomes

$$k_1(0) = \frac{2b^*}{\kappa+1} \mu_0 \sqrt{b}, \tag{C.183}$$

where, from (C.171)

$$\begin{aligned} b^* &= \sqrt{P^* \frac{\kappa+1}{2\pi\alpha(1+\alpha)}}, \\ P^* &= \frac{P}{\mu_0 R}. \end{aligned} \tag{C.184}$$

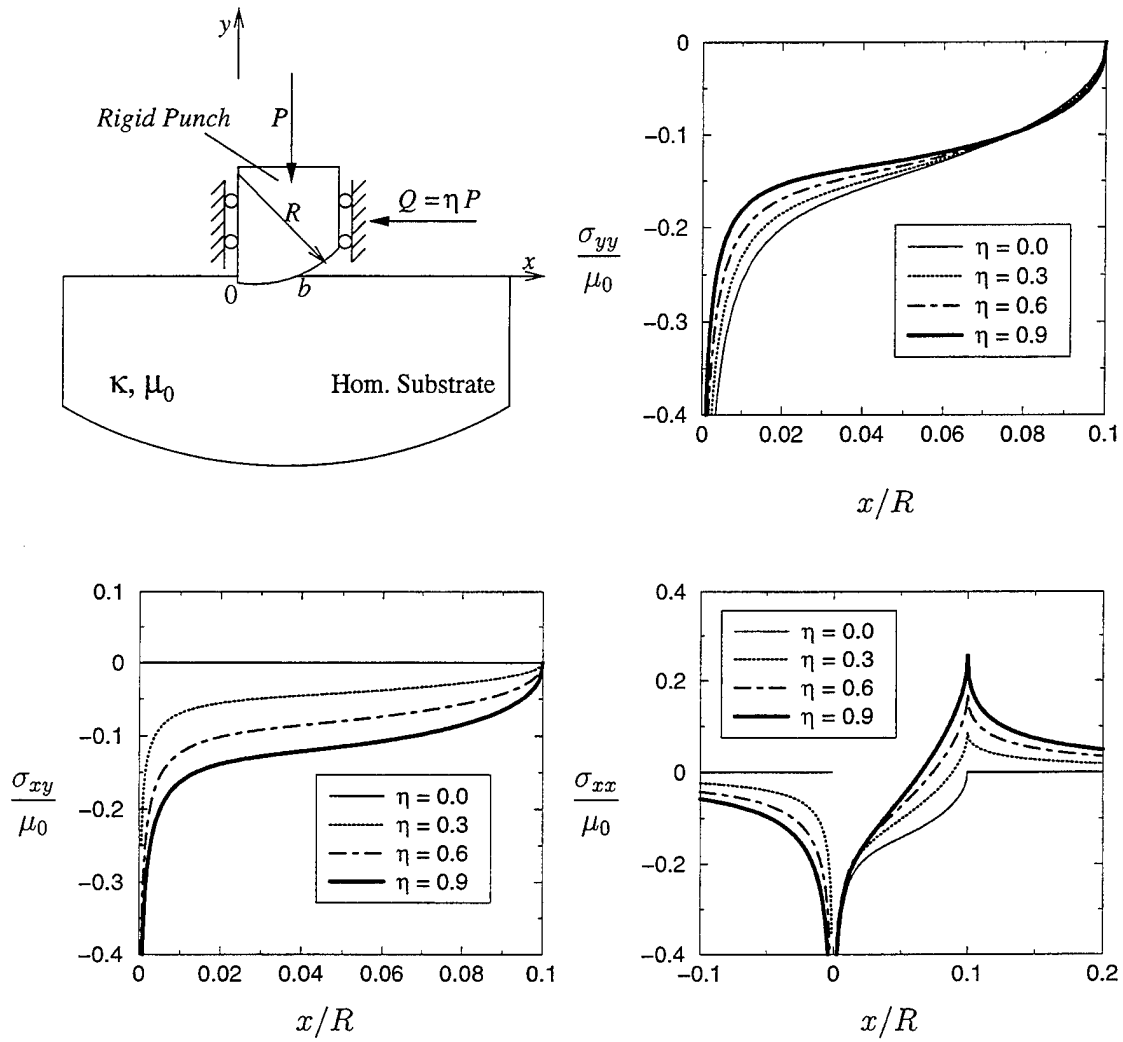

Figure C.9: Stress distribution on the surface of a homogeneous medium under a semi-circular punch for various values of the friction coefficient, η

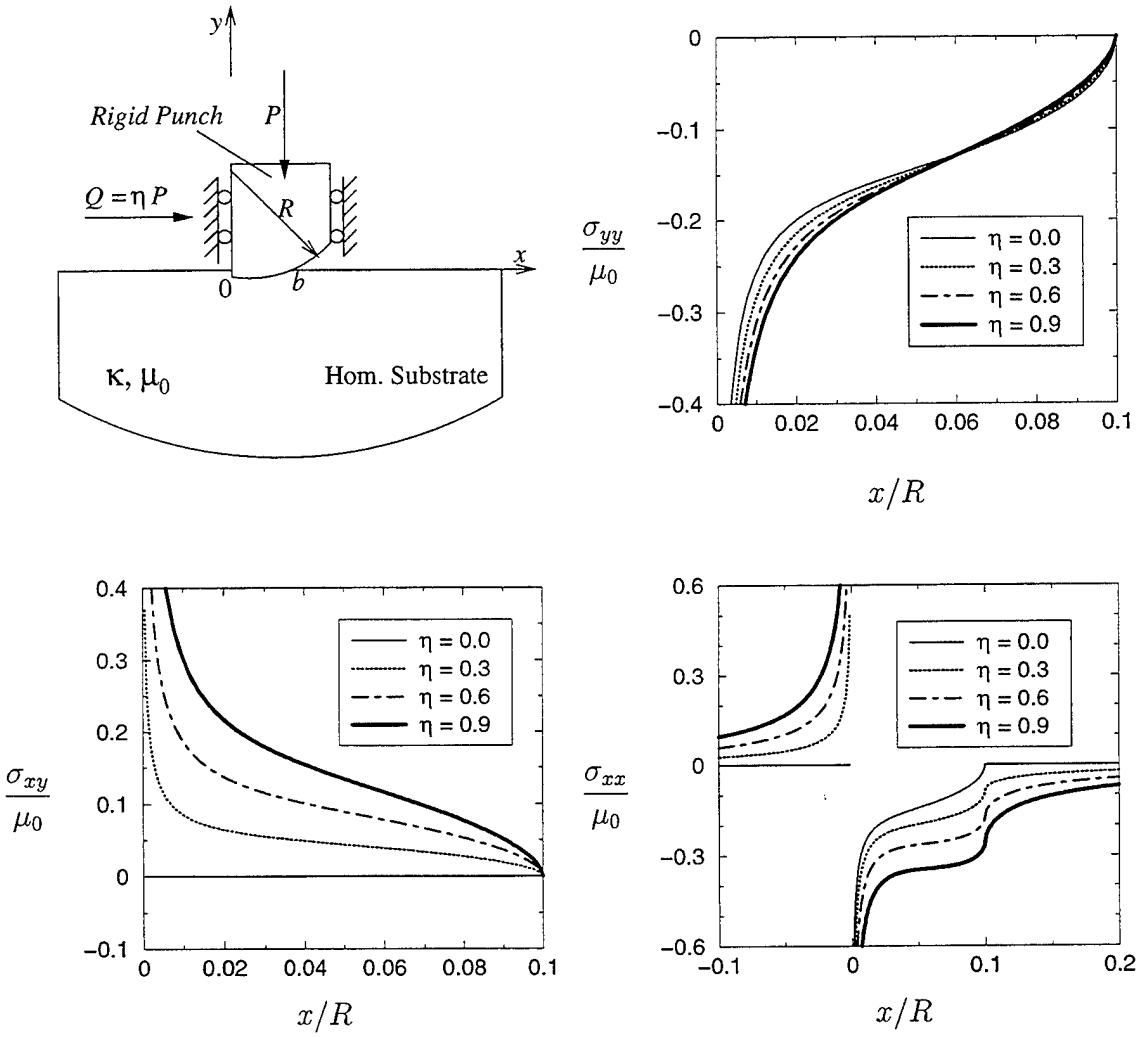

Figure C.10: Stress distribution on the surface of a homogeneous medium under a semi-circular punch for various values of the friction coefficient, η

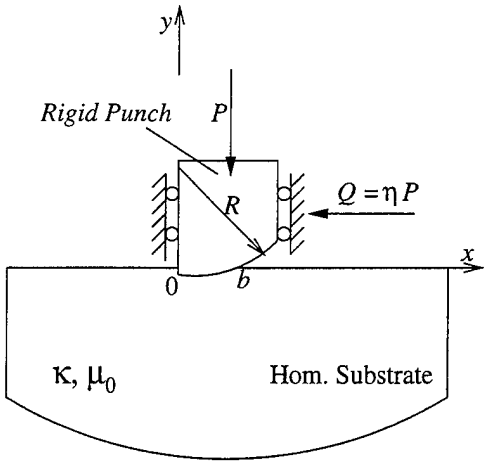

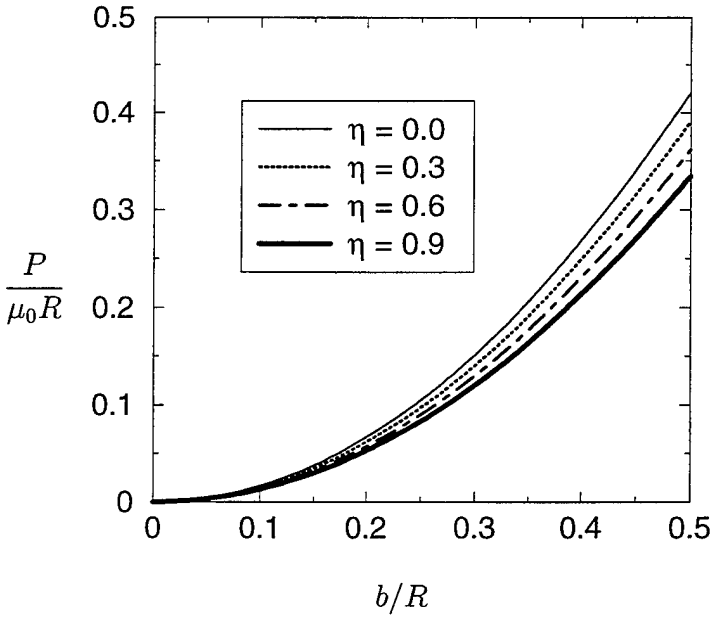

Figure C.11: The load versus the contact length for a homogeneous medium under a semi-circular punch for various values of the friction coefficient, η

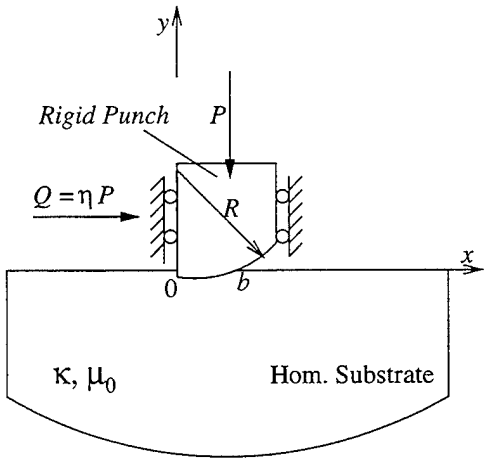

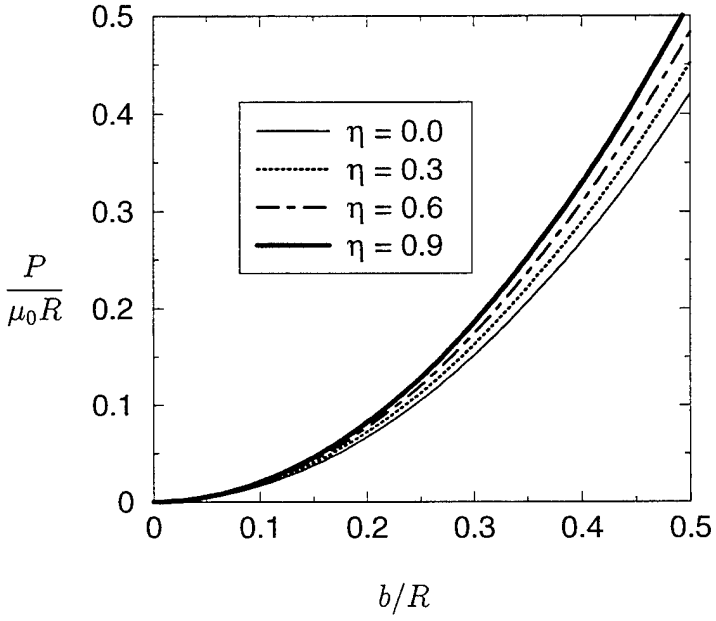

Figure C.12: The load versus the contact length for a homogeneous medium under a semi-circular punch for various values of the friction coefficient, η

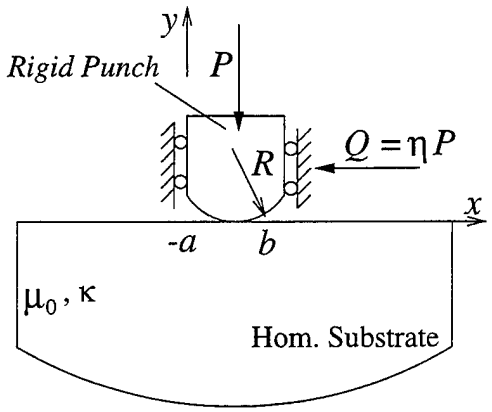

Figure C.13: Geomety of the parabolic punch problem for the homogeneous medium

C.7 Parabolic punch

The problem geometry can be seen in Figure C.13. Using the following tractions on the boundary

$$\sigma_{yy}(x,0) = -p(x), \qquad \sigma_{xy}(x,0) = -\eta p(x), \qquad -a < x < b, \tag{C.185}$$

$$\sigma_{yy}(x,0) = \sigma_{xy}(x,0) = 0, \qquad x < -a, \quad x > b, \tag{C.186}$$

equation (C.57) becomes

$$Ap(x) + \frac{B}{\pi}\int_{-a}^{b} \frac{p(t)}{t-x}dt = \lambda \frac{\partial}{\partial x} v(x,0), \tag{C.187}$$

where

$$A = \frac{\kappa - 1}{\kappa + 1}\eta, \tag{C.188}$$

$$B = -1, \tag{C.189}$$

$$\lambda = \frac{4\mu_0}{\kappa + 1}, \tag{C.190}$$

$$\frac{\partial}{\partial x} v(x,0) = \frac{x}{R}. \tag{C.191}$$

The equilibrium equation for this geometry is

$$\int_{-a}^{b} p(t)dt = P. \tag{C.192}$$

In order to solve the integral equation the limits of integration have to be normalized. Now setting

$$t = t^* R, \tag{C.193}$$

$$x = x^* R, \tag{C.194}$$

$$b = b^* R, \tag{C.195}$$

$$a = a^* R, \tag{C.196}$$

$$p(t) = p^*(t^*), \tag{C.197}$$

(C.187) and (C.192) can be written as

$$Ap^*(x^*) + \frac{B}{\pi}\int_{-a^*}^{b^*} \frac{p^*(t^*)}{t^* - x^*}dt^* = \lambda x^*, \tag{C.198}$$

$$\int_{-a^*}^{b^*} p^*(t^*)dt^* = \frac{P}{R}. \tag{C.199}$$

Further normalizing the integration limits from $(-a^*, b^*)$ to $(-1, 1)$ by using the following change of variables

$$t^* = \frac{b^* + a^*}{2}s + \frac{b^* - a^*}{2}, \qquad -1 < s < 1 \tag{C.200}$$

$$x^* = \frac{b^* + a^*}{2}r + \frac{b^* - a^*}{2}, \qquad -1 < r < 1 \tag{C.201}$$

$$p^*(t^*) = \frac{\lambda}{2}\phi(s), \tag{C.202}$$

one obtains

$$A\phi(r) + \frac{B}{\pi}\int_{-1}^{1} \frac{\phi(s)ds}{s - r} = (b^* + a^*)r + (b^* - a^*), \qquad -1 < r < 1. \tag{C.203}$$

$$\int_{-1}^{1} \phi(s)ds = \frac{4}{b^* + a^*} \frac{P}{\lambda R}. \tag{C.204}$$

Also defining

$$A_1 = \frac{b+a}{R} = b^* + a^*, \tag{C.205}$$

$$B_1 = \frac{b-a}{R} = b^* - a^*, \tag{C.206}$$

(C.203) becomes

$$A\phi(r) + \frac{B}{\pi} \int_{-1}^{1} \frac{\phi(s)ds}{s-r} = f(r), \qquad -1 < r < 1. \tag{C.207}$$

where

$$f(r) = A_1 r + B_1.$$

Now assuming a solution of the form

$$\phi(s) = \sum_{0}^{\infty} c_n w(s) P_n^{(\alpha,\beta)}(s), \qquad w(s) = (1-s)^{\alpha} (1+s)^{\beta}, \tag{C.208}$$

(C.207) becomes

$$\sum_{0}^{\infty} c_n \left[A w(r) P_n^{(\alpha,\beta)}(r) + \frac{B}{\pi} \int_{-1}^{1} \frac{w(s) P_n^{(\alpha,\beta)}(s) \phi(s) ds}{s-r} \right] = f(r), \qquad -1 < r < 1. \tag{C.209}$$

Using the property of Jacobi Polynomials given in Appendix A equation (A.6), equation (C.209) may be expressed as

$$\sum_{0}^{\infty} c_n \left[-\frac{2^{-\kappa_0} B}{\sin \pi\alpha} P_{n-\kappa_0}^{(-\alpha,-\beta)}(r) \right] = f(r). \tag{C.210}$$

where κ_0 is the index of the problem which is

$$\kappa_0 = -(\alpha + \beta) = -1,$$

In this problem, after the application of a given load, the ends of the contact length(i.e. b^* and a^*) is unknown. However since the index of the problem is ($\kappa_0 = -1$) the following consistency condition has to be satisfied.

$$\int_{-1}^{1} f(t)\frac{dt}{w(t)} = 0. \tag{C.211}$$

Since $f(t)$ is a function of (A_1, B_1), for a fixed contact length $b^* + a^* = A_1$, we can find B_1 from the consistency condition (C.211) as

$$\int_{-1}^{1} f(t)\frac{dt}{w(t)} = \int_{-1}^{1} \frac{A_1 t + B_1}{w(t)} dt = 0 \tag{C.212}$$

The integral can be evaluated in closed form by expanding $A_1 t + B_1$ into Jacobi Polynomials $P_j^{(-\alpha,-\beta)}(t)$ as follows

$$A_1 t + B_1 = 2A_1 P_1^{(-\alpha,-\beta)}(t) + \left[B_1 - (\beta - \alpha) A_1\right] P_0^{(-\alpha,-\beta)}(t), \tag{C.213}$$

$$\begin{aligned} \int_{-1}^{1} \frac{A_1 t + B_1}{w(t)} dt &= \int_{-1}^{1} \frac{2A_1 P_1^{(-\alpha,-\beta)}(t)}{w(t)} dt + \int_{-1}^{1} \frac{\left[B_1 - (\beta - \alpha) A_1\right] P_0^{(-\alpha,-\beta)}(t)}{w(t)} dt \\ &= \left[B_1 - (\beta - \alpha) A_1\right] \theta_0(-\alpha, -\beta) \\ &= \left[B_1 - (\beta - \alpha) A_1\right] \frac{\pi}{\sin \pi\alpha} = 0, \end{aligned} \tag{C.214}$$

which means that

$$B_1 - (\beta - \alpha) A_1 = 0. \tag{C.215}$$

Therefore

$$B_1 = (\beta - \alpha) A_1. \tag{C.216}$$

Hence the right hand side of equation (C.210)(i.e. $f(r)$) is known and if we cut the series at $n = N$, (C.210) becomes

$$\sum_{0}^{N} c_n \left[\frac{2}{\sin \pi\alpha} P_{n+1}^{(-\alpha,-\beta)}(r)\right] = f(r). \tag{C.217}$$

We have $N+1$ unknowns (i.e. $c_0, c_1, ..., c_N$) to determine. The easiest way to determine these unknowns is to expand both sides of equation (C.210) into series of Jacobi Polynomials $P_j^{(-\alpha,-\beta)}(r)$, and to compare the coefficients. Thus, using the orthogonality relations equation (C.217) becomes

$$\frac{2}{\sin \pi\alpha}\theta_j(-\alpha,-\beta)\, c_{j-1} = F_j, \qquad j = 0, 1, ...N+1, \tag{C.218}$$

where

$$F_j = \int_{-1}^{1} \frac{P_j^{(-\alpha,-\beta)}(t)}{w(t)} f(t)\, dt = \int_{-1}^{1} \frac{P_j^{(-\alpha,-\beta)}(t)}{w(t)} (A_1 t + B_1)\, dt. \tag{C.219}$$

The first equation in (C.218) reads as

$$\frac{2}{\sin \pi\alpha}\theta_0(-\alpha,-\beta)\, c_{-1} = F_0. \tag{C.220}$$

where

$$F_0 = \int_{-1}^{1} f(t)\frac{dt}{w(t)}. \tag{C.221}$$

which is the consistency condition (C.211). Therefore we can formally assume that

$$c_{-1} = 0. \tag{C.222}$$

and the unknown coefficients become

$$c_{j-1} = \frac{\sin \pi\alpha}{2\theta_j(-\alpha,-\beta)} F_j, \qquad j = 1, 2, ..., N+1. \tag{C.223}$$

$N+1$ unknowns (i.e. $c_0, c_1, ..., c_N$) can then be found by expanding the right hand side of equation (C.217) as in equation (C.213). The only nonzero coefficient is

$$c_0 = A_1 \sin \pi\alpha = (b^* + a^*) \sin \pi\alpha. \tag{C.224}$$

The solution of the problem becomes

$$\phi(s) = c_0 w(s), \qquad w(s) = (1-s)^{\alpha}(1+s)^{\beta}, \tag{C.225}$$

In order to find the pressure distribution, substitute (C.225) into (C.202)

$$\frac{p^*(t^*)}{\mu_0} = \frac{2}{\kappa+1} c_0 (1-s)^{\alpha} (1+s)^{\beta}, \tag{C.226}$$

where

$$s = \frac{2t^* - b^* + a^*}{b^* + a^*}. \tag{C.227}$$

Using (C.194) and (C.185) we find

$$\begin{aligned} \sigma_{yy}(x^*, 0) &= -p^*(x^*) \\ &= -\frac{4\mu_0}{\kappa+1} \sin \pi\alpha \, (b^* - x^*)^{\alpha} (x^* + a^*)^{\beta}. \end{aligned} \tag{C.228}$$

Therefore normalized pressure distribution becomes

$$\frac{\sigma_{yy}(x, 0)}{\mu_0} = -\frac{4}{\kappa+1} \sin \pi\alpha \, (b^* - x^*)^{\alpha} (x^* + a^*)^{\beta}. \tag{C.229}$$

In order to find the relation between b^* and a^* we use equation (C.216) and substitute B_1 and A_1 from (C.205) and (C.206)

$$b^* - a^* = (\beta - \alpha)(b^* + a^*).$$

Therefore

$$b^* = \frac{\beta}{\alpha} a^*. \tag{C.230}$$

The Load displacement relation can be found from the equilibrium equation (C.204)

$$\int_{-1}^{1} \phi(s) ds = \frac{4}{A_1} \frac{P}{\lambda R}. \tag{C.231}$$

Using the orthogonality of Jacobi Polynomials we have

$$c_0 \theta_0 (\alpha, \beta) = \frac{4}{A_1} \frac{P}{\lambda R}, \tag{C.232}$$

where, for $\kappa_0 = -(\alpha+\beta) = -1$,

$$\begin{aligned}\theta_0(\alpha,\beta) &= \int_{-1}^{1} w(t)\,dt = \frac{2^{\alpha+\beta+1}\Gamma(\alpha+1)\Gamma(\beta+1)}{\Gamma(\alpha+\beta+2)} \\ &= \frac{2\pi\alpha\beta}{\sin\pi\alpha},\end{aligned} \tag{C.233}$$

Therefore the relation between the load and the contact length becomes

$$P^* = \frac{P}{\mu_0 R} = \frac{2\pi\alpha\beta}{\kappa+1}\left(b^*+a^*\right)^2. \tag{C.234}$$

The stress $\sigma_{xx}(x,0)$ can be found by using equation (C.68). Since $\sigma_{yy}(x,0)$ is zero outside the contact region ($-a<x<b$) (C.68) can be written as

$$\sigma_{xx}(x,0) = \begin{cases} \sigma_{yy}(x,0) + \dfrac{2}{\pi}\displaystyle\int_{-a}^{b}\frac{\sigma_{xy}(t,0)}{t-x}dt, & -a<x<b, \\ \dfrac{2}{\pi}\displaystyle\int_{-a}^{b}\frac{\sigma_{xy}(t,0)}{t-x}dt, & x\notin[-a,b]. \end{cases} \tag{C.235}$$

Defining

$$\sigma_{xx}(x,0) = -\frac{\lambda}{2}q(r), \tag{C.236}$$

and substituting $\sigma_{xy}(t,0)$ from (C.185) and using (C.192), (C.194)and (C.225), equation (C.235) may be expressed as

$$q(r) = \begin{cases} \phi(r) + \dfrac{2\eta}{\pi}\displaystyle\int_{-1}^{1}\frac{\phi(s)}{s-r}ds, & -1<r<1, \\ \dfrac{2\eta}{\pi}\displaystyle\int_{-1}^{1}\frac{\phi(s)}{s-r}ds, & |r|>1, \end{cases} \tag{C.237}$$

where

$$\phi(r) = c_0 w(r), \qquad w(r) = (1-r)^{\alpha}(1+r)^{\beta}.$$

Substituting $\phi(r)$ into (C.237) and using (C.236) we have

$$\frac{\sigma_{xx}(x,0)}{\mu_0} = \begin{cases} -\dfrac{2}{\kappa+1}w(r)c_0 - \dfrac{4\eta}{(\kappa+1)\pi}c_0 L_0(r), & -1<r<1, \\ -\dfrac{4\eta}{(\kappa+1)\pi}c_0 L_0(r), & |r|>1, \end{cases} \tag{C.238}$$

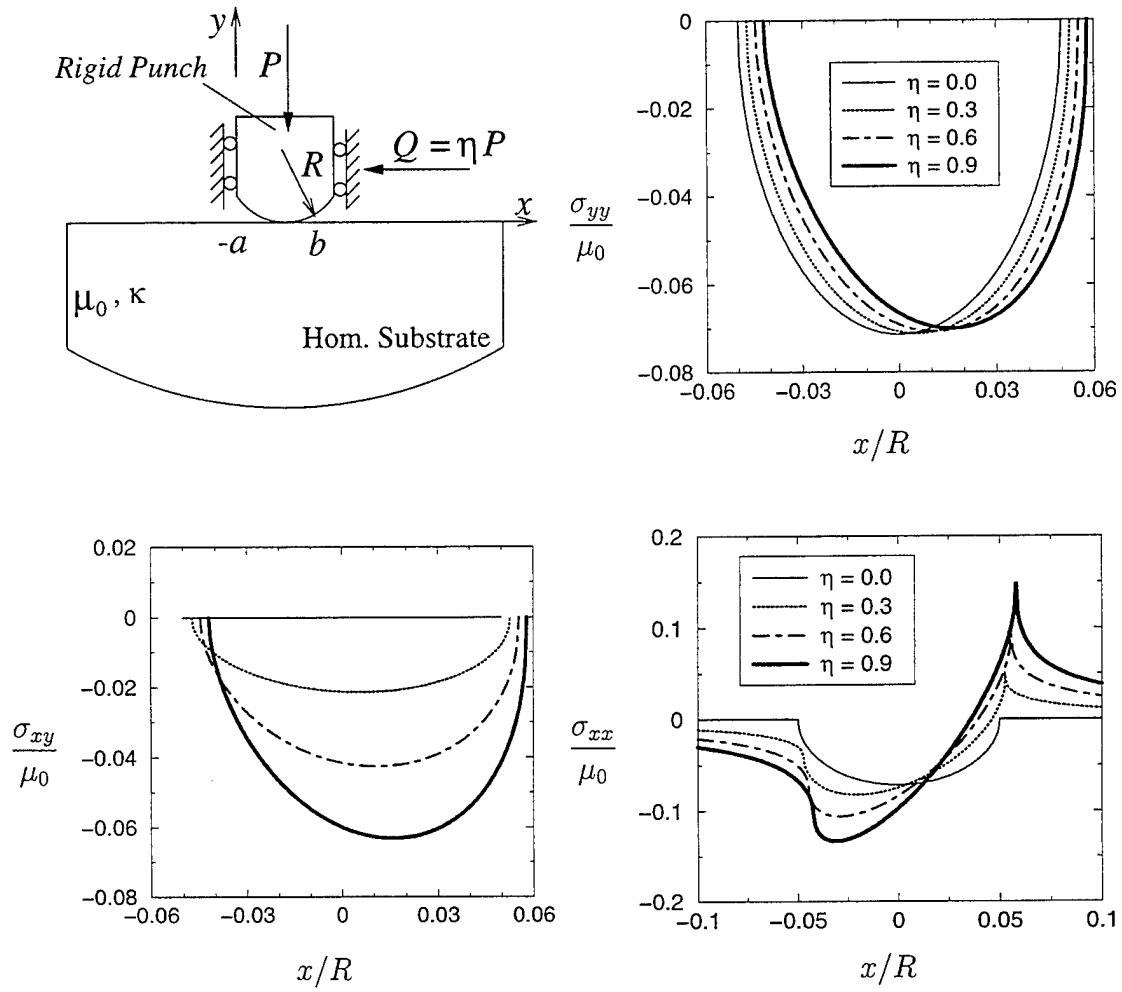

Figure C.14: Stress distribution on the surface of a homogeneous medium under a cylindrical punch for various values of the friction coefficient, η

where $L_0(r)$ is calculated in closed form in equation (B.52) as follows

$$L_0(r) = \frac{\pi}{\sin \pi\alpha} \begin{cases} -(-r+1)^{\alpha}(-r-1)^{\beta} - r + \alpha - \beta, & -\infty < r < -1, \\ (1-r)^{\alpha}(1+r)^{\beta}\cos \pi\alpha - r + \alpha - \beta, & -1 < r < 1, \\ (r-1)^{\alpha}(r+1)^{\beta} - r + \alpha - \beta, & 1 < r < \infty. \end{cases} \tag{C.239}$$

Appendix D

Problems with two deformable homogeneous solids

D.1 The Homogeneous problem

The mixed boundary value problem depicted in Figure D.1 give rise to the singular integral equation of the second kind. Consider the following basic formulas for the elastic half plane relating the surface tractions to the displacement derivatives

$$-\omega_2\sigma_{2xy}(x,0) - \frac{1}{\pi}\int_{-\infty}^{\infty}\frac{\sigma_{2yy}(t,0)}{t-x}dt = \lambda_2\frac{\partial}{\partial x}v_2(x,0), \tag{D.1}$$

$$-\omega_3\sigma_{3xy}(x,0) + \frac{1}{\pi}\int_{-\infty}^{\infty}\frac{\sigma_{3yy}(t,0)}{t-x}dt = \lambda_3\frac{\partial}{\partial x}v_3(x,0), \tag{D.2}$$

$$\omega_2\sigma_{2yy}(x,0) - \frac{1}{\pi}\int_{-\infty}^{\infty}\frac{\sigma_{2xy}(t,0)}{t-x}dt = \lambda_2\frac{\partial}{\partial x}u_2(x,0), \tag{D.3}$$

$$\omega_3\sigma_{3yy}(x,0) + \frac{1}{\pi}\int_{-\infty}^{\infty}\frac{\sigma_{3xy}(t,0)}{t-x}dt = \lambda_3\frac{\partial}{\partial x}u_3(x,0), \tag{D.4}$$

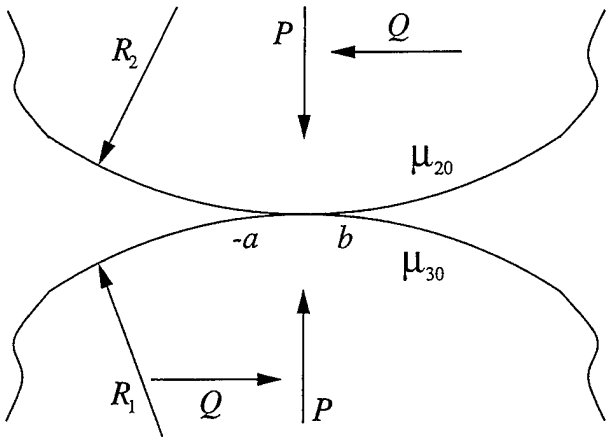

Figure D.1: The Geometry of the problem with two deformable homogeneous bodies

where

$$\omega_2 = \frac{\kappa_2 - 1}{\kappa_2 + 1}, \tag{D.5}$$

$$\omega_3 = \frac{\kappa_3 - 1}{\kappa_3 + 1}, \tag{D.6}$$

$$\lambda_2 = \frac{4\mu_{20}}{\kappa_2 + 1}, \tag{D.7}$$

$$\lambda_3 = \frac{4\mu_{30}}{\kappa_3 + 1}. \tag{D.8}$$

Defining

$$\sigma_{2yy}(x,0) = \sigma_{3yy}(x,0) = \sigma(x), \tag{D.9}$$

$$\sigma_{2xy}(x,0) = \sigma_{2xy}(x,0) = \tau(x), \tag{D.10}$$

(D.1) and (D.2) becomes

$$-\frac{\omega_2}{\lambda_2}\tau(x) - \frac{1}{\lambda_2 \pi}\int_{-\infty}^{\infty}\frac{\sigma(t)}{t-x}dt = \frac{\partial}{\partial x}v_2(x,0), \tag{D.11}$$

$$-\frac{\omega_3}{\lambda_3}\tau(x) + \frac{1}{\pi\lambda_3}\int_{-\infty}^{\infty}\frac{\sigma(t)}{t-x}dt = \frac{\partial}{\partial x}v_3(x,0), \tag{D.12}$$

For , relatively small contact regions, the vertical displacement for respectively the upper and lower half media may be expressed as

$$v_2(x,0) = v_{20} - \frac{x^2}{2R_1}, \tag{D.13}$$

$$v_3(x,0) = -v_{30} + \frac{x^2}{2R_2}. \tag{D.14}$$

Therefore

$$\frac{\partial}{\partial x} v_2(x,0) = -\frac{x}{R_1}, \tag{D.15}$$

$$\frac{\partial}{\partial x} v_3(x,0) = +\frac{x}{R_2}. \tag{D.16}$$

Subtracting (D.16) from (D.15), we have

$$\frac{\partial}{\partial x} v_3(x,0) - \frac{\partial}{\partial x} v_2(x,0) = \frac{x}{R}, \tag{D.17}$$

where

$$\frac{1}{R} = \frac{1}{R_2} + \frac{1}{R_1} = \frac{R^*}{R_2}, \tag{D.18}$$

$$R^* = 1 + \chi, \tag{D.19}$$

$$\chi = \frac{R_2}{R_1}. \tag{D.20}$$

Subtracting (D.12) from (D.11), and using (D.17) we have

$$-C\tau(x) + \frac{D}{\pi}\int_{-\infty}^{\infty} \frac{\sigma(t)}{t-x} dt = \frac{xR^*}{R_2},$$

where

$$C = \frac{\omega_3}{\lambda_3} - \frac{\omega_2}{\lambda_2} = \frac{C^*}{\mu_{30}},$$

$$D = \frac{1}{\lambda_3} + \frac{1}{\lambda_2} = \frac{D^*}{\lambda_3},$$

$$C^* = \frac{(\kappa_3 - 1) - (\kappa_2 - 1)\Gamma}{4},$$

$$D^* = \frac{(\kappa_3 + 1) + (\kappa_2 + 1)\Gamma}{4},$$

$$\Gamma = \frac{\mu_{30}}{\mu_{20}}.$$

Or in a more compact form

$$-A^*\tau(x) + \frac{1}{\pi}\int_{-\infty}^{\infty}\frac{\sigma(t)}{t-x}dt = \frac{\mu_{30}R^*}{D^*}\frac{x}{R_2}, \tag{D.21}$$

where

$$A^* = \frac{C}{D} = \frac{(\kappa_3 - 1) - (\kappa_2 - 1)\,\Gamma}{(\kappa_3 + 1) + (\kappa_2 + 1)\,\Gamma}. \tag{D.22}$$

Applying the following tractions on the boundary

$$\left.\begin{aligned} \sigma_{2yy}(x,0) = \sigma_{3yy}(x,0) = \sigma(x) = -p(x), \\ \sigma_{2xy}(x,0) = \sigma_{3xy}(x,0) = \tau(x) = -\eta p(x), \end{aligned}\right\} \quad -a < x < b, \tag{D.23}$$

$$\sigma_{2yy}(x,0) = \sigma_{2xy}(x,0) = 0, \qquad x < -a, \quad x > b,$$

(D.21) reduces to

$$Ap\,(x) + \frac{B}{\pi}\int_{-a}^{b}\frac{p(t)}{t-x}dt = \frac{\mu_{30}R^*}{D^*}\frac{x}{R_2}, \tag{D.24}$$

where

$$\begin{aligned} A &= A^*\eta, \\ B &= -1. \end{aligned}$$

Also the equilibrium equation becomes

$$\int_{-a}^{b} p(t)dt = P. \tag{D.25}$$

D.2 Solution of the integral equation

In order to solve the integral equation (D.24) the limits of integration have to be normalized. Now setting

$$t = t^* R_2, \tag{D.26}$$

$$x = x^* R_2, \tag{D.27}$$

$$b = b^* R_2, \tag{D.28}$$

$$a = a^* R_2, \tag{D.29}$$

$$p(t) = p^*(t^*), \tag{D.30}$$

(D.24) and (D.25) can be written as

$$Ap^*(x^*) + \frac{B}{\pi}\int_{a^*}^{b^*} \frac{p^*(t^*)}{t^* - x^*} dt^* = \frac{\mu_{30} R^*}{D^*} x^*, \tag{D.31}$$

$$\int_{-a^*}^{b^*} p^*(t^*) dt^* = \frac{P}{R_2}, \tag{D.32}$$

where

$$A = -\eta \frac{(\kappa_3 - 1) - (\kappa_2 - 1)\Gamma}{(\kappa_3 + 1) + (\kappa_2 + 1)\Gamma}, \tag{D.33}$$

$$B = -1, \tag{D.34}$$

$$R^* = 1 + \chi, \tag{D.35}$$

$$\chi = \frac{R_2}{R_1}, \tag{D.36}$$

$$\Gamma = \frac{\mu_{30}}{\mu_{20}}, \tag{D.37}$$

Further normalizing the integration limits from $(-a^*, b^*)$ to $(-1, 1)$ by using the following change of variables

$$t^* = \frac{b^* + a^*}{2} s + \frac{b^* - a^*}{2}, \qquad -1 < s < 1 \tag{D.38}$$

$$x^* = \frac{b^* + a^*}{2} r + \frac{b^* - a^*}{2}, \qquad -1 < r < 1 \tag{D.39}$$

$$p^*(t^*) = \frac{\mu_{30} R^*}{2D^*} \phi(s), \tag{D.40}$$

one obtains

$$A\phi(r) + \frac{B}{\pi}\int_{-1}^{1}\frac{\phi(s)ds}{s-r} = (b^* + a^*)\, r + (b^* - a^*)\,, \qquad -1 < r < 1. \tag{D.41}$$

Also defining

$$A_1 = \frac{b+a}{R_2} = b^* + a^*, \tag{D.42}$$

$$B_1 = \frac{b-a}{R_2} = b^* - a^*, \tag{D.43}$$

(D.41) becomes

$$A\phi(r) + \frac{B}{\pi}\int_{-1}^{1}\frac{\phi(s)ds}{s-r} = f\,(r)\,, \qquad -1 < r < 1. \tag{D.44}$$

where

$$f\,(r) = A_1 r + B_1. \tag{D.45}$$

Now assuming a solution of the form

$$\phi(s) = \sum_{0}^{\infty} c_n w(s) P_n^{(\alpha,\beta)}(s), \qquad w\,(s) = (1-s)^{\alpha}\,(1+s)^{\beta}\,, \tag{D.46}$$

(D.44) becomes

$$\sum_{0}^{\infty} c_n \left[A w(r) P_n^{(\alpha,\beta)}(r) + \frac{B}{\pi}\int_{-1}^{1}\frac{w(s)P_n^{(\alpha,\beta)}(s)\phi(s)ds}{s-r}\right] = f\,(r)\,, \qquad -1 < r < 1. \tag{D.47}$$

Using the property of Jacobi Polynomials given in Appendix A equation (A.6), equation (D.47) may be expressed as

$$\sum_{0}^{\infty} c_n \left[\frac{2}{\sin\pi\alpha} P_{n+1}^{(-\alpha,-\beta)}(r)\right] = f\,(r)\,. \tag{D.48}$$

where κ_0 is the index of the problem which is

$$\kappa_0 = -\,(\alpha+\beta) = -1,$$

The same solution approach can be used as in the case of parabolic punch. Thus the solution is

$$\phi(s) = c_0 w(s), \qquad w(s) = (1-s)^{\alpha}(1+s)^{\beta}, \tag{D.49}$$

where

$$c_0 = A_1 \sin \pi\alpha = (b^* + a^*) \sin \pi\alpha. \tag{D.50}$$

In order to find the pressure distribution, substitute (D.49) into (D.40), giving

$$p^*(x^*) = \frac{\mu_{30} R^*}{2D^*} \phi \left(\frac{2x^* - b^* + a^*}{b^* + a^*} \right). \tag{D.51}$$

Now by using (D.30) and (D.23) we find

$$\begin{aligned} \sigma_{yy}(x^*, 0) &= -p^*(x^*) = -\frac{\mu_{30} R^*}{2D^*} c_0 w \left(\frac{2x^* - b^* + a^*}{b^* + a^*} \right), \\ &= -\frac{\mu_{30} R^*}{2D^*} c_0 w \left(\frac{2x^* - b^* + a^*}{b^* + a^*} \right). \end{aligned}$$

Since

$$w \left(\frac{2x^* - b^* + a^*}{b^* + a^*} \right) = \frac{2}{b^* + a^*} (b^* - x^*)^{\alpha} (x^* + a^*)^{\beta},$$

$$\sigma_{yy}(x^*, 0) = -\frac{\mu_{30} R^*}{D^*} \sin \pi\alpha \, (b^* - x^*)^{\alpha} (x^* + a^*)^{\beta}, \tag{D.52}$$

the normalized pressure distribution becomes

$$\frac{\sigma_{yy}(x, 0)}{\mu_{30}} = -\frac{R^*}{D^*} \sin \pi\alpha \, (b^* - x^*)^{\alpha} (x^* + a^*)^{\beta}. \tag{D.53}$$

Also, the relation between b^* and a^* is found to be

$$b^* = \frac{\beta}{\alpha} a^*. \tag{D.54}$$

The Load displacement relation can be found from the equilibrium equation (D.32) and (D.49) (D.40)

$$\int_{-1}^{1} \phi(s) ds = \frac{4D^*}{R^* (b^* + a^*)} \frac{P}{\mu_{30} R_2}. \tag{D.55}$$

Using the orthogonality of Jacobi Polynomials we have

$$c_0\theta_0(\alpha,\beta)=\frac{4D^*}{R^*(b^*+a^*)}\frac{P}{\mu_{30}R_2}, \tag{D.56}$$

where

$$\theta_0(\alpha,\beta)=\frac{2\pi\alpha\beta}{\sin\pi\alpha}. \tag{D.57}$$

Therefore the relation between the load and the contact length becomes

$$P^*=\frac{P}{\mu_{30}R_2}=\frac{R^*}{4D^*}2\pi\alpha\beta(b^*+a^*)^2. \tag{D.58}$$

Defining

$$\sigma_{xx}(x,0)=-\frac{\mu_{30}R^*}{2D^*}q(r), \tag{D.59}$$

one may easily calculate $q(r)$ as follows

$$q(r)=\begin{cases} w(r)c_0+\frac{2\eta}{\pi}c_0L_0(r), & -1<r<1, \\ \frac{2\eta}{\pi}c_0L_0(r), & |r|>1, \end{cases}$$

where $L_0(r)$ is calculated in closed form in Appendix B equation (B.52)

D.2.1 The bearing problems

For the problems involving negative curvatures the only difference would be in the right hand side of the integral equation and the curvature of the lower half plane. Thus,

$$\frac{\partial}{\partial x}v_2(x,0)=\frac{x}{R_1},$$

$$\frac{\partial}{\partial x}v_3(x,0)-\frac{\partial}{\partial x}v_2(x,0)=\frac{x}{R}, \tag{D.60}$$

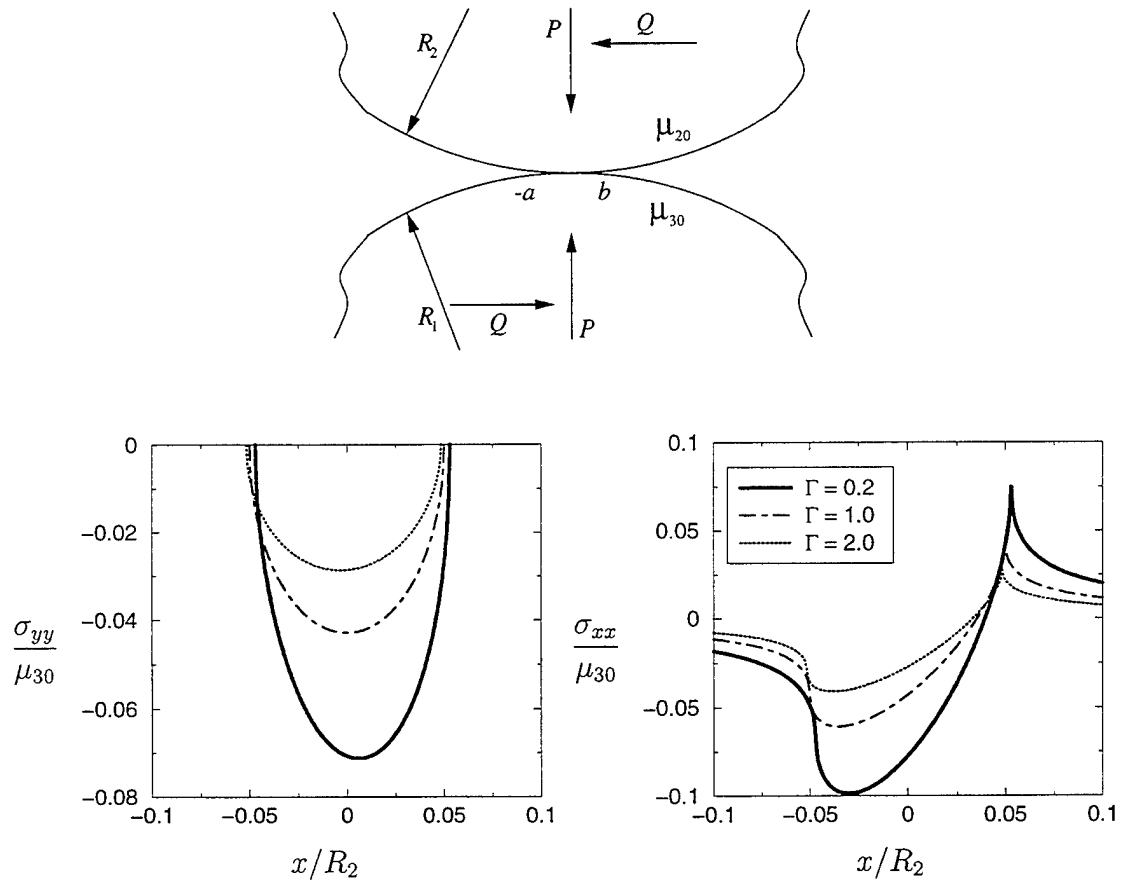

Figure D.2: Stress distribution on the surface of the elastic cylinders for various values of the stiffness ratios, $\Gamma = \mu_{30}/\mu_{20}$, $\chi = R_2/R_1 = 0.2$, $\eta = 0.5$, $(b+a)/R_2 = 0.1$

where

$$\frac{1}{R} = \frac{1}{R_2} - \frac{1}{R_1} = \frac{R^*}{R_2}, \tag{D.61}$$

$$R^* = 1 + \chi, \tag{D.62}$$

$$\chi = -\frac{R_2}{R_1}. \tag{D.63}$$

Note that $R_2 < R_1$. and the range of χ is $(-1 < \chi < 0)$

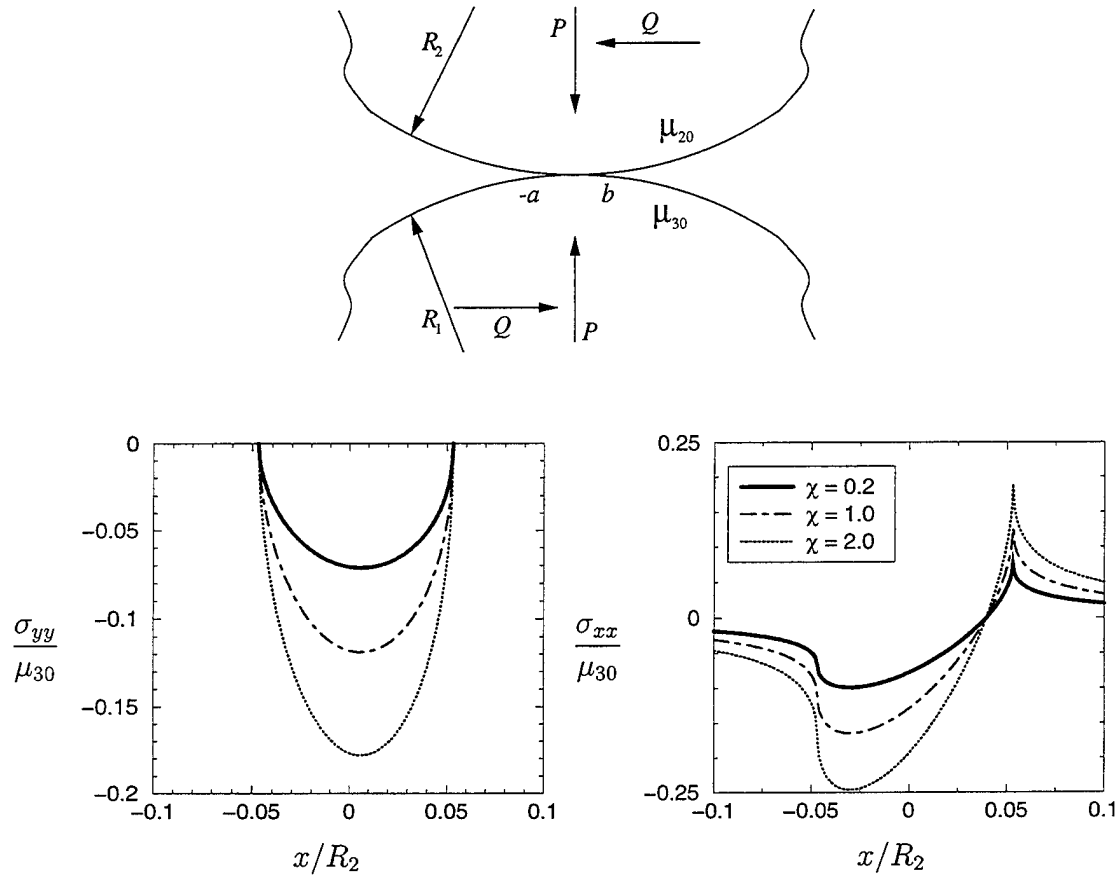

Figure D.3: Stress distribution on the surface of the elastic cylinders for various values of the curvature ratios, $\chi = R_2/R_1$, $\Gamma = \mu_{30}/\mu_{20} = 0.2$, $\eta = 0.5$, $(b+a)/R_2 = 0.1$

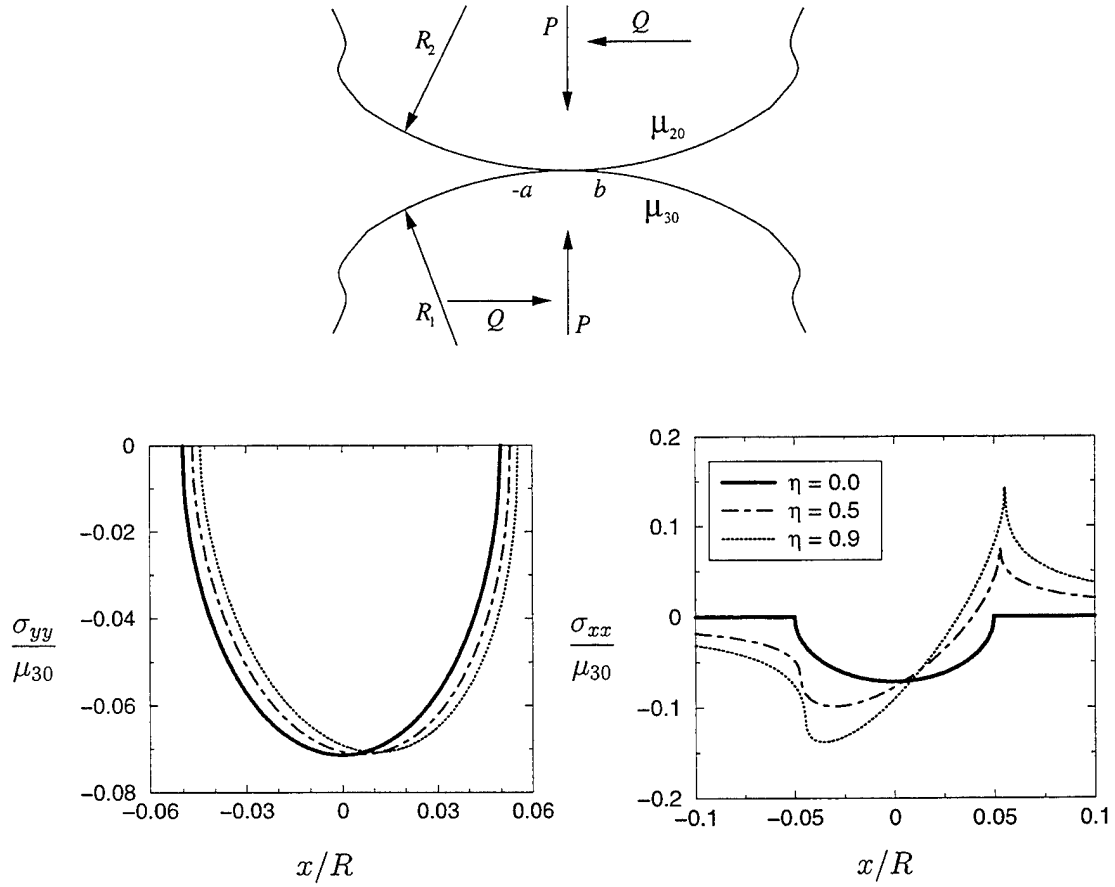

Figure D.4: Stress distribution on the surface of the elastic cylinders for various values of the coefficient of friction, η, $\chi = R_2/R_1 = 0.2$, $\Gamma = \mu_{30}/\mu_{20} = 0.2$, $\eta = 0.5$, $(b+a)/R_2 = 0.1$

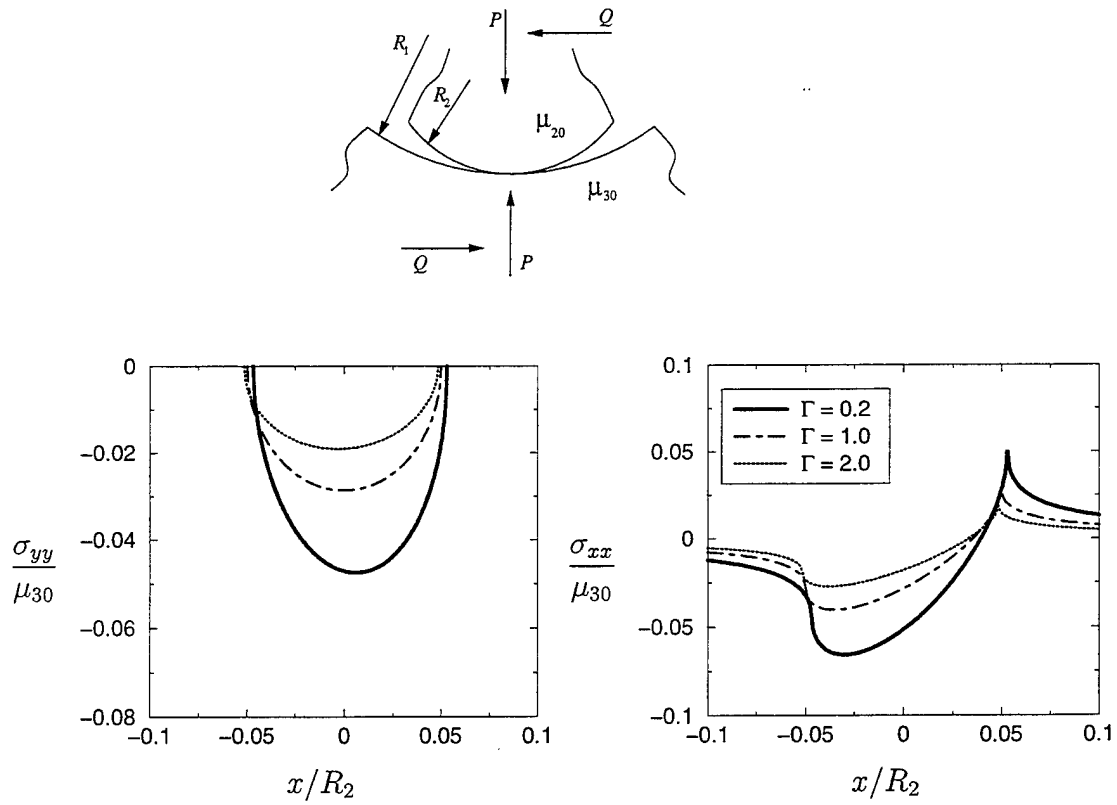

Figure D.5: Stress distribution on the surface of the elastic cylinders for various values of the stiffness ratios, $\Gamma = \mu_{30}/\mu_{20}$, $\chi = R_2/R_1 = 0.2$, $\eta = 0.5$, $(b+a)/R_2 = 0.1$

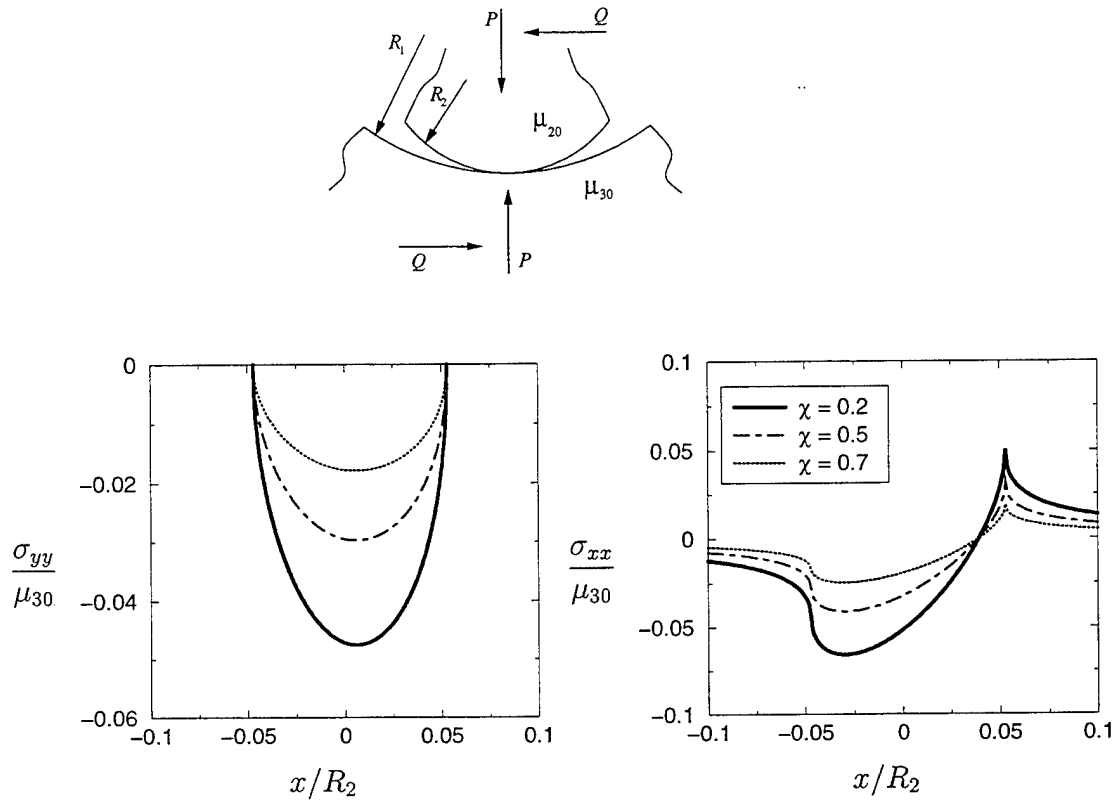

Figure D.6: Stress distribution on the surface of the elastic cylinders for various values of the curvature ratios, $\chi = R_2/R_1$, $\Gamma = \mu_{30}/\mu_{20} = 0.2$, $\eta = 0.5$, $(b+a)/R_2 = 0.1$

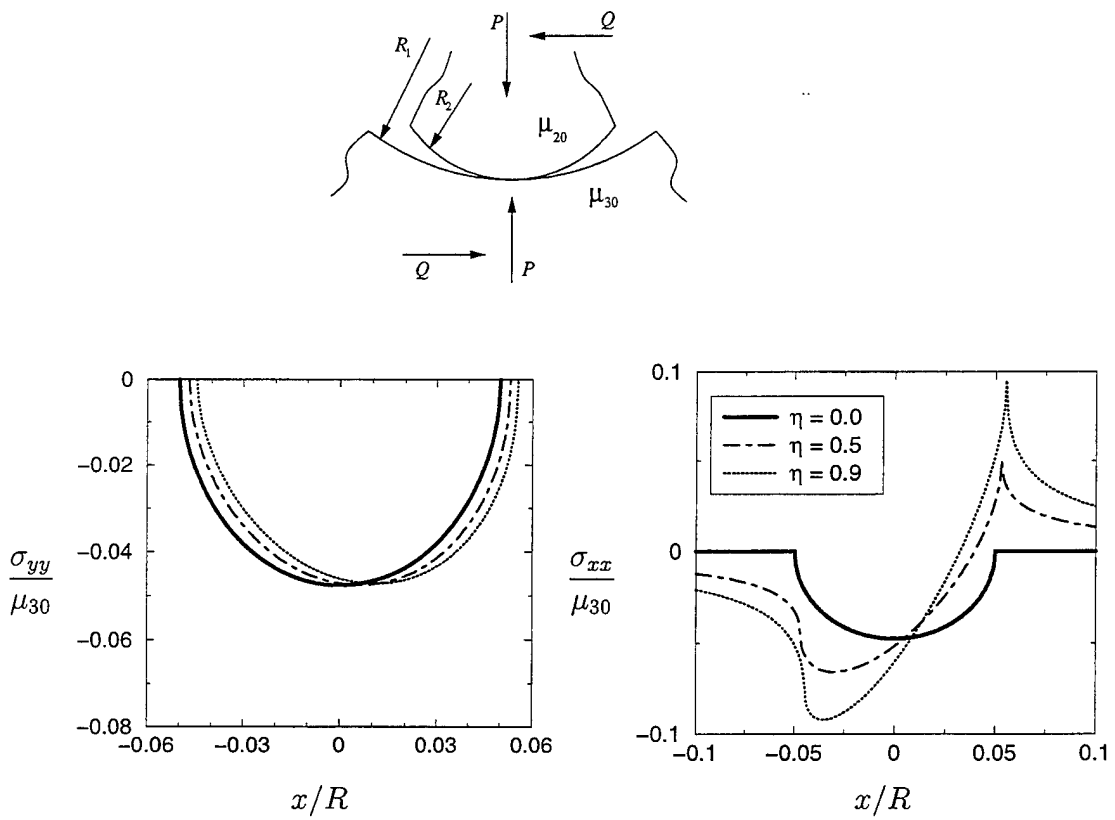

Figure D.7: Stress distribution on the surface of the elastic cylinders for various values of the coefficient of friction, η, $\chi = R_2/R_1 = 0.2$, $\Gamma = \mu_{30}/\mu_{20} = 0.2$, $\eta = 0.5$, $(b+a)/R_2 = 0.1$

Appendix E

Asymptotic Analysis of Kernels

E.1 Introduction

In the derivation of the integral equations , an important step is to find the asymptotic values of the the infinite integrals in (2.165)-(2.168) and (3.159)-(3.162). There are two reasons why we asymptotically expand the infinite integrals as $\alpha \to \infty$. First the singular behavior of the integral equation and that of its solution comes from the leading order term in the large α expansion of the kernel in integrands (2.165)-(2.168) and (3.159)-(3.162). The second reason is that the subsequent terms in the expansion facilitate computational efficiency when we numerically solve the singular integral equations (4.3) and (4.4).

E.2 The Upper half plane

Before starting to analyse the behaviour of the integrands in equations (2.110)-(2.113) assymptotically as $\alpha \to \infty$, the variables used in the integrands can be written as

$$h_{11}(\alpha, y) = -\frac{i\alpha(\kappa_2 - 1)}{\Delta_3}\left(y_1\overline{r_4} + \overline{y_1}r_4\right), \tag{E.1}$$

$$h_{12}(\alpha, y) = \frac{i\alpha}{\Delta_3}\left(-y_1\overline{r_2} + \overline{y_1}r_2\right), \tag{E.2}$$

$$h_{21}(\alpha, y) = -\frac{i\alpha}{\Delta_3}\left(y_2\overline{r_2} + \overline{y_2}r_2\right), \tag{E.3}$$

$$h_{22}(\alpha, y) = -\frac{i\alpha(\kappa_2 - 1)}{\Delta_3}\left(y_2\overline{r_4} - \overline{y_2}r_4\right), \tag{E.4}$$

where

$$y_1(\alpha, y) = e^{n_2 y} + r_1 e^{-h_2(n_1 - n_2) + n_1 y} + r_3 e^{-h_2(\overline{n_1} - n_2) + \overline{n_1} y}, \tag{E.5}$$

$$y_2(\alpha, y) = a_2 e^{n_2 y} + a_1 r_1 e^{-h_2(n_1 - n_2) + n_1 y} - \overline{a_1} r_3 e^{-h_2(\overline{n_1} - n_2) + \overline{n_1} y}, \tag{E.6}$$

$$r_2 = z_{12} + z_{11} r_1 e^{-h_2(n_1 - n_2)} + \overline{z_{11}} r_3 e^{-h_2(\overline{n_1} - n_2)}, \tag{E.7}$$

$$r_4 = z_{22} + z_{21} r_1 e^{-h_2(n_1 - n_2)} - \overline{z_{21}} r_3 e^{-h_2(\overline{n_1} - n_2)}, \tag{E.8}$$

$$z_{11} = (3 - \kappa_2)(i\alpha)a_1 + (\kappa_2 + 1)n_1, \tag{E.9}$$

$$z_{12} = (3 - \kappa_2)(i\alpha)a_2 + (\kappa_2 + 1)n_2, \tag{E.10}$$

$$z_{21} = a_1 n_1 + i\alpha, \tag{E.11}$$

$$z_{22} = a_2 n_2 + i\alpha, \tag{E.12}$$

$$\Delta_3 = -(r_2\overline{r_4} + \overline{r_2}r_4), \tag{E.13}$$

$$r_1 = \frac{1}{\Delta_2}\left(s_2\overline{t_1} + \overline{s_1}t_2\right), \tag{E.14}$$

$$r_3 = \frac{1}{\Delta_2}\left(s_2 t_1 - s_1 t_2\right), \tag{E.15}$$

$$\Delta_2 = -(s_1\overline{t_1} + \overline{s_1}t_1), \tag{E.16}$$

$$\begin{aligned}
s_1 &= i\lambda_2\alpha a_1 + \Lambda_2\left(\kappa_2+1\right)n_1\kappa_1 + \left(\kappa_1^2-1\right)|\alpha|, && \text{(E.17)}\\
s_2 &= i\lambda_2\alpha a_2 + \Lambda_2\left(\kappa_2+1\right)n_2\kappa_1 + \left(\kappa_1^2-1\right)|\alpha|, && \text{(E.18)}\\
t_1 &= a_1\left[\chi_2\kappa_1 n_1 + |\alpha|(\kappa_1+1)\right] + i\alpha\left[\kappa_1\chi_2 - (\kappa_1-1)\right], && \text{(E.19)}\\
t_2 &= a_2\left[\chi_2\kappa_1 n_2 + |\alpha|(\kappa_1+1)\right] + i\alpha\left[\kappa_1\chi_2 - (\kappa_1-1)\right], && \text{(E.20)}\\
\lambda_2 &= \kappa_1^2 + \kappa_1\left(\Lambda_2\left(3-\kappa_2\right)-2\right)+1, && \text{(E.21)}\\
\Lambda_2 &= \chi_2\frac{\kappa_1-1}{\kappa_2-1}, && \text{(E.22)}\\
\chi_2 &= \frac{\mu_{10}}{\mu_1}, && \text{(E.23)}
\end{aligned}$$

$$a_j(\alpha) = \frac{1}{\alpha}\frac{2i\alpha^2 - |\alpha|(\kappa_2+1)\delta_2\gamma_2}{2n_j + \gamma_2(3-\kappa_2)}, \qquad j=1,2 \tag{E.24}$$

$$a_j(\alpha) = \frac{1}{\alpha}\frac{2i\alpha^2 + |\alpha|(\kappa_2+1)\delta_2\gamma_2}{2n_j + \gamma_2(3-\kappa_2)}, \qquad j=3,4 \tag{E.25}$$

$$\begin{aligned}
n_1 &= \frac{1}{2}\left(-\gamma_2 + \sqrt{\gamma_2^2 + 4(\alpha^2 + i|\alpha||\gamma_2|\delta_2)}\right), && \text{(E.26)}\\
n_2 &= \frac{1}{2}\left(-\gamma_2 - \sqrt{\gamma_2^2 + 4(\alpha^2 + i|\alpha||\gamma_2|\delta_2)}\right), && \text{(E.27)}\\
n_3 &= \frac{1}{2}\left(-\gamma_2 + \sqrt{\gamma_2^2 + 4(\alpha^2 - i|\alpha||\gamma_2|\delta_2)}\right), && \text{(E.28)}\\
n_4 &= \frac{1}{2}\left(-\gamma_2 - \sqrt{\gamma_2^2 + 4(\alpha^2 - i|\alpha||\gamma_2|\delta_2)}\right), && \text{(E.29)}\\
\delta_2^2 &= \frac{3-\kappa_2}{\kappa_2+1}. && \text{(E.30)}
\end{aligned}$$

A straightforward asymptotic analysis of the integrands of the infinite integrals would start with the asymptotic expansion of the roots (2.44)-(2.47). We start by analyzing the roots of the characteristic equation asymptotically. Defining new variables

$$r = \frac{|\gamma_2|}{|\alpha|}, \qquad s = \frac{|\gamma_2|}{\gamma_2}, \tag{E.31}$$

the first two roots of the characteristic equation (2.40) becomes

$$n_1 = \frac{1}{2}\left(-\gamma_2 + \sqrt{\gamma_2^2 + 4(\alpha^2 + i|\alpha||\gamma_2|\delta_2)}\right) = \frac{|\alpha|}{2}N_1, \tag{E.32}$$

$$n_2 = \frac{1}{2}\left(-\gamma_2 - \sqrt{\gamma_2^2 + 4(\alpha^2 + i|\alpha||\gamma_2|\delta_2)}\right) = \frac{|\alpha|}{2}N_2, \tag{E.33}$$

$$\delta_2 = \sqrt{\frac{3-\kappa_2}{\kappa_2+1}}, \tag{E.34}$$

where

$$N_1 = -sr + \sqrt{r^2 + 4 + 4i\delta_2 r}, \tag{E.35}$$

$$N_2 = -sr - \sqrt{r^2 + 4 + 4i\delta_2 r}. \tag{E.36}$$

As $\alpha \to \infty$ or $r \to 0$

$$n_1 \to |\alpha|, \tag{E.37}$$

$$n_2 \to -|\alpha|. \tag{E.38}$$

In the expression for $y_1(\alpha, y)$ and $y_2(\alpha, y)$ given in (E.5) and (E.6), the exponential terms becomes

$$e^{n_2 y} \to e^{-|\alpha|y}, \tag{E.39}$$

$$e^{-h_2(n_1-n_2)+n_1 y} \to e^{-|\alpha|(2h_2-y)} \to 0, \tag{E.40}$$

$$e^{-h_2(\overline{n}_1-n_2)+\overline{n}_1 y} \to e^{-|\alpha|(2h_2-y)} \to 0, \tag{E.41}$$

since the range of y is $0 < y < h_2$ in the FGM coating. Therefore, as $\alpha \to \infty$,

$$y_1(\alpha, y) \to e^{-|\alpha|y}, \tag{E.42}$$

$$y_2(\alpha, y) \to a_2 e^{-|\alpha|y}. \tag{E.43}$$

Similarly in the expression for r_2 and r_4 given in (E.7) and (E.8) the exponential tems tends to

$$e^{-h_2(n_1-n_2)} \to e^{-2|\alpha|h_2} \to 0, \tag{E.44}$$

$$e^{-h_2(\overline{n}_1-n_2)} \to e^{-2|\alpha|h_2} \to 0. \tag{E.45}$$

Therefore

$$r_2 \rightarrow z_{12}, \tag{E.46}$$

$$r_4 \rightarrow z_{22}. \tag{E.47}$$

Also as $\alpha \rightarrow \infty$, Δ_3 tends to

$$\Delta_3 = -(r_2\overline{r}_4 + \overline{r}_2 r_4) \rightarrow \Delta_{30}, \tag{E.48}$$

where

$$\Delta_{30} = -(z_{12}\overline{z}_{22} + \overline{z}_{12}z_{22}). \tag{E.49}$$

Therefore using equations (E.42), (E.43), (E.46), (E.47) and (E.48), equations (2.114)-(2.117) becomes

$$h_{11}(\alpha, y) \rightarrow i\frac{\alpha}{|\alpha|}e^{-|\alpha|y}\sum_{n=0}^{13}\mathcal{A}_n r^n, \tag{E.50}$$

$$h_{12}(\alpha, y) \rightarrow e^{-|\alpha|y}\sum_{n=0}^{13}\mathcal{B}_n r^n, \tag{E.51}$$

$$h_{21}(\alpha, y) \rightarrow i\frac{\alpha}{|\alpha|}e^{-|\alpha|y}\sum_{n=0}^{13}\mathcal{C}_n r^n, \tag{E.52}$$

$$h_{22}(\alpha, y) \rightarrow e^{-|\alpha|y}\sum_{n=0}^{13}\mathcal{D}_n r^n, \tag{E.53}$$

where

$$
\begin{aligned}
\mathcal{A}_0 &= -\frac{\kappa_2+1}{4} \\
\mathcal{A}_1 &= \frac{s\,(\kappa_2+5)}{8} \\
\mathcal{A}_2 &= -\frac{5}{8} \\
\mathcal{A}_3 &= \frac{s}{4} \\
\mathcal{A}_4 &= -\frac{1}{32}\,\frac{5\,\kappa_2-8}{\kappa_2+1} \\
\mathcal{A}_5 &= \frac{1}{16}\,\frac{(\kappa_2-3)}{\kappa_2+1}s \\
\mathcal{A}_6 &= -\frac{1}{128}\,\frac{5\,{\kappa_2}^2-36\,\kappa_2+57}{(\kappa_2+1)^2} \\
\mathcal{A}_7 &= \frac{1}{64}\,\frac{(\kappa_2-7)\,(\kappa_2-3)\,s}{(\kappa_2+1)^2} \\
\mathcal{A}_8 &= -\frac{1}{512}\,\frac{5\,{\kappa_2}^3-84\,{\kappa_2}^2+375\,\kappa_2-493}{(\kappa_2+1)^3} \\
\mathcal{A}_9 &= \frac{1}{256}\,\frac{(\kappa_2-3)\,({\kappa_2}^2-18\,\kappa_2+61)\,s}{(\kappa_2+1)^3} \\
\mathcal{A}_{10} &= -\frac{1}{2048}\,\frac{5\,{\kappa_2}^4-152\,{\kappa_2}^3+1318\,{\kappa_2}^2-4324\,\kappa_2+4783}{(\kappa_2+1)^4} \\
\mathcal{A}_{11} &= \frac{1}{1024}\,\frac{(\kappa_2-7)\,(\kappa_2-3)\,({\kappa_2}^2-26\,\kappa_2+85)\,s}{(\kappa_2+1)^4} \\
\mathcal{A}_{12} &= -\frac{5}{8192}\,\frac{{\kappa_2}^5-48\,{\kappa_2}^4+682\,{\kappa_2}^3-4026\,{\kappa_2}^2+10479\,\kappa_2-9958}{(\kappa_2+1)^5} \\
\mathcal{A}_{13} &= \frac{1}{4096}\,\frac{(\kappa_2-3)\,({\kappa_2}^4-52\,{\kappa_2}^3+734\,{\kappa_2}^2-3748\,\kappa_2+6217)\,s}{(\kappa_2+1)^5}
\end{aligned}
\tag{E.54}
$$

$$
\begin{aligned}
\mathcal{B}_0 &= -\frac{\kappa_2 - 1}{4} \\
\mathcal{B}_1 &= \frac{s\,(\kappa_2 + 1)}{8} \\
\mathcal{B}_2 &= -\frac{1}{4} \\
\mathcal{B}_3 &= \frac{s}{16} \\
\mathcal{B}_4 &= -\frac{1}{16}\,\frac{\kappa_2 - 3}{\kappa_2 + 1} \\
\mathcal{B}_5 &= \frac{1}{64}\,\frac{(\kappa_2 - 4)\,s}{\kappa_2 + 1} \\
\mathcal{B}_6 &= -\frac{1}{64}\,\frac{(\kappa_2 - 3)\,(\kappa_2 - 7)}{(\kappa_2 + 1)^2} \\
\mathcal{B}_7 &= \frac{1}{256}\,\frac{({\kappa_2}^2 - 12\,\kappa_2 + 29)\,s}{(\kappa_2 + 1)^2} \\
\mathcal{B}_8 &= -\frac{1}{256}\,\frac{(\kappa_2 - 3)\,({\kappa_2}^2 - 18\,\kappa_2 + 61)}{(\kappa_2 + 1)^3} \\
\mathcal{B}_9 &= \frac{1}{1024}\,\frac{({\kappa_2}^3 - 24\,{\kappa_2}^2 + 147\,\kappa_2 - 257)\,s}{(\kappa_2 + 1)^3} \\
\mathcal{B}_{10} &= -\frac{1}{1024}\,\frac{(\kappa_2 - 3)\,(\kappa_2 - 7)\,({\kappa_2}^2 - 26\,\kappa_2 + 85)}{(\kappa_2 + 1)^4} \\
\mathcal{B}_{11} &= \frac{1}{4096}\,\frac{s\,({\kappa_2}^4 - 40\,{\kappa_2}^3 + 446\,{\kappa_2}^2 - 1844\,\kappa_2 + 2531)}{(\kappa_2 + 1)^4} \\
\mathcal{B}_{12} &= -\frac{1}{4096}\,\frac{(\kappa_2 - 3)\,({\kappa_2}^4 - 52\,{\kappa_2}^3 + 734\,{\kappa_2}^2 - 3748\,\kappa_2 + 6217)}{(\kappa_2 + 1)^5} \\
\mathcal{B}_{13} &= \frac{1}{16384}\,\frac{s\,({\kappa_2}^5 - 60\,{\kappa_2}^4 + 1050\,{\kappa_2}^3 - 7530\,{\kappa_2}^2 + 23535\,\kappa_2 - 26610)}{(\kappa_2 + 1)^5}
\end{aligned}
\tag{E.55}
$$

$$
\begin{aligned}
\mathcal{C}_0 &= -\frac{\kappa_2+1}{4} \\
\mathcal{C}_1 &= \frac{s\,(\kappa_2+1)}{8} \\
\mathcal{C}_2 &= -\frac{1}{8} \\
\mathcal{C}_3 &= 0 \\
\mathcal{C}_4 &= -\frac{1}{32}\,\frac{\kappa_2-4}{\kappa_2+1} \\
\mathcal{C}_5 &= 0 \\
\mathcal{C}_6 &= -\frac{1}{128}\,\frac{{\kappa_2}^2-12\,\kappa_2+29}{(\kappa_2+1)^2} \\
\mathcal{C}_7 &= 0 \\
\mathcal{C}_8 &= -\frac{1}{512}\,\frac{{\kappa_2}^3-24\,{\kappa_2}^2+147\,\kappa_2-257}{(\kappa_2+1)^3} \\
\mathcal{C}_9 &= 0 \\
\mathcal{C}_{10} &= -\frac{1}{2048}\,\frac{{\kappa_2}^4-40\,{\kappa_2}^3+446\,{\kappa_2}^2-1844\,\kappa_2+2531}{(\kappa_2+1)^4} \\
\mathcal{C}_{11} &= 0 \\
\mathcal{C}_{12} &= -\frac{1}{8192}\,\frac{{\kappa_2}^5-60\,{\kappa_2}^4+1050\,{\kappa_2}^3-7530\,{\kappa_2}^2+23535\,\kappa_2-26610}{(\kappa_2+1)^5} \\
\mathcal{C}_{13} &= 0
\end{aligned}
\tag{E.56}
$$

$$
\begin{aligned}
\mathcal{D}_0 &= \frac{\kappa_2 - 1}{4} \\
\mathcal{D}_1 &= -\frac{s\,(\kappa_2 + 1)}{8} \\
\mathcal{D}_2 &= \frac{1}{4} \\
\mathcal{D}_3 &= -\frac{1}{16}\,s \\
\mathcal{D}_4 &= \frac{1}{16}\,\frac{\kappa_2 - 3}{\kappa_2 + 1} \\
\mathcal{D}_5 &= -\frac{1}{64}\,\frac{(\kappa_2 - 4)\,s}{\kappa_2 + 1} \\
\mathcal{D}_6 &= \frac{1}{64}\,\frac{(\kappa_2 - 3)\,(\kappa_2 - 7)}{(\kappa_2 + 1)^2} \\
\mathcal{D}_7 &= -\frac{1}{256}\,\frac{({\kappa_2}^2 - 12\,\kappa_2 + 29)\,s}{(\kappa_2 + 1)^2} \\
\mathcal{D}_8 &= \frac{1}{256}\,\frac{(\kappa_2 - 3)\,({\kappa_2}^2 - 18\,\kappa_2 + 61)}{(\kappa_2 + 1)^3} \\
\mathcal{D}_9 &= -\frac{1}{1024}\,\frac{({\kappa_2}^3 - 24\,{\kappa_2}^2 + 147\,\kappa_2 - 257)\,s}{(\kappa_2 + 1)^3} \\
\mathcal{D}_{10} &= \frac{1}{1024}\,\frac{(\kappa_2 - 3)\,(\kappa_2 - 7)\,({\kappa_2}^2 - 26\,\kappa_2 + 85)}{(\kappa_2 + 1)^4} \\
\mathcal{D}_{11} &= -\frac{1}{4096}\,\frac{s\,({\kappa_2}^4 - 40\,{\kappa_2}^3 + 446\,{\kappa_2}^2 - 1844\,\kappa_2 + 2531)}{(\kappa_2 + 1)^4} \\
\mathcal{D}_{12} &= \frac{1}{4096}\,\frac{(\kappa_2 - 3)\,({\kappa_2}^4 - 52\,{\kappa_2}^3 + 734\,{\kappa_2}^2 - 3748\,\kappa_2 + 6217)}{(\kappa_2 + 1)^5} \\
\mathcal{D}_{13} &= -\frac{1}{16384}\,\frac{s\,({\kappa_2}^5 - 60\,{\kappa_2}^4 + 1050\,{\kappa_2}^3 - 7530\,{\kappa_2}^2 + 23535\,\kappa_2 - 26610)}{(\kappa_2 + 1)^5}
\end{aligned}
\tag{E.57}
$$

Finally the assymptotic expansions of the integrands in (2.165)-(2.168) becomes

$$h_{11}(\alpha, y) \rightarrow -i\frac{\alpha}{|\alpha|}\frac{\kappa_2 + 1}{4}e^{-|\alpha|y}, \tag{E.58}$$

$$h_{12}(\alpha, y) \rightarrow -\frac{\kappa_2 - 1}{4}e^{-|\alpha|y}, \tag{E.59}$$

$$h_{21}(\alpha, y) \rightarrow -i\frac{\alpha}{|\alpha|}\frac{\kappa_2 + 1}{4}e^{-|\alpha|y}, \tag{E.60}$$

$$h_{22}(\alpha, y) \rightarrow \frac{\kappa_2 - 1}{4}e^{-|\alpha|y}. \tag{E.61}$$

E.3 The lower half plane

The variables used in the integrands of the infinite integrals in equations (3.108)-(3.111) can be written as

$$h_{31}(\alpha, y) = -\frac{i\alpha(\kappa_3 - 1)}{\Delta_5}\left(y_3\overline{r_8} + \overline{y_3}r_8\right), \tag{E.62}$$

$$h_{32}(\alpha, y) = \frac{i\alpha}{\Delta_5}\left(-y_3\overline{r_6} + \overline{y_3}r_6\right), \tag{E.63}$$

$$h_{41}(\alpha, y) = -\frac{i\alpha}{\Delta_5}\left(y_4\overline{r_6} + \overline{y_4}r_6\right), \tag{E.64}$$

$$h_{42}(\alpha, y) = -\frac{i\alpha(\kappa_3 - 1)}{\Delta_5}\left(y_4\overline{r_8} - \overline{y_4}r_8\right), \tag{E.65}$$

where

$$y_3(\alpha, y) = e^{n_5 y} + r_5 e^{-h_3(n_5 - n_6) + n_6 y} + r_7 e^{-h(n_5 - \overline{n_6}) + \overline{n_6} y}, \tag{E.66}$$

$$y_4(\alpha, y) = a_5 e^{n_5 y} + a_6 r_5 e^{-h_3(n_5 - n_6) + n_6 y} - \overline{a_6} r_7 e^{-h_3(n_5 - \overline{n_6}) + \overline{n_6} y}, \tag{E.67}$$

$$\Delta_5 = -(r_6\overline{r_8} + \overline{r_6}r_8), \tag{E.68}$$

$$r_6 = z_{55} + z_{56} r_5 e^{-h_3(n_5 - n_6)} + \overline{z_{56}} r_7 e^{-h_3(n_5 - \overline{n_6})}, \tag{E.69}$$

$$r_8 = z_{65} + z_{66} r_5 e^{-h_3(n_5 - n_6)} - \overline{z_{66}} r_7 e^{-h_3(n_5 - \overline{n_6})}, \tag{E.70}$$

$$z_{55} = (3 - \kappa_3)(i\alpha)a_5 + (\kappa_3 + 1)n_5, \tag{E.71}$$

$$z_{56} = (3 - \kappa_3)(i\alpha)a_6 + (\kappa_3 + 1)n_6, \tag{E.72}$$

$$z_{65} = a_5 n_5 + i\alpha, \tag{E.73}$$

$$z_{66} = a_6 n_6 + i\alpha, \tag{E.74}$$

$$r_5 = \frac{1}{\Delta_4}\left(s_5\overline{t_6} + \overline{s_6}t_5\right), \tag{E.75}$$

$$r_7 = \frac{1}{\Delta_4}\left(s_5 t_6 - s_6 t_5\right), \tag{E.76}$$

$$\Delta_4 = -\left(s_6\overline{t_6} + \overline{s_6}t_6\right), \tag{E.77}$$

$$s_5 = i\lambda_3\alpha a_5 + \Lambda_3\left(\kappa_3+1\right)n_5\kappa_4 - \left(\kappa_4^2-1\right)|\alpha|, \tag{E.78}$$

$$s_6 = i\lambda_3\alpha a_6 + \Lambda_3\left(\kappa_3+1\right)n_6\kappa_4 - \left(\kappa_4^2-1\right)|\alpha|, \tag{E.79}$$

$$t_5 = a_5\left[\chi_3\kappa_4 n_5 - |\alpha|(\kappa_4+1)\right] + i\alpha\left[\kappa_4\chi_3 - (\kappa_4-1)\right], \tag{E.80}$$

$$t_6 = a_6\left[\chi_3\kappa_4 n_6 - |\alpha|(\kappa_4+1)\right] + i\alpha\left[\kappa_4\chi_3 - (\kappa_4-1)\right], \tag{E.81}$$

$$\lambda_3 = \kappa_4^2 + \kappa_4\left(\Lambda_3\left(3-\kappa_3\right)-2\right)+1, \tag{E.82}$$

$$\Lambda_3 = \chi_3\frac{\kappa_4-1}{\kappa_3-1}, \tag{E.83}$$

$$\chi_3 = \frac{\mu_{40}}{\mu_4}, \tag{E.84}$$

$$a_j(\alpha) = \frac{1}{\alpha}\frac{2i\alpha^2 - |\alpha|(\kappa_3+1)\delta_3\gamma_3}{2n_j+\gamma_3(3-\kappa_3)}, \qquad j=5,6 \tag{E.85}$$

$$a_j(\alpha) = \frac{1}{\alpha}\frac{2i\alpha^2 + |\alpha|(\kappa_3+1)\delta_3\gamma_3}{2n_j+\gamma_3(3-\kappa_3)}, \qquad j=7,8 \tag{E.86}$$

$$n_5 = \frac{1}{2}\left(-\gamma_3 + \sqrt{\gamma_3^2 + 4(\alpha^2 + i|\alpha||\gamma_3|\delta_3)}\right), \tag{E.87}$$

$$n_6 = \frac{1}{2}\left(-\gamma_3 - \sqrt{\gamma_3^2 + 4(\alpha^2 + i|\alpha||\gamma_3|\delta_3)}\right), \tag{E.88}$$

$$n_7 = \frac{1}{2}\left(-\gamma_3 + \sqrt{\gamma_3^2 + 4(\alpha^2 - i|\alpha||\gamma_3|\delta_3)}\right), \tag{E.89}$$

$$n_8 = \frac{1}{2}\left(-\gamma_3 - \sqrt{\gamma_3^2 + 4(\alpha^2 - i|\alpha||\gamma_3|\delta_3)}\right). \tag{E.90}$$

We start by analyzing the roots of the characteristic equation (3.37) asymptotically. Defining new variables

$$r = \frac{|\gamma_3|}{|\alpha|}, \qquad s = \frac{|\gamma_3|}{\gamma_3}, \tag{E.91}$$

the first two roots of the characteristic equation (3.37) becomes

$$n_5 = \frac{1}{2}\left(-\gamma_3 + \sqrt{\gamma_3^2 + 4(\alpha^2 + i|\alpha||\gamma_3|\delta_3)}\right) = \frac{|\alpha|}{2}N_5, \tag{E.92}$$

$$n_6 = \frac{1}{2}\left(-\gamma_3 - \sqrt{\gamma_3^2 + 4(\alpha^2 + i|\alpha||\gamma_3|\delta_3)}\right) = \frac{|\alpha|}{2}N_6, \tag{E.93}$$

$$\delta_3 = \sqrt{\frac{3-\kappa_3}{\kappa_3+1}}, \tag{E.94}$$

where

$$N_5 = -sr + \sqrt{r^2 + 4 + 4i\delta r}, \tag{E.95}$$

$$N_6 = -sr - \sqrt{r^2 + 4 + 4i\delta r}. \tag{E.96}$$

As $\alpha \to \infty$ or $r \to 0$

$$n_5 \to |\alpha|, \tag{E.97}$$

$$n_6 \to -|\alpha|. \tag{E.98}$$

In the expression for $y_3(\alpha, y)$ and $y_4(\alpha, y)$ the exponential terms becomes

$$e^{n_5 y} \to e^{|\alpha| y}, \tag{E.99}$$

$$e^{-h_3(n_5 - n_6) + n_6 y} \to e^{-|\alpha|(2h_3 + y)} \to 0, \tag{E.100}$$

$$e^{-h_3(n_5 - \overline{n}_6) + \overline{n}_6 y} \to e^{-|\alpha|(2h_3 + y)} \to 0, \tag{E.101}$$

since the range of y is $-h_3 < y < 0$. Therefore

$$y_3(\alpha, y) \to e^{|\alpha| y}, \tag{E.102}$$

$$y_4(\alpha, y) \to a_5 e^{|\alpha| y}. \tag{E.103}$$

Similarly in the expression for r_6 and r_8 the exponential tems tends to

$$e^{-h_3(n_5 - n_6)} \to e^{-2|\alpha| h_3} \to 0, \tag{E.104}$$

$$e^{-h_3(n_5 - \overline{n}_6)} \to e^{-2|\alpha| h_3} \to 0, \tag{E.105}$$

Thus

$$r_6 \to z_{55}, \tag{E.106}$$

$$r_8 \to z_{65}, \tag{E.107}$$

and

$$\Delta_6 \to \Delta_{60}, \tag{E.108}$$

where

$$\Delta_0 = -\left(z_{55}\overline{z}_{65} + \overline{z}_{55}z_{65}\right). \tag{E.109}$$

Therefore equations (3.118)-(3.121) becomes

$$h_{31}(\alpha, y) \rightarrow -\frac{i\alpha(\kappa_3 - 1)e^{|\alpha|y}}{\Delta_0}\left(\overline{z}_{65} + z_{65}\right), \tag{E.110}$$

$$h_{32}(\alpha, y) \rightarrow \frac{i\alpha e^{|\alpha|y}}{\Delta_0}\left(-\overline{z}_{55} + z_{55}\right), \tag{E.111}$$

$$h_{41}(\alpha, y) \rightarrow -\frac{i\alpha e^{|\alpha|y}}{\Delta_0}\left(a_5\overline{z}_{55} + \overline{a}_5 z_{55}\right), \tag{E.112}$$

$$h_{42}(\alpha, y) \rightarrow -\frac{i\alpha(\kappa_3 - 1)e^{|\alpha|y}}{\Delta_0}\left(a_5\overline{z}_{65} - \overline{a}_5 z_{65}\right). \tag{E.113}$$

Expanding equations (E.110)-(E.113) asymptotically as $\alpha \rightarrow \infty$ we obtain

$$h_{31}(\alpha, y) \rightarrow i\frac{\alpha}{|\alpha|}e^{|\alpha|y}\sum_{n=0}^{13}\mathcal{E}_n r^n, \tag{E.114}$$

$$h_{32}(\alpha, y) \rightarrow e^{|\alpha|y}\sum_{n=0}^{13}\mathcal{F}_n r^n, \tag{E.115}$$

$$h_{41}(\alpha, y) \rightarrow i\frac{\alpha}{|\alpha|}e^{|\alpha|y}\sum_{n=0}^{13}\mathcal{G}_n r^n, \tag{E.116}$$

$$h_{42}(\alpha, y) \rightarrow e^{|\alpha|y}\sum_{n=0}^{13}\mathcal{H}_n r^n, \tag{E.117}$$

where

$$
\begin{aligned}
\mathcal{E}_0 &= \frac{\kappa_3+1}{4} \\
\mathcal{E}_1 &= \frac{s\,(\kappa_3+5)}{8} \\
\mathcal{E}_2 &= \frac{5}{8} \\
\mathcal{E}_3 &= \frac{s}{4} \\
\mathcal{E}_4 &= \frac{1}{32}\,\frac{5\,\kappa_3-8}{\kappa_3+1} \\
\mathcal{E}_5 &= \frac{1}{16}\,\frac{s\,(\kappa_3-3)}{\kappa_3+1} \\
\mathcal{E}_6 &= \frac{1}{128}\,\frac{5\,\kappa_3^2-36\,\kappa_3+57}{(\kappa_3+1)^2} \\
\mathcal{E}_7 &= \frac{1}{64}\,\frac{(\kappa_3-3)\,(\kappa_3-7)\,s}{(\kappa_3+1)^2} \\
\mathcal{E}_8 &= \frac{1}{512}\,\frac{5\,\kappa_3^3-84\,\kappa_3^2+375\,\kappa_3-493}{(\kappa_3+1)^3} \\
\mathcal{E}_9 &= \frac{1}{256}\,\frac{(\kappa_3-3)\,(\kappa_3^2-18\,\kappa_3+61)\,s}{(\kappa_3+1)^3} \\
\mathcal{E}_{10} &= \frac{1}{2048}\,\frac{5\,\kappa_3^4-152\,\kappa_3^3+1318\,\kappa_3^2-4324\,\kappa_3+4783}{(\kappa_3+1)^4} \\
\mathcal{E}_{11} &= \frac{1}{1024}\,\frac{(\kappa_3-3)\,(\kappa_3-7)\,(\kappa_3^2-26\,\kappa_3+85)\,s}{(\kappa_3+1)^4} \\
\mathcal{E}_{12} &= \frac{5}{8192}\,\frac{\kappa_3^5-48\,\kappa_3^4+682\,\kappa_3^3-4026\,\kappa_3^2+10479\,\kappa_3-9958}{(\kappa_3+1)^5} \\
\mathcal{E}_{13} &= \frac{1}{4096}\,\frac{(\kappa_3-3)\,(\kappa_3^4-52\,\kappa_3^3+734\,\kappa_3^2-3748\,\kappa_3+6217)\,s}{(\kappa_3+1)^5}
\end{aligned}
\tag{E.118}
$$

$$
\begin{aligned}
\mathcal{F}_0 &= -\frac{\kappa_3 - 1}{4} \\
\mathcal{F}_1 &= -\frac{(\kappa_3 + 1)\, s}{8} \\
\mathcal{F}_2 &= -\frac{1}{4} \\
\mathcal{F}_3 &= -\frac{s}{16} \\
\mathcal{F}_4 &= -\frac{1}{16}\,\frac{\kappa_3 - 3}{\kappa_3 + 1} \\
\mathcal{F}_5 &= -\frac{1}{64}\,\frac{s\,(\kappa_3 - 4)}{\kappa_3 + 1} \\
\mathcal{F}_6 &= -\frac{1}{64}\,\frac{(\kappa_3 - 3)\,(\kappa_3 - 7)}{(\kappa_3 + 1)^2} \\
\mathcal{F}_7 &= -\frac{1}{256}\,\frac{s\,(\kappa_3^2 - 12\,\kappa_3 + 29)}{(\kappa_3 + 1)^2} \\
\mathcal{F}_8 &= -\frac{1}{256}\,\frac{(\kappa_3 - 3)\,(\kappa_3^2 - 18\,\kappa_3 + 61)}{(\kappa_3 + 1)^3} \\
\mathcal{F}_9 &= -\frac{1}{1024}\,\frac{s\,(\kappa_3^3 - 24\,\kappa_3^2 + 147\,\kappa_3 - 257)}{(\kappa_3 + 1)^3} \\
\mathcal{F}_{10} &= -\frac{1}{1024}\,\frac{(\kappa_3 - 3)\,(\kappa_3 - 7)\,(\kappa_3^2 - 26\,\kappa_3 + 85)}{(\kappa_3 + 1)^4} \\
\mathcal{F}_{11} &= -\frac{1}{4096}\,\frac{s\,(\kappa_3^4 - 40\,\kappa_3^3 + 446\,\kappa_3^2 - 1844\,\kappa_3 + 2531)}{(\kappa_3 + 1)^4} \\
\mathcal{F}_{12} &= -\frac{1}{4096}\,\frac{(\kappa_3 - 3)\,(\kappa_3^4 - 52\,\kappa_3^3 + 734\,\kappa_3^2 - 3748\,\kappa_3 + 6217)}{(\kappa_3 + 1)^5} \\
\mathcal{F}_{13} &= -\frac{1}{16384}\,\frac{s\,(\kappa_3^5 - 60\,\kappa_3^4 + 1050\,\kappa_3^3 - 7530\,\kappa_3^2 + 23535\,\kappa_3 - 26610)}{(\kappa_3 + 1)^5}
\end{aligned}
\tag{E.119}
$$

$$
\begin{aligned}
\mathcal{G}_0 &= \frac{\kappa_3 + 1}{4} \\
\mathcal{G}_1 &= \frac{(\kappa_3 + 1)\, s}{8} \\
\mathcal{G}_2 &= \frac{1}{8} \\
\mathcal{G}_3 &= 0 \\
\mathcal{G}_4 &= \frac{1}{32} \frac{\kappa_3 - 4}{\kappa_3 + 1} \\
\mathcal{G}_5 &= 0 \\
\mathcal{G}_6 &= \frac{1}{128} \frac{\kappa_3^2 - 12\,\kappa_3 + 29}{(\kappa_3 + 1)^2} \\
\mathcal{G}_7 &= 0 \\
\mathcal{G}_8 &= \frac{1}{512} \frac{\kappa_3^3 - 24\,\kappa_3^2 + 147\,\kappa_3 - 257}{(\kappa_3 + 1)^3} \\
\mathcal{G}_9 &= 0 \\
\mathcal{G}_{10} &= \frac{1}{2048} \frac{\kappa_3^4 - 40\,\kappa_3^3 + 446\,\kappa_3^2 - 1844\,\kappa_3 + 2531}{(\kappa_3 + 1)^4} \\
\mathcal{G}_{11} &= 0 \\
\mathcal{G}_{12} &= \frac{1}{8192} \frac{\kappa_3^5 - 60\,\kappa_3^4 + 1050\,\kappa_3^3 - 7530\,\kappa_3^2 + 23535\,\kappa_3 - 26610}{(\kappa_3 + 1)^5} \\
\mathcal{G}_{13} &= 0
\end{aligned}
\tag{E.120}
$$

$$
\begin{aligned}
\mathcal{H}_0 &= \frac{\kappa_3 - 1}{4} \\
\mathcal{H}_1 &= \frac{(\kappa_3 + 1)\, s}{8} \\
\mathcal{H}_2 &= \frac{1}{4} \\
\mathcal{H}_3 &= \frac{s}{16} \\
\mathcal{H}_4 &= \frac{1}{16} \frac{\kappa_3 - 3}{\kappa_3 + 1} \\
\mathcal{H}_5 &= \frac{1}{64} \frac{s\,(\kappa_3 - 4)}{\kappa_3 + 1} \\
\mathcal{H}_6 &= \frac{1}{64} \frac{(\kappa_3 - 3)\,(\kappa_3 - 7)}{(\kappa_3 + 1)^2} \\
\mathcal{H}_7 &= \frac{1}{256} \frac{s\,(\kappa_3^2 - 12\,\kappa_3 + 29)}{(\kappa_3 + 1)^2} \\
\mathcal{H}_8 &= \frac{1}{256} \frac{(\kappa_3 - 3)\,(\kappa_3^2 - 18\,\kappa_3 + 61)}{(\kappa_3 + 1)^3} \\
\mathcal{H}_9 &= \frac{1}{1024} \frac{s\,(\kappa_3^3 - 24\,\kappa_3^2 + 147\,\kappa_3 - 257)}{(\kappa_3 + 1)^3} \\
\mathcal{H}_{10} &= \frac{1}{1024} \frac{(\kappa_3 - 3)\,(\kappa_3 - 7)\,(\kappa_3^2 - 26\,\kappa_3 + 85)}{(\kappa_3 + 1)^4} \\
\mathcal{H}_{11} &= \frac{1}{4096} \frac{s\,(\kappa_3^4 - 40\,\kappa_3^3 + 446\,\kappa_3^2 - 1844\,\kappa_3 + 2531)}{(\kappa_3 + 1)^4} \\
\mathcal{H}_{12} &= \frac{1}{4096} \frac{(\kappa_3 - 3)\,(\kappa_3^4 - 52\,\kappa_3^3 + 734\,\kappa_3^2 - 3748\,\kappa_3 + 6217)}{(\kappa_3 + 1)^5} \\
\mathcal{H}_{13} &= \frac{1}{16384} \frac{s\,(\kappa_3^5 - 60\,\kappa_3^4 + 1050\,\kappa_3^3 - 7530\,\kappa_3^2 + 23535\,\kappa_3 - 26610)}{(\kappa_3 + 1)^5}
\end{aligned}
\tag{E.121}
$$

Finally as $\alpha \to \infty$ or $r \to 0$ the behaviour of the integrands become

$$h_{31}(\alpha, y) \;\to\; i\frac{\kappa_3 + 1}{4}\frac{\alpha}{|\alpha|}e^{|\alpha|y}, \tag{E.122}$$

$$h_{32}(\alpha, y) \;\to\; -\frac{\kappa_3 - 1}{4}e^{|\alpha|y}, \tag{E.123}$$

$$h_{41}(\alpha, y) \;\to\; i\frac{\kappa_3 + 1}{4}\frac{\alpha}{|\alpha|}e^{|\alpha|y}, \tag{E.124}$$

$$h_{42}(\alpha, y) \;\to\; \frac{\kappa_3 - 1}{4}e^{|\alpha|y}, \tag{E.125}$$

Appendix F

Numerical Evaluation of Fredholm Kernels

F.1 The Infinite Integral

In solving equations such as (4.24), the accuracy is very highly dependent on the correct evaluation of the Fredholm kernels $k^*_{ij}(s,r)(i = 1,...,4, \quad j = 1,2)$. The Fredholm kernels contain integrals with infinite upper limit. Evaluation of the infinite integrals to a high degree of accuracy is essential.

We shall treat the integrands with sine and cosine terms separately. Integration of $k^*_{ij}(s,r)$ is done by separating the integration limits, i.e.

$$\begin{aligned} k_{i1}(s,r) &= -\frac{4}{\kappa+1}\left[\int_0^{A^*} + \int_{A^*}^{\infty}\right] \Phi^*_{i1}(\zeta)\sin\zeta(s-r)d\zeta, \\ k_{i2}(s,r) &= -\frac{4}{\kappa+1}\left[\int_0^{A^*} + \int_{A^*}^{\infty}\right] \Phi^*_{i2}(\zeta)\cos\zeta(s-r)d\zeta, \end{aligned}$$

First integrals in $k_{ij}(s,r)$ are bounded and are evaluated numerically. However, the second integrals are evaluated using the 13 term approximation in the asymptotic expansion.

For the 0 to A^* part, integration is done by using a Gaussian quadrature. We can choose A^* so that $\left|\frac{\gamma^*}{A^*}\right|^{13}$ is small to any degree we want. For a particular nonhomogeneity constant, $\gamma_3 h_3$, there is a point where any further increase in A^* will only serve to tax the numerical effort. If A^* becomes larger in 0 to A^* integral, there will be more computing effort to calculate this integral.

The second integrals consist of

$$\int_{A^*}^{\infty} \Phi_{i1}^*(\zeta) \sin\zeta(s-r)d\zeta, \qquad \int_{A^*}^{\infty} \Phi_{i2}^*(\zeta) \cos\zeta(s-r)d\zeta \tag{F.1}$$

For the A^* to infinity part, the integrands $\Phi_{i1}^*(\zeta)$ and $\Phi_{i2}^*(\zeta)$ are asymptotically expanded as shown in Appendix E for $\zeta \to \infty$ as follows:

$$\Phi_{11}^*(\zeta) = \sum_{n=1}^{13} \mathcal{A}_n \left|\frac{\gamma^*}{\zeta}\right|^n \sin\zeta(s-r), \tag{F.2}$$

$$\Phi_{21}^*(\zeta) = \sum_{n=1}^{13} \mathcal{C}_n \left|\frac{\gamma^*}{\zeta}\right|^n \sin\zeta(s-r), \tag{F.3}$$

$$\Phi_{31}^*(\zeta) = \sum_{n=1}^{13} \mathcal{E}_n \left|\frac{\gamma^*}{\zeta}\right|^n \sin\zeta(s-r), \tag{F.4}$$

$$\Phi_{41}^*(\zeta) = \sum_{n=1}^{13} \mathcal{G}_n \left|\frac{\gamma^*}{\zeta}\right|^n \sin\zeta(s-r), \tag{F.5}$$

$$\Phi_{12}^*(\zeta) = \sum_{n=1}^{13} \mathcal{B}_n \left|\frac{\gamma^*}{\zeta}\right|^n \cos\zeta(s-r), \tag{F.6}$$

$$\Phi_{22}^*(\zeta) = \sum_{n=1}^{13} \mathcal{D}_n \left|\frac{\gamma^*}{\zeta}\right|^n \cos\zeta(s-r), \tag{F.7}$$

$$\Phi_{32}^*(\zeta) = \sum_{n=1}^{13} \mathcal{F}_n \left|\frac{\gamma^*}{\zeta}\right|^n \cos\zeta(s-r), \tag{F.8}$$

$$\Phi_{42}^*(\zeta) = \sum_{n=1}^{13} \mathcal{H}_n \left|\frac{\gamma^*}{\zeta}\right|^n \cos\zeta(s-r). \tag{F.9}$$

where $\mathcal{A}_n$, $\mathcal{B}_n$, $\mathcal{C}_n$, $\mathcal{D}_n$, $\mathcal{E}_n$, $\mathcal{F}_n$, $\mathcal{G}_n$, and $\mathcal{H}_n$ are given in equations (E.54)-(E.57) and

(E.118)-(E.121).Thus we need to calculate the integrals of the form

$$S_k = \int_{A^*}^{\infty} \frac{\sin\zeta\,|s-r|}{\zeta^k} d\zeta, \tag{F.10}$$

$$C_k = \int_{A^*}^{\infty} \frac{\cos\zeta\,|s-r|}{\zeta^k} d\zeta. \tag{F.11}$$

First note that

$$Si(x) = \int_0^x \frac{\sin(t)}{t} dt = \left(\int_0^{\infty} - \int_x^{\infty}\right) \frac{\sin(t)}{t} dt = \frac{\pi}{2}\frac{|x|}{x} - \int_x^{\infty} \frac{\sin(t)}{t} dt, \tag{F.12}$$

$$Ci(x) = \int_0^x \frac{\cos(t)}{t} dt = \gamma_0 + log|x| - \int_0^{|x|} \frac{1-cost}{t} dt, \tag{F.13}$$

where

$$\gamma_0 = 0.57721566490.$$

Therefore

$$\int_x^{\infty} \frac{\sin(t)}{t} dt = \frac{\pi}{2}\frac{|x|}{x} - Si(x), \tag{F.14}$$

$$\int_x^{\infty} \frac{\cos(t)}{t} dt = \left(\int_0^{\infty} - \int_0^{x}\right) \frac{\cos(t)}{t} dt$$

$$= -\gamma_0 - log|x| + \int_0^{|x|} \frac{1-cost}{t} dt. \tag{F.15}$$

S_1 and C_1 may be obtained as

$$S_1 = \frac{|s-r|}{s-r} \int_{A^*}^{\infty} \frac{\sin\zeta\,|s-r|}{\zeta} d\zeta = \frac{|s-r|}{s-r}\left[\frac{\pi}{2} - Si(A^*\,|s-r|)\right], \tag{F.16}$$

$$C_1 = \int_{A^*}^{\infty} \frac{\cos\zeta\,|s-r|}{\zeta} d\zeta = -Ci\,(A^*\,|s-r|) \tag{F.17}$$

The necessary recursive formulas may therefore be obtained by integrating by parts.

$$S_k = \left(\frac{\sin A\,|s-r|}{A^{k-1}(k-1)} + \frac{|s-r|}{k-1}\int_A^{\infty} \frac{\cos\zeta\,|s-r|}{\zeta^{k-1}} d\zeta\right)\frac{s-r}{|s-r|}$$

$$= \frac{1}{k-1}\left(\frac{\sin A\,|s-r|}{A^{k-1}} + |s-r|\,C_{k-1}\right)\frac{s-r}{|s-r|}, \qquad k>1 \tag{F.18}$$

$$
\begin{aligned}
C_k &= \frac{\cos A\,|s-r|}{A^{k-1}(k-1)} - \frac{|s-r|}{k-1}\int_A^\infty \frac{\sin\zeta\,|s-r|}{\zeta^{k-1}}d\zeta \\
&= \frac{1}{k-1}\left[\frac{\cos A\,|s-r|}{A^{k-1}} - (s-r)\,S_{k-1}\right], \qquad k>1 \qquad \text{(F.19)}
\end{aligned}
$$